



THE UNIVERSITY *of* EDINBURGH

This thesis has been submitted in fulfilment of the requirements for a postgraduate degree (e. g. PhD, MPhil, DClinPsychol) at the University of Edinburgh. Please note the following terms and conditions of use:

- This work is protected by copyright and other intellectual property rights, which are retained by the thesis author, unless otherwise stated.
- A copy can be downloaded for personal non-commercial research or study, without prior permission or charge.
- This thesis cannot be reproduced or quoted extensively from without first obtaining permission in writing from the author.
- The content must not be changed in any way or sold commercially in any format or medium without the formal permission of the author.
- When referring to this work, full bibliographic details including the author, title, awarding institution and date of the thesis must be given.

The phylogeny, evolution, and anatomy of
Taeniodonta (Mammalia: Eutheria) and
implications for the mammalian evolution after
the Cretaceous-Palaeogene mass extinction

Zoi Kynigopoulou



Thesis submitted for the degree of
Doctor of Philosophy

The University of Edinburgh
School of Geosciences

2023

To Prof. George D. Koufos,
my first mentor in palaeontology

Author's declaration

I declare that this thesis has been composed solely by myself, except where otherwise acknowledged. No part of the thesis has been submitted in order to apply for any other degree at this or any other institution.

Zoi Kynigopoulou

January 2023

Abstract

Mammals originated in the Mesozoic and were among the survivors of the Cretaceous-Palaeogene (K-Pg) mass extinction. However, the mode and the tempo of evolution for the eutherian mammals, the placental mammals and their close relatives remain unclear. Right after the K-Pg extinction, there were many groups of “archaic” mammals in the Palaeogene. Among these mammals are the Taeniodonta, a rather enigmatic group, known for their worn teeth. Taeniodonts are believed to have crossed the K-Pg boundary and started their diversification early in the Paleocene.

Fossils of taeniodonts have been found only in North America and their worn teeth and robust bodies are distinctive among other animals of their time. There are nine genera of taeniodonts, traditionally arranged into two families: the smaller Conoryctidae, which are believed to have had a more generalised body plan, and the robust Stylinodontidae, adapted for digging.

The main aim of this thesis is to shed light on the species-level inner relationship of Taeniodonta and to understand the morphological adaptations and functional morphology of the early members of this group. Central to this study are the numerous new fossils from the San Juan Basin in New Mexico, USA. These include new elements of dentition assigned to various members of Taeniodonta, as well as postcranial elements belonging to the genus *Conoryctes comma*.

Chapter one reviews previous work that was carried out for taeniodonts and provides a background on the anatomy and evolution of the group. Well-known palaeontologists such as Cope, Wortman, Matthew and others have studied taeniodonts and were among the first to assign many new materials to new genera.

More recent studies have focused on the anatomy of taeniodonts, their functional morphology and the structure of their unique teeth. There have been very few attempts to analyse their phylogeny.

In Chapter two, new dental fossils from the Puercan and Torrejonian of the San Juan Basin are described and used to understand the unique dentition of taeniodonts. Using these specimens and various others that were studied in many museums, a detailed species-level cladistic analysis is presented. It includes 133 taxa, scored for 630 dental, cranial, and postcranial characters. Among these are fourteen species of taeniodonts and other taxa that are potentially related to the group. All the previous phylogenetic studies of taeniodonts included only dental characters. The present study captures the dental, cranial and postcranial morphology. The dataset was then analysed under maximum parsimony to create a strict consensus topology. Using the first and last appearance of the taxa, a time-calibrated tree was created.

The results of this analysis show that Taeniodonta is a monophyletic group and excludes the Cretaceous taxon *Schowalteria* which has been a dubious member of the group. The interrelationship of Taeniodonta generally conforms to previous studies as the group is divided into two clades, corresponding to the Conoryctidae, and the Stylinodontidae. Interestingly, *Huerfanodon polecatensis* is resolved as a sister taxon to a clade of *Huerfanodon torrejonius* and *Conoryctes comma*. This topology of the phylogenetic tree and other anatomical features led to questions about the validity of the genus *Huerfanodon*. The results also propose that, among the numerous Palaeogene mammals in the dataset, Taeniodonta are cimolestids and potentially related to other groups including the leptictids and the palaeonodonts. These relationships need to be further tested with a broader spectrum of phylogenetic characters in a matrix that includes more taxa.

Chapter three presents a detailed anatomical description of the new postcranial elements of the genus *Conoryctes comma*. Previously, the postcranial skeleton of this genus was represented only by partial humerus and radius, leading to unanswered questions about the postcranial anatomy and locomotion of this animal. This chapter includes detailed descriptions and photographs of nine new specimens from the San Juan Basin. These specimens include elements of the vertebrae, forelimb and hindlimb of *Conoryctes*, and were compared with the skeletons of other taeniodonts and Palaeogene mammals. These comparisons and the functional anatomy of the postcranial fossils suggest a digging mode of life for *Conoryctes*.

The final chapter concludes the findings of this thesis. Based on the cladistic analysis and the fossil record, taeniodonts share common dental characteristics such as the progressively smaller molars in the tooth row and the absence of ectoflexus in the upper molars, while there are various similarities in the postcranial anatomy too. Unlike previous studies that consider only Stylinodontidae as highly specialised animals, this study finds that even early Paleocene *Conoryctes* had a specialised skeleton, with robust forelimbs and hindlimbs and sharp claws. This points to a high degree of fossoriality in both clades of Taeniodonta. Therefore, digging adaptations is a common trait in all taeniodonts, possibly shared with their closest relatives too. This mode of life might have impacted the survivability of their ancestors during the Cretaceous-Palaeogene extinction and led taeniodonts to radiate in the Paleocene.

Lay summary

Mammals are often considered to be among the most successful animals because they have adapted their skeletons to be able to live in many ecological niches; from small bats that fly, to enormous whales living in the sea. This is thanks to a series of adaptations that started hundreds of million years ago. The ancestors of mammals, changed over time and gave rise to the three major groups of living mammals: the monotremes, the marsupials and the placentals. The monotremes are the mammals that lay eggs, the marsupials give birth to poorly developed young that carry later in their pouch, and the placentals give birth to fully-developed young. When mammals split into these three groups is still unknown. To answer this question there needs to be a study of key animals that lived right before and right after the Cretaceous-Palaeogene mass extinction.

The Cretaceous-Palaeogene mass extinction killed almost 75% of all species on Earth, leading the non-avian dinosaurs to extinction. Many mammals survived and started to diversify and occupy different ecological areas. In order to do that, they changed their skeleton and teeth from generalised structures to more specialised anatomical features. This led to the variety of modern mammals we have today. A group of mammals that lived right after the extinction and whose relationships with modern mammals is unknown is called “archaic mammals”. They are an important link in understanding the diversification of mammals after the Cretaceous-Palaeogene extinction.

One such group of “archaic mammals” is Taeniodonta. They are unique animals that lived in North America from 66 to 45 million years ago. Some of them were only a few kilos but later became bigger, reaching up to 100 kilos, similar in size and build

like a warthog. One common characteristic in all taeniodonts is the high level of wear on their teeth and their massive canines. The early forms of the group, Conoryctidae, are thought to be small with generalised body plans. The more derived taeniodonts, Stylinodontidae, had specialised teeth for feeding on abrasive vegetation, such as roots and tubers, massive upper and lower canines and robust bodies with big claws, perfectly adapted for digging.

The San Juan Basin of New Mexico, USA is an area where many taeniodonts have been found. In the second chapter of this thesis, new specimens from the San Juan Basin are assigned to four species. Most of the new specimens show a low level of wear, making it easy to observe their dental anatomy. The anatomical features of mammalian teeth are very important in understanding the relationship among mammals. This is one of the reasons why Taeniodonta has remained an enigmatic group for many decades. Using the new dental specimens attributed to a better diagnosis for taeniodonts and led to a better understanding of the relationships within the group.

The study of the new dental specimens led to a few interesting conclusions. The first is the presence of more complicated lower teeth for the “generalised” group of Taeniodonta than previously proposed. The second interesting conclusion is that one of the more derived taeniodont, *Ectoganus* changed drastically the anatomy of its upper molars likely as a result of a diet of more hard vegetation. After studying the distribution of the enamel and the dentine, it is clear that *Ectoganus* shifted one of the smaller cusps to create a more squared-shaped upper molar. This is an anatomical change that is observed in other mammals too and is often due to changes in the diet and environment.

Dental anatomy is very important when working on the phylogeny of mammals. The method of finding relationships among animals is called a phylogenetic analysis and it uses anatomical features, called characters, which are scored for many animals. The matrix of a phylogenetic analysis can include an abundance of characters and animals to better portray their relationships. Similar analyses have been done on Taeniodonta but never to a species level and only including characters of their teeth. Using the new observations on the dental anatomy, the skull and the skeleton, all species of taeniodonts were scored. The matrix used is based on previous studies, and it was modified by adding a few characters and more taxa that previous studies find related to taeniodonts.

The results show that Taeniodonta is a monophyletic clade, consisting of the two known clades of Conoryctidae and Stylinodontidae. The most parsimonious tree finds *Schowalteria*, which was previously thought to belong to Stylinodontidae, outside of Taeniodonta. A detailed overview of the specimen followed, pointing out the differences between *Schowalteria* and taeniodonts. Another important result is that *Huerfanodon torrejonius* is found as a sister taxon to *Conoryctes comma* and outside of that clade is the other species of the genus, *Huerfanodon polecatensis*. A study of the two genera led to synonymise *Huerfanodon* under *Conoryctes*.

The third chapter of this thesis includes a detailed study of the skeleton of *Conoryctes comma*, a member of the Conoryctidae family. This animal was known from a few parts of the postcranial skeleton, and new specimens from the San Juan Basin led to a better understanding of almost all its skeleton. The new specimens include parts of the vertebrae column, the forelimb, the manus, the pelvis, and the hindlimb. These were compared to other taeniodonts and Palaeogene taxa. A study

of the functional morphology shows that *Conoryctes* was a scratch-digging animal, like pangolins.

Combining the results of the study, *Conoryctes*, a member of the Conoryctidae family, had a digging mode of life. Some of these anatomical features are seen in *Onychodectes*, the oldest member of Conoryctidae, and *Wortmania*, the oldest member of Stylinodontidae. All that indicates that the common ancestor of Taeniodonta was most likely an animal with adaptations for some degree of fossoriality, that potentially helped them survive after the Cretaceous-Palaeogene mass extinction.

Acknowledgements

Looking back to the past four and a half years I can recall countless stressful and difficult times, and challenges that helped me grow on an academic and personal level, but also amazing and unique experiences. None of that would have been possible without the help of many important people that guided me with their knowledge and support.

First and foremost, I would like to express my deep gratitude to my supervisors: Steve Brusatte, Tom Williamson and Sarah Shelley. Not only they believed in my abilities and gave me the opportunity to study at the University of Edinburgh, but they trusted me to share their enthusiasm for this special group of mammals. I would like to thank Steve for the guidance, motivation and encouragement during all the stages of this journey. I would also like to thank you Steve for giving me opportunities to teach, improve my outreach skills and attend conferences. Tom Williamson has been tremendously helpful in understanding the stratigraphy of the San Juan Basin and the Paleocene mammals, so a very special thank you goes to him. Thanks, Tom, for passing on your enthusiasm for taeniodonts and of course for giving me access to all the specimens and photos you have. I would like to thank Sarah for teaching me how to take excellent photos, a technique that was passed down to her by Tom. Thank you, Sarah, for all the times you sat down with me and helped me with datasets and gave me useful advice on how to improve my work. I sincerely thank all three of my supervisors for all the moments we shared in the field, in conferences and museums and for the overall excellent experience I had as their PhD student.

I would also like to thank the members of the PaIM group that have been my fellow travellers on this journey. Special thank you to John Wible for sharing all of his

knowledge on anatomy and having the patience to explain even the smallest detail. I would also like to thank Fernando Perini for sharing important information on *Xenarthra* and Greg Funston for providing me with photos and teaching me about palaeohistology. Ornella Bertrand has been a great companion during fieldwork and conferences. Thanks, Ornella, for all the help, the valuable support and the nice long walks. I would also like to thank the other PhD students of the team Sofia Holpin, Paige dePolo and Hans Puschel Rouliez for being great friends. To all the people of the PaIM group, thank you for the countless head-scratching moments and the fun times we shared.

A special thank you also to Ken Rose for inviting me to look into some Eocene specimens of taeniodonts and for the interesting conversations we had. I would like to thank various curators that helped me during my museum visits, such as Nicole Ridgwell (NMMNH&S) for helping me pack and borrow specimens; Judy Galkin (AMNH) for always being extremely helpful; Amanda Millhouse (USNM) for sending me photos of specimens after my visit; and Daniel Brinkman (YPM).

My PhD was funded by ERC and I would also like to thank the IT of the University of Edinburgh for awarding me with a graphic tablet to work on the drawings and photos of my thesis. I would also like to thank EAVP for awarding me with a travel grant.

A special thanks go to Ian Butler, the University of Edinburgh, that was patient enough to scan the specimen I needed twice. Another staff member of the University of Edinburgh I would like to thank is Sophie Ramette for sharing important information and guidance.

Major supporters along this journey are my fellow PhD students. Many thanks to fellow palaeontologists of Edinburgh such as Davide, Michella, Natalia, and especially Julia and Amy for the nice walks and brunches. I would like to thank previous and current PhD students of the “Attic” such as Mylene, Hugo and my boothmates Berit, Chris and Sophie.

I would like to thank the members of “The University of Shenanigans”: Becca, Elizabeth, and Dylan. Thank you for all the amazing experiences, the adventures, the pranks, and the laughs we had all these years. But also, thanks for the stress and responsibilities you drugged me into when we joined the Grad School Committee.

Many thanks go to my friend Nokwazi for assisting me in finding cool coffee shops in Edinburgh. Even though they were far away, my friends Christina and Sophia have greatly supported me with valuable cat videos and more.

I would not have made it this far if it wasn't for my family's support. I would like to thank my sister Angelliki for being a great role model ever since we were kids. I want to thank my brother-in-law, Gregory, for his support and my niece, Eleni-Myrsini, for teaching me to focus on the important things in life. A special thank you goes to my partner, Daniel, for his contagious optimism. Finally, I thank my parents for their endless support and love, especially during the writing stage of this thesis. I want to thank my mother Athina, who has offered many times to help me, and my father Kostas, who made sure I had enough coffee every day.

Contents

Author's declaration	i
Abstract	iii
Lay summary	vii
Acknowledgements	xi
Contents	xv
Institutional Abbreviations	xvii
CHAPTER 1	1
Introduction	1
Cretaceous – Palaeogene mammals	6
Historical background of Taeniodonta	9
Outline of the present study	20
CHAPTER 2	23
Systematics and phylogeny of Taeniodonta	23
Introduction	25
Background on the affinities and phylogenetic analyses of Taeniodonta	26
Methods	37
Basic terminology	37
Methodological Protocols	118
Results	122
Discussion	135
Relationships within Taeniodonta	137
Relationships with other mammals	150
Evolution of Taeniodonta	150
CHAPTER 3	153
The postcranial skeleton of <i>Conoryctes comma</i>	153
Introduction	155
Materials and methods	165
Comparative description	173
Vertebrae	173
Humerus	183
Ulna	190
Radius	196
Metacarpals	202

Innominate.....	206
Femur	213
Patella.....	223
Tibia.....	224
Astragalus	234
Calcaneum	242
Metatarsals	251
Results and Discussion	254
CHAPTER 4	259
Conclusions.....	259
Summary.....	261
Future work.....	269
References	271
Appendix.....	285
Appendix to Chapter 2	285
Appendix to Chapter 3	389

Institutional Abbreviations

AMNH: American Museum of Natural History, New York City, New York, USA

FMNH, P or PM: Field Museum of Natural History, Chicago, Illinois, USA

NMMNH&S: New Mexico Museum of Natural History and Science, Albuquerque, New Mexico, USA

TMM: Texas Memorial Museum, University of Texas, Austin, Texas, USA

UM: Museum of Paleontology, University of Michigan, Ann Arbor, Michigan, USA

USGS: U.S. Geological Survey, Paleontology and Stratigraphy Branch, Denver, Colorado

USNM: National Museum of Natural History, Washington, D. C., USA

YPM (PU): Peabody Museum of Natural History, Yale University, New Haven, Connecticut, USA

CHAPTER 1

Introduction



San Juan Basin, New Mexico, fieldwork May 2019

“...οἱ δ’ ὄλως ἀπολιθοῦν τὰ τιθέμενα εἰς ἑαυτούς”

ΠΕΡΙ ΛΙΘΩΝ, Θεόφραστος

“...whereas other (rocks) can turn into stone what is placed on top of them”

ON STONES, Theophrastus (c. 371 – c. 287 BC)

Mammals are among the most successful animals on Earth since they have a variety of sizes and they occupy most habitats; from small flying bats to large whales capable of deep diving. These variations are a result of many million years of diverse locomotion and dietary adaptations that started from a synapsid ancestor (Kielan-Jaworowska, *et al.* 2004). During the Mesozoic mammals originated and were already occupying different ecological niches (Luo, 2007). The asteroid impact that caused the Cretaceous-Palaeogene (K-Pg) mass extinction killed almost 75% of all species on Earth, including the non-avian dinosaurs. Many mammals survived, diversified and occupied different ecological niches, making the Cenozoic, the age of mammals. Among the mammals that lived right after the extinction is the Taeniodonta. The present study focuses on the anatomy and phylogeny of these enigmatic mammals, due to their worn teeth.

There are three major groups of modern mammals: the monotremes, the marsupials and the placentals. The monotremes lay eggs and the only living monotremes today are the platypus and the four species of echidna. All the extinct and extant monotremes and their close relatives form the Australosphenida, which split off from early mammals in the Jurassic (Luo, 2007). Another subclass of mammals is Theria, which includes the extinct and extant marsupials and placentals and their close relatives (Luo, 2007; O'Leary *et al.*, 2013). Marsupials are mammals that give birth to poorly developed young and are later developed in a pouch. Placentals, like humans, are mammals that give birth to well-developed young.

Understanding the relationships of mammals, and particularly placentals, and placing the time of their diversification is still a subject of many studies today. Recent studies on genome analyses conclude that placental mammals originated 83.3-77.6

million years ago (Álvarez-Carretero *et al.*, 2022) or even earlier than that, around 102 million years ago (Foley *et al.*, 2022). However, Upham *et al.* (2021) argued that molecular analyses should include fossil evidence to help understand mammalian diversification.

There are currently five models for the diversification of placentals. The three of these, the short, the long fuse and the explosive, were proposed by Archibald and Deutschman (2001). The explosive model, also supported by the analysis of O'Leary *et al.* (2013) hypothesises that all placentals originated and explosively diversified after the Cretaceous-Palaeogene (K-Pg) mass extinction. Some new researchers exclude this model a priori in their analyses (Álvarez-Carretero *et al.*, 2022). The long and short fuse models have been supported by many molecular analyses (Springer *et al.*, 2003; Foley *et al.*, 2016 short-fused, Brininda-Emonds *et al.*, 2007 long fuse) proposing that the root of Placentalia is before the K-Pg. The long fuse hypothesises that Placentalia originated early, but much of the diversification within placentals occurred later in the Cretaceous and Paleocene. The short fuse model suggests that the origin and much of the major diversification of Placentalia happened early, in the Cretaceous (Figure 1).

The two recently proposed models, the soft explosive and the trans-KPg model, are intermediate between the explosive and long fuse models. The soft explosive model (Phillips, 2016) proposes that placentals originated in the Cretaceous, and only the interordinal clades were living before the K-Pg and the extinction led to the origin of the intraordinal clades. The trans-KPg model (Liu *et al.*, 2017) is very similar to the long fuse model but places the origin of placentals during the Upper Cretaceous.

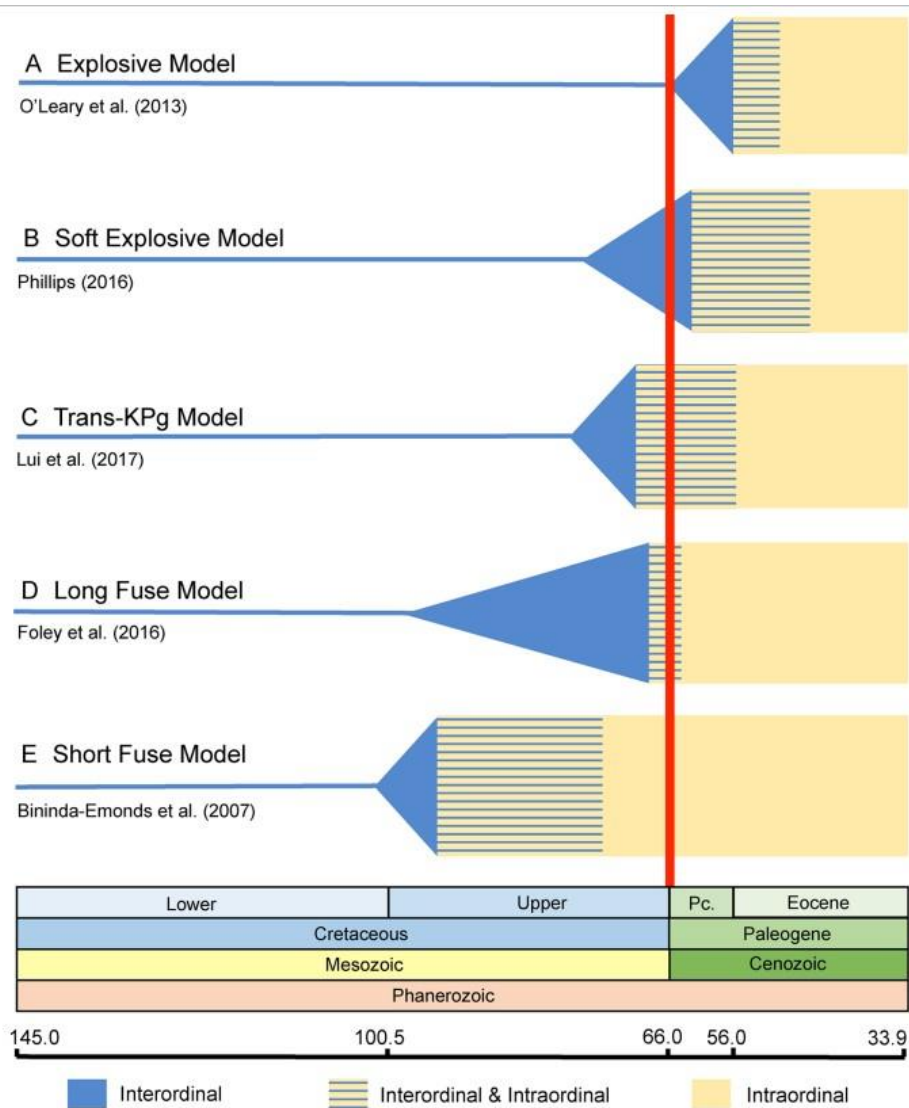


Figure 1: A graphic representation of the five models of Placentalia diversification as seen in the Springer *et al.* (2019) paper (figure 1).

Therefore, a detailed study of the fossil record, along with molecular data is essential for understanding the evolutionary history of placental mammals. Particularly understanding the anatomy and phylogeny of the Paleocene mammals that diversified and lived after the K-Pg extinction can hold important information for the origin of placentals. The PaIM (Paleocene Mammal) working group, which I am part of, is trying to answer the enigmas around the rise of placental mammals. We have scored dental,

cranial and postcranial characters for over 200 taxa of extant and extinct mammals. My contribution to the team and the scope of this thesis is to study taeniodonts and other late Cretaceous and early Palaeogene mammals.

Cretaceous – Palaeogene mammals

After the Cretaceous-Palaeogene mass extinction, many placental mammals and their close relatives, early eutherians, thrived in the Palaeogene. However, there are still unanswered questions for some mammals that lived right after the extinction, during the early Palaeogene, and their phylogenetic position on the mammalian tree has been the subject of debate. Their relationship with Cretaceous mammals is uncertain and it is unclear whether they left any obvious modern descendants (Rose 2006). These mammals belong to the “archaic” groups, and they are a key component in understanding the evolution of placental mammals. Some of the “archaic” mammals are grouped in wastebaskets like the “condylarths”, ungulate-like mammals, and insectivorous “cimolestans” (Rose 2006). Other “archaic” mammals are phylogenetic enigmas, such as pantodonts, tillodonts, and taeniodonts.

Taeniodonta (Cope, 1876) is an enigmatic group of “archaic” mammals, known from localities of North America only. The lowest putative taeniodont stratigraphically is *Schowalteria* found in the Upper Cretaceous Scollard Formation of Alberta, Canada (Fox and Naylor, 2003). Therefore, taeniodonts are proposed to have originated before the K-Pg boundary, making them among the animals that survived the extinction.

One of their unique features is the enamel distribution and the level of wear on their teeth. The enamel is usually worn on the lingual side of their upper teeth and the

buccal side on the lower teeth, indicative of an abrasive diet (Koenigswald *et al.*, 2010). This led them to develop hypsodont teeth, meaning that the tooth crown, which is covered in enamel, is high (White, 1959). All the teeth of the most derived animal of the group, *Stylinodon*, had reached an ever-growing condition, hypselodonty. Moreover, their unique wear patterns and enamel distribution puzzled many researchers who tried to understand their diet (Schoch, 1986; Turnbull, 2004; Koenigswald 2011). In addition to their peculiar teeth, they reached large sizes ranging from medium-sized animals (5-10kg), like small species of pangolins, up to 110 kg (Schoch, 1986), like a warthog or armadillo.

Paterson (1949b) proposed that dental adaptations, the enlarged canines and the jaw movement, led to cranial and postcranial adaptations in the subfamily of Stylinodontidae, while the subfamily of Conoryctidae was “generalised in structure”. This term was used to indicate the resemblance in the anatomy with the primitive therian morphotype, like *Didelphis*, and the presence of few specializations in the functional morphology of the postcranial skeleton (Gregory 1910; Matthew 1937; Schoch, 1986). Many Paleocene mammals have been proposed as having a skeletons lacking adaptations for specific locomotion types, but a recent study by Shelley *et al* (2021) showed a high diversity of the tarsal morphology. The current study is trying to evaluate whether conoryctids lacked any specialised features or possessed postcranial adaptations. For this, a detailed in-group phylogeny to understand the evolution of the Taeniodonta is the primary goal of the study.

The phylogeny of Taeniodonta is problematic and there have been many studies trying to assess their relationships with other Palaeogene and Cretaceous taxa, and the modern mammalian orders. Wortman (1897), after studying their teeth

and their postcranial anatomy, suggested that they fall in the order of Edentata, particularly close to ground sloths. Later Matthew (1937) suggested connections with palaeodonts, Xenarthra and Pholidota. The name Edentata was introduced by Cuvier (1798) to unite animals that had fewer or no teeth, and a robust skeleton, such as armadillos, sloths, anteaters, pangolins and armadillos. Many taxa had been placed in that order, including taeniodonts as mentioned above. Novacek (1986, 1992) and Novacek and Wyss (1986) proposed using the term Edentata to include only Pholidota and Xenarthra and Palaeodontia. Many phylogenetic analyses failed to find Edentata as a monophyletic clade, with Xenarthra being more closely related to Afrotheria and Pholidota to Laurasatheria (Gunnell and Rose, 2008; O'Leary *et al.*, 2013), whereas palaeodonts fall close to Pholidota (Rose, 2008; O'Leary *et al.*, 2013).

Based on more recent studies, Taeniodonta is believed to belong to Cimolesta (McKenna, 1975), primitive eutherian mammals (Wible *et al.*, 2007, 2009) and *Alveugena* is the sister taxon of taeniodonts (Eberle, 1999; Rook and Hunter, 2011; 2013). However, recent analyses showed that there are still questions regarding the relationships within Taeniodonta (Williamson and Brusatte, 2013). Their position within Eutheria is still debatable and that is outside of the scope of the current study but is part of the PaIM group research.

The second goal of this study is to understand the anatomy and functional morphology of *Conoryctes* and to address the level of its postcranial adaptations. Williamson and Brusatte (2013), when describing the new postcranial skeleton of an early Puercan taeniodont, *Wortmania*, highlighted important features pointing to some degree of fossoriality not only for *Wortmania* but also for a conoryctid, *Onychodectes*.

Finding the timing of the diversification within taeniodonts could help understand the diversification of mammals before and after the K-Pg extinction.

The San Juan Basin in New Mexico, USA, has a temporally well-constrained record of the latest Cretaceous and Paleocene animals that have been studied for many decades. Many of the early Paleocene taeniodonts and other taxa have been found there. The basin has been studied with extensive fieldwork, and detailed studies of the biostratigraphy have been carried out (Flynn, *et al.*, 2020; Williamson, 1996). However, specimens found in the early 1900s in the basin, and other areas, lack precise geographic and stratigraphic information, so the biostratigraphy of most early-collected specimens of taeniodonts is poorly resolved.

Many new specimens of taeniodonts were collected from the San Juan Basin and were used for the current study. The new material helped to understand the intriguing dental morphology of the group and added an abundance of characters in the phylogenetic analysis, as seen in chapter two. Among the new specimens are associated postcranial bones of the taeniodont *Conoryctes comma*, which helped understand the functional morphology of this animal. *Conoryctes* is a Paleocene taeniodont known mostly from dental and cranial specimens from the Torrejonian of the San Juan Basin.

Historical background of Taeniodonta

Taeniodonta has always puzzled researchers who tried to find possible affinities and groups to associate them with. Marsh (1874) was the first one to describe a taeniodont, naming it *Stylinodon mirus*. He believed they were related to *Toxodon*, a

South American mammal of the Late Miocene. The following year, though, after naming Tillodontia, an extinct order of Palaeogene mammals with elongated incisors, Marsh (1875) included in them the family Stylinodontidae. Cope (1874) described *Calamodon gliriformis* (synonym now to *Ectoganus gliriformis*) and *Ectogonus* (Cope, 1874). He also formed the new suborder of Taeniodonta based on these two animals, with the two families of Ectoganidae and Calamodontidae. While describing *Calamodon*, Cope (1876) pointed to similarities with Edentata and the Insectivora. Insectivora included both lipotyphlans and “archaic insectivores”, such as leptictids, palaeoryctids, pantolestids, apatemyids, mixodectids and other families (Rose, 2006). The relationships of these animals in the mammalian tree are better resolved in recent studies, and Insectivora is not supported by molecular evidence (O’Leary *et al.*, 2013) and therefore the term is considered a wastebasket taxonomically.

Marsh (1876) described *Dryptodon* (synonym now to *Ectoganus*). In the following year (1877) he placed Stylinodontidae still in Tillodontia and said that tillodonts are not related to Edentata. A series of descriptions of new genera followed by Cope, such as *Conoryctes* (Cope, 1881a), *Psittacotherium* (Cope, 1882a), *Hemiganus vultuosus* (Cope, 1882c), *Hexodon molestus* (now a synonym of *Conoryctes comma*) (Cope, 1884a), *Hemiganus otariidens* (now synonym to *Wortmania*) (Cope, 1885; Cope, 1888), and *Onychodectes tisonensis* (Cope, 1888). However, he did not place these in Taeniodonta but referred them to Tillodontia. When describing *Hexodon*, Cope (1884a) believed there were similarities with *Periptychus*, a member of condylarths, another group of “archaic mammals”. Later Cope (1888) dropped this suggestion and instead observed similarities between *Hexodon*, *Onychodectes* and *Hemiganus*. In that study, he also placed *Hemiganus otariidens* in Creodonta. Osborn and Earle (1895) when describing the skulls (AMNH 785) of

Onychodectes tisonensis and of *Onychodectes rarus* (AMNH 8240) referred the genus *Onychodectes* to Tillodontia.

It was Wortman who in his studies (Wortman, 1896a,b; 1897) united *Hemiganus*, *Psittacotherium*, *Stylinodon*, *Ectoganus* and *Onychodectes* and *Conoryctes* forming the new suborder of Ganodonta. Wortman (1897) described many of the known materials, such as the skull of *Onychodectes* and *Conoryctes*. In his study, he also transferred the type of *Hemiganus* to the genus *Psittacotherium*. This would be noticed later by Hay (1899) who proposed the name *Wortmania otariidens* for that specimen.

Wortman (1897) also introduced the idea that Ganodonta was a suborder under Edentata, with the family of Conoryctidae related to armadillos, and the family of Stylinodontidae to ground sloths. The family of Conoryctidae include the taxa of *Onychodectes* and *Conoryctes*, while *Hemiganus*, *Psittacotherium*, *Calamodon* and *Stylinodon* belonged to the Stylinodontidae. The classification of these two families was based on the orientation of the lower posterior premolars (p2, p4) on the jaw, as it is oblique in Conoryctidae; an observation that is seen in all taeniodonts. The similarities that Wortman (1897) noticed in his studies between Ganodonta and Edentata are focused not only on the teeth but the postcranial skeleton too. Particularly, the teeth of derived taeniodonts, such as *Stylinodon*, show a lack of enamel around the tooth while they are also rootless. The robustness of the forelimb, the manus and the femur, also reminded Wortman of ground sloths and led to his assumptions.

However, this idea was not well received by many researchers and Ganodonta were provisionally placed under Edentata. Among the researchers that rejected the

affinities were Scott (1905), Ameghino (1897, 1902, 1906a, b) and Winge (1915), with the latter giving detailed explanations as to why these resemblances are due to convergence. Winge later (1917; 1923) pointed out that the group resembled more Insectivora taxa and Leptictidae, particularly referring to Stylinodontidae and Insectivora with Leptictidae, Tillotheriidae and Periptychidae (Winge, 1917). The anatomical similarities he noticed were on the short nasals, the cusps on the stylar shelf on the upper molars and the elongated canines. Winge (1917) also noticed differences between *Onychodectes* and *Conoryctes*, naming three subfamilies, the Onychodectinae, the Conoryctinae and the Stylinodontinae.

This view was accepted by Matthew (1937), who changed the name of Ganodonta to Taeniodonta since it was the first proposed name for the group by Cope (1876). He proposed the interrelationships of taeniodonts as divided into one family, Stylinodontidae, with four subfamilies, the Onychodectinae, the Conoryctinae, the Psittacotheriinae (including *Wortmania*, *Psittacotherium* and *Calamodon*) and the Stylinodontinae. In his detailed study, Matthew (1937) also pointed out that taeniodonts are possibly related to palaeodonta, Xenarthra and Pholidota and he excluded any relationships with Tillodontia, apart from a possible common insectivore ancestor (Figure 2). Matthew (1878) had previously discussed possible relationships between palaeodonta and edentates.

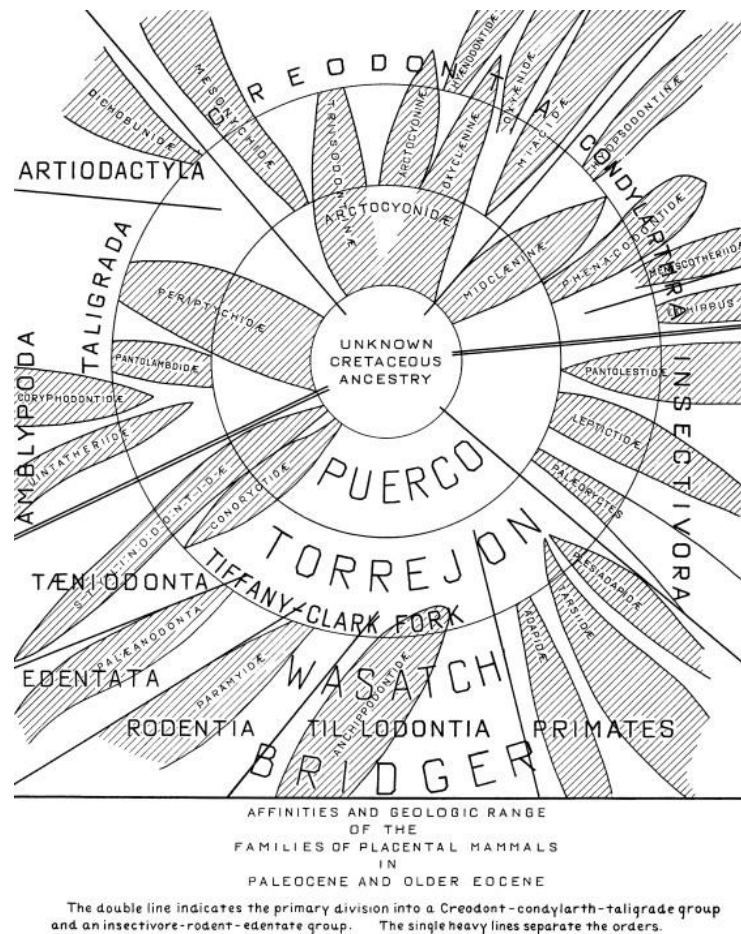


Figure 2: The affinities of placental mammals from the Paleocene and Eocene as seen in Matthew (1937, figure 83).

In his study, Matthew (1937) also described and illustrated many specimens, giving revised diagnoses of Taeniodonta while referencing all the work that was previously done on these animals. He also synonymized *Conoryctes comma* (Cope, 1881a) with *Hexodon molestus* (Cope, 1884a) and accepted *Hemiganus vultuosus* (Cope, 1882c) under *Psittacotherium multifragum* (Cope, 1882a), naming the other genus as *Wortmania otariidens*.

A new specimen, intermediate in size between *Onychodectes* and *Conoryctes*, was later found in Dragon Canyon, of northeast Utah. Gazin (1939), described it and

created the new genus of *Conoryctella*. Accepting the detailed work of Matthew, Simpson (1945) later proposed keeping only the two subfamilies for Taeniodonta: the Conoryctinae (*Onychodectes*, *Conoryctella*, *Conoryctes*) and the Stylinodontinae (*Wortmania*, *Psittacotherium*, *Ectoganus* and *Stylinodon*). In 1949b Patterson introduced *Lampadophorus*, a genus synonymised with *Ectoganus*. In the same year, he published a detailed revision of Taeniodonta, studying evolutionary stages within the group. He believed that conoryctids are more primitive compared to stylinodontids, with *Onychodectes* being the most primitive of all taeniodonts. The evolutionary changes he noticed were on the teeth, particularly the canine, the jaw and the chewing mechanism and the foot, particularly the claw, and as a result a change in the size. His views are described in more detail in chapter two of the current study.

A few studies followed trying to indicate relationships between Taeniodonta with other groups. Lillegraven (1969) proposed *Procerberus formicarum* as a sister taxon to Taeniodonta based on the morphology of their teeth. McKenna (1969) also proposed connections with “*Procerberus* or similar palaeoryctoid”. Based on the dental anatomy, McKenna (1975) introduced the order Cimolesta, which included Taeniodonta with Didelphodonta, Pantodonta and Apatotheria. Looking at the tarsals, Szalay (1977) placed taeniodonts in the Lepticticomorpha order; Leptictinae, Palaeoryctinae, Pantolestidae and Microsyopidae were also included. Szalay’s idea of “leptictimorph tarsals” is still a term used to describe the tarsals of many animals, including Taeniodonta. The “leptictimorph astragalocalcaneal morphology” is observed in the anatomy of the distal tibia and the tarsals and is associated with extreme plantar flexion and increased lateral stability in the tibial-astragalar joint (Szalay, 1977). Kielan-Jaworowska *et al.* (1979) suggested affinities of taeniodonts with *Cimolestes* and *Procerberus* based on dental similarities.

Schoch (1986) did a detailed study on Taeniodonta for his PhD thesis and several papers, naming new taxa and proposing new affinities. In 1981 Schoch and Lucas described a new smaller species of *Stylinodon* that they named *Stylinodon inexplicatus* (PU 16102). Many years later, Turnbull (2004) concluded that the smaller dental dimensions of the specimen (PU 16102), compared to *Stylinodon mirus*, is commonly seen in juvenile animals with extreme levels of hypsodonty. Therefore, the species of *Stylinodon inexplicatus* may no longer be valid. Schoch and Lucas (1981b) later introduced a new genus *Huerfanodon* included two species: *Huerfanodon torrejonius*, the type of the genus, and *Huerfanodon polecatensis*. The first species was based on two specimens of a partial skull and mandible (USNM 15412) from the Nacimiento Formation of the San Juan Basin, and another partial skull (MCZ 20181), from Rock Bench Quarry, Fort Union Formation, Wyoming. *H. polecatensis* is known only from a partial mandible (PU 14718). The later study of Schoch and Lucas (1981c) introduced a new species of *Conoryctella* from the San Juan Basin, *Conoryctella pattersoni* (NMMNH P-25056), a specimen of an almost complete mandible, part of the upper dentition and a portion of the forelimb. Schoch (1985;1981) also established two species for *Ectoganus*, with two subspecies each based on the crown morphology, primarily the level of hypsodonty and root development: *E. copei copei*, *E. copei bighornensis*, *E. gliriformis gliriformis*, and *Ectoganus gliriformis lobdelli*. Schoch (1986) mentioned these new taxa and hypothesised about their digging adaptations, and their coarse diet of roots and tubers, studied the biostratigraphy of taeniodonts and attempted to draw their phylogenetic relationships, but did not perform a numerical phylogenetic analysis. Later, Archibald (1993) used the phylogenetic relationships of taeniodonts proposed by Schoch (1986) as a case study of true extinction events.

Schoch (1986) also excluded a few taxa from Taeniodonta that were found outside of North America and placed them in Tillodontia. Some of these include *Basalina basalensis* (Dehm and Oettingen-Spielberg, 1958) found in the middle Eocene of Kuldana Formation, Pakistan and *Chungchienia sichuanica* (Chow, 1963) found in the upper Eocene of south Henan, China and *Lessnessina* from the early Eocene of Abbey Wood, UK. The latter was first described as a condylarth by Hooker (1979) based on the dental morphology. The upper molars of *Lessnessina* are very different from taeniodonts and they have a well-formed post-cingulum, typically minuscule or absent in Taeniodonta, as discussed thoroughly in chapter two.

Another observation by Schoch (1986), following Patterson (1949b), is the general rarity of taeniodonts in the fossil faunas. Patterson (1949b) believed this is due to their primarily small-sized populations, while Schoch (1986) suggested that taeniodonts lived in areas that were less likely to get fossilised, “away from the riverine floodplains”. The rarity of Taeniodonta in the fossil record was also raised by Coombs (1983) who included taeniodonts in her study about large, clawed mammals. Her comparative study associated taeniodonts with digging adaptations and their “unusual” dentition indicative of an abrasive diet.

Gingerich (1989), when describing the Eocene faunas of Wyoming, rejected the idea of subspecies for *Ectoganus* but argued there were four separate species. He also proposed that *E. copei* is more closely related to the *E. lobdeli* and *E. gliriformis* lineage. Rose *et al.* (2012) presented a new specimen of *Ectoganus* from Wyoming and followed Gingerich (1989)’s classification of four species and no subspecies.

A putative new species, known from an isolated lower molar that was found in the Eocene of Baixo Mondego, Portugal, was named *Eurodon silveirinhensis* by

Estravis and Russell (1992) and placed in a new subfamily, the Eurodontidae, belonging to Taeniodonta. In his review of Taeniodonta, Rose (2006) pointed out there is not enough evidence to support that connection. Indeed, the affinities of *Eurodon* to taeniodonts are not well-supported. The small size of *Eurodon*, the lack of at least some level of hypsodonty, the posteriorly extended talonid and the enlarged hypoconulid, are significant differences. Moreover, early Eocene taeniodonts had a much more complex dental anatomy on the lower teeth than *Eurodon*. In chapter two new specimens of lower molars of four Paleocene taeniodonts are described and they demonstrate different anatomy to the lower third molar, m3, of *Eurodon*. Therefore, the current analysis excludes *Eurodon silveirinhensis*.

Lucas and Williamson (1993) described a new genus, *Schochia* that was thought to be the sister taxon of the Stylinodontidae. *Schochia* was later named *Robertschochia* by Lucas (2011). McKenna and Bell (1997) listed Taeniodonta as a suborder within the order of Cimolesta and placed *Schochia* within Stylinodontidae. A new finding supported the idea of a relationship between Taeniodonta and Cimolesta: the partial skull with the upper dentition of a cimolestid that Eberle (1999) named *Alveugena carbonensis* found in the middle Puercan of the Ferris Formation, Hanna Basin, Wyoming. That study included the first-ever numerical phylogenetic analysis and included one member of taeniodonts, the early Puercan *Onychodectes*. Particularly, the results of that analysis showed *Alveugena* was a sister taxon to *Onychodectes*.

A few years later, a new specimen from the Late Cretaceous of Alberta, Canada was found, consisting of a partial skull and an almost complete mandible. Fox and Naylor (2003) described the specimen, assigning it to a new genus *Schowalteria*

clemensi and discussed anatomical features that point to stylinodontid affinities. Since *Schowalteria* was found in the Upper Cretaceous, if correctly identified as a taeniodont, it would be the oldest member of the group, pushing the origin of the clade before the Cretaceous-Palaeogene mass extinction. The next year Turnbull (2004) described the youngest (Bridgerian- Uintan) member of taeniodonts, *Stylinodon*, using specimens from the Washakie Formation, Wyoming, USA.

Rose (2006) in his book “The Beginning of the Age of Mammals”, using previous work included Taeniodonta, under Cimolesta and gave a brief review of the group. He addressed the possibility that the dental features of *Schowalteria* could be convergent with those of taeniodonts. Later Koenigswald *et al.* (2010) studied the enamel microstructure and dental wear patterns of *Stylinodon*. They concluded that the derived taeniodonts, *Ectoganus* and *Stylinodon*, had an abrasive diet. When it comes to the chewing mechanism, they proposed a “one-phase” orthal power stroke. The following year, Koenigswald (2011) studied the diversity of hypsodont teeth and categorised the hypsodont molars of *Stylinodon* as “enamel-band hypsodonty”. Most importantly he raised three major parameters for describing hypsodonty teeth, i.e. the extension of the ontogenetic phase, the degree of hypsodonty, and the type of wear.

There have been very few phylogenetic analyses for Taeniodonta. Rook and Hunter (2011) used some of the characters proposed by Schoch (1986) and Eberle (1999) to test the relationships within the group, at a generic level. A later study by Rook and Hunter (2013) followed, using the Wible *et al.* (2009) matrix and scoring *Schowalteria* and *Alveugena* to understand the affinities of taeniodonts with other mammals. Wible *et al.* (2009) focused on the early divergences of Eutheria and close groups, and so their phylogenetic matrix included many Cretaceous taxa and dental,

cranial and postcranial characters. The results of Rook and Hunter (2011) showed that *Schowalteria* is a basal taeniodont and *Alveugena* is the sister taxon of Taeniodonta. Clemens (2013) described a new specimen of *Wortmania*, from the lower Paleocene (Pu 2/Pu 3) of Montana, the first reported occurrence of a Puercan stylinodontid outside of the San Juan Basin. In his discussion, Clemens wrote a small overview of taeniodonts, using the phylogenetic tree produced by Rook and Hunter (2011). He also pointed out the need for more specimens to connect the Cretaceous and Palaeogene taxa.

Williamson and Brusatte (2013), when describing new specimens of *Wortmania*, revised the genus of *Robertschochia* (Lucas, 2011) from the Puercan of the San Juan Basin (type NMMNH P-9000), which was previously named *Schochia* by Lucas and Williamson (1993). In their study they synonymized *Robertschochia* with *Wortmania*. Williamson and Brusatte used the same matrix by Rook and Hunter (2011) and scored more characters using the new specimens of *Wortmania*. *Schowalteria* was found to be outside of Stylinodontidae in their results too. They were also the first to mention that digging adaptations are present in even the most basal taeniodonts such as *Wortmania* and *Onychodectes*.

Several workers recently have presumed taeniodonts to be members of Cimolesta. Taeniodonts were described as cimolestids in various recent studies of Cimolesta taxa, such as in Fox's (2015) study of the three new genera of "*Cimolestes*" and in Clemens (2017) study of *Procerberus*. However, *Schowalteria* is still considered an enigmatic taeniodont. Fox (2016) wrote a detailed paper on the scoring of the previous numerical phylogenetic studies of taeniodonts (Rook and Hunter, 2011; 2013; Williamson and Brusatte, 2013), pointing out the reasons why *Schowalteria* is a

stylinodontid. In a more inclusive phylogenetic analysis (Halliday and Goswami, 2016; Halliday *et al.*, 2019), only *Onychodectes* is used as a member of Taeniodonta. In chapter two, these phylogenetic studies are discussed in more detail.

Recent studies have also looked into the endocranial anatomy of Taeniodonta. Napoli *et al.* (2018) studied the brain and inner ear of *Onychodectes*. Their results show that *Onychodectes* had a brain similar to other eutherians, with big olfactory bulbs, possibly possessing a keen sense of smell. Bertrand *et al.* (2022) included taeniodonts in their analysis of the brain evolution of placental mammals. They found that the small brain volume of Paleocene mammals relative to their body sizes, including taeniodonts, is a result of their rapid increase in body size after the Cretaceous-Palaeogene mass extinction.

Outline of the present study

For this study, I visited the collections of the AMNH, YPM, USNM, and NMMNH&S and examined specimens of Taeniodonta. I also studied a variety of cimolestids and leptictids in the same museums. The current study includes new specimens found in the San Juan Basin, New Mexico, USA. The basin contains a very rich record of early Paleocene taeniodonts. Recent specimens are accompanied by precise geographic and stratigraphic data. The new specimens also provided much new information on the anatomy and allowed an examination of the phylogeny of Taeniodonta.

The second chapter describes some of the dental specimens found that belong to four genera of taeniodonts. These led to a better understanding of dental anatomy

and helped clarify some differences among the genera. Using these specimens as well as many specimens of taeniodonts and other Paleocene mammals from various museums in North America, I did a species-level phylogenetic analysis for Taeniodonta. This is the first attempt to understand the affinities within taeniodonts on a species level and includes dental, cranial and postcranial characters. The new dataset is based on the Shelley_2020 matrix, modified from Wible *et al.* (2009) and Shelley (2018), and new characters and taxa have been added. The new matrix was subjected to parsimony analysis, using the software TNT, to produce a phylogeny for taeniodonts that shows their in-group relationships. A time-calibrated analysis of a partial most parsimonious tree with the first and last appearances of the taxa, allowed an understanding of the timing of Taeniodonta evolution and their diversification. All the new information is also contributing to the broader concept of the evolution of placental mammals right before and after the end-Cretaceous mass extinction.

The third chapter of the thesis is focused on new postcranial elements from the San Juan Basin. These are described in detail, and compared with other taxa of Taeniodonta, potential relatives and a few other Palaeogene mammals. Based on associated dental elements, stratigraphic evidence, measurements, and observations, all the new postcranial elements described in that chapter are assigned to the genus *Conoryctes comma*. The skeleton of this genus was previously known only from a partial radius and incomplete humerus and manus. The new material helps reconstruct the skeleton of *Conoryctes* and indicates a small size variation within the genus. The postcranial elements were also studied for their functional anatomy, showing *Conoryctes* had digging adaptations.

Each chapter includes photographs of the specimens unless it is mentioned that these can be found in the Appendix. The references and appendices are placed at the end of the thesis, including tables of measurements and photographs of the specimens, as well as the time intervals and code used in R for the time-calibrated tree. The supplementary material includes the final phylogenetic matrix used and the synapomorphies found in the study.

CHAPTER 2

Systematics and phylogeny of Taeniodonta



Jay Matterenes, 1960
Bridger Basin in Wyoming during the Eocene, mural at the NMMNH&S

“...as complete and perfect a phylum as has ever been deciphered within the whole range of paleontology”

Jacob L. Wortman (1856-1926)

Introduction

Many researchers have worked on taeniodonts and there have been a few attempts to understand their phylogenetic affinities. The cladistic analysis in this chapter uses more anatomical characters than any previous phylogenetic studies and focuses on the interrelationships within Taeniodonta. Furthermore, the broad sample of fossil and extant mammals allows for a further evaluation of their phylogenetic position in the mammalian tree.

To fill the knowledge gap in the dental anatomy of taeniodonts new material from the San Juan Basin proved very useful. The San Juan Basin in New Mexico of the USA is an area where many early Paleocene taeniodonts have been found. Fieldwork done at different localities in the basin over the past years has recovered many new specimens. Moreover, the stratigraphy of the San Juan Basin is well-studied and so provided precise biostratigraphic information for the new specimens. Table 1 in the Appendix summarises the studied specimens and the localities in which they were found. These belong to the Geoscience Collections of the New Mexico Museum of Natural History and Science (NMMNH&S).

Part of the study in this chapter is based on these new specimens from the NMMNH&S. These specimens gave useful insight into the dental anatomy of five genera, *Onychodectes*, *Conoryctella*, *Conoryctes*, *Huerfanodon* and *Psittacotherium*. Observations on the dental anatomy of these specimens led to new phylogenetic characters that were added for this study, as described below.

Background on the affinities and phylogenetic analyses of Taeniodonta

Taeniodonta (Cope, 1876) has been considered a suborder by McKenna and Bell (1997), but is mostly viewed as an order of Cimolesta (Schoch, 1986; Rose, 2006; Rook and Hunter, 2013; Williamson and Brusatte, 2013). Their worn teeth and the rarity of some taxa in the fossil record are some of the reasons why their phylogeny remains unclear. Very early in their study, they were thought to be related to tillodonts (Cope, 1882a; Marsh, 1875; Osborn and Earle, 1895) due to their enlarged incisors, resembling the large canines of the taeniodonts.

Wortman (1896; 1897) demonstrated that the big teeth of taeniodonts are the canines, whereas tillodonts have big incisors. He also speculated that Taeniodonta, which he called Ganodonta, is a suborder of Edentata and related to ground sloths and armadillos. He also described evolutionary steps and highlighted that they form a “perfect and complete phylum”.

The theory that they are related to Edentata, was not accepted and Winge (1923) referred Ganodonta to the “Insectivora”. Later Simpson (1931) published a study on *Metacheiromys*, in which he proposed Taeniodonta have a common ancestor with the Palaeonodonta. Matthew (1937) recognised the order of Ganodonta but change the name back to Taeniodonta as it was originally proposed by Cope (1876). In his attempt to find affinities with other groups, Matthew (1937) recognised Taeniodonta as a separate order, related to palaeonodonts, Xenarthra and Pholidota. This was of course before it was clear that Xenarthra is not related to Pholidota (Springer *et al.*, 2003; Gunnell and Rose, 2008; O’Leary *et al.*, 2013). Matthew (1937)

pointed out again that Taeniodonta and Tillodontia share a common ancestor from a “proto-insectivore stock”.

One of the first substantial attempts to study the evolution of Taeniodonta is the work of Patterson (1949b). In his analysis, Patterson (1949b) studied the dental, cranial, and postcranial anatomy of the known taxa at length, noting the evolution of taeniodonts through time. He focused mainly on the changes in the canine, the skull and the foot of the two families (Figure 3). He also agreed with Matthew (1937) about taeniodonts originating in the Late Cretaceous from insectivore ancestors. Based on Patterson (1949b) the enlargement and the posterior buttress of the canine happened in the Puercan and Torrejonian to separate taxa like *Onychodectes* and *Wortmania*. These changes in the canine led to the specialisation of the jaw and the skull. Patterson (1949b) suggested that the changes in the manus, like the shortening of the metatarsals and the curved and laterally compressed claws, were rapid at first and then gradual in Stylinodontidae. Lastly, he commented, agreeing with previous workers, that the rarity of Taeniodonta in the fossil record is due to the rarity and isolated groups of them in the fauna of the Palaeogene.

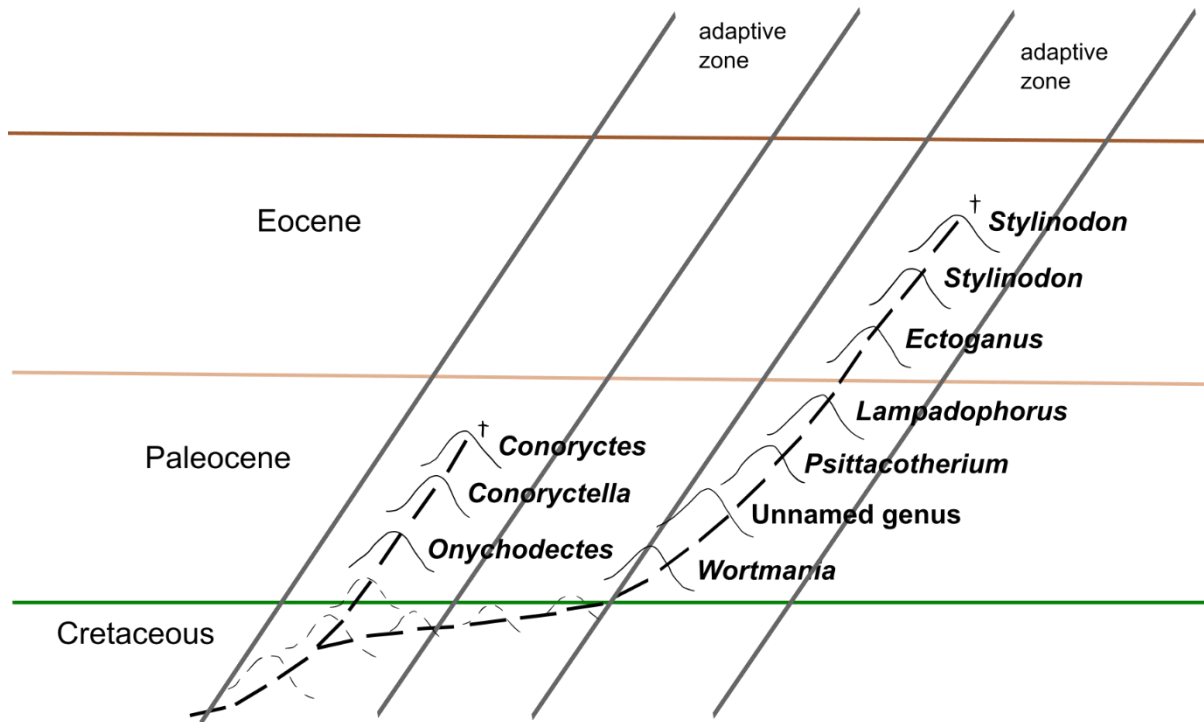


Figure 3: Drawing of the diagram seen in Patterson (1949b, figure 7) for the evolution of Taeniodonta. The bold dashed lines indicate phylogeny, the frequency curves represent known and inferred stages (dashed curves).

Later based on Patterson's (1949b) analysis of Taeniodonta, Lillegraven (1969) and McKenna (1969) proposed a connection of the group with "*Procerberus* or similar palaeoryctid". McKenna (1975), looking into the dental anatomy, proposed the order Cimolesta and included in there Taeniodonta with Didelphodonta, Pantodonta, and Apatotheria. Based on the study on the tarsals Szalay (1977) put taeniodonts in the Lepticticomorpha order which included Leptictinae, Palaeoryctinae, Pantolestidae, and Microsypidae, in the Glires cohort which included the order of Rodentia and Lagomorpha. In the same group of "Infraclade Eutheria", there is the "?Edentata cohort" including the orders of Palaeonodonta, Xenarthra, and Pholidota. Szalay's idea that primitive taeniodonts have "leptictimorph tarsals" is still accepted by researchers, and evidence of this can be seen further in chapter three, where the tarsals of

Conoryctes are described and compared to other taeniodonts and a variety of Palaeogene mammals.

Robert Schoch worked on taeniodonts for several years as part of his PhD dissertation. He introduced a few new species, and he was among the first to attempt a cladistic analysis using the anatomical features of these animals. Although it is not a numerical phylogenetic analysis based on parsimony, he followed in Patterson's footsteps, looking into the anatomy first and then the evolutionary patterns of the group. Schoch (1986) proposed in his cladogram that Taeniodonta was divided among two families: the Conoryctidae including the genera *Onychodectes*, *Conoryctella*, *Conoryctes*, and *Huerfanodon*, and the Stylinodontidae including *Wortmania*, *Psittacotherium*, *Ectoganus* and *Stylinodon*. Schoch (1986) suggested that the ancestor of taeniodonts was a *Procerberus*-like animal. Later, Archibald (1993) used that cladogram and plotted biostratigraphy data to it as a case study for his work.

Schochia sullivanii (Lucas and Williamson, 1993), a genus that was later changed to *Robertschochia* (Lucas, 2011) and then made a junior synonym of *Wortmania* (Williamson and Brusatte, 2013), was proposed to be the sister taxon to the Stylinodontidae. A study that followed after the new genus of *Schochia*, by McKenna and Bell (1997) found Taeniodonta as a suborder within the order of Cimolesta, which was in the Grandorder of Ferae that included the other suborders of Didelphodonta, Apatotheria, Tillodontia, Pantodonta, Pantolestia, Pholidota and Ernanodontia. A few years later, a specimen from the Hanna Basin in Wyoming was found including the upper palate and dentition of a new animal, *Alveugena carbonensis* (Eberle, 1999). In that study, the similarities with primitive taeniodonts such as *Onychodectes* were discussed and a phylogenetic analysis using the PAUP

software was conducted. This is the first time a numerical analysis was applied to taeniodonts and possible outgroup taxa. The analysis used 15 dental characters, scored for *Procerberus formicarum*, *Procerberus grandis*, *Alveugena carbonensis*, and *Onychodectes tisonensis*, with *Cimolestes* spp., as the outgroup. The phylogenetic analysis recovered *Alveugena carbonensis*, a cimolestid, as the sister taxon to Taeniodonta.

After a few years, a new specimen from Red Deep River Valley, in Alberta, Canada was found and assigned to *Schowalteria clemensi*, a new genus of Stylinodontidae (Fox and Naylor, 2003). It consists of an almost complete mandible, rostrum, and upper dentition. The upper and lower anterior teeth (canine, premolars) are better preserved than the posterior teeth (molars). What is perhaps most interesting about this specimen is that it dates to the Late Cretaceous. If the assertions that it is a taeniodont are true, this would push back the proposed origin of Taeniodonta before the Cretaceous-Palaeogene mass extinction, especially because the Stylinodontidae family was considered to be, in many ways, more derived than the members of the Conoryctidae. According to Fox and Naylor (2003), *Schowalteria* shows characteristics such as the restricted enamel on the canines, and the “posterior buttress” of the lower canine, which are seen in stylinodontids. Therefore, if *Schowalteria* is a stylinodontid, the split of the two families must have happened before the Cretaceous-Palaeogene extinction. In that way, taeniodonts became a valuable group in understanding the diversification of eutherian mammals, as described in the Introduction chapter.

However, Fox and Naylor (2003) used only anatomical observations to assign the new specimen to Stylinodontidae, rather than phylogenetic analyses. Among the

first studies that used *Schowalteria* in a phylogenetic analysis was Weinstein (2009). Later these phylogenetic and stratocladistic analyses were published by the same team (Rook and Hunter, 2011) using a matrix of 37 dental characters -some of which were ordered-, that combined the anatomical observations of Schoch (1986) and the analysis of Eberle (1999). They also scored other taxa such as *Cimolestes*, *Procerberus formicarum*, *Procerberus grandis* and *Alveugena* as “taeniodont Ancestors”. Their results showed that *Schowalteria* is not a stylinodontid but rather the most basal taeniodont. They questioned the restriction of the enamel as an anatomical feature and pointed out that it could be due to breakage. The distribution of the enamel, or the “level of hypsodonty” are features I am also very sceptical about in the current study, discussed later in this chapter. Rook and Hunter (2011) also addressed other features that point to *Schowalteria* as not a stylinodontid using *Onychodectes* and *Conoryctella* for comparison and proving that they also shared some of the supposed stylinodontid features mentioned by Fox and Naylor (2003). This strengthened their phylogenetic results that *Schowalteria* shares features with both families since it is the most basal taeniodont. Because *Schowalteria* has derived characters that are not seen in *Wortmania*, Rook and Hunter (2011) questioned whether Taeniodonta is a monophyletic clade if *Schowalteria* is a stylinodontid. This was not something proposed by Fox and Naylor (2003) and is not implied by the stratigraphic gap between the two clades.

In Rook and Hunter (2011), Taeniodonta is divided into two clades: the Conoryctidae with taxa of *Conoryctes*, *Conoryctella* and *Huerfanodon*, excluding *Onychodectes*, and the Stylinodontidae with *Wortmania*, *Schochia*, *Psittacotherium*, *Ectoganus* and *Stylinodon*. A few years later they performed the same analysis and found the same results for the inner group relationships (Rook and Hunter, 2013).

They added more taxa of cimolestids such as *Didelphodus*, *Acmeodon*, *Aaptoryctes*, and *Palaeoryctes* with *Protictis* as the outgroup. In order to examine the relationships of Taeniodonta with other eutherian taxa, Rook and Hunter (2013) performed an analysis including only the taxon of *Schowalteria* as a representative of Taeniodonta. For this, they used the Wible *et al.* (2009) matrix and the taxa included in it. This was the first attempt to check the positions of Taeniodonta in the mammalian tree using phylogenetic characters and computed methods. The Wible *et al.* (2009) matrix has 408 dental, cranial as well as postcranial characters of 69 taxa aiming at understanding the phylogeny of extinct eutherians.

Their results (Rook and Hunter, 2013) are similar to Rook and Hunter (2011) and show *Schowalteria* as a basal taeniodont, *Onychodectes* is the sister taxon to Stylinodontidae, and *Alveugena* is the sister taxon of Taeniodonta. *Alveugena* is more closely related to *Cimolestes* than to *Procerberus* in that study. They also found that in the phylogenetic analysis that included other mammalian taxa, taeniodonts are stem placentals. One of the points they addressed again was the monophyletic group of Taeniodonta and that *Schowalteria* is not a stylinodontid. Combining this and the position of taeniodonts they concluded that stem placentals were diversifying in the Palaeogene. An erratum followed (Rook and Hunter, 2013b) that corrected some of the scorings and gave the correct name of *Robertschochia* (Lucas, 2011) to *Schochia*. The topology produced after these corrections was the same as in their previous paper (Rook and Hunter, 2013).

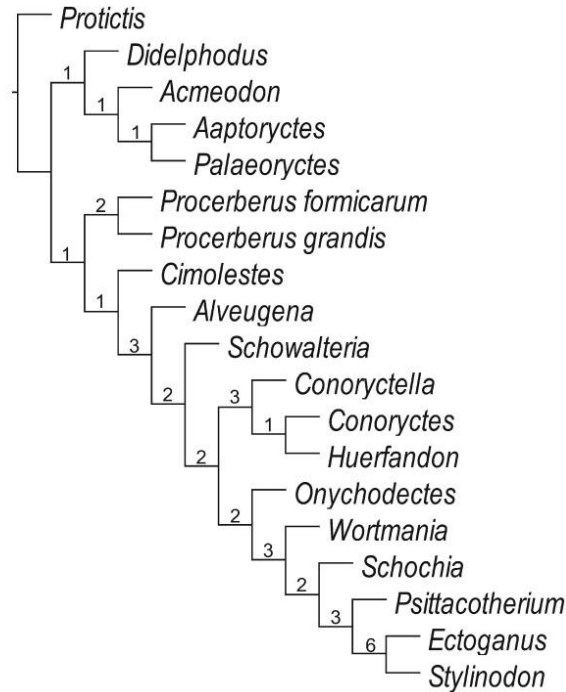


Figure 4: Phylogenetic tree by Rook and Hunter (2013, figure 1) with Bremer support values.

Based on the matrix of 37 characters from Rook and Hunter (2011), another study was conducted by Williamson and Brusatte (2013). In that paper, new specimens of the genus *Wortmania* were found that led to redescribing the genus and synonymising *Robertschochia* with *Wortmania*. Williamson and Brusatte (2013) obtained substantially different results. *Schowalteria* was still the most basal taeniodont, but *Onychodectes* was found more basal and not a sister taxon to Stylinodontidae. The Conoryctidae was a monophyletic clade, however, when using unordered characters *Conoryctes*, *Conoryctella* and *Huerfanodon* formed a polytomy. Similarly, there is a polytomy formed with *Wortmania*, *Psittacotherium* and an *Ectoganus* + *Stylinodon* clade when characters are unordered. Based on the authors, these polytomies would be resolved when adding new characters and taxa to the analysis. Williamson and Brusatte (2013) were also the first researchers to suggest

that based on the postcranial features, there was at least some degree of digging behaviour to all taeniodonts.

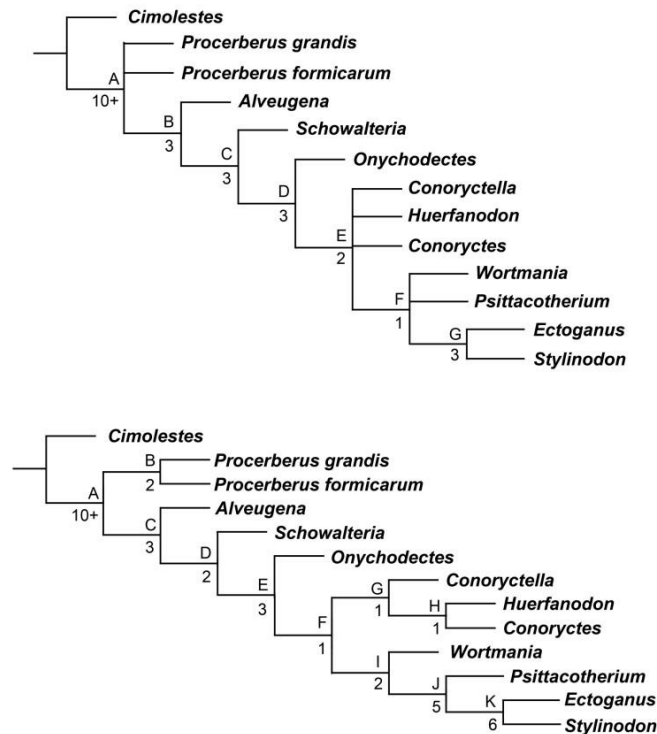


Figure 5: Phylogenetic trees by Williamson and Brusatte (2013, figure 14) with Bremer support values shown on the nodes. Unordered characters are used for the tree on the top and ordered for the tree at the bottom.

A review of these studies (Rook and Hunter, 2013; 2013b; Williamson and Brusatte, 2013) followed by Fox (2016), in which he gave detailed criticism on the scoring of the taxa and the interpretation of the results. He pointed out that Taeniodonta has always been considered a monophyletic clade, and the presence of a stylinodontid, *Schowalteria* in the Late Cretaceous does not imply otherwise. Instead, it extends the stratigraphic range of Stylinodontidae, and Taeniodonta, and implies that there is a ghost lineage of more primitive taeniodonts which are not found yet. Fox (2016) strongly highlighted again that regardless of the two previous

phylogenetic analyses, *Schowalteria* is a stylinodontid and blamed the lack of such characters in the matrix to help place it near that clade. He also pointed out that the authors of both studies have not seen the specimen in person, and therefore should not be dismissive of the anatomical evidence pointing to Stylinodontidae.

Fox (2016) also pointed out that *Onychodectes*, having insectivore-like features seen in the skull proportions and anatomy should be considered a basal taeniodont and not just basal to Stylinodontidae. Lastly, one other argument Fox (2016) raised was the use of a “wastebasket” as an outgroup. To avoid this, in the current study the three genera of *Altacreodus*, *Ambilestes*, and *Scollardius* are scored, following Fox (2015).

The relationship of *Schowalteria* to taeniodonts is key to understanding the origin of Taeniodonta and its diversification. As pointed out by Clemens (2013; 2017), if taeniodonts are closely related to *Alveugena* and *Procerberus*, then these lineages had arisen before the late Cretaceous. Moreover, the appearance of cf. *Wortmania*, a Paleocene taeniodont, in Montana, indicates that maybe taeniodonts originated outside of the Western Interior (Clemens, 2013).

In a broader scope, the diversification of Taeniodonta can help better understand the radiation of eutherians. In a recent study about the evolution of Eutheria from the Cretaceous and Palaeogene, *Onychodectes* was included instead of *Schowalteria* as a representative of taeniodonts (Halliday and Goswami, 2016). In that analysis, *Onychodectes* is found to be the sister taxon to *Escavadodon*, close to taxa *Wyolestes*, and *Leptacodon*. The most interesting feature of that analysis is that *Onychodectes* is found within Placentalia, rather than a stem taxon of Placentalia. In the following analysis by the same team (Halliday *et al.*, 2019), in the consensus tree

of 248 taxa scored for 748 characters, *Onychodectes* is not only found as the sister taxon to *Escavadodon*, but they form a group that is related to *Palaeonodon*, *Tubulodon* and a *Eurotamandua-Eomanis* group. The Halliday *et al.* (2019) study also suggests that late stem and early crown placentals may not show a lot of anatomical differences, making it more difficult to identify members of the crown Placentalia in the Cretaceous fossil record. A similar analysis trying to understand the radiation of placental mammals was conducted by O'Leary *et al.* (2013), but it did not include any Taeniodonta and just a few cimolestids and leptictids. As mentioned earlier, in the study of the PalM group, I have scored some genera of Taeniodonta. Since that matrix is bigger, with more characters and taxa, and includes genomic data, it will be more valuable to explain the position of taeniodonts in the mammalian tree. The focus of the current study is the group's interrelationships and secondarily to explain their affinities with potential close relatives of Taeniodonta.

One conclusion that can be drawn from the previous studies, that aimed to understand the relationships of taeniodonts over the past one hundred years, is the necessity of new specimens. All these researchers were considering the specimens and means available to them and gave justifiable examples of their reasoning. Similarly, my attempt to understand the inter phylogeny on a species level of Taeniodonta is based on the information and specimens available to me. Contrary to previous studies that scored only dental characters for taeniodonts, the matrix of the current thesis uses cranial and postcranial characters. Using the phylogenetic characters that were scored only for the characters with strong evidence, I conducted the following phylogenetic analysis.

Methods

Measurements of the new dental specimens were made using digital callipers to the nearest two decimals and are provided in the Appendix (tables A2-A4). When needed, digital measurements were taken using the software ImageJ 1.6.0 (Schneider *et al.*, 2012). The teeth were coated with magnesium oxide before photographing them. Photos of all the studied specimens were taken with a Nikon D3500 camera and an 18-55mm lens or a 105mm macro lens. I used a photo stacking technique using Helicon Focus 8.0.4. The photos were later edited, using the Inkscape 0.92.3 software.

Basic terminology

This chapter uses the cusp nomenclature by Szalay (1969) and Williamson *et al.* (2014) for the dental anatomy. Figures 6 and 7 follows Szalay (1969) and includes some additional anatomical features on the upper (Figure 6) and lower teeth (Figure 7). Following the dental formula by O'Leary *et al.* (2013, figure 3), I am referring to the first and second premolars (upper/lower) as P1/p1 and P2/p2 respectively. The P3/p3 is seen in basal eutherians as a retained deciduous tooth (not seen in taxa studied), whereas I am using the terminology P4/p4 for the penultimate molar, and P5/p5 for the ultimate premolar O'Leary *et al.* (2013).

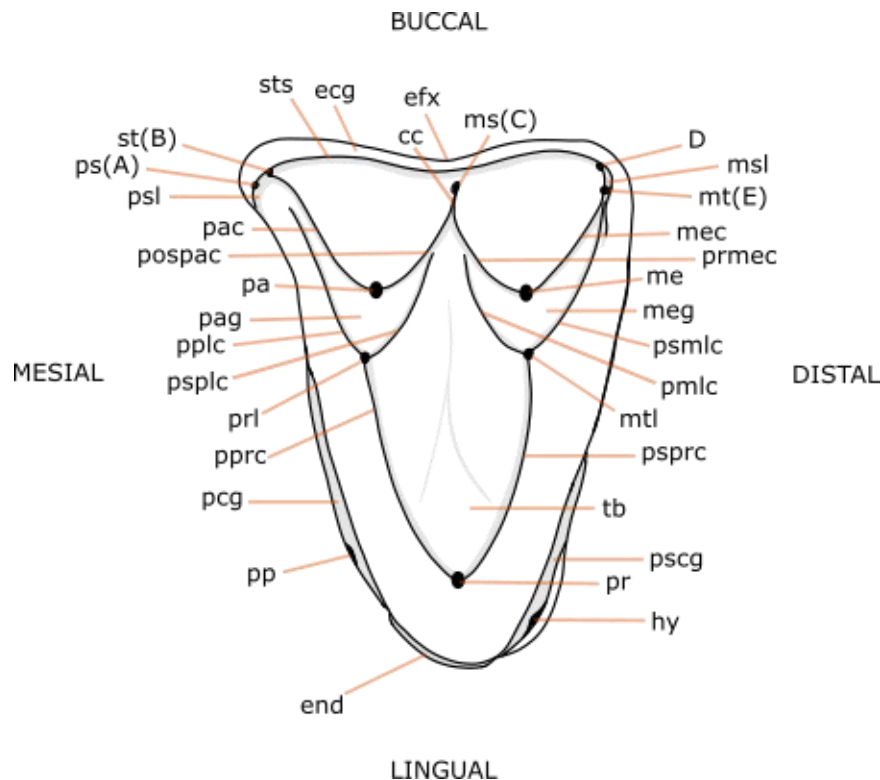


Figure 6: Line drawing of the upper molar cusp nomenclature used, based on Szalay (1969) and Williamson *et al.* (2014).

cc: centrocrista (postparacrista & premetacrista)

D: D cusp

ecg: ectocingulum

efx: ectoflexus

end: endocingulum

hy: hypocone

me: metacone

mec: metacrista (postmetacrista)

meg: metacingulum

ms: mesostyle (C cusp)

msl: metastylar lobe

mt: metastyle (E cusp)

mtl: metaconule

pa: paracone

pac: paracrista (preparacrista)

pag: paracingulum

pcg: precingulum

pmlc: premetaconule crista

pospac: postparacrista

pp: protostyle (pericone)

pplc: preparaconule crista

pprc: preprotocrista

pr: protocone

prl: paraconule

prmec: premetacrista

ps: parastyle

pscg: postcingulum

psl: parastylar lobe

psmlc: postmetaconule crista

psplc: postparaconule crista

psprc: postprotocrista

st: stylocone (B cusp)

sts: stylar shelf

tb: trigon basin

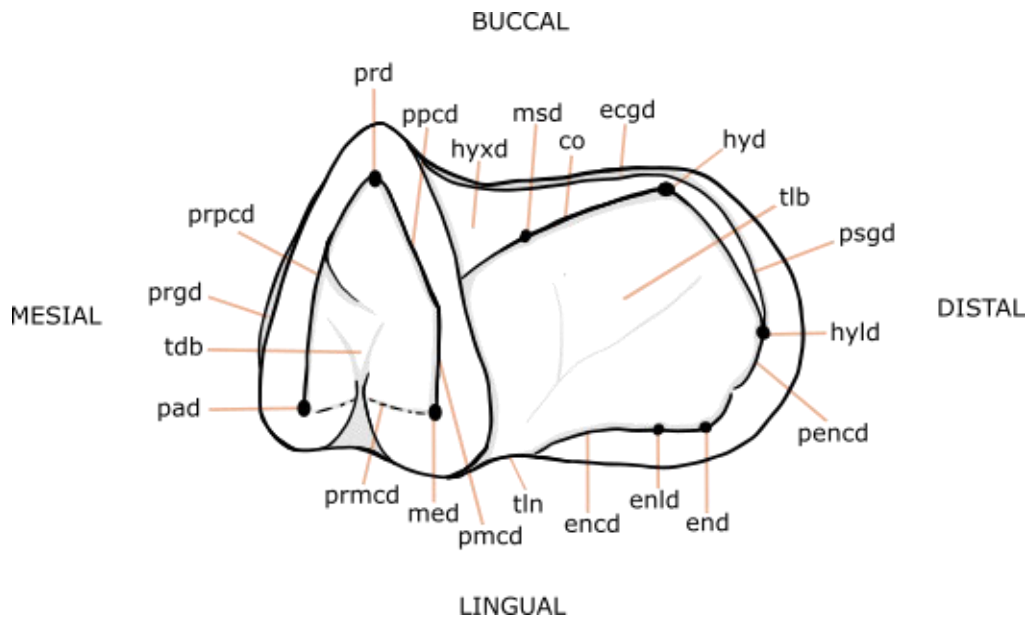


Figure 7: Line drawing of the lower molar cusp nomenclature used, based on Szalay (1969) and Williamson *et al.* (2014).

- co: cristid obliqua
- ecgd: ectocingulid
- encd: entocristid
- enld: entoconulid
- end: entoconid
- hyd: hypoconid
- hyl: hypoconulid
- hyxd: hypoflexid
- med: metaconid
- msd: mesoconid
- pad: paraconid
- pencd: postentocristid
- pmcd: postmetacristid
- ppcd: postprotocristid
- prd: protoconid
- prgd: precingulid
- prmcd: premetacristid
- prpcd: preprotocristid
- psgd: postcingulid
- tdb: trigonid basin
- tlb: talonid basin
- tln: talonid notch

Taxonomic sampling

The current study uses the Wible *et al.* (2009) matrix that was modified by Shelley (2018, PhD dissertation) and Shelley (2020, modified version of Shelley 2018). I will refer to it as the Shelley_2020 matrix in the text. In that dataset there are 172 taxa scored for 617 characters, mostly focused on resolving the relationships within Periptychidae. Periptychidae is another enigmatic Paleocene group of mammals and so the Shelley_2020 matrix contains a lot of characters and taxa essential for the scope of the current study.

Following Wible *et al.* (2009), *Nanolestes* is set *a priori* as the outgroup, rooting the tree. The matrix (supplementary file_S1) was built using the online platform Morphobank (O'Leary and Kaufman, 2012). Some taxa were excluded from Shelley_2020 and others were added for the purpose of my study.

Since they are outside of the scope of this study, I excluded many of the “condylarths” from the Shelley_2020 matrix, such as *Oxyacodon apiculatus*, *Oxyacodon archibaldi*, *Oxyacodon ferronensis*, *Oxyacodon josephi*, *Oxyacodon marshater*, *Oxyacodon priscilla*, *Pleuraspidotherium*, *Ectoconus symbolus*, *Paleoungulatum hooleyi*, *Tinuvial eurydice*, *Maiorana ferrisensis*, *Mimatuta makpialutae*, *Mimatuta morgoth*, *Mithrandir oligistus*, *Mithrandir onostus*, *Goleroconus alfi*, *Haploconus elachistus*, *Conacodon cophater*, *Conacodon delphae*, *Conacodon harbourae*, *Conacodon kohlbergeri*, *Conacodon matthewi*, *Anisonchus willeyi*, *Auraria urbana*, *Carsioptychus coarctatus*, *Ampliconus antoni*, *Anisonchus athelas*, *Anisonchus eowynae*, *Anisonchus fortunatus*. I also excluded *a priori* *Lainodon* and *Sheikhdzheilia* since they were scored for fewer than 100 characters, out of the 630

characters of the final matrix. As mentioned in Shelley (2018), *Didelphodus altidens* is a problematic taxon that needs rescoring, for this, I excluded it *a priori*. Following Fox (2015), I replaced *Cimolestes* with the three new genera formerly considered to be species of *Cimolestes*, *Ambilestes cerberoides*, *Scollardius propalaeoryctes*, and *Altacreodus magnus*.

Palaeogene taxa

The taxa added to this study are known cimolestids such as *Ambilestes cerberoides*, *Scollardius propalaeoryctes*, *Altacreodus magnus*, *Palaeoryctes*, *Pantolestes*, *Puercolestes simpsoni* and the cimolestids that are potentially close relatives (Rook and Hunter, 2013; Williamson and Brusatte, 2013) to Taeniodonta *Alveugena carbonensis*, *Procerberus sp. cf. P. grandis* and *Procerberus formicarum*. Since Leptictida shares similar tarsal anatomy with Taeniodonta and they are another enigmatic group (Szalay, 1977), I scored in the matrix *Prodiacodon puercensis* and *Prodiacodon crustulum*. In a few phylogenetic analyses on early mammals, *Onychodectes* is the sister taxon to *Escavadodon zygus* (Halliday *et al.*, 2016; 2019). I also noticed a few similarities with taeniodonts and therefore added this animal to the dataset. Here is information on the taxa, the publications, and the specimens used in the current study.

Ambilestes cerberoides (Lillegraven, 1969)

(=*Cimolestes cerberoides*, Fox, 2015)

Lectotype: UALVP 2973, partial left maxilla with P4, P5, M1, M2

Type locality: KUA-1, Griffith Farm, Red Deer River Valley, Alberta

Age: Lancian

Distribution: Lower Scollard Formation, Alberta; Hell Creek Formation, Montana

Sources: Illustrations and text in Fox (2015)

Scollardius propalaeoryctes (Lillegraven, 1969)

(=*Cimolestes propalaeoryctes*, Fox, 2015)

Holotype: UALVP 3756, partial right dentary with two incisors, c, p1-5, m1-3

Type locality: KUA-1, Griffith Farm, Red Deer River Valley, Alberta

Age: Lancian

Distribution: Lower Scollard Formation, Alberta; Hell Creek Formation, Montana

Sources: Illustrations and text in Fox (2015)

Altacreodus magnus (Clemens and Russell, 1965)

(=*Cimolestes magnus*, Fox, 2015)

Holotype: UALVP 622, left dentary with p4, m1-3

Type locality: KUA-1, Griffith Farm, Red Deer River Valley, Alberta

Age: Lancian

Distribution: Lower Scollard Formation, Alberta; Lance Formation, Wyoming; Hell Creek Formation, Montana; Hell Creek Formation, North Dakota; Frenchman Formation, Saskatchewan

Sources: Illustrations and text in Fox (2015; 2016), specimens AMNH 105157, AMNH 128544

Palaeoryctes (Matthew, 1913)

(scored for both species *P. punctatus* and *P. jepseni*)

Holotype: *P. punctatus* AMNH 15850, maxillary fragment with M1-3; broken P5-M2 and M3; distal left humerus, proximal ulna

P. jepseni UM 109156, right alveoli of c, p2 and p4-m3

Type locality: SC-I02 (?) Fort Union Formation, Park County, Wyoming, Clarks Fork Basin, Montana

Age: Middle and late Tiffanian of western North America (Ti-4, Ti-5)

Middle to late Clarkforkian land-mammal age (Cf-2, Cf-3)

Sources: Illustrations and text in Bloch *et al.* (2004)

Pantolestes (Cope, 1872)

(=*Anisacodon*, Marsh, 1872, *Passalacodon*, Marsh, 1872)

(mostly scored for *P. longicaudis*)

Holotype: AMNH 5142, left p4, m1, m2 and m3, associated postcranial elements

Type locality: Lower Bridger Station, Wyoming

Age: early middle Eocene

Sources: Illustrations and text in Dunn and Townsend (2019), Dorr (1977), Szalay (1977)

Puercolestes simpsoni (Reynolds, 1936)

Holotype: UCMP 36658, partial skull with left roots of C-P4, P5-M1, right roots of C-P4, P5, M1-3

Type locality: Fossil Zone A, From the De-na-zin Wash area, San Juan Basin, New Mexico

Age: Puercan (Pu2)

Sources: Illustrations and text in Williamson *et al.* (2011), Clemens (2019)

Alveugena carbonensis (Eberle, 1999)

Holotype: UW 26559, right I2, broken C, P1, P2, P5, M1-3 and left I2, C, P1-P5, M1-3 and partial cranium with fragments of nasals, frontals, turbinals, vomer, palatine, lacrimal and premaxillae and maxilla

Type locality: UW locality V-91005, upper Ferris Formation, western Hanna Basin, Wyoming

Age: early- middle Puercan (Pu2)

Sources: Illustrations and text in Eberle (1999)

Note: The partial mandible described in Rook and Hunter (2011) referred to this taxon is not scored in the current analysis, since it is dubious if it belongs to *Alveugena*.

Procerberus formicarum (Sloan and van Valen, 1965)

Holotype: UMVP 1460, fragmentary dentary with p4, p5 and m1

Type locality: Bug Creek Anthills locality in western McCone County, northeast Montana

Age: early Puercan (Pu1)

Sources: Illustrations and text in Clemens (2017) and specimen AMNH 96358

Procerberus sp. cf. P. grandis (Middleton and Dewar, 2004)

Referred specimens: UCMP 137189, fragmentary maxillary with P4-M3, UCMP 150024, fragment of a lower molar

Type locality: UCMP V77136, Tullock Member, Fort Union Formation, Wyoming

Age: early Puercan (Pu1)

Sources: Illustrations and text in Clemens (2017) and specimen AMNH 118024

Prodiacodon puercensis (Matthew, 1929)

(=*Diacodon (Palaeolestes) puercensis*, Matthew and Granger, 1918)

Holotype: AMNH 16011, partial skeleton

Type locality: Torrejon, San Juan Basin, New Mexico

Age: late Torrejonian to late Tiffanian

Sources: Illustrations and text in Gunnell *et al.* (2007) and specimens AMNH 100318, AMNH 100658, AMNH 100831, AMNH 87708, NMMNH P-72176

Prodiacodon crustulum (Novacek, 1977)

(=*Palaeolestes*, Matthew and Granger, 1918)

Holotype: UCMP 114990 left upper molar (M1 or M2)

Type locality: Biscuit Springs, Tullock Formation, Montana

Age: early Puercan (Pu1)

Sources: Illustrations and text in Clemens (2015)

Escavadodon zygus (Rose and Lucas, 2000)

Holotype and referred specimens: NMMNH P-232, right upper molar (M1 or M2), NMMNH P-567, left p4; NMMNH P-679, left p5; NMMNH P-2489, left m1; NMMNH P-1901, left m2; and NMMNH P-2401, right m3

Type locality: NMMNH locality 2708, Escavada Wash, Sandoval County, New Mexico

Age: late Torrejonian

Sources: Illustrations and text in Rose and Lucas (2000) and NMMNH P-22051 postcranial elements including

Taeniodonta

The aim of this chapter is the interrelationships of Taeniodonta, and after a careful study of their anatomy, there needs to be an updated revision of the taxa. The following pages use previous diagnoses (Schoch, 1986; Gingerich, 1989; Fox and Naylor, 2003; Williamson and Brusatte, 2013) on the genera of taeniodonts and added with new observations. The sources of information for scoring these taxa are also reported. Based on the new diagnoses the new dental specimens from the San Juan Basin are also assigned to genera. A short description of some of the new specimens follows, and there are photos of all the new specimens, as well as measurements of all the specimens, in the Appendix (tables A2-A4, figures A1-A22).

Schowalteria (Fox and Naylor, 2003)

Distribution: KUA-1, Griffith's Farm, Scollard Formation, Red Deep River Valley, Alberta

Diagnosis: as in Fox and Naylor, 2003

Schowalteria clemensi (Fox and Naylor, 2003)

Holotype: RTMP 93.90.01 incomplete skull with right C, P1-P5, M1, M2 partial mandible with right c, p1-p5, m1-m3, left p4, m2

Type locality: *same as genus*

Distribution and Diagnosis: *same as genus*

Sources: Illustrations and text in Fox and Naylor (2003), Fox (2016), specimen RTMP 93.90.01

Onychodectes (Cope, 1888)

Distribution: Puercan (Pu1, Pu2) of New Mexico and Utah

Revised Diagnosis: small taeniodont, upper molars moderately hypsodont; three incisors; P5 with a protocone, paracone and incipient metacone, parastyle, stylocone and metastyle; upper molars have pre- and postcingula minuscule to absent; lower molars bear a long trigonid and the talonid has a high hypoconid, entoconid and a hypoconulid; entoconids distolingually to hypoconid, presence of mesoconid varies, minuscule mesiolingual cingulid; mandibular angular process on the same level as the vertical level of the condyloid process

Onychodectes tisonensis (Cope, 1888)

(=*Onychodectes tisonensis* Cope, 1888

Onychodectes tisonensis Matthew, 1937

Onychodectes n. sp.? Robison and Lucas, 1980

Onychodectes tisonensis tisonensis Schoch, 1981b)

Holotype: AMNH 3405, right and left maxillae with P5-M3, left m2, associated right astragalus

Type locality: Puercan strata, Nacimiento Formation, San Juan Basin, New Mexico

Distribution and Diagnosis: *same as genus*

Sources: Illustrations and text in Schoch (1986), Matthew (1937), specimens AMNH 16410, AMNH 785, AMNH 3405, AMNH 16528, AMNH 3411, AMNH 3406, USNM

15536, AMNH 36070, AMNH 16411, AMNH 16410, AMNH 3411, AMNH 16405, AMNH 16408, AMNH 16528, AMNH 3404, AMNH 3576a

Comments: The subspecies *O. tisonensis rarus* was used to describe specimens with better developed “internal accessory cusp” which is placed further buccally to the cristid obliqua. In general, this study is not down to the subspecies level, and so *O. tisonensis rarus* is not scored.

New specimens: NMMNH P-46299, NMMNH P-63948 (NMMNH P-47450, NMMNH P-81239 in the Appendix)

New specimen NMMNH P-46299 (Figure 8) from the L-8348 locality, “Taeniolabis zone,” De-na-zin Wash (Pc2), consists of a partial left mandible with a few damaged lower teeth. The p1, p2 are broken off, and so are the mesial cusp of the p4. The lower p5 is almost complete, while m1 is missing the mesial end of the trigonid and m2 the distal end of the talonid. There is a mental foramen under the p4 on the buccal side of the mandible. Although the specimen is damaged, the small cuspids distally on the p4, the mesial cingulid on p5, and the prominent paraconid and its paracristid on the m2, are characteristics seen in other specimens of *Onychodectes*. Specimen NMMN P-46299 resembles the partial jaw of *O. tisonensis*, particularly with specimen AMNH 16409, in the lower premolars. For all these reasons it is assigned to *O. tisonensis*.

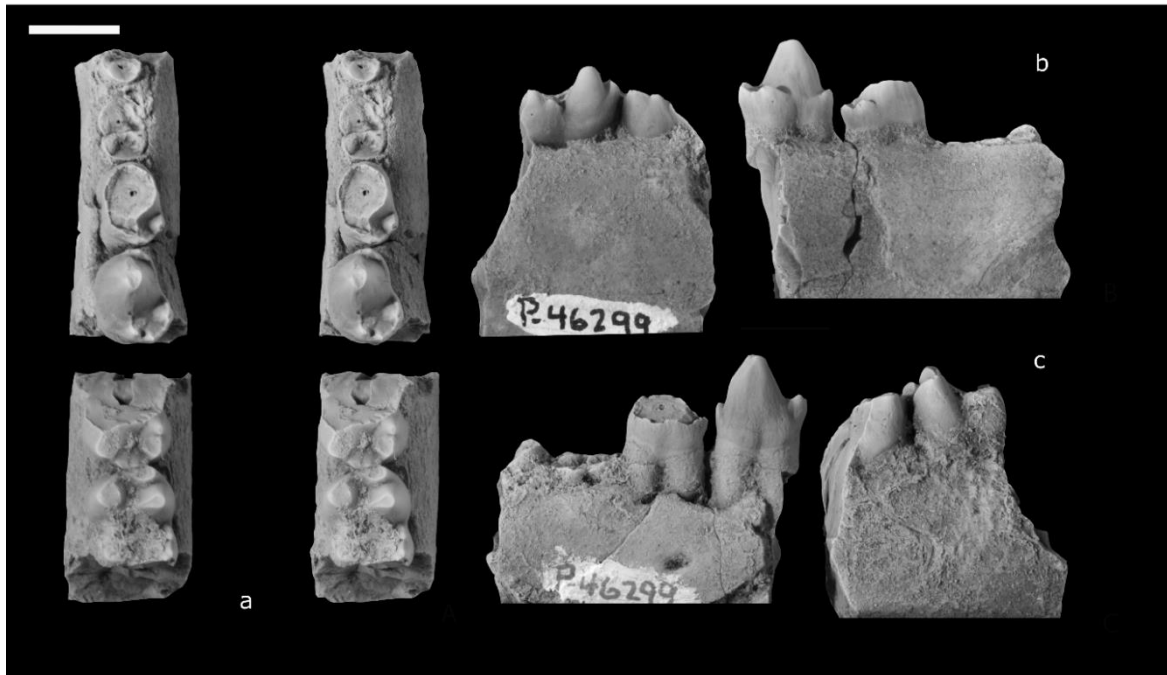


Figure 8: Specimen NMMNH P-46299 of *Onychodectes tisonensis* in occlusal (a), lingual (b) and buccal (c) views. Photos were taken by Thomas Williamson, edited by me. The teeth that are not damaged are p5 and m2. Scale bar is 1cm.

Specimen NMMNH P-63948 was found in locality L-8348, Taeniolabis zone, in the De-na-zin Wash (Pc2) and is a partial right mandible with p1, p4, m2 and the roots in place of the mandible of the right canine, p2, p5, m1 and m3. There are roots for two incisors; a small mesial one and a larger lateral one. Looking at the anatomy of the m2, and its resemblance with other specimens, such as NMMNH P-47450 (Appendix, Figure A1). NMMNH P-63948 is also assigned to *Onychodectes tisonensis*.

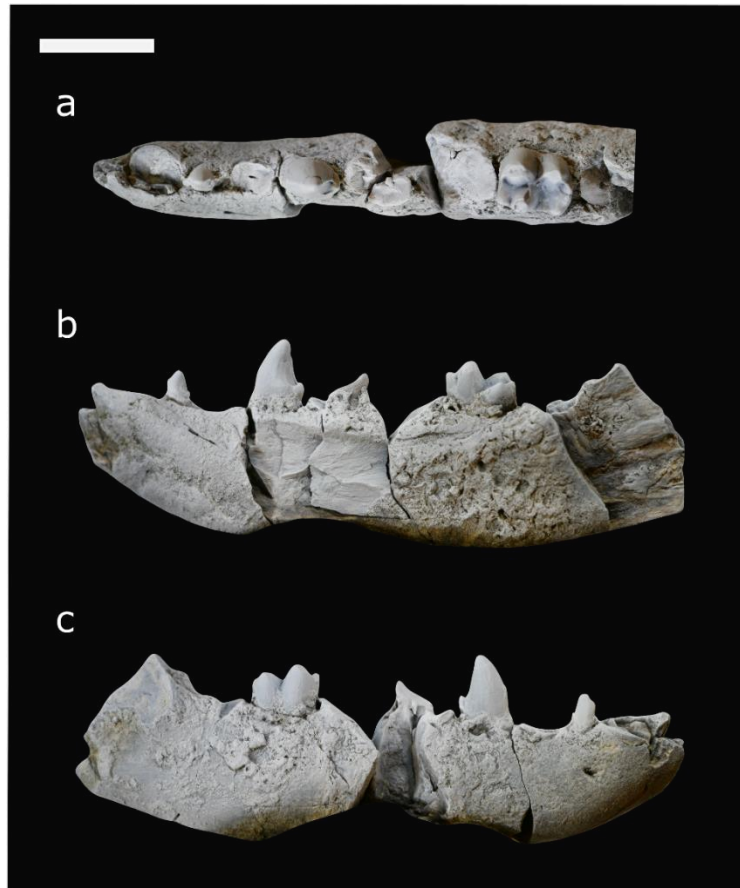


Figure 9: Specimen NMMNH P-63948 of *Onychodectes tisonensis* in occlusal (a), lingual (b) and buccal (c) views. Photos were taken by Thomas Williamson, edited by me. The teeth that are not damaged are p1, p4 and m2. Scale bar is 1cm.

Wortmania (Hay, 1899)

(=*Hemiganus* Wortman, 1897

Wortmania Hay, 1899

Wortmania Matthew, 1937

Schochia Lucas and Williamson, 1993

Robertshochia Lucas, 2011

Wortmania Williamson and Brusatte, 2013)

Distribution: Puercan (Pu1, Pu2), San Juan Basin, New Mexico

Revised Diagnosis: intermediate taeniodont, upper and lower canines oval in cross-section; upper premolar P2 has only a protocone lacking a lingual cingulum; P5 lacks a metacone; upper molars have an incipient ectocingulum; upper M2 is wider than long; lower molars with an anteroposteriorly compressed trigonid; trigonids wider than talonids; mandibular symphysis unfused; radius has one fossa in articulation with the carpals

Wortmania otariidens (Cope, 1885)

(=*Hemiganus otariidens* Cope, 1885

Hemiganus otariidens Cope, 1888

Hemiganus otariidens Wortman, 1897

Wortmania otariidens Matthew, 1937

Schochia sullivanii Lucas and Williamson, 1993

Schochia sullivanii Williamson, 1996

Robertschochia sullivanii, Lucas 2011

Wortmania otariidens Williamson and Brusatte, 2013)

Lectotype: AMNH 3394, partial skull with right C, P4, P5, left I3?, C, upper teeth, mandible with left i, c and p4-p5, m1 and postcranial elements

Type locality: Puerco Formation, San Juan Basin, New Mexico

Distribution and Diagnosis: *same as the genus*

Sources: Illustrations and text in Schoch (1986), Matthew (1937), Williamson and Brusatte (2013), specimens AMNH 3394, AMNH 3413, USNM 17655, USNM 17654, USNM 15428, NMMNH P-64001

Conoryctella (Gazin, 1939)

Conoryctes Taylor, 1981

Distribution: Torrejonian (To2) of New Mexico and Utah

Revised Diagnosis: intermediate in size and level of hypsodonty between *Onychodectes* and *Conoryctes*; P5 with a protocone, paracone and incipient metacone, minuscule stylocone and parastyle; upper molar metastylar and parastylar lobe subequal with a small mesostyle; triangular lower canines with a long root, bearing grooves; ultimate lower premolar p5 longer than p4, with a protoconid and a moderately developed talonid and no anterolingual cingulid; lower molars with relative large paraconids and enclosed lingually talonids with an entocristid reaching the distal wall of the metaconid, presence of a mesoconid, hypoconulids with more than one cuspid, presence of a pre-entoconulid; symphysis of jaw unfused

Conoryctella dragonensis (Gazin, 1939)

(=*Conoryctella dragonensis* Gazin, 1939

Conoryctella dragonensis Gazin, 1941

Conoryctella dragonensis Schoch and Lucas, 1981c)

Holotype: USNM 15704, left maxilla with alveolus for P4 and P5, M1 and M2

Type locality: Dragon local fauna, upper North Horn Formation, Emery County, Utah

Age: Torrejonian (To1) of the North Horn Formation, Emery County, Utah

Revised Diagnosis: same as genus; larger species of *Conoryctella*; P5 with better-developed metacone and incipient stylocone

Sources: Illustrations and text in Schoch and Lucas (1981c), Schoch (1986), specimen USNM 15704

Conoryctella pattersoni (Schoch and Lucas, 1981c)

(=*Conoryctella dragonensis* Gazin, 1939

Conoryctella Schoch and Lucas, 1981a

Conoryctes comma Taylor, 1981

Conoryctella pattersoni Schoch and Lucas, 1981c)

Holotype: NMMNH P-25056 (=UNM B-1258 old label), left and right maxilla with left P5, M1, M2 and M3, and right mandible with c1, p4, p5, m1, m2 and m3, partial right and left ulnae

Type locality: locality B-1096, Kuts Canyon, Nacimiento Formation, San Juan Basin, New Mexico

Age: Torrejonian (To2) of the Nacimiento Formation, San Juan, New Mexico

Revised Diagnosis: smaller species of *Conoryctella*; P5 lacks a parastyle, stylocone and metacone and the postprotocrista is less developed

Sources: Illustrations and text in Schoch and Lucas (1981c), Schoch (1986), specimen NMMNH P-25056

New specimens: NMMNH P-53990, NMMNH P-53835 (NMMNH P-21380 in Appendix)

The specimen NMMNH P-53990 (Figure 10) consists of one upper tooth that is a left upper molar; probably the left M1. It can't be M3 since there is an alveolus for a smaller tooth distally, nor it can be P5 since the buccal cingulum is well formed. It is found in the locality Kutz Canyon (Tj3).

The size of the tooth is smaller than *Onychodectes* and not as big as *Conoryctes* or *Huerfanodon*. Although the length is similar to *Conoryctes* and *Huerfanodont*, it is not as wide as the M1 and M2 of the former genera. The parastylar and metastylar lobes are expanding less mesiobuccally and distobuccally than in *Onychodectes*. Compared to the two species of *Conoryctella*, NMMNH P-53990 is similar to *C. pattersoni* (Schoch and Lucas, 1981c).

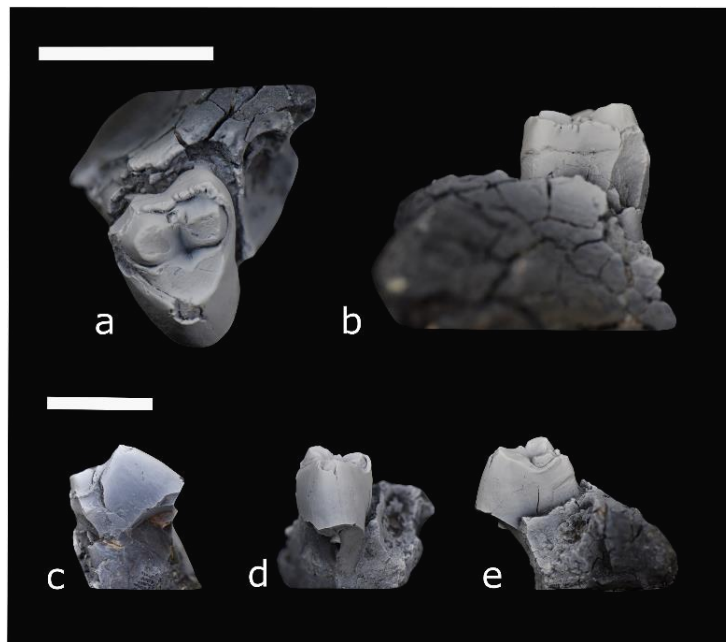


Figure 10: Specimen NMMNH P- 53990, upper M1 of *Conoryctella pattersoni*, in occlusal (a), buccal (b), mesial (c), lingual (d), and distal (e) views. Scale bar is 1cm.

Specimen NMMNH P-53835 (Figure 11) was found in locality L-6390 of the Kutz Canyon (Tj3). It consists of a small part of a left jaw with one lower molar present and the roots of another bigger tooth. The tooth that is preserved is m2 based on the size and the position of the paraconid.

The trigonid of NMMNH P- 53835 is taller than the talonid but not to the degree seen in *Onychodectes* and the m2 is also bigger than the m2 of the latter genus.

Specimen NMMNH P- 53835 has a tall crown, so the level of hypsodonty is higher than *Onychodectes* but not as high as seen in *Conoryctes*. More importantly, it shows no signs of any cingulids and there is no additional cusp posterior to the entoconid, which is named in this study as post-entoconulid. A post-entoconulid is present in *Conoryctes* and *Huerfanodon*. Another distinctive feature is that the enamel is equally distributed lingually and buccally, unlike in taxa *Conoryctes* and *Huerfanodon*. The small cusp mesially to the entoconulid is very similar to the m2 of *Conoryctella pattersoni* (NMMNH P-25056 type). The latter specimen is worn and so there is no evidence of a mesoconid. For these reasons, I am assigning specimen NMMNH P-53835 to *Conoryctella pattersoni*.

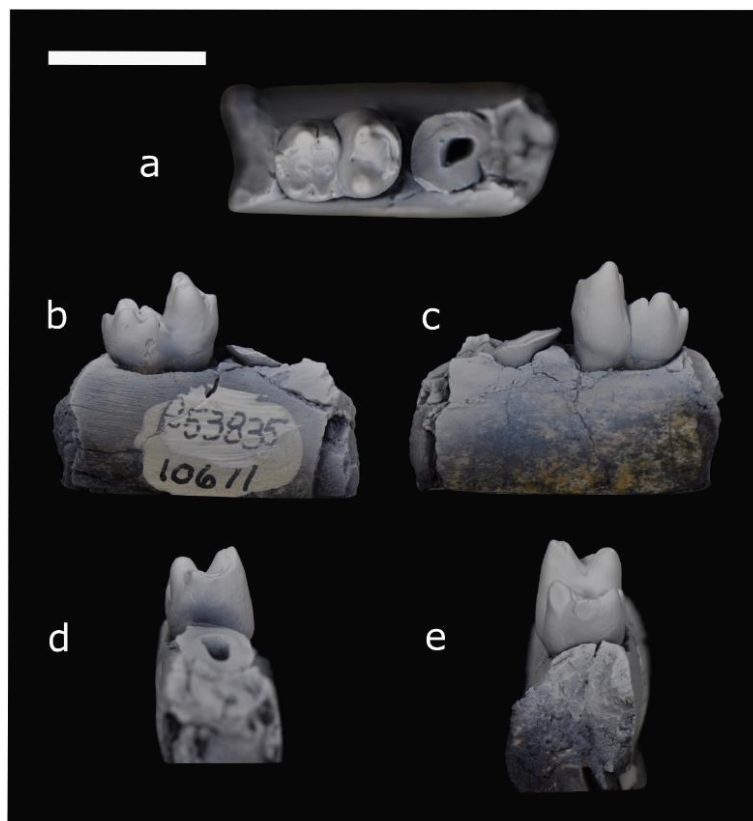


Figure 11: Specimen NMMNH P-53835, lower m2, of *Conoryctella pattersoni* in occlusal (a), lingual (b), buccal (c), mesial (d) and distal (e) views. Scale bar is 1cm.

Conoryctes (Cope 1881a)

(=*Conoryctes* Cope, 1881a

Hexodon Cope, 1884a

non *Hexodon* Olivier, 1789)

Distribution: Torrejonian to Tiffanian (To2, To3) of the Nacimiento Formation, San Juan Basin, New Mexico

Emended Diagnosis: intermediate taeniodont, upper and lower canines with internal groove; upper premolar P1 is absent; P4 bears a minuscule to small metacone and a minuscule to well-formed lingual cingulum; P5 molariform with a paracone, metacone, small parastyle, metastyle, no stylocone or stylar shelf; upper molars with paracones, metacones, stylar shelf cuspidated with prominent parastyle, metastyle and the mesostyle vary from absent to well developed; lower premolar p5 with a protoconid, and a cuspidate talonid, lacking paraconid and metaconid; talonid and trigonid subequal; lower molars bearing a mesoconid, a large hypoconid similar in size as the entoconid, cuspidate hypoconulid, a mesial (pre-) and a distal (post-) entoconulid

Conoryctes comma (Cope, 1881a)

(=*Conoryctes comma* Cope, 1881a

Conoryctes comma Cope, 1881b

Hexodon molestus Cope, 1884a

Conoryctes comma Cope, 1884b

Conoryctes comma (= *Hexodon molestus*) Cope, 1888

Conoryctes comma Wortman, 1897

Conoryctes comma Matthew, 1937

Conoryctes comma Wilson, 1956

non *Conoryctes comma* Van Valen, 1978

non *Conoryctes comma* Taylor, 1981)

Holotype: AMNH 3395, isolated right canine, left partial mandible with p5, m1 and m2 and alveolus for p2, p4 and m3

Type locality: Torrejonian strata, Nacimiento Formation, San Juan Basin, New Mexico

Distribution and Diagnosis: *same as the genus*

Sources: Illustrations and text in Schoch (1986), Matthew (1937), specimens AMNH 3395, USNM 22484, AMNH 3396, AMNH 16029, NMMNH P-16200 (=UNM B-890, old label)

New specimens: NMMNH P-61799, NMMNH P-47921, NMMNH P-19976, (NMMNH P- 54106, P-48434, NMMNH P-47943, NMMNH P-54419, NMMNH P-16182, NMMNH P-41519, NMMNH P-02705, NMMNH P-77882, NMMNH P-51827, NMMNH P-51828 in Appendix)

The new specimen NMMNH P-61799 (Figures 12 and 13) is very interesting since it resembles both genera of *Conoryctes* and *Huerfanodon*. It was found in locality L-8182 on the lower horizon of the West Flank Torreon Wash (Tj4). It consists of partial left and right maxillae with upper dentition, part of the cranium and one right canine, an incisor and numerous smaller unidentifiable elements.

The left side of the upper dentition is almost complete, consisting of a canine, an anterior-most premolar, followed by the roots for the next premolar, a complete posteriormost premolar and the two molars, lacking the most distal molar. Interestingly, there is a gap between the upper left canine and the preserved premolar. As in other *Conoryctes* specimens though the P1 is absent (Schoch, 1986). The right

dentition of the specimen includes three teeth in part of the maxilla and an isolated canine and another isolated tooth. Based on the size and comparing it to the left side of the same individual, the isolated tooth is the M3, while the other three are the P4, P5 and M1. This is because the one in the middle has parastylar and metastylar lobes but no buccal cingulum, meaning it is a P5. Based on this specimen the zygomatic arch originated at the level of the M1-M2 as seen in other specimens of *Conoryctes comma* (USNM 22484).

The size, the age and the molariform P5 of NMMNH P-61799 point to either *Conoryctes* or *Huerfanodon*. It is hard to distinguish differences in the upper dentition between the two taxa. Based on the diagnosis of *Huerfanodon* the P4 is submolariform bearing protocone, paracone and metacone (Schoch and Lucas, 1981b). There are no differences between the molars of the two taxa. It is true though that the holotype of *Huerfanodon torrejonus* (USNM 15412) has a more molariform P4 than *Conoryctes*. In USNM 15412 there are more cusps lingually, resembling more a protocone and a mesial and a distal smaller cuspule, while the metacone is absent. Regardless of the terminology used, specimen AMMH 3396 of *C. comma* also bears a somewhat molariformed P4 that although it has a prominent metastylar lobe, the lingual lobe is less prominent and developed as the type of *H. torrejonus*. Specimen AMNH 3396 of *C. comma* however has a lingually extended lobe on the P4. Photos of the P4 of *Conoryctes* and *H. torrejonus* can be seen in the Appendix (Figures A26, A27). With these in mind, and since specimen NMMNH P- 61799 has a submolariform P4 with fewer cups lingually than USNM 15412, I am assigning it to *Conoryctes comma*.

This particular specimen, therefore, is important, not only because it opens the question of the difference between the taxa of *Conoryctes* and *Huerfanodon*, but also because the less worn lingual area of the left M2 revealed unknown anatomical features of the upper molars of *Conoryctes*. The way the M2 is worn indicates that it is quite possible the upper molars- at least the M1 and M2- of *Conoryctes* had one paraconule and two metaconules (Figure 12). To put that in perspective, out of all the known specimens of *Conoryctes*, none has unworn molars to provide this evidence. *Huerfanodon* (type USNM 15412) also bears paraconules and metaconules, however, because these cuspids have never been found before in specimens of *Conoryctes* does not reject the potential presence in the latter genus. Similarly, the worn teeth of all the specimens of *Conoryctella* and *Wortmania* cannot prove- or disprove- the presence of paraconules and metaconules. Only in specimen USNM 3405, the type of *Onychodectes tisonensis*, the molars are less worn and there are hints of the presence of the conules based on the wear patterns.

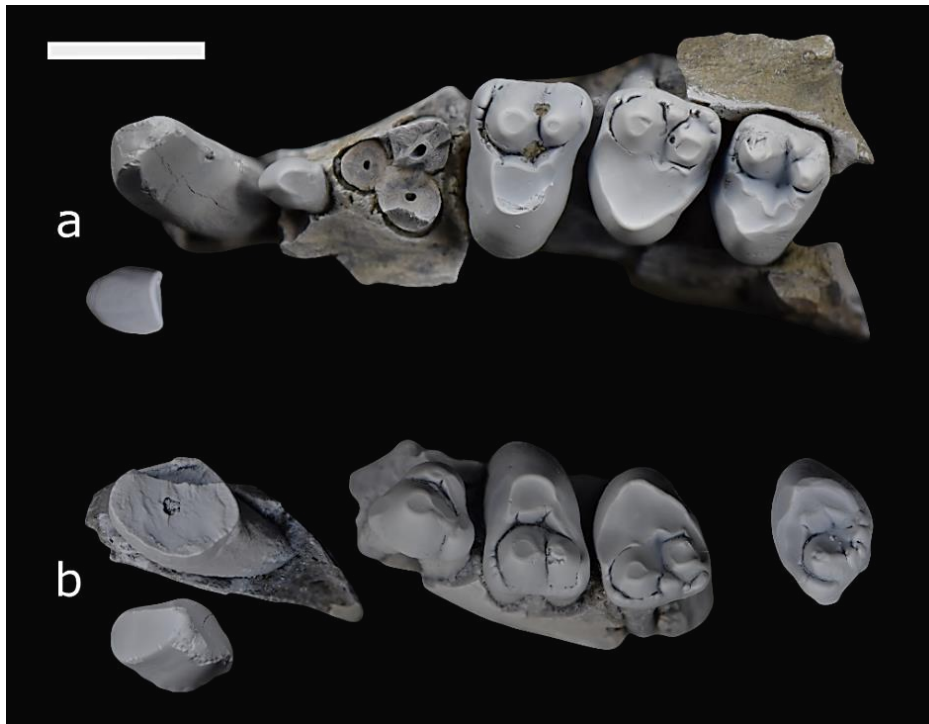


Figure 12: Occlusal view of specimen NMMNH P-61799, *Conoryctes comma* left side (a) and right side (b). The Scale bar is 1cm.

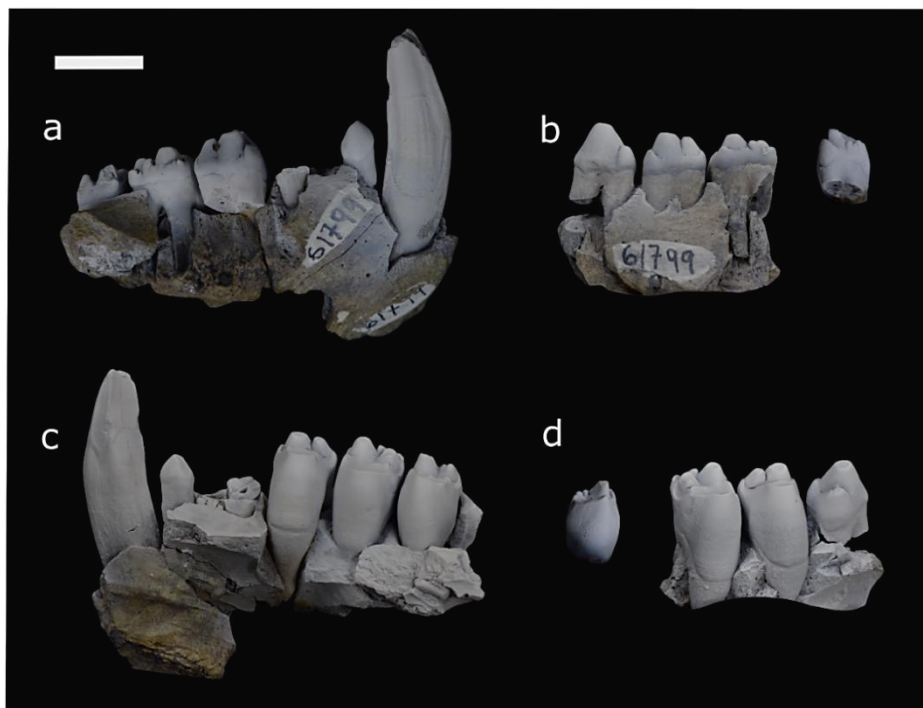


Figure 13: Left side (a, c) and right side (b, d) of the upper dentition of specimen NMMNH P-61799, *Conoryctes comma*, in buccal view (a, b) and lingual view (c, d). Scale bar is 1cm.

Specimen NMMNH P-47921 (Figure 14) was found in L-6419, Angel Peak, Kutz Canyon (Tj4). It also consists of a lower molar, probably an m1 or m2. The less prominent paraconid that is almost as high as the metaconid and extends less mesially, the large pre-entoconulid (i.e. an entoconulid, mesial to the entoconid) and post-entoconulid (distal to the entoconid), point more to the genus *Conoryctes* than *Huerfanodon*. For these reasons, NMMNH P-47921 is assigned to *Conoryctes comma*.

Specimen NMMNH P-19976 (Figure 15) was found at the locality L-8182, lower horizon of West Flank Torreon Wash (Tj6). It consists of an almost complete left mandible, missing the anterior part of the mandibular body and the coronoid process. On the mandible, there is also an alveolus for p4, a worn p5 and molars. All the teeth in the mandible are worn, yet there are still some informative features on the occlusal side. The robust mandible is similar to bigger taeniodonts, like *Conoryctes*.

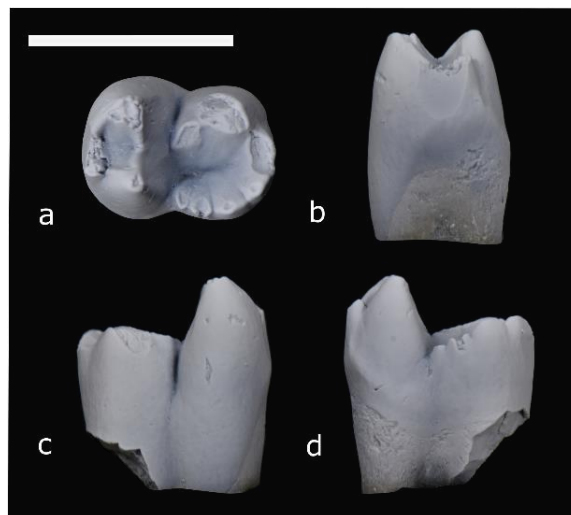


Figure 14: Specimen NMMNH P-47921 of *Conoryctes comma* in occlusal (a), mesial (b), buccal (c) and lingual (d) views. Scale bar is 1cm.

The size, age and level of hypsodonty point to the Conoryctidae family and particularly to *Conoryctes* and *Huerfanodon*. Specimen NMMNH P-19976 was compared with the mandibles and lower dentition of these two taxa. Because the p5 of NMMNH P-19976 has only one cusp in the trigonid, I am excluding *Huerfanodon polecatensis*. When comparing these to the species *Conoryctes comma* and *Huerfanodon torrejonius*, I was unable to find anatomical differences between them, primarily due to the worn dentition of the former. The diagnosis for the genus of *Conoryctes comma* suggests that lower molars have small paraconids, which based on my observations, these characters could also apply to the specimens of *Huerfanodon*.

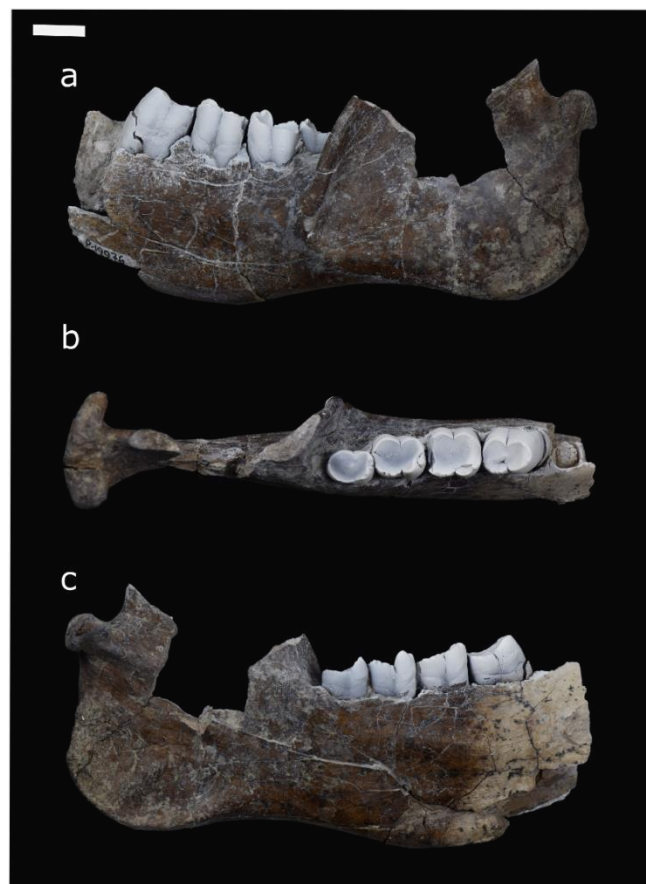


Figure 15: Specimen NMMNH P-19976 of *Conoryctes comma* in buccal (a), occlusal (b) and lingual (c) views. Scale bar is 1cm.

The diagnosis for *Huerfanodon* also suggests that the paracristids are prominent (Shoch and Lucas, 1981b), which is also true for specimen AMNH 16029 of *Conoryctes comma*. Moreover, the cuspidate talonid lingually is similar in the USNM 15412, the type of *Huerfanodon torrejoni*, as well as both molars of the specimen AMNH 16029 of *Conoryctes comma*. These specimens also have in common a relatively large hypoconid, a moderate mesoconid, two cusps on the hypoconulid area, a pre-entoconulid and a smaller post-entoconulid (distal entoconulid, between the entoconid and the hypoconulid). In general, the main difference is that the paraconid is slightly bigger in *Huerfanodon torrejoni* and relatively more appressed in *Conoryctes comma*. Understanding that the teeth distinction between these two genera is problematic, I used the shape of the mandible to identify NMMNH P-19976. Although there are only two partial jaws of *Huerfanodon* (USNM 15412 and PU 14718), the resembles in the anatomy and morphology of NMMNH P-19976 with the jaws of *Conoryctes comma* (AMNH 3395 type, USNM 22484, AMNH 3398, AMNH 3396 and AMNH 3397) led to assign this new specimen to *Conoryctes comma*.

An interesting observation on NMMNH P- 19976 is the wearing pattern of the enamel. This can be seen in other specimens of *Conoryctes* too. The more worn teeth are the p5 and the m1 and all the teeth are mostly worn posterior-buccally. The most distal parts of the trigonid, the paraconid area, are well preserved in m2 and m3, while lingually all the teeth preserve the most lingual parts of the enamel, i.e., the cuspid in the entoconulid area. Moreover, there is almost a big pit in the middle of the talonid, due to a probably very strong protocone. Animals like *Conoryctes* probably had a very big protocone for crushing their food. However, the exposing of the dentine creates a sharp shearing surface on the enamel, so potentially they had a secondary shearing phase while chewing. In an attempt to preserve that shearing area lingually, they

probably enhanced the buccal area of their teeth by adding more cusps, i.e., the cuspidate buccal cingulum in the upper molars, and the pre- and post-entoconulid in the lower molars.

For all the reasons described above, the distinction between *Conoryctes* and *Huerfanodon*, particularly *H. torrejonius*, is very challenging. This study will focus on their anatomical differences in order to understand their affinities.

Huerfanodon (Schoch and Lucas, 1981b)

Distribution: Torrejonian of Big Horn Basin, Wyoming and San Juan Basin, New Mexico

Emended diagnosis: same as in Schoch and Lucas (1981b)

Huerfanodon polecatensis (Schoch and Lucas, 1981b)

Holotype: PU 14718, incomplete right mandible, alveoli c,p1-p2, lower p4-p5, m1-m2 and alveolus for m3

Type locality: “Rock Bench Quarry Beds”, Polecat Bench Formation, Rock Bench Quarry, Big Horn Basin, Wyoming

Age: Torrejonian (To2)

Diagnosis: as in Schoch and Lucas (1981b)

Sources: Illustrations and text in Schoch and Lucas (1981b), Schoch (1986), specimen PU 14718

Huerfanodon torrejonius (Schoch and Lucas, 1981b)

Holotype: USNM 15412, partial skull with upper dentition P4, M1, M2 and M3 and partial mandible with lower teeth c1, p5, m1, m3

Type locality: T23N, R9W, Kimbetoh Arroyo, Nacimiento Formation, San Juan Basin, New Mexico

Age: Torrejonian (To2)

Diagnosis: as in Schoch and Lucas (1981b)

Sources: Illustrations and text in Schoch and Lucas (1981b), Schoch (1986), specimen USNM 15412

Psittacotherium (Cope, 1882a)

(=*Hemiganus* Cope, 1882c)

Distribution: Torrejonian (To2, To3) of Wyoming and New Mexico; Torrejonian to Tiffanian of Montana and Texas

Revised Diagnosis: intermediate in size between *Wortmania* and *Ectoganus*, enlarged, rooted canines with anteriorly limited enamel; I3 enlarged; upper canines with grooved enamel; premolars and molars show hypsodonty; roots of the upper premolars and molars fused; P5 lacking a metastyle; upper premolars transversely elongated with a large paracone and protocone connected with low cristae; upper molars transversely elongated bearing paracones and metacones with incipient centrocrista, postmetacrista and metastylar lobe, which are even smaller on M2 and M3, distinct paraconule and a larger metaconule; lower incisor moderately sized; lower premolar p1 reduced and single-rooted; p2 single rooted with a protoconid and a metaconid; p5 submolariform with a protoconid and metaconid, lacking a paraconid,

the talonid is small and lingually placed talonid; lower molars with broader trigonids than talonids, with more lingually placed talonids; mandibular condyle same level as the tooth row; mandibular symphysis is fused

Psittacotherium multifragum (Cope, 1882a)

(=*Psittacotherium multifragum* Cope, 1882a

Psittacotherium multifragum Cope, 1882b

Psittacotherium aspasiae Cope, 1882b

Hemiganus vultuosus Cope, 1882c

Psittacotherium multifragum Cope, 1884b

Psittacotherium aspasiae Cope, 1884b

Hemiganus vultuosus Cope, 1884b

Psittacotherium megalodus Cope, 1887

Psittacotherium multifragum Wortman, 1897

Psittacotherium multifragum Matthew, 1937

Psittacotherium aspasiae Matthew, 1937

Psittacotherium multifragum Simpson, 1937

Psittacotherium multifragum Wilson, 1956

Psittacotherium multifragum? Simpson, 1959

Psittacotherium cf. *P. multifragum* Wilson, 1967

Psittacotherium multifragum Rigby, 1980

Psittacotherium multifragum Schoch, 1981a)

Holotype: AMNH 3413, mandible with left i3, c1, alveoli for left m2-3, right p2, m1, m2 and alveoli for p1 and m3

Type locality: Torrejonian strata, Huerfano Peak, Nacimiento Formation, San Juan Basin, New Mexico

Distribution and Diagnosis: *same as the genus*

Sources: Illustrations and text in Schoch (1986), Matthew (1937), specimens USNM 15411, USNM 15410, AMNH 754, AMNH 88383, USNM 15413, AMNH 16560, AMNH 15938

New specimens: NMMNH P-30630, NMMNH P-19838 (NMMNH P-30628, NMMNH P-47826, NMMNH P-44908, NMMNH P-19800, NMMNH P-57845 NMMNH P-16230 in the Appendix)

New specimen NMMNH P-30630 (Figure 16) is found in L-4344, Kutz Canyon indet. It consists of three teeth, a fragmented anterior premolar and two upper molars. Because of the size, the small metacone and the incipient parastyle, these are second upper molars (M2). The right M2 is similar to the left but damaged mesially at the paracone. Interestingly, the lingual area is less worn and it is evident that the preprotocrista is slightly cuspidate and the same applies to the postprotocrista. There is a distinctively larger cuspule in the middle of the postprotocrista, like in the left M2, similar to a metaconule.

The anatomy, the transversely elongated shape, the hypsodonty, the distribution of the enamel around each tooth, the minuscule buccal cingulum and parastylar lobe- are very similar to *Psittacotherium multifragum* (Schoch, 1986). So, specimen NMMNH P-30630 is assigned to this *P. multifragum*. The similarities can also be observed while studying the upper dentition of USNM 15411 and TMM 40537-61 and 40537-33 BB *P. multifragum*. Interestingly the new specimen NMMNH P-30630 provides a lot of insight into the metaconule and paraconule since it is the first unworn M2 ever found of the genus.

Specimen NMMNH P-19838 (Figure 17) found in L-2590, Kutz Canyon indet., consists of five isolated lower teeth. One of them is smaller and conical and so it is a lower incisor. The rest have a square shape with a distinguished talonid and a trigonid and so they are lower premolars and molars. They are an m1, a p5 and a p4.

The p5 is very similar to specimen AMNH 16661. The shape of the teeth, the enamel distribution and the locality as well as the resemblance with other specimens, lead to assign NMMNH P-19838 to *Psittacotherium multifragum*.



Figure 16: Specimen NMMNH P-30630, left M2 (left), right M2 (centre), upper premolar (right) of *Psittacotherium multifragum* in occlusal (a), buccal (b), distal (c) mesial (d) and lingual (e) views. The scale bar is 1cm.

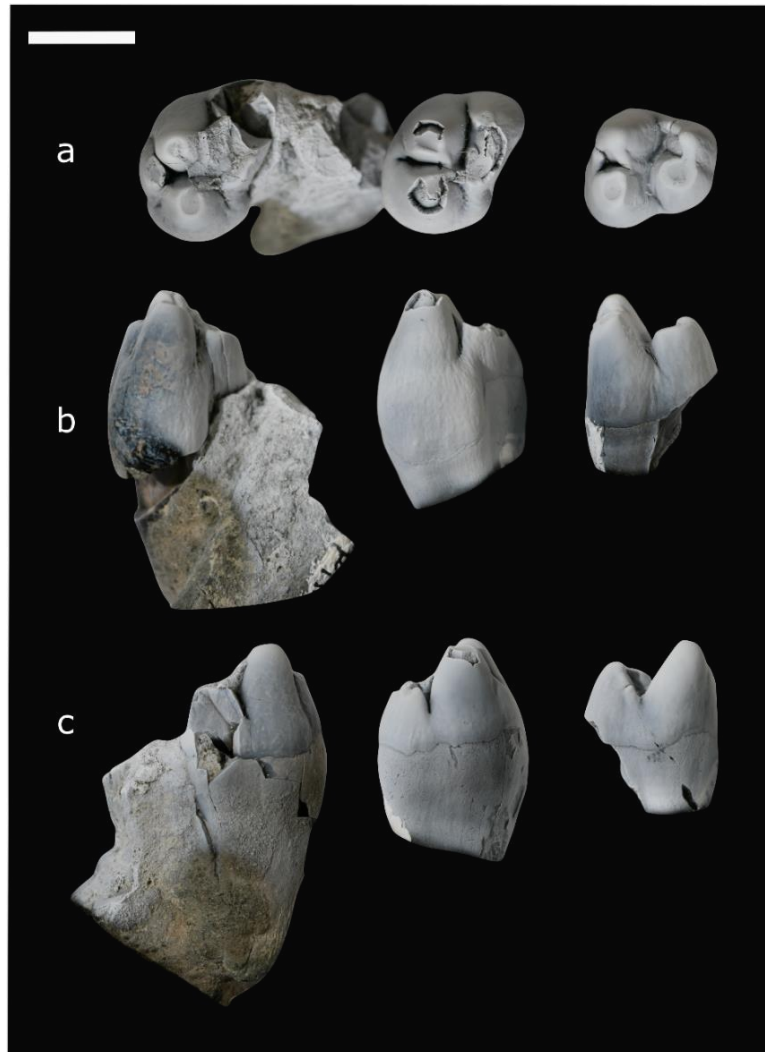


Figure 17: Specimen NMMNH P-19838, m1 (left), p4 (centre), p5 (right) of *Psittacotherium multifragum* in occlusal (a), buccal (b) and lingual (c). Photos were taken by Thomas Williamson and edited by me. Scale bar is 1cm.

Ectoganus (Cope, 1874)

(=*Ectoganus* Cope, 1874

Calamodon Cope, 1874

Dryptodon Marsh, 1876

Conicodon Cope, 1894

non *Calamodon* Amaral, 1935

Lampadophorus Patterson, 1949a)

Distribution: Tiffanian-Wasatchian of Colorado, Clarkforkian of Montana, Clarkforkian-Wasatchian of Wyoming and Wasatchian of New Mexico

Revised Diagnosis: large taeniodont; enlarged, rootless canines, enamel restricted anteriorly, and the dentine is compressed posteriorly; cheek teeth moderate to extreme hypsodont; upper molars lacking stylar shelf, parastyle, stylocone and metastyle, metacone lingually to paracone, presence of a distolingual cusp lingually, absent of postprotocrista to connect distolingual cusp to protocone giving a bilophodont shape to the upper molars; lower premolars p4, p5 submolariform with narrower, lingually placed talonids than trigonids; lower molars lacking cristid obliqua and entocristid, giving them a bilophodont shape

Ectoganus bighornensis (Schoch, 1981b)

(=*Ectoganus copei copei* Schoch, 1981b

Ectoganus bighornensis Gingerich, 1989)

Holotype: PU 14678, canine fragments, right P4, M1-2, left P4, M3 and right m1

Type locality: lower Willwood Formation, southern tip of Polecat Bench, T. 55 N., R. 100 W., Bighorn Basin, Wyoming

Age: early Wasatchian (Wa0)

Revised Diagnosis: small *Ectoganus* with less hypsodont premolars and molars; cusps on upper premolars smaller than in *E. copei*

Sources: Illustrations and text in Schoch (1986), specimen PU 14678

Comments: Following Gingerich (1989) this study acknowledges the two subspecies of *Ectoganus copei* as two different species, *Ectoganus copei* and *Ectoganus bighornensis*

Ectoganus copei (Schoch, 1981b)

(=*Ectoganus gliriformis* Gazin, 1936

Ectoganus copei copei Schoch, 1981b

Ectoganus copei Schoch, 1983a

Ectoganus copei Gingerich, 1989)

Holotype: USNM 12714, skull with right I3, C, P1-4, dp5, M1, left dp5, M1, I3, C, P1-4, dp5, M1-2, alveolus M3, mandible with right roots of c, p2, m1, m3, left c, p2, dp5, m1-2

Type locality: Wasatchian strata, Willwood Formation, Bighorn Basin, Wyoming

Age: Clarkforkian

Revised Diagnosis: small *Ectoganus* with extreme hypsodont canines, incisors and P1-P2 and p1-p2; upper P1- P2 with a paracone and an enlarged protocone; lower molars with a vestigial paraconid

Sources: Illustrations and text in Schoch (1986), specimen USNM 12714

Ectoganus gliriformis (Cope, 1874)

(=*Ectoganus gliriformis* Cope, 1874

Calamodon simplex Cope, 1874

Calamodon arcamaenus Cope, 1874

Calamodon novomehicanus Cope, 1874

Dryptodon crassus Marsh, 1876

Ectoganus novomehicanus Cope, 1877

Ectoganus gliriformis Cope, 1877

Calamodon arcamaenus Cope, 1877

Calamodon simplex Cope, 1877

Calamodon simplex Cope, 1884b

Calamodon simplex Wortman, 1897

Ectoganus gliriformis Gazin, 1936

Ectoganus cf. *simplex* Guthrie, 1967

Ectoganus simplex Schankler, 1980

Ectoganus gliriformis gliriformis Schoch, 1981b

Ectoganus gliriformis Gingerich, 1989)

Holotype: USNM 1137, canine fragments, right P4, M1-2, left P4, M3 and right m1

Type locality: Wasatchian strata, San Jose Formation, probably Almagre Arroyo, San Juan Basin, New Mexico

Age: Wasatchian (Wa3)

Revised Diagnosis: large *Ectoganus* with extreme hypsodont canines, incisors and P1-P2 and p1-p2; upper P1- P2 and p1-p2 with a paracone and an enlarged and obliquely placed protocone; lower molars with a vestigial paraconid; dorsal root of the

mandibular angular process level with the vertical level of the condyloid process; later trochlear keel of the astragalus greater than the medial

Sources: Illustrations and text in Schoch (1986), specimens USNM 1017, AMNH 16771, AMMH 16244, AMNH 15633, AMNH 4287

Comments: Following Gingerich (1989) I am acknowledging the two subspecies of *Ectoganus gliriformis* as two different species, *Ectoganus gliriformis* and *Ectoganus lobdelli*

Ectoganus lobdelli (Simpson, 1929b)

(=*Psittacotherium* sp. indet. Simpson, 1929a

?*Psittacotherium lobdelli* Simpson, 1929b

?*Psittacotherium* sp. Patterson, 1936

Lampadophorus expectatus Patterson, 1949a

Lampadophorus lobdelli Patterson, 1949a

cf. *Lampadophorus* sp. Rose, 1981

Ectoganus gliriformis lobdelli Schoch, 1981b

Ectoganus gliriformis lobdelli Schoch, 1985

Ectoganus gliriformis lobdelli Schoch, 1981b

Ectoganus lobdelli Gingerich, 1989)

Holotype: AMNH 22234, right M3

Type locality: Clarkforkian strata, Fort Union Formation, Eagle Coal Mine, Bear Creek, Montana

Age: Wasatchian (Wa1-2)

Revised Diagnosis: large *Ectoganus* with p2, P2 less hypsodont; P4-M3 and p4-m3 moderately hypsodont with relatively low, rounded, bulbous crowns and relative shallow roots

Sources: Illustrations and text in Schoch (1986), specimens PU 21499, PU 20864

Stylinodon (Marsh, 1874)

(=*Stylinodon* Marsh, 1874

Calamodon Cope, 1881c

Calamodon Cope, 1884b)

Distribution: Late Wasatchian of Colorado and Wyoming, Bridgerian of Colorado and Wyoming, Uintan of Utah and Bridgerian or Uintan of western Texas

Revised Diagnosis: largest taeniodont; all of the teeth ever-growing (hypsodont); enamel restricted only buccal and lingually; upper and lower canines compressed posteriorly; anterior premolars P1-P2 and p1-p2 longer than posterior premolars; p1 and P1 "L shaped"; upper molars subequal in size; lower molars subequal in size; mandibular condyle approximately one molar length above the tooth row; deltopectoral region extends more than half the humeral shaft

Stylinodon mirus (Marsh, 1874)

(=*Stylinodon mirus* Marsh, 1874

Calamodon cylindrifer Cope, 1881c

Calamodon cylindrifer Cope, 1884b

Stylinodon mirus Marsh, 1897

Stylinodon mirus Wortman, 1897

Stylinodon cylindrifer Wortman, 1897

Stylinodon cylindrifer White, 1952

Stylinodon sp. Robinson, 1966

Stylinodon cylindrifer Guthrie, 1971

Stylinodon mirus Schoch and Lucas, 1981d

Stylinodon inexplicatus Schoch and Lucas, 1981d

Stylinodon mirus Turnbull, 2004)

Holotype: YPM 11095, fragments of the mandible with left p4-m1 and alveoli for lower cheek teeth

Type locality: Bridgerian strata, Bridger Formation, near Millersville, Bridger Basin, Wyoming

Age: Bridgerian- Uintan

Distribution and Diagnosis: *same as genus*

Sources: Illustrations and text in Schoch (1986), Turnbull (2004) specimens PU 16102, YPM 11095, AMNH 107954

Comments: As pointed out by Turnbull (2004) *Stylinodon inexplicatus* (Schoch and Lucas, 1981d), is a juvenile specimen of *S. mirus*.

Conoryctidae (Wortman, 1896b)

Type Genus *Conoryctes* (Cope, 1881)

Included Genera *Conoryctella* (Gazin, 1939); *Conoryctes* (Cope, 1881a); *Huerfanodon* (Schoch and Lucas, 1981b)

New specimens: NMMNH P-25014

Specimen NMMNH P-25014 (Figures 18 and 19) from the L-00625 locality, Kutz Canyon (Tj2) consists of a partial right mandible. Although damaged there is a strong coronoid crest and a deep masseteric fossa. The proximal area of the mandible is broken and missing, while there are four lower teeth, three molars and the last premolar. The last premolar is a deciduous tooth since it is molariformed and the enamel is evenly distributed lingually and buccally. The lighter colour of the enamel also indicates that it is thinner and therefore a deciduous tooth.

To study the permanent p5, specimen NMMNH P-25014 was scanned at the University of Edinburgh by Ian Butler, using a 4D μ CT (cone beam, pixel size 0.2mm, voxel size 0.45mm). Later the scanned images were processed in Avizo Lite 2019.4, shared license University of Edinburgh, Palaeontology group. Using the "Image segmentation" module in Avizo the outline of the permanent p5 on each slide was captured. The selected areas were then used to generate a surface with the "Generate Surface" module. That way, it is able now to visualise and measure the permanent p5 within the jaw.

The molars of NMMNH P-25014 are unworn, m1 is bigger than all of the molars and m1 and m2 have an almost square shape. The last molar is more elongated distally. The cuspids of the molars are bulbous and well-separated and the trigonid is not too high compared to the talonid. The m1 has a big protoconid and an almost equally big metaconid and a smaller paraconid. The paraconid is lower than the other cuspids of the trigonid and there is no paracristid. The talonid consists of a smaller mesoconid, a big hypoconid, two small cuspids in the hypoconulid area, a moderate entoconid and a smaller post-entoconulid. The m2 is very similar to m1 with

the only difference being a very prominent paracristid and a more lingually placed paraconid that is almost as tall as the metaconid. The m3 is very similar to m2, with a prominent paracristid, a more lingually oriented paraconid. The hypoconulids are placed more distally, giving m3 a more elongated shape and there is no mesoconid. The enamel distribution has almost the same height lingually and buccally.

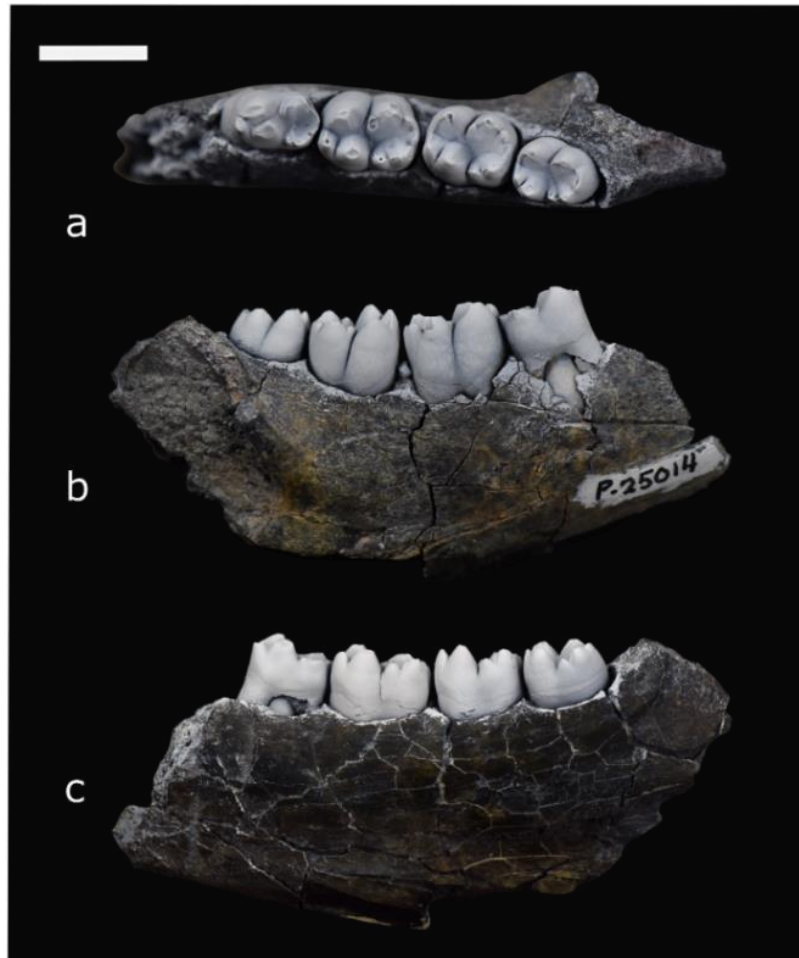


Figure 18: Specimen NMMNH P-25014 in occlusal (a), buccal (b) and lingual (c) views with dp5, m1, m2 and m3. Scale bar is 1cm.

The p5 of NMMNH P-25014 (Figure 19) has one big cuspid mesially, the protoconid, and there is also a bulging mesio-buccally, in the metaconid position. The trigonid is taller than the distal talonid, which is narrow. Unfortunately, the specimen

was filled with iron oxide, which causes lower contrast between the sediment and the tooth. Therefore, I was not able to segment the cuspids and have a detailed view of the talonid.

NMMNH P-25014 is a very interesting specimen and the locality and age suggest an early taeniodont (Figure A28-A30). It is bigger than *Schowalteria*, i.e. length of m1 is 5.04mm for *Schowalteria*, and the length of the m1 is 9mm for NMMNH P-25014. The lack of lingual cingulid rules out that this specimen is of *Onychodectes*. The size of the premolar and the molars are intermediate between *Conoryctes* and *Conoryctella* (Appendix tables A2, A3 and A4). The talonid of NMMNH P-25014 is almost as high as the trigonid, which is not the case with the lower molars of *Conoryctella*. Looking at the molars, the main difference between *Conoryctes* and *H. torrejonius* is the lack of a posterior entoconulid in the talonid and the enamel that is even distributed lingually and buccally. The segmented p5 show that there is only one major cusp in the anterior area, meaning that it is lacking a metaconid. *H. polecatensis* has a metaconid on the p5, therefore NMMNH P-25014 does not belong to that genus.

The bulbous cuspids resemble more the lower dentition of members of the Stylinodontidae family. All the known specimens of *Wortmania* are worn, however, the molars of *Wortmania* (specimen NMMNH P-64001) have similar enamel distribution with NMMNH P-25014. Proportionally it is different to *Wortmania* since the lower molars of *Wortmania* have a narrow talonid than trigonid on the m1 and m2. The lower molars of NMMNH P-25014 have trigonids and talonids subequal in size. The mandible of NMMNH P-64001 is bigger though than NMMNH P-25014, even though the latter is of a juvenile. Moreover, the lower teeth of *Wortmania* are tilted more lingually in the jaw, something not seen in NMMNH P-25014. Compared to

Psittacotherium, NMMNH P-25014 is smaller and the canines would be much smaller in size. The trigonid of the lower premolars and molars of *Psittacotherium* (Figures A21 and A22 in Appendix) bears more cuspids distolingually than NMMNH P-25014. Specimen NMMNH P-25014 is also too small, and too old stratigraphically, to belong to either *Ectoganus* or *Stylinodon*.

Another interesting aspect of this specimen is the pits in the enamel probably due to wear. On the m1, there is a small circular area where the enamel was wearing out at the entoconid and post-entoconulid areas. That wear spot is bigger on the m2, and the most lingual hypoconulid is slightly worn. The deciduous p5 also shows a similar pattern with the talonid more worn than the trigonid. These areas were conducting a probably strong protocone during mastication. The diet must have been very abrasive considering there are already signs of wear even though the animal of NMMNH P- 25014 was still a juvenile. Since it is a subadult it is best to name it *Conoryctidae* indet. and not create a new genus.

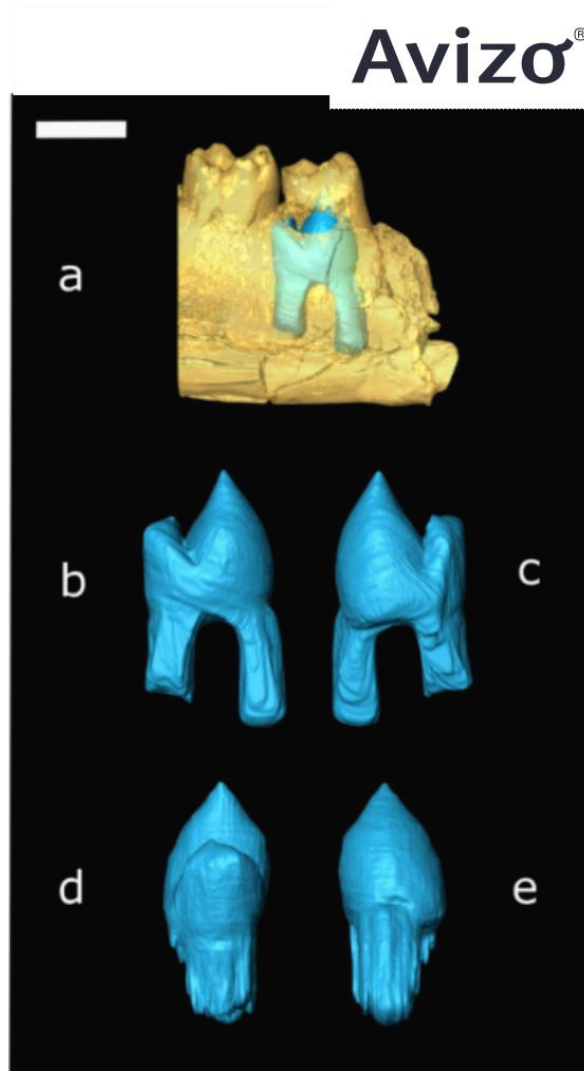


Figure 19: The scanned image of specimen NMMNH P-25014 with the permanent p5 in the jaw after segmentation in Avizo (a). The p5 in lingual (b), buccal (c), distal (d) and mesial (e) views. Scale bar is 1cm.

Character sampling

The Shelley_2020 matrix that was used for this analysis includes 271 dental characters, 267 cranial, and 92 postcranial characters. The upper and lower teeth are scored separately, and each individual tooth is scored separately apart from the molars. I did not separate each molar, because, in the case of Taeniodonta, there is a lot of information missing due to their worn teeth. So, dividing characters for each tooth would minimise the characters scored for taeniodonts. Since there are more differences between the first molars with the last molar, there are characters that are only scored for the last molar, to make sure this is distinguished.

For the purpose of this study, I checked if the characters proposed by previous phylogenetic analyses on Taeniodonta were included in the Shelley_2020 matrix. Each of the character lists in the publications was reviewed to assess whether each character was included in the Shelley_2020 matrix. If there were important characters in the published analyses that were missing from the Shelley_2020 matrix, I made sure to include them. I also added new characters to the matrix based on my observations on Taeniodonta. The full list of the matrix and the characters used for this study can be seen as Supplementary material (S1). Note that the first character is numbered 0.

Based on previous phylogenetic analyses on Taeniodonta

Using the observations of Patterson (1949b) and his study, Schoch (1986) listed the anatomical features that were apomorphic for each taxon. Since this was not done using numerical cladistics analysis, he created a cladogram by hand and united

taxa by creating “nodes”. Based on Schoch’s anatomical features and the matrix of Eberle (1999), an introduction and phylogenetic study of *Alveugena*, a few phylogenetic analyses followed. These analyses were performed either to check the intra (Rook and Hunter, 2013a, b; Williamson and Brusatte, 2013) or inter (Rook and Hunter 2011; 2013) relationships of Taeniodonta. The second analysis by Rook and Hunter (2013), in which they used only *Alveugena* and *Schowalteria*, is already based on a modified matrix by Wible *et al.* (2007; 2009) as is the Shelley_2020 matrix and will not be discussed.

In the text below, I will go through the anatomical features mentioned in Schoch (1986, figure 56), and check how these were turned into phylogenetic characters in the other phylogenetic analyses. I will point out the characters in the Shelley_2020 matrix that are already capturing the information from previous studies. The way these characters were scored for Taeniodonta will also be discussed below. In case these are not in that matrix, I will explain how new characters were made, or why I dismissed them.

Node 1 in Schoch (1986, figure 56) has many anatomical features that unite all taeniodonts.

- A feature that is seen in all taeniodonts (Schoch, 1986) is the presence of protocones, which is in the Shelley_2022 matrix character **ch.174**, upper molar protocone presence: present (0), absent (1). All taeniodonts have a protocone, however, *Stylinodon* has very worn teeth and even the presence of a protocone is dubious and was not scored.

- The size of the protocone on the upper molars is a character seen in the analyses by Rook and Hunter (2011; 2013) and Williamson and Brusatte (2013). The Shelley_2022 matrix captures this in **ch.175**, “Upper molar protocone development: small without trigon basin (0), small with distinct trigon basin (1), larger basin somewhat expanded mesiodistally (2), distal portion expanded (3)”. Scoring that for taeniodonts is difficult considering the level of wear on some of their teeth. Taxa like *Schowalteria*, *Conoryctella*, *Wortmania*, and *Stylinodon* were not scored for ch.175 due to a lack of unworn upper molars. Similarly, *Huerfanodon polecatensis* is not scored for this character since it is known only from a partial jaw. *Onychodectes* (AMNH P-3405), *Huerfanodon torrejoni* (USNM 15412), *Conoryctes comma* (NMMNH P-61799) and *Psittacotherium* (NMMNH P-30630) are scored as having small protocones with distinct trigon basin, but not mesiodistally expanded (state 1).

- The presence and position of paraconules and metaconules were also characters in the studies of Eberle (1999) and Rook and Hunter (2011; 2013) and Williamson and Brusatte (2013). The Shelley_2020 matrix includes these as characters **ch.156-157** and **ch.158-159** respectively. Character 156 is capturing the presence of the paraconule on the upper molars, with state 0 as absent and state 1 as present. Character 157 is describing the position of the paraconule as closer to the protocone (0), or midway, closer to the paracone (1). Similarly to the protocone, the lingual area of the upper dentition is worn in many taeniodonts, and so these characters are not scored for all the taxa. For those taxa with less worn upper molars, the paraconules are present. These are *Onychodectes tisonensis* (AMNH 3405), *Conoryctes comma* (NMMNH P-61799), *Huerfanodon torrejoni* (USNM 15412), *Psittacotherium multifragum* (NMMNH P-30630), *Ectoganus copei* (USNM 12714). For all of these taxa, the paraconules are midway between the paracone and protocone (state 1),

apart from *Ectoganus copei* (see figures 21, 22 and 23, and discussion on the distolingual cusp below), which is closer to the protocone (state 0).

Similarly, for the metaconule, character 158 is capturing the absence (1) and presence (0), while character 159 is capturing the position, closer to protocone (0), midway or closer to metacone (1). These were scored like the paraconule. The second upper molar of *Conoryctes* (NMMNH P-61799) has a less worn area and it is possible to see the paraconule and metaconule based on the wear patterns, however, their position relative to the protocone is not clear. Therefore, *Conoryctes* is not scored for characters 157 and 159.

- Another feature is the size of paracones and metacones seen in Schoch (1986) and in the phylogenetic analyses of Rook and Hunter (2011; 2013), and Williamson and Brusatte (2013). In the Shelley_2020 matrix, the relative position and size of paracone and metacone are captured with characters **ch.138-139**. Character 138 is scored for the relative size of the metacone and paracone on M2 with the states: metacone noticeably smaller than paracone (0), metacone and paracone subequal (1) and metacone larger than paracone (2). Metacone is subequal to the paracone on the M2 in *Onychodectes tisonensis* (AMNH 3405), *Conoryctella pattersoni* (NMMNH P-25056, Schoch and Lucas, 1981c) and *Wortmania otariidens* (NMMNH P-64001, Williamson and Brusatte, 2013). The metacone on the M2 is noticeably smaller in *Conoryctes comma* (NMMNH P-61799, NMMNH P-16200, Schoch and Lucas, 1981b) *Huerfanodon torrejoni* (USNM 15412, Schoch and Lucas, 1981b), *Psittacotherium multifragum* (USNM 15411) and *Ectoganus bighornensis* (USNM 527725, Rose *et al.*, 2012).

Character 139 captures the relative position of the metacone and paracone on the M1 and M2 as either the metacone placed labial to paracone (0), the metacone and paracone on the same level (1) and the metacone lingual to the paracone (2). All taeniodonts scored for this character as having the metacone and paracone on the same level, apart from *Ectoganus copei* (USNM 12714).

- The “reduced styler shelves” as Schoch (1986) describes them are character “Stylar margin on upper molars” in Eberle (1999), Rook and Hunter (2011; 2013) and Williamson and Brusatte (2013). In the Shelley_2020 matrix that information is captured with two characters; **ch.116** the presence of the styler shelf (state 0 for absence, state 1 for presence) and **ch.117** which quantifies the width of the shelves compared to the total tooth width. All scored taeniodonts have a styler shelf, apart from *Ectoganus* which is absent in all the species, while *Huerfanodon polecatensis* was not scored due to the lack of upper dentition for the species. The juvenile specimen of *Stylinodon mirus* (YPM PU 16102, upper M3) was used to score the lack of styler shelf for the genus.

For character 117 the states of the size of the styler shelf are present and 50% or more of the tooth width (0), present but less than 50% but more than 25% (1), present but less than 25% (2). All taeniodonts were scored as state 2 since the styler shelf is very narrow. The species of *Ectoganus* and *Stylinodon* lack a styler shelf and so this character (ch.117) is inapplicable.

- Another anatomical feature (Schoch, 1986) is the absence of precingula and postcingula. This is the character “Lingual cingula on upper molars” in Eberle (1999), Rook and Hunter (2011; 2013) and Williamson and Brusatte (2013). In the current matrix the presence of precingulum is **ch.182** and of postcingulum **ch.185**. The

precingulum is absent in all the taeniodonts, while due to the level of wear it is unknown for *Schowalteria*. In *Onychodectes tisonensis* (AMNH 3405 and USNM 15536) there is a minuscule precingulum that is not seen in all specimens of the species though; it is missing in AMNH 16528 and AMNH 785. The precingulum is also small in specimen NMMNH P-9000 of *Wortmania otariidens*, however specimen NMMNH P-64001 is lacking that feature (Williamson and Brusatte, 2013). Therefore, character 182 is scored as polymorphic (present and absent) for *Onychodectes tisonensis* and *Wortmania otariidens*.

Character 185 is scored for the presence (0) or absence (1) of the postcingulum. All scored taeniodonts are lacking a postcingulum, while this is not a character scored for *Schowalteria* due to damaged upper molars lingually. Only *Onychodectes tisonensis* is scored as polymorphic as there is a minuscule postcingulum in some specimens (AMNH 3405), that is missing in others (AMNH 16528). The juvenile specimen of *Stylinodon mirus* (YPM PU 16102) was used to score the lack of precingulum and postcingulum for the genus.

- One very interesting feature in the taxa of Taeniodonta is the absence of a hypocone mentioned by Schoch (1986). The more derived taxa though are thought to have a hypocone that “developed by a splitting-off from the protocone” (Schoch, 1986). There is a presence/absent character in the Shelley_2020 matrix (**ch.191**). However, I wanted to capture the unique “hypocones” of the derived taeniodonts and added a new character based on the new approach of the “hypocone” morphology. There is a lengthy discussion in the section below.

- The first node in Schoch (1986, figure 56) also has anatomical features of the lower molars such as the lack of lower molars cingulids. This is a character in the

Shelley_2020 matrix, **ch.227**, capturing the presence (1) or absence (0) of the lingual cingulids on the first and second lower molars. This character was not scored for *Schowalteria* due to the level of wear on the first two molars, and it is also unscored for *Conoryctella dragonensis* since the lower dentition of this taxon is unknown. The rest of the taeniodonts are scored as state 0, absent or weak lingual cingulids.

- The size of the protoconid relative to the metaconid is mentioned in Schoch (1986) and is character **ch.223** in the Shelley_2020 matrix. The height of the protoconid is measured either as the tallest cusp on the trigonid (0), subequal to the metaconid and/or the paraconid (1) or smaller than the metaconid and/or the paraconid (2). All taeniodonts are scored as having the protoconid subequal to the metaconid and/or the paraconid (1). The taxa that are known only from worn lower molars, *Schowalteria Wortmania otariidens*, *Stylinodon mirus*, or are not known from lower teeth, *Conoryctella dragonensis*, were not scored for this character.

- The most common characteristic of Taeniodonta is the level of hypsodonty on the cheek teeth (Schoch, 1986), which is the character “Crown hypsodonty” in Eberle (1999) and “Molar hypsodonty” in Rook and Hunter (2011; 2013) and Williamson and Brusatte (2013). In the Shelley_2020 matrix, this is character **ch.18** for the incisors and **ch.256-257** for the lower molars. Character 18 is capturing the position of the root of the upper anteriormost incisor. This could be either as closed and rooted (0), therefore no hypsodont anteriormost incisor, or hypsodont with the root of the incisor in the premaxilla only (1), or extending into the maxilla (2), or even further in the maxilla (3). Very few taeniodont taxa are known from their upper incisors. The incisors of *Onychodectes* are closed (0), while more derived forms show hypsodonty incisors. These are *Ectoganus copei* (USNM 12714) has the incisor extending further into the

maxilla (2) and *Stylinodon* in the maxilla (3). The upper incisor of *Wortmania* is closed, but it was not found in the skull, so it wasn't scored.

The hypsodonty of the lower molars is scored for character 256 and the degree of hypsodonty as character 257. These characters might need to be evaluated further, especially since establishing the level of hypsodonty is problematic when the teeth are extremely worn, which is the case for taeniodonts. Moreover, as will be discussed below, there are different types of hypsodonty (Koenigswald, 2011). Apart from *Onychodectes*, *Wortmania* and *Conoryctella pattersoni*, all taeniodonts are scored as having hypsodonty on the lower molars. *Wortmania* (NMMNH P-64001) is known only from too worn lower molars, so this score is prone to change. *Schowalteria* has extremely worn lower molars, apart from the trigonid of the third lower molars, and so it was not scored for characters 256 and 257.

- Schoch (1986, figure 56) mentioned some uniting similarities regarding the size of taeniodonts dentition. Considering the extreme level of wear, the observations of relative sizes are important for this group. One of these observations is the subequal trigonids and talonids of the lower molars. The following analyses (Eberle, 1999; Rook and Hunter, 2011; 2013; Williamson and Brusatte, 2013) checked this feature for the three molars separately. In the Shelley_2020 matrix, this is captured by character **ch.236** for all the lower molars. This character is not divided into three, one for each lower molar, because there is no variation among the lower molars in all the taxa of taeniodonts. Character 236 measures the length of the trigonid relative to the talonid and the states are: long more than 75% of the total tooth length (0), some shortening 51% to 75% of the total tooth length (1) and anteroposterior compression of trigonid, 50% or less of the total tooth length (2). *Onychodectes* has a relatively long trigonid

(state 0) and so does *Huerfanodon torrejoni* (USNM 15412). *Conoryctes* (AMNH 16029), *Huerfanodon polecatensis*, *Conoryctella pattersoni* (NMMNH P- 25056), and *Ectoganus copei* (USNM 12714) have a shorter trigonid, almost subequal to the talonid (state 1). *Wortmania* (NMMNH P-64001) is scored as having an anteroposterior compression (state 2). This character is referring to the m1 and m2 because it is common for the talonid to be more distally expanding. Therefore, *Schowalteria* which has only the m3 less worn was not scored for character 236.

- The height of the trigonid relative to the talonid is a feature noticed by Schoch (1986) and is a phylogenetic character in the other datasets too (Eberle, 1999; Rook and Hunter, 2011; 2013; Williamson and Brusatte, 2013) and is **ch.235** in the Shelley_2020 matrix. Similarly to character 236 which was described above, this is not scored separately for each lower molar. Character 235 measures the height of the trigonid relative to the height of the talonid. The height of the trigonid is scored as, twice or more the height of the talonid (0), less than twice the height of the talonid (1) and subequal to the talonid (2). All taeniodonts are scored as having tall trigonids, less than twice the height of the talonids (state 1).

- Another noticeable anatomical characteristic of taeniodonts is the posterior decrease in size of the molars (Schoch, 1986). That is a character in Eberle (1999) as “Size of M2 relative to M1” and was used by the following studies too (Rook and Hunter, 2011; 2013, and Williamson and Brusatte, 2013). In the Shelley_2020 matrix, the relative size of the upper molars (**ch.105-107**) and lower molars (**ch.108-110**) is addressed. Character 105 compares the size area of the upper molar M1 to M2 with these states: M1 is much larger, more than 120% or larger (0), both teeth are subequal, 80% to 120% (1) and M1 is much smaller, less than 80% (2). Similarly, character 106

compares M2 to M3 and character 107 M1 to M3. For all taeniodonts, the area of M2 is larger than M3, and the area of M1 is larger than M3. When comparing M1 to M2 (character 105) *Onychodectes* (AMNH 3405), *Conoryctella pattersoni* (NMMNH P-25056), *Conoryctella dragonensis* (USNM 15704), *Wortmania* (NMMNH P-64001) and *Ectoganus copei* (USNM 12714) have subequal M1 and M2. *Conoryctes* (USNM 22484), *Huerfanodon torrejonus* (USNM 15412) and *Psittacotherium* (USNM 15411) have a much larger area of M1 compared to M2. For *Stylinodon*, all upper molars are subequal in size (state 1 for characters 105, 106 and 107). Even though *Schowalteria* seems to have a larger M2 compared to M1, since these teeth are not complete, they were not scored.

For the lower teeth, characters 108, 109 and 110 compare the size area of the m1 to m2 (ch.108), m2 to m3 (ch.109) and m1 to m3 (ch.110). The states of character 108 are: m1 is much larger, more than 120% or larger (0), both teeth are subequal, 80% to 120% (1) and m1 is much smaller, less than 80%. These states are similar for characters 109 and 110. For all taeniodonts, the area of the m3 is larger than the m2, and the m1 area is larger than the m3. The area of the m1 is subequal to m2 in *Onychodectes* (AMNH 16528, AMNH 3411), *Conoryctella pattersoni* (NMMNH P-25056), *Conoryctes* (USNM 22484, NMMNH P-19976, Figure 15, NMMNH P-54106 Figure A6), *Wortmania* (AMNH 3394), and *Psittacotherium* (UNM NP-220), *Ectoganus copei* (USNM 12714), *Ectoganus bighornensis* (USNM 527725). Only *Huerfanodon polecatensis* seems to have a much bigger area of m1 relative to the m2. The lower molars of *Stylinodon* and *Schowalteria* are all subequal in size (state 1 for characters 108, 109 and 110).

Node 2 in Schoch (1986, figure 56) unites all Conoryctidae because of the following anatomical features.

- “Narrow triangular-shaped P3-P5” which is based on the new nomenclature P4-P5 and I will refer to these numbers using the new nomenclature (Wible, 2009; O’Leary et al., 2013). This is the character “Lingual length of upper molars and posterior premolars” in Eberle (1999), and “Upper molar lingual length” in Rook and Hunter (2011, 2013) and Williamson and Brusatte (2013). In the Shelley_2020 matrix, this is character **ch.77**, comparing the length of P4 relative to the length of the P5. The states for this character are: P4 is much shorter, P4 to P5 length <0.7 (0), P4 is somewhat shorter 0.7 to 0.84 (1), P4 is subequal to P5 0.85 to 0.99 (2), P4 is longer than P5 >1.0 (3). *Onychodectes* (AMNH 16528, AMNH 3405), *Conoryctella pattersoni* (NMMNH P-25056), *Wortmania* (NMMNH P-64001), *Psittacotherium* (USNM 15411), and *Stylinodon* (PM 3895) fall within the range of subequal P4 to P5. The P4 is shorter than the P5 (state 1) for the taxa *Schowalteria* (RTMP 1993.090.0001) and *Conoryctes* (NMMNH P-16200). Specimen USNM 12714 of *Ectoganus copei* has deciduous dP5, so it was not scored for this character

- In the Conoryctidae node, Schoch (1986, figure 56) also included the presence of an “incipient metacone” in the ultimate upper premolar. Only the presence of the metacone was captured in the character “P4 morphology” in Rook and Hunter (2011; 2013) and Williamson and Brusatte (2013) with states “0 = triangular, 1 = submolariform, 2 = molariform”. State 2 indicates the presence of a metacone on the P5(P4). In the Shelley_2020 matrix, the presence of the metacone on the P5 is scored as character **ch.65**, states present (0) and absent (1). *Conoryctes*, *C. pattersoni*, *C. dragonensis*, *Psittacotherium*, *Ectoganus copei*, *E. gliriformis*, *E. bighornensis*, and *E.*

lobdelli (PU 21499), have a metacone on their P5. This is absent in *Wortmania* (Williamson and Brusatte, 2013). Since the teeth are too worn, this is not scored for *Stylinodon*.

The size of the metacone on the P5 is character 66 in the Shelley_2020 matrix and the states are: swelling metacone connate to paracone (0), large metacone and paracone, distinctly separated (1). In all the taxa that a metacone is present, it is a small swelling very close to the paracone (state 1), while only on *Conoryctes* this is more separated (state 2).

- For the lower ultimate premolar Schoch (1986) points out the presence of a “small talonid heel” that is a character in Rook and Hunter (2011; 2013) and Williamson and Brusatte (2013). In the Shelley_2020 matrix, there is a character for the presence and absence of the talonid on the ultimate lower premolar, p5 (**ch.99**) and a separate character for its size (**ch.100**). All taeniodonts that the p5 is known of have a talonid heel. Character 100 is capturing the width of the talonid compared to the trigonid on the p5, either as narrower (state 0) or equally wide (state 1). For the taxa *Schowalteria*, *Onychodectes*, *Huerfanodon polecatensis*, *Conoryctella pattersoni*, *Wortmania*, and *Psittacotherium* the talonid is narrower than the trigonid on the p5. The talonid is as wide as the trigonid on the p5 of *Conoryctes* and *H. torrejonius* (USNM 15412).

Node 3 of Schoch (1986, figure 56) is a feature only for *Onychodectes*.

-Schoch (1986) pointed out that the P4 of *Onychodectes* has “incipient parastyle, stylocone, metastyle and meta-stylocone”. Eberle (1999) captured this in the character “Styles on P4”. In Rook and Hunter (2011) and in Williamson and Brusatte (2013) there are the characters “P4 morphology, states 0=triangular, 1=submolariform,

2=molariform”, also the characters “P4 parastyle”, “P4 stylocone” and “P4 metastyle” with states to capture presence /absence and size. These were later changed to “P5 morphology”, “P5 parastyle”, “P5 stylocone” and “P5 metastyle” in Rook and Hunter (2013) to follow the new nomenclature. These features are not in the Shelley_2020 matrix. I added them as characters **ch.616** “P5 parastyle”, **ch.617** “P5 stylocone” and **ch.618** “P5 metastyle” with the states of “0=absent, 1=present” for all three of these new characters.

Character 616 captures the presence of the parastyle on the P5. All taeniodonts have a parastyle on the P5, while the presence of a stylocone (ch.617) and metastyle (ch.618) varies in Taeniodonta. The taxa that have a stylocone on the P5 are *Onychodectes*, *Conoryctes comma* (NMMNH P-16200, NMMNH P-61799), and *Psittacotherium* (USNM 15411). The taxa that lack a stylocone on the P5 are *Conoryctella dragonensis*, *Conoryctella pattersoni*, and *Schowalteria* (Fox, 2016). The metastyle on the P5 is present in *Onychodectes*, *Conoryctes comma* (NMMNH P-16200, NMMNH P-61799), *Conoryctella pattersoni* (NMMNH P-25056), *Wortmania* (Williamson and Brusatte, 2013), but is absent in *Psittacotherium* (USNM 15411) and *Ectoganus* (Rose *et al.*, 2012).

Nodes 4 and 5 are to distinguish the accessory cuspid that is observed only in two specimens of *Onychodectes*. This study is not on the subspecies level. Some characters will be scored as polymorphic reflecting the variability of *O. tisonensis*. Therefore, this accessory cuspid is not a vital character.

Node 6 in Schoch (1986, figure 56) unites the genera *Conoryctella*, *Conoryctes* and *Huerfanodon*.

-The anatomical feature mentioned by Schoch (1986) is the reduced paraconids and very narrow molars. In Rook and Hunter (2011) this was turned into the character “Paraconids” with the states “0=small, 1=moderate, 2=large” and “Paraconids versus metaconids” with states “0=not equal, 1=subequal”. Similarly, these are found in Rook and Hunter (2013) and Williamson and Brusatte (2013). In the Shelley_2020 matrix, the presence/absence of paraconid is captured by character **ch.210** and its height is compared to the metaconid by character **ch.213**. For the narrow molars, there is the character **ch.237** in the Shelley_2020 matrix to measure how narrow the lower molars are by comparing the talonid to the trigonid width.

Character 213 in Shelley_2020 is comparing the height of the paraconid to the metaconid with the states: paraconid shorter than metaconid (0), subequal to metaconid (1) and paraconid taller than metaconid (2). For all the taeniodonts, that this is scored, the paraconid is shorter than the metaconid.

Character 237 is comparing the talonid width to the trigonid of the lower molars. The states of this character are: very narrow trigonid, subequal to the base of the metaconid (0), talonid narrower than trigonid (1), talonid subequal to wider than trigonid (2). The width of the talonid is subequal to the trigonid in the taxa *Onychodectes* (AMNH 16528), *Conoryctes* (NMMNH P-54106, Figure A6, NMMNH P-19976, Figure 15), *Huerfanodon torrejonius* (USNM 15412), *Huerfanodon polecatensis* (YPM PU 14718), *Conoryctella pattersoni* (NMMNH P-25056), *Ectoganus copei* (USNM 12714), *E. gliriformis* (AMNH 4286), *E. bighornensis* (USNM 527725) and *Wortmania* (NMMNH P-64001). Only the lower molars of *Schowalteria*

and *Psittacotherium* (AMNH 754 m1, USNM 1017 m2?) have a narrower talonid than trigonid.

Nodes 7, 8 and 9 in Schoch (1986, figure 56) describe the two species of *Conoryctella*.

- One of the features is “lower canine triangular in cross-section and deeply rooted”. The shape is due to the wear of the tooth and similarly to the enamel distribution, I did not score a feature that is a product of wear, since this could lead to the misidentification of unworn specimens. As for the roots of the lower canines, that is also a character in Rook and Hunter (2011; 2013) and Williamson and Brusatte (2013). In the Shelley_2020 matrix, character **ch.34** describes the size of the lower canines and **ch.35** the number of the roots.

Character 34 captures the size of the lower canines, and the states are enlarged (0) and small (1). The number of roots for the lower canine, character 35, has the states: two (0) and one (1). All taeniodonts, whose lower canine is known, have an enlarged lower canine with one root.

- Another feature that is used in Schoch (1986) to distinguish the two species of *Conoryctella* is the “slightly more molariform” P5. As mentioned above, that could be the shape and the presence of cusps and conules on the P5. In the Shelley_2020 matrix, there are characters about the presence and morphology of protocone, metacone, lobes, and conules of the ultimate upper premolar (**ch.63-66, 74, 75**), capturing what previous studies meant by “molariform premolar”. Characters 65 and 66 in Shelley_2020 have been described above.

Character 63 is capturing the presence of the protocone in P5, states are present (0) and absent (1). All taeniodonts that are known from P5, are scored as having a protocone on the P5.

The size of the protocone relative to the paracone on the P5 is scored for character 64. The states are the protocone is smaller than the paracone (0), and the protocone approaches the paracone in height (1). This is not scored for many members of Taeniodonta because the protocone is usually too worn to capture its height. Even in less worn specimens like NMMNH P-61799, the protocone is worn and seems to be smaller than the paracone, but it is unclear if this is due to wear.

The presence of paraconule on the P5 is captured in character 74, with the states absent (0) and present (1). Character 75 is scored for the presence of the metaconule on P5 as absent (0) and present (1). All taeniodonts lack paraconules. *Onychodectes* (AMNH 3405) and *Conoryctella pattersoni* (NMMNH P-25056) are the only taeniodonts that there is a potential presence of a metaconule on the P5. Schoch proposed the presence of paraconule and metaconule on the P5 for *Psittacotherium* and *Ectoganus* (*Psittacotherium* AMNH 16731, *E. copei* FMNH P 15575, *E. gliriformis* PU 13173, *E. lobdelli* PU 21499). I was able to see that only in the specimens of *Ectoganus*.

Node 10 (Schoch, figure 56) has common anatomical features that unite *Conoryctes comma* and the two species of *Huerfanodon* and these are the following.

-The absence of P1 and molariform P5 are the characters used by Schoch (1986). The P5 has been described above. The character "P1 presence" is also a character in previous studies (Rook and Hunter, 2011; 2013; Williamson and Brusatte, 2013). In

the Shelley_2020 matrix, this is captured by character **ch.39** “Number of premolars”. It would be better if there was a character for the presence/absence of all teeth separately, but to avoid homoplasy this was done differently. Character 39 for the number of premolars has the states: five, including retained dP3 (0), four (1), three (2), two or less (3). All taeniodonts, whose number of premolars is known, are scored as having four (state 1), apart from *Conoryctes* which has three (AMNH 3396, NMMNH P-61799 figures 12 and 13). Specimen USNM 15412 of *Huerfanodon torrejonius* is missing some premolars, and it is believed to have only three upper premolars (Schoch and Lucas, 1981b).

Node 11 in Schoch (1986, figure 56) has a characteristic for *Conoryctes comma*. This is the presence of very small paraconids. This is a character in the Shelley_2020 that was described above, Character 213 (**ch.213**).

Node 12 has characteristics that are seen in *Huerfanodon*.

-There is a submolariform P3 (P4 with the current nomenclature). In Eberle (1999), there is a character “Upper premolar morphology” that describes the presence of molariform/non-molariform premolars. This is later used only for the penultimate upper premolar in later studies as “P3 morphology” with the states of “0=triangular, 1=submolariform, 2=molariform” (Rook and Hunter, 2011; 2013; Williamson and Brusatte, 2013). In the Shelley_2020 matrix, this is captured in characters **51**, **52**, and **54**.

Character 51 is scoring the presence of a protocone on the P4, with the states absent (0) and present (1). The development of the protocone on the P4 is captured in character 52 and is either a small lingual bulge (0) or large and basined (1). The

taeniodonts that have a protocone that is large and basined (state 1) on the P4 are *Onychodectes* (AMNH 16528), *Huerfanodon torrejonus* (USNM 15412), *Wortmania* (NMMNH P-64001), *Ectoganus copei* (USNM 12714), *E. gliriformis* (PU 21499), *Psittacotherium* (USNM 15411). Looking into various specimens of *Conoryctes comma*, some specimens seem to have a protocone (NMMNH P-61799, AMNH 3396 NMMNH P-16200) that is just a lingual bulge, but the protocone is absent in other specimens of the same genus (AMNH 3398). Also, *Schowalteria* could potentially have a protocone on the P4, but it is not clear due to wear, so it was not scored for character 51.

The presence of a metacone on the P4 is scored in character 54 as absent or vestigial (0) or as present (1). All taeniodonts are scored as having a vestigial metacone on the P4.

-The characteristic used by Schoch for *Huerfanodon* is a well-developed mesostyle on the upper molars. The size of the mesostyle in the upper molars is character “M1 and M2 mesostyle” with states “0=absent, 1=small, 2=moderate and 3=well-developed” in later studies (Rook and Hunter, 2011; 2013; Williamson and Brusatte, 2013). In the Shelley_2020 matrix, there is a character for the presence/absence of the mesostyle, **ch.129** “Upper molar stylar cusp C mesostyle”. The reason why there is no other character to describe the size of the mesostyle is because while studying the specimens, particularly of *Conoryctes* and *Huerfanodon*, the mesostyle is very variable even between the left and right sides of individuals. This is seen in specimen NMMNH P-16200, on which the mesostyle is prominent on the molars of the left side, but not so on those on the right side (Figure 20).

- Another feature is the “internal groove” of the lower canine. This is modified in Eberle (1999) as “Wear pattern on upper molars and premolars” with the states “0=not pronounced over the entire occlusal surface, 1=pronounced over the entire occlusal surface, i.e. taeniodont-like”. This was also a character in the studies that followed (Rook and Hunter, 2011; 2013; Williamson and Brusatte, 2013). Similar to the “level of hypsodonty”, this is a characteristic of taeniodonts that is prone to the level of wear. This could lead to problems when there is an unworn canine with the “internal groove” and enamel, whereas when worn it would look like the rest of the worn canines of taeniodonts. Therefore, it is not captured by Shelley_2020 and I did not create a new character.

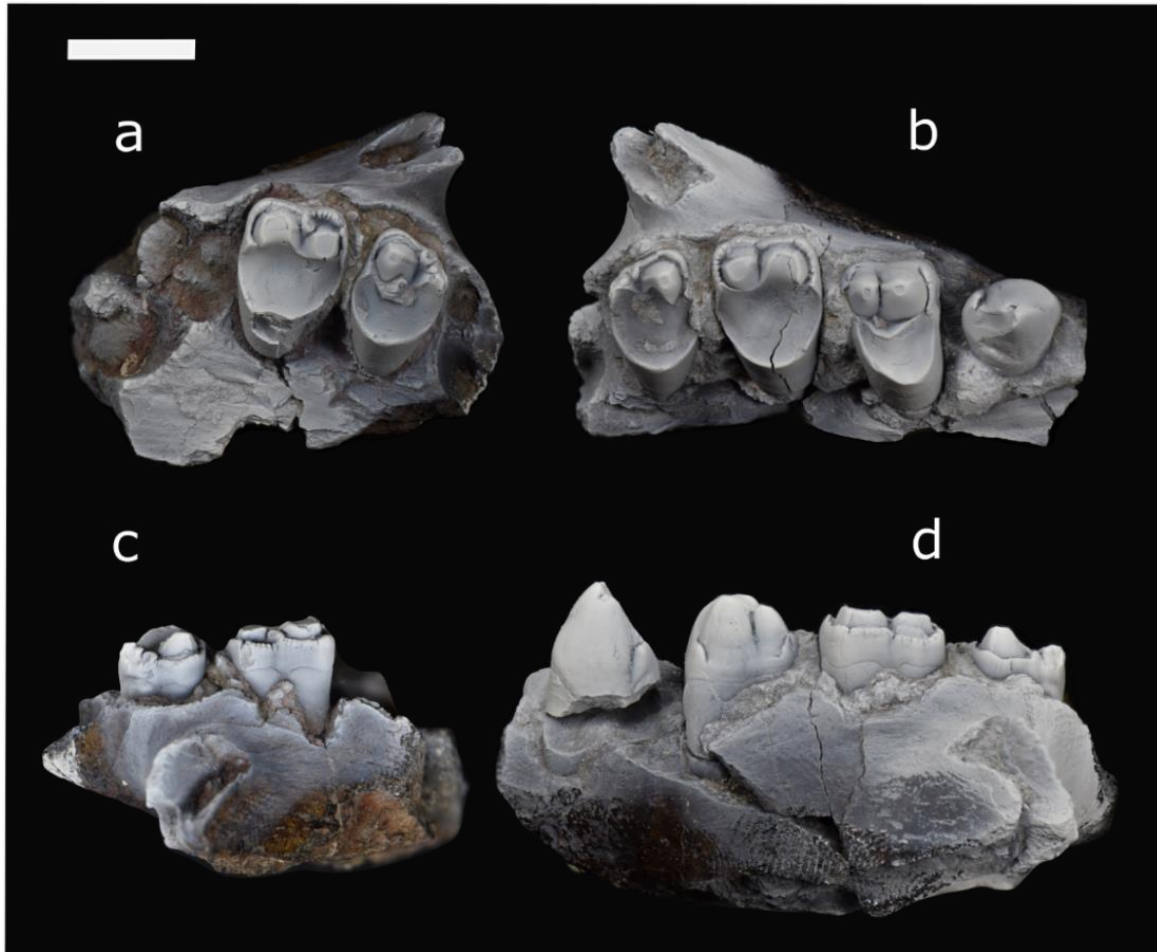


Figure 20: Upper teeth of specimen NMMNH P- 16200, *Conoryctes comma*, in occlusal view left side (a) and right side (b) and in buccal view left side (c), right side (d). Notice the prominent mesostyle on the left M1 and M2 (a and c) and only a minuscule mesostyle on the right M1 (b and d). Scale bar is 1cm.

Node 14 as seen in Schoch (1986, figure 56) points out the difference between *Huerfanodon torrejonius* and *Huerfanodon polecatensis*.

- A noticeable difference on the contrary between *Huerfanodon torrejonius* and *H. polecatensis* is the presence of a metaconid on the ultimate lower premolar in the latter. This is found as character “p4” / “p5 morphology, 0= nonmolariform, 1= submolariform, 2= molariform” in the latest analyses (Rook and Hunter, 2011; 2013; Williamson and Brusatte, 2013). In the Shelley_2020 matrix, there is the character,

ch.95 for the presence (0), and absence (1) of a metaconid in the ultimate lower premolar. The ultimate premolar of *Huerfanodon polecatensis* (YPM PU 14718), *Psittacotherium* (Schoch, 1986), *Ectoganus lobdelli* (PU 18994) and *E. gliriformis* (PU 13713) have a metaconid on the p5. This is not seen in the taxa of *Conoryctella pattersoni* (NMMNH P-25056), *Conoryctes comma* (NMMNH P-54106), *Huerfanodon torrejonius* (USNM 15412) and *Onychodectes* (AMNH 16405).

Node 15 in Schoch (1986) has characteristics that unite all Stylinodontidae.

-One of these is the large canines, which is in the Shelley_2020 matrix, character **ch.34** for the lower canines and it is as described above. Character 31 is scored for the upper canines as either enlarged (0) or small (1). All members of Taeniodonta are scored as having enlarged upper canines.

- Another feature seen in Stylinodontidae based on Schoch (1986) is the transversely placed premolars on the jaw. This is seen in Rook and Hunter (2011) as the character "Premolars set obliquely" and it is in the other analyses on taeniodonts that followed. In the Shelley_2020 matrix, this is scored with character **ch.80** "First lower premolar p1 orientation, 0=in line with the jaw axis, 1=oblique". The lower p1 is known for few taxa, and even fewer of them are found in the jaw, making this character unscored for many taxa. *Schowalteria* (RTMP 1993.090.0001) has the p1 placed in line with the jaw, whereas *Onychodectes* (AMNH 16528), *Wortmania* (AMNH 3394), *Conoryctes* (USNM 22484, NMMNH P- 54106), *Psittacotherium* (AMNH 754) have this set obliquely in the jaw.

- The stylinodontids are known for having robust limb bones and claws modified for scratch digging. None of the phylogenetic analyses performed for taeniodonts include

postcranial characters. In the Shelley_2020 matrix, the robustness of the skeleton is captured with **ch.544**.

The extension of the humeral deltopectoral crest relative to the humeral shaft is scored in character 544. The states are: does not extend beyond 50% of the length of the humerus shaft (0), extends distally over 50% of the length of the shaft (1). *Onychodectes* (AMNH 16528), and *Ectoganus copei* (FMN 26090) have a humerus that the deltopectoral crest is not extending more than 50% of the total length of the humerus (state 0). However, the very robust *Stylinodon* (YPM 11096) has a very distally protruding deltopectoral crest (state 1).

-Another feature pointed out for Stylinodontidae, is the presence of recurved claws on the manus. This is not a well-defined character, and the level of “recurved” claw is not set in a measurable way. Also, this is not only seen in Stylinodontidae, as proposed by the new postcranial elements of *Conoryctes comma* (see chapter three). For the purpose of this study -and since all the taxa of whom the ungual phalanges of the manus are known, have recurved claws- this is not a helpful character for understanding the inner phylogeny of taeniodonts, so this was not added to the matrix.

Node 18 of Schoch (1986, figure 56) has features for *Ectoganus* and *Psittacotherium*.

-These are the number of incisors, that was turned into “upper incisor number” and “lower incisor number” phylogenetic characters in Rook and Hunter (2011; 2013) and Williamson and Brusatte (2013). These are characters **ch.11** and **ch.12** respectively in the Shelley_2020 matrix. The number of incisors is unknown for most of the studied taxa. *Onychodectes* (AMNH 16528) has three upper and three lower incisors,

Conoryctes (USNM 22484, AMNH 15939) has only two upper and three lower incisors, *Wortmania* (AMNH 3394) and *Psittacotherium* (AMNH 754) have one upper and one lower. *Ectoganus copei* (USNM 12714) has two upper incisor and *E. gliriformis* (AMNH 4286) has one lower incisor. *Stylinodon* (PM 3895) has two upper incisors and one lower incisor.

Node 17 in Schoch (1986, figure 56) is uniting *Psittacotherium*, *Ectoganus* and *Stylinodon* based on the well-developed hypsodonty. Other nodes (20,26) also refer to the hypsodonty of the premolars and the molars.

-To capture the extreme level of hypsodonty for the more derived forms of Taeniodonta I added in the Shelley_2020 matrix four new characters. Characters **ch.624** and **ch.625** are regarding the presence/absence of hypselodonty in the upper premolars and molars respectively. The characters **ch.626** and **ch.627** are for the lower premolars and molars hypselodonty.

Character 624 is scored for the absence (0) or presence (1) of hypselodonty on the upper premolars. It is scored as absent in all taeniodonts, apart from *Stylinodon*. The presence of hypselodont upper molars is scored in character 625, with the states absent (0) and present (1). This is also scored as present only for *Stylinodon* (PM 3895, Turnbull, 2004).

Character 626 is scored for the presence of hypselodont lower premolars, absent is state 0 and present is state 1. The hypselodonty of the lower molars is scored in character 627 as absent (0), or present (1). Both of these characters (ch.626 and ch.627) are scored as present only for *Stylinodon* (PM 3895, Turnbull, 2004).

Node 19 is a character that is seen only in *Psittacotherium* (Schoch, 1986, figure 56).

-When it comes to the postcranial anatomy Schoch (1986) pointed out the small third trochanter of the femur in *Psittacotherium*. This is character **ch.569** in the Shelley_2020 matrix: “Femur third trochanter size, 0=large, 1=moderate, 2=small”. In the current study, this is scored for other taxa too. It is scored as moderate for *Onychodectes* (AMNH 3405), *Conoryctes* (NMMNH P-79457, see chapter three), and *Wortmania* (AMNH 3394) and as small for *Psittacotherium* (AMNH 16560), *Ectoganus gliriformis* (Schoch, 1986) and *Stylinodon mirus* (UW 2270).

In node 20 (Schoch, 1986, figure 56), the term “bilophodont molars” is mentioned. This was later made into a phylogenetic character in the phylogenetic studies (Rook and Hunter, 2011; 2013; Williamson and Brusatte, 2013). I believe this is not a “true bilophodont” tooth as mentioned in Scot and Symon (1952) but have a similar shape. This is due to the presence of the “hypocone” in *Ectoganus*, which is addressed in length below. To avoid any homoplasies with other taxa, I did not score this as a character in the matrix of the current study.

Node 27 in Schoch (1986, figure 56) states the characteristics seen in *Stylinodon*.

-What is very typical for *Stylinodon* is the elongation of the enlarged p1 and P1. There are no characters to score these in the Shelley_2020 matrix, and so I added two characters (**ch.628** and **629**).

Character 628 is capturing the size of the lower premolar p1 with the states: smaller than posterior premolars (0), and longer than posterior premolars (1). Similarly, character 629 is scored for the upper anterior premolars (0=smaller than posterior premolars, 1=longer than posterior premolars). In all taeniodonts, both upper and lower anterior premolars are smaller than the posterior upper and lower premolars respectively. Apart from *Stylinodon* (UW 2270, PM 3895) that has very long anterior premolars compared to the posterior ones, both for the upper and the lower premolars.

There are a few phylogenetic characters in Eberle (1999), Rook and Hunter (2011; 2013) and Williamson and Brusatte (2013) that are not mentioned in Schoch (1986). These are the presence of metacrista, the development of ectoflexus and the styler margin on the upper molars. There are phylogenetic characters for these features in the Shelley_2020 matrix (**ch.146, 136, 137, 119-123**).

Character 146 is capturing the presence of the postmetacrista (absent=0 and present=1). All taeniodonts have a postmetacrista, apart from *Psittacotherium* and *Ectoganus copei*.

The ectoflexus is scored in the Shelley_2020 matrix for its presence, character 136 (present=0, absent=1), and the development on the molars is scored as character 137. The states of ch.137 are present only on the penultimate molar M2 (0), present on the penultimate and preceding molars M1, M2 (1), present on all molars (2), present on M2 and M3 (3). All members of Taeniodonta are scored as lacking ectoflexus, apart

from *Schowalteria* (RTMP 1993.090.0001) which has an ectoflexus at least on the M1 and M2 (M3 is missing).

There are many characters in the Shelley_2020 to describe the morphology of the styler margins of the upper molars. Character 119 is for scoring the presence of the parastylar lobe (present=0, absent=1) on the upper molars and character 120 is for the metastylar lobe (present=0, absent=1) on the upper molars. All taeniodonts have a parastylar lobe on the upper molars apart from *Ectoganus copei* (USNM 12714), *E. gliriformis* (AMNH 16244, Schoch, 1986), *E. bighornensis* (USNM 527725). The metastylar lobe is also present in all taeniodonts on the upper molars, apart from *Psittacotherium* (USNM 15411), *E. copei* (USNM 12714), *E. gliriformis* (AMNH 16244, Schoch, 1986) and *E. bighornensis* (USNM 527725). Using the M3 of PU 16102 shows that there is probably no parastylar, nor a metastylar lobe on the upper molars of *Stylinodon*.

The buccal extent of the parastylar and metastylar lobes is captured by character 121. The states for this character are: parastylar more buccal (0), lobes subequal (1), metastylar more buccal (2). The parastylar reaches more buccally in the upper molars of *Schowalteria*, *Onychodectes* (AMNH 3405, AMNH 16405) and *Wortmania* (NMMNH P-64001). The lobes are reaching the same level (state 1) in the taxa *Conoryctes* (NMMNH P-16200), *H. torrejonius* (USNM 15412) and *Conoryctella pattersoni* (NMMNH P-25056), *Conoryctella dragonensis* (USNM 15704). Moreover, for the taxa mentioned above that lack a parastylar lobe and/or a metastylar lobe, character 121 is considered inapplicable.

For the relative position of the parastylar lobe to the paracone on the M1, character 122 is describing this with the states: anterolabial to paracone (0), anterior

to paracone (1). The parastylar lobe on the M1 is anterolabial to the paracone in all taeniodonts.

The size of the parastylar lobe is scored with character 123. The width of the parastylar lobe is measured to the stylocone (or the stylocone position) on the M2. The states for this character are the parastylar width is more than 30% of the total width (0), less than 30% but more than 20% (1), and 20% or less (2). All taeniodonts have a parastylar lobe whose width is 20% less than the total width of the tooth (state 1). Apart from the taxa *Schowalteria* (RTMP 1993.090.0001) and *Onychodectes* (AMNH 3405, AMNH 16405) that the width of the parastylar lobe is between 30% and 20% of the total width of M2.

Lastly, there is a character introduced by Eberle (1999) that was used by Rook and Hunter (2011; 2013) called “Relative Transverse Width (RTW) of upper molars” and is calculated by dividing the “Maximum Transverse Width” to the “Anteroposterior length” of the upper molars. In the Shelley_2020 matrix character **ch.115** “Upper molar M2 shape” calculates the shape of M2 by dividing the maximum mesio-distal (=anteroposterior) length to the maximum buccal-lingual (=transverse) width. Therefore character ch.115 is the inverse RTW fraction. Since the information captured is the same, I did not add this as a new character in the matrix. Taxa *Onychodectes*, *Huerfanodon torrejoni*, *C. pattersoni*, *C. dragonensis*, *Psittacotherium* and *Ectoganus copei* are scored as wider than long. Taxa *Conoryctes*, *Wortmania* and *Stylinodon* have a much wider than long M2.

To sum up, all the characters mentioned by previous studies that attempted to explain the interrelationships of taeniodonts are included in the matrix of the current

study. The new characters mentioned above that I added to the Shelley_2020 matrix based on these previous studies are:

Ch.616: P5 parastyle, 0=absent, 1=present

Ch.617: P5 stylocone, 0=absent, 1=present

Ch.618: P5 metastyle, 0=absent, 1=present

Ch.624: Upper premolars hypselodonty, 0=absent, 1=present

Ch.625: Upper molars hypselodonty, 0=absent, 1=present

Ch.626: Lower premolars hypselodonty, 0=absent, 1=present

Ch.627: Lower molars hypselodonty, 0=absent, 1=present

Ch.628: Lower anterior premolars size, 0=smaller than posterior premolars, 1=longer than posterior premolars

Ch.629: Upper anterior premolars size, 0=smaller than posterior premolars, 1=longer than posterior premolars

Based on new observations on Taeniodonta

In order to include more information on taeniodonts in the dataset, some new characters were added to describe anatomical features in the upper (**ch.619, 620**) and lower teeth (**ch.621-623**).

As it is already captured in the dataset, all taeniodonts lack a well-distinguished postcingulum and a true hypocone, a cusp that originates from the postcingulum (Hunter and Jernvall, 1995; de Muizon *et al.*, 2019). However, Schoch and Lucas

(1981b) in the diagnosis of the genus *Huerfanodon* added the presence of a hypocone on the P5. Later, Schoch (1986) mentions that there is a hypocone on the upper molars of the more derived forms, such as a minuscule hypocone seen in *Psittacotherium* and a large one in *Ectoganus*. For this, he also stated that the “metacone-hypocone” of *Ectoganus* is due to the splitting of the protocone. In his attempt to visualize the relationships of Taeniodonta Schoch (1986, figure 56) uses the absence of a hypocone or “developed by a splitting-off from the protocone” to unite all taeniodonts. Patterson (1949b) when writing on Stylinodontidae, named that cusp as a postero-internal cusp and put the word “hypocone” in parenthesis. While describing a new specimen of upper dentition and partial lower jaw of *Ectoganus bighornensis* Rose *et al.* (2012) named that cusp a hypocone joined with the metacone thus creating a metaloph.

Studying the holotype of *Huerfanodon torrejonius*, the type species of the genus, it is clear that there is no hypocone on the P5 since there is no postcingulum. The upper molars of the species also lack a hypocone and a postcingulum, and on the right M2, there is a twinned metaconule. The right and left upper molars of *Psittacotherium* (NMMNH P-30630, TMM 40537-61 and TMM 40537-33) also show two cusps in the metaconular area. In the specimens of *Ectoganus* (better seen in USNM 12714) there is a large cusp, in the hypocone position, however, there is no hypocone. Given that a true hypocone is not seen in earlier taeniodonts and the lack of postcingulum, I believe that the distolingual cusp in *Ectoganus* is not a true hypocone (Hunter and Jernvall, 1995; Muizon *et al.*, 2019). It would have functionally served as a hypocone; however, this cusp does not originate from a postcingulum to be named a true hypocone. This distolingual cusp is either a duplication of the protocone or a metaconular pseudohypocone.

One way to examine the origin of the distolingual cusp in USNM 12714, *Ectoganus copei*, is by tracing the Enamel Dentine Junction (EDJ) of the left M1. Anemone *et al.* (2012) when investigating the origin of the pseudohypocone in Eocene primates studied the morphology of the crests using EDJ. The EDJ helps to identify the morphological development of the tooth crown and they pointed out how useful this is for worn teeth. Following the same technique as in Anemone *et al.* (2012), the EDJ was traced to evaluate the relationship between the distolingual cusp and the metaconule and protocone.

Specimen USNM 12714 of *Ectoganus copei* was scanned using CT (voxel size 0.0573) and the files were processed in Avizo Lite 2019.4. The M1 was used to check the origin of the distolingual cusp by tracing and segmenting the Enamel Dentine Junction (EDJ). Then using the “Generate Surface” module the EDJ surface was created. Figure 21 shows the EDJ on the M1 in purple, while the dentine is in red for the whole tooth and in green for the distolingual cusp. Where the dentine is exposed, on the protocone area, there is no EDJ.

In Figure 21 there is a clear separation of the EDJ between the protocone and the distolingual cusp. A cross-section of the M1 (Figure 22) shows that the enamel is separated between the protocone and the distolingual cusp. The enamel is including the distolingual cusp and the metaconule (Figure 22). Therefore, *Ectoganus* does not have a hypocone, but a distolingual cusp that originated from a lingual shifting of a metaconule.

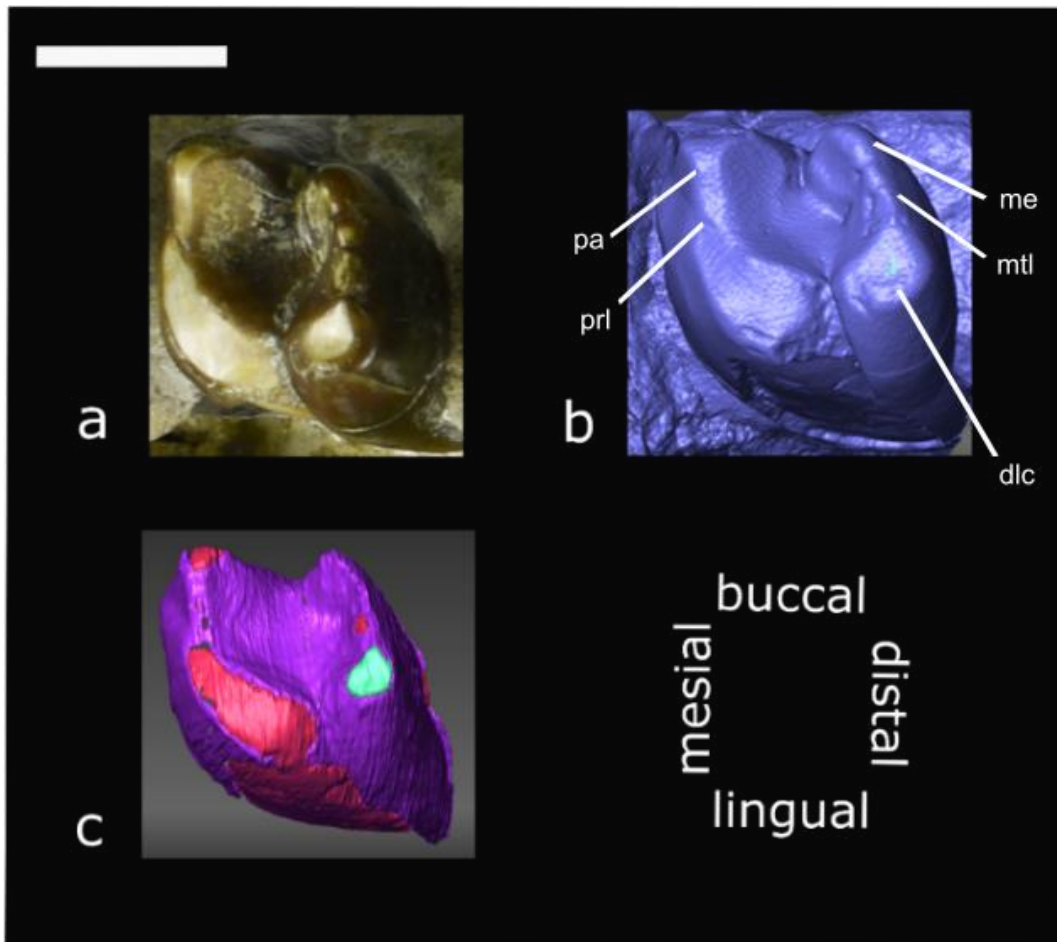


Figure 21: The left M1 of USNM 12714, *Ectoganus copei*. Photo of the M1 in occlusal view (a), representation of the M1 after scanned and processed in Avizo (b). The surface model of the EDJ (c), with purple colour is the EDJ, with red and green is exposed dentine with red and green is exposed dentine where EDJ is worn, the green patch of the dentine is the distolingual cusp. pa: paracone, prl: paraconule, me: metacone, mtl: metaconule, dlc: distolingual cusp. Scale bar is 1 cm.

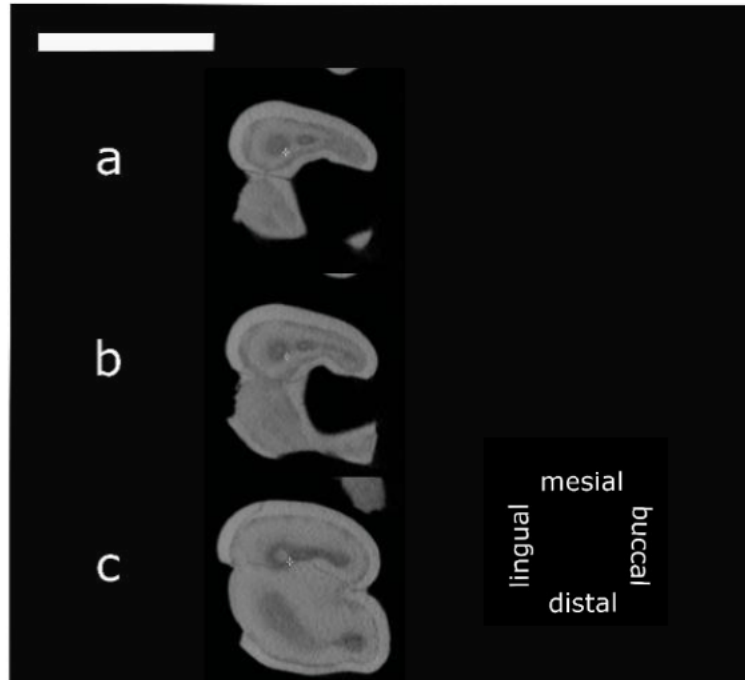


Figure 22: A cross-section of the M1 (USNM 12714), *Ectoganus copei*, on different levels starting from near the occlusal surface of the tooth (a), towards the root (c). Scale bar is 1cm.

This is based only on one specimen and the EDJ needs to be tested on other specimens of *Ectoganus*. Moreover, as pointed out by previous researchers, changes in the occlusal function need to be tested with both the upper and lower dentition (Van Vale, 1994; Davis, 2011). A study that focuses on the upper and lower teeth will give a complete image of the dental morphology of *Ectoganus* and help in understanding the formation of the distolingual cusp. Similarly, it would be worth looking into the less worn teeth of *Stylinodon*.

The study of the upper molars of *Huerfanodon*, *Psittacotherium* and *Ectoganus* shows that there needs to be a character in the Shelley_2020 to capture the presence of two metaconules on the upper molars. This is character **ch.620**, “twinned metaconule on upper molars”, and the states are absent (0) and present (1). The twinned metaconule is present in *Huerfanodon torrejonus* and *Psittacotherium*. It

could possibly be present in other Taeniodonta, but that is not possible to examine given the high level of wear.

To capture the distolingual cups on the upper molar of *Ectoganus* character **ch.619** was added in the Shelley_2020 matrix. Character 619 “distolingual cusp on upper molars” has the states absent (0) and present (1). This was scored only as present for *Ectoganus* (Figure 23).

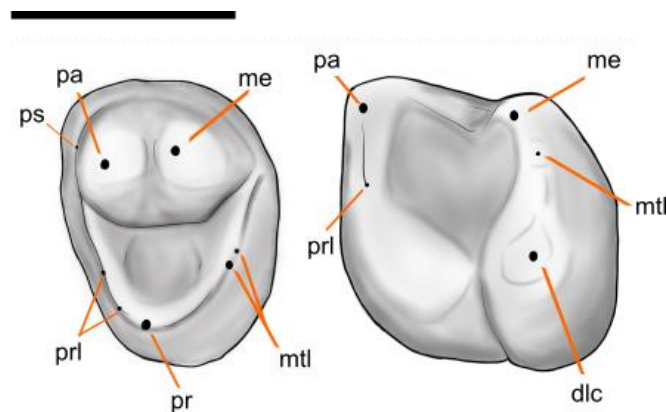


Figure 23: Drawing of the M2 of *Psittacotherium multifragum* (NMMNH P-30630) on the left and of the M1 of *Ectoganus copei* (USNM 12714) on the right. pa: paracone, me: metacone, ps: parastyle, prl: paraconule, pr: protocone, mtl: metaconule, dlc: distolingual cusp. Scale bar is 1cm.

Regarding the lower dentition, some taxa of taeniodonts have more cuspid than others. There is an extra cuspid in the lingual view, distally to the entoconid. To distinguish that extra cuspid, I named the mesial cuspid pre-entoconulid (i.e entoconulid), and the distal cuspid post-entoconulid (Figure 24). The presence of these cuspid is added in the Shelley_2020 matrix as **ch.621** and **ch.622**. Character 621 is “lower molar pre-entoconulid, 0=absent, 1=present” and character 622 is “lower molar post-entoconulid, 0=absent, 1=present”. The pre-entoconulid is present in various taxa and is polymorphic for *Onychodectes*. The post-entoconulid is only

scored as present for *Conoryctes* and *Huerfanodon torrejonus*, and *Onychodectes* and *Conoryctella* are lacking one (Figure 24).

Another addition on the lower molars are small cuspids in the hypoconulid position; these are not well-separated. Therefore, I added a character (**ch.623**) to capture the presence of more than one hypoconulid in that area. Character 623 is described as “lower molars multicuspid in the hypoconulid position” and the states are absent, hypoconulid consists of one cuspid (0) and present, more than one cuspid (1). In case there is no hypoconulid on the lower molars, this character is inapplicable. *Onychodectes* has only one hypoconulid (Figure 24) and so does *Ectoganus*. The lower molars of *Conoryctes* (NMMNH P-47921) and *Huerfanodon torrejonus* (USNM 15412) have a multicuspid hypoconulid. The lower m3 of a young *Psittacotherium* (USNM 15413) shows that there are many cuspids in the hypoconulid area too. This is also seen in the new lower molar of *Psittacotherium*, NMMNH P-19800 (Figure A20 in the Appendix). Figure 24 has drawings of some taeniodonts lower molars to point out the presence of pre- and post-entoconulid as well as the numbers of cuspids in the hypoconulid area.

Summarizing, the characters added to Shelley_2020 based on my observations on Taeniodonta are:

Ch.619: Distolingual cusp on upper molars, 0=absent, 1=present

Ch.620: Twinned metaconule on upper molars, 0=absent, 1=present

Ch.621: Lower molars pre entoconulid, 0=absent, 1=present

Ch.622: Lower molars post entoconulid, 0=absent, 1=present

Ch.623: Lower molars multicuspid in the hypoconulid position, 0=absent one cuspid as hypoconulid, 1=present more than one cuspid

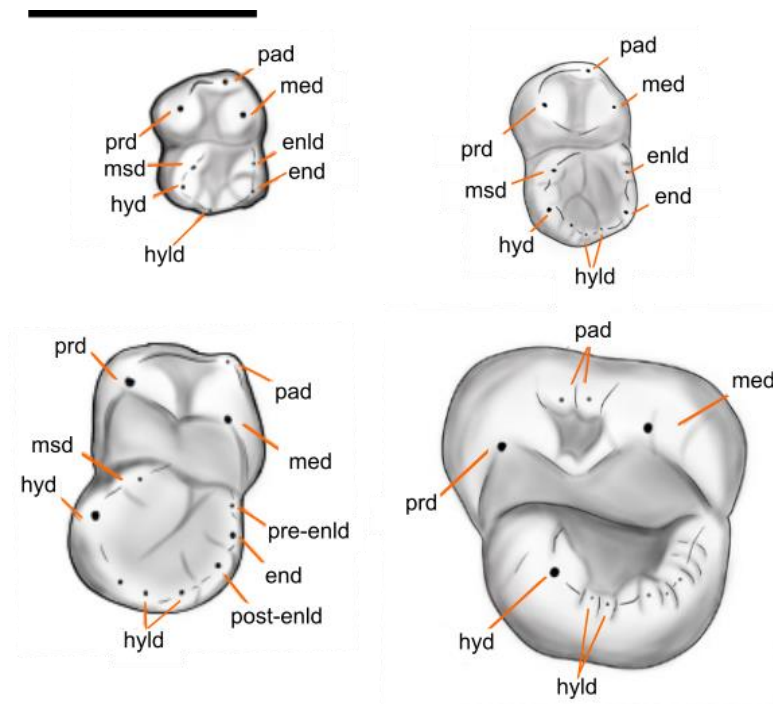


Figure 24: Drawing of *Onychodectes tisonensis* (NMMNH P- 46299, m2) on the top left, *Conoryctella pattersoni* (NMMNH P-53835, m2) top right, *Conoryctes comma* (NMMNH P-47921, lower molar) bottom left, and *Psittacotherium multifragum* (NMMNH P-19800, lower molar) bottom right. pad: paraconid, med: metaconid, prd: protoconid, msd: mesoconid, hyd: hypoconid, hyld: hypoconulid, post-enld: post-entoconulid, end: entoconid, pre-enld: pre-entoconulid. Scale bar is 1cm.

Methodological Protocols

Cladistics

As mentioned above, there were a few modifications on the Shelley_2020 matrix, mostly adding taxa and characters to help with the understanding of taeniodonts phylogeny. So, the matrix of the current study consists of 630 characters, 78 of which are ordered, and 134 scored taxa, with *Nanolestes* being the outgroup as proposed previously (Shelley 2018; Wible *et al.*, 2009). To analyse the matrix, the software TNT v1.5 (Goloboff *et al.*, 2008) was used to perform phylogenetic analysis with maximum parsimony as the optimality criterion.

Firstly, the matrix was analysed under the New Technology search, using the sectorial search (Goloboff, 1999), ratchet (Nixon, 1999), drift (Goloboff, 1999) and tree fusing (Goloboff, 1999) options, with default parameters. Sectorial search is used when working on a large dataset that has more than 100 taxa and 100 characters because it creates reduced datasets which are then subjected to additional search (Goloboff *et al.*, 2008). The ratchet search uses Tree Bisection Reconnection (TBR) method and consists of two phases: perturbation (using original weights, upweighting or deleting) and search (Nixon, 1999). The drift algorithm is similar to the ratchet algorithm, but instead of reweighting the characters in the perturbation phase evaluates the tree-swapping based on the relative and absolute fit difference (Goloboff, 1999). The tree fusing evaluates the sub-tree exchanges performed by the previous searches and keeps those with the best score (Goloboff *et al.*, 2008). Lastly, a driven search was selected, meaning the above calculations continued until the best score (the minimum tree length) is found at a given set of times. In this analysis,

replications ran until the minimum tree length was found 10 times and then the trees were saved in RAM. The trees that were generated after the New Technology search were then analysed under the Traditional search that uses only a Tree Bisection reconnection (TBR) branch-swapping algorithm.

After the combination of these analyses, the consistency index, and the retention index were calculated. The consistency index (CI) measures the amount of homoplasies in the dataset which are less if the CI value is closer to 1. The retention index (RI) accounts for how well the synapomorphies explain the trees. The support of individual clades was calculated with the absolute and relative Bremer's support values and the Jackknife percentages (Goloboff *et al.*, 2008). The Bremer support quantifies the number of steps needed to make a clade fall apart in the strict consensus tree. The smaller a number is, the easier it is to break that branch, therefore the weaker the clade is. The Jackknife technique uses the trees produced from the TBR, which is done after the New Technology Search and is a resampling procedure. During Jackknife the topology is analysed again, and characters are deleted randomly without replacement. For this reason, the topology produced after this analysis is not necessarily the same as the consensus tree. The percentage of each node shows the percentage that it was recovered in the analysis, being an estimator of accuracy. The higher the percentage, the more times this node had been found during this analysis and the stronger the support is.

From the pool of trees found after the New Technology search and the Traditional search methods, the relative and absolute Bremer support values were calculated. The Jackknife percentages were later calculated. The Jackknife technique is estimating the variability in the tree by reanalysing the phylogeny as characters are

randomly deleted. This analysis was done with output results as absolute frequencies, using a traditional search for the resampling.

A pruning of poorly known taxa was done a posteriori calculating the Bremer support values. The taxa that were eliminated were scored for less than the median of the unscored characters in the dataset. The unscored characters are 49,922 and so, only taxa that were scored for over 370 characters were used. Figure A31 in the Appendix shows a pruned a posteriori Bremer support consensus tree. I also include *Nanolestes* which is set as the outgroup and *Ambilestes* which is set as an outgroup for Cimolesta.

Time calibrated Phylogeny

For this analysis, the software R and the cal3 time-scaling methodology, which is proposed by Bapst (2014) and used by Bertrand *et al.* (2021), were used. A copy of the code can be found in the Appendix, as well as the time intervals and FAD and LAD of the taxa used (tables A5-A6a,b). For this analysis, I used only part of the consensus tree, which includes only the species *E. copei* and *E. gliriformis*. The polytomy seen in the strict consensus tree after the analyses is probably due to the lack of scored characters for the species *E. bighornensis* and *E. lobdelli*, therefore they were excluded. The taxa that were used are: *Puercolestes simpsoni*, *Procerberus formicarum*, *Procerberus* sp.cf. *P. grandis*, *Prodiacodon crustulum*, *Prodiacodon puercensis*, *Escavadodon zygus*, *Alveugena carbonensis*, *Schowalteria clemensi*, *Onychodectes tisonensis*, *Conoryctes comma*, *Huerfanodon torrejoni*, *Huerfanodon polecatensis*, *Conoryctella pattersoni*, *Conoryctella dragonensis*, *Wortmania*

otariidens, *Psittacotherium multifragum*, *Ectoganus copei*, *Ectoganus gliriformis* and *Stylinodon mirus*.

The cal3 method is a stochastic time-scaling technique that keeps the appearance of the taxa in the geological record consistent but shifts randomly the ages of the nodes. Therefore, the calibration does not rely only on the first and last appearances of a taxon in the fossil record, but it also takes into account “ghost” evolutionary history. Three rates need to be calculated in advance: the sampling rate, the branching rate and the rate of extinction.

For the sampling rate, I calculated the maximum likelihood (Foote, 1997) based on the distribution of stratigraphic ranges. Then using the function `sProb2sRate` I converted the probability of sampling per time interval to the instantaneous rate of sampling per lineage/time unit. For the true extinction rate (`divRate`), I divided the extinction rate it was calculated (`spRes`) by the interval ranges (`meanInt`). In Bapst (2014) it is mentioned that the branching rates can be set as equal to the extinction rates and I did so in the code `extRate=divRate` and `brRate=divRate` when performing the “`bin_cal3TimePaleoPhy`”. Since it is a stochastic method, R gives a warning not to interpret only a single tree and so I ran this analysis 100 times (`ntrees=100`). To get the consensus time-calibrated tree I used the “`averageTree`” function and calculated the minimal distance between taxa for different trees with the “`quadratic.path.difference`” method. Then I plotted the median diversity curve for each lineage across the time intervals. To plot the time-calibrated tree, I used the “`geoscalePhylo`” function and set *Puercolestes simpsoni* as the outgroup. I also added the first and last appearances of each taxon, which are plotted as bold lines on the tree.

Results

The results from the New Technology Search gave 23 most parsimonious trees with best score 4259, the consistency index is 0.173 and the retention index is 0.546. Afterwards, the Traditional Search yielded 240 total most parsimonious trees. In the Appendix (Figures A31-A32), there is also the topology after the Jackknife resampling and the support values of the clades, as well as the topology and the Bremer support values after a posteriori pruning.

The results of the analysis show that the topology of the taxa studied is well resolved (Figure 25). The basal taxa are plotted as seen in the previous studies that used a former version of this matrix (Wible *et al.* 2009; Shelley, 2018). There are not many polytomies and even taxa that were not scored by myself seem to not have been impacted by the taxa I added to the dataset. One interesting observation is that some groups are found as polyphyletic, such as Zhelestidae, and Leptictida, which are monophyletic in Wible *et al.* (2007; 2009). This could be due to the addition of the new cimolestid taxa, however, the position of *Prodiacodon* is unexpected. Moreover, *Purgatorius* is also not grouped near Primates, but in leptictids and Zhelestidae, similar to the results in Wible *et al.* (2009) and Shelley (2018).

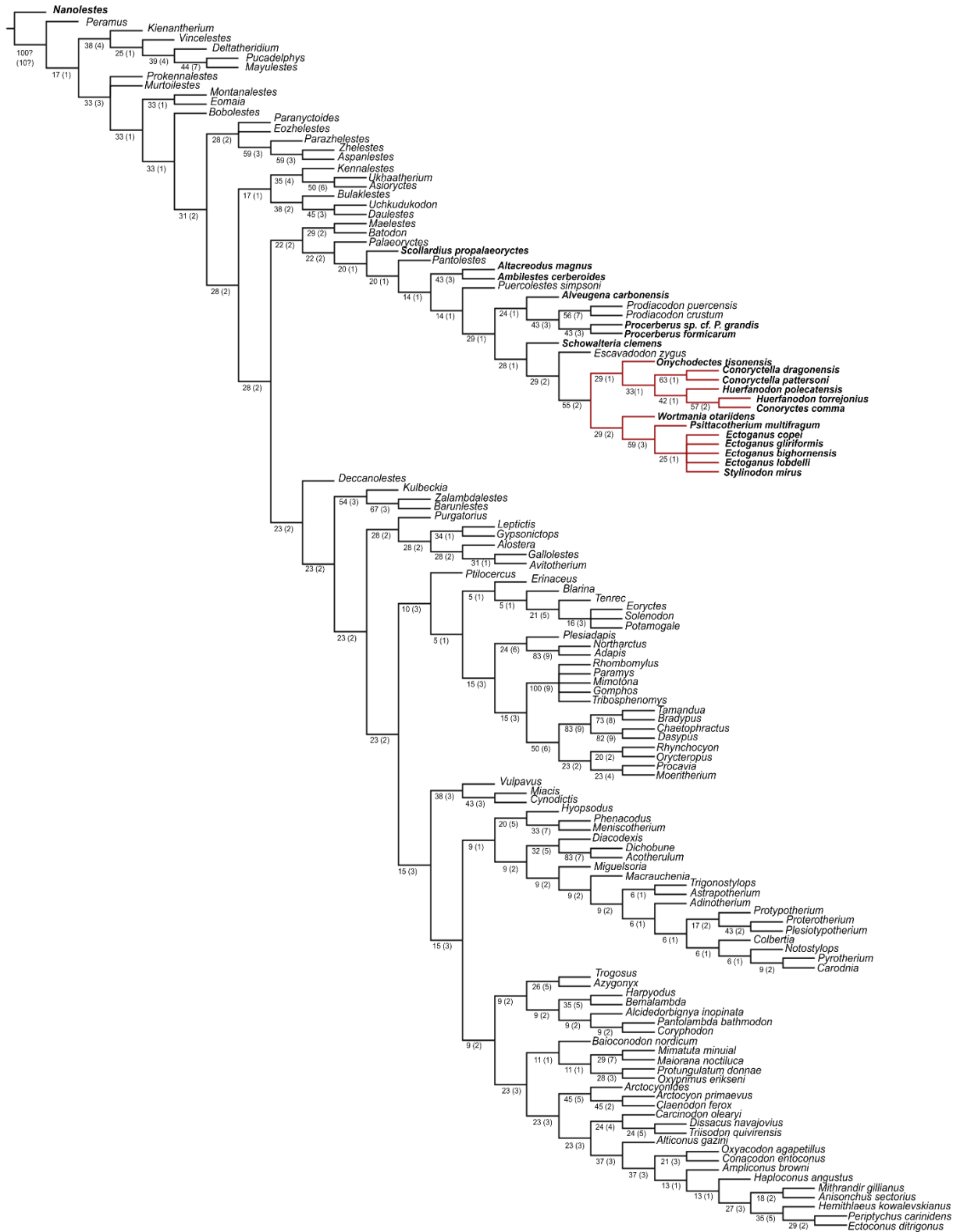


Figure 25: Strict consensus tree of 240 parsimonious trees, after a New Technology search and a Traditional search. Taeniodonta and potential related taxa based on previous studies are highlighted in bold. The clades of taeniodonts are in red. Under each clade are the Bremer support relative values and in parentheses the absolute values.

The consensus tree finds Taeniodonta outside of placentals and within a group of mostly cimolestids (Figure 25). In this, there is also the leptictid *Prodiacodon*, which is not near *Leptictis* or *Gypsonictops*, and the palaeodont *Escavadodon*. *Prodiacodon* and *Procerberus* share a close common ancestor, but this relationship needs further testing. Regarding Taeniodonta, *Schowalteria* is not found as either within taeniodonts or as their sister taxon, rather *Escavadodon* is found to be the sister taxon of Taeniodonta. The position of *Schowalteria* will be discussed further in the discussion of this chapter.

In general, for Taeniodonta, there are two clades found: the *Wortmania* + *Psittacotherium* + *Ectoganus gliriformis* + *Ectoganus copei* + *Stylinodon mirus* clade and the *Onychodectes* + *Conoryctella dragonensis* + *Conoryctella pattersoni* + *Huerfanodon polecatensis* + *Huerfanodon torrejonius* + *Conoryctes comma* clade. The clades within Conoryctidae are better resolved and supported. The low values of support in some cases, for example, the polytomy of the four species of *Ectoganus* and *Stylinodon*, is a result of the few characters that are scored in the dataset, only represented by slightly over one fourth of the total characters; roughly 179 characters scored for each of these species out of the 630 characters. Moreover, their worn teeth do not allow for more anatomical observations, or for adding new characters in phylogenetic analyses. Both absolute and relative support of the *Conoryctes comma* and *Huerfanodon torrejonius* node is very high and it was found 93% of the time in the Jackknife analysis, which is one of the best well-supported nodes within taeniodonts. The weakest is the node the polytomy of *Ectoganus* and *Stylinodon*.

Time-calibrated tree

As explained earlier, the cal3 algorithm is a stochastic time-scaling technique which uses the given taxa, their range, and a given topology and calculates branching times for ancestor-descendant relationships (Figure 26). Moreover, the stratigraphic ranges of the taxa can be seen too, while the last stratigraphic occurrence is where the name of each clade is plotted. The time was divided into almost equal intervals, and the algorithm showed that altogether the mean is 0.67 million years (meanlt in the code), with a sampling rate of 0.42 for the data.

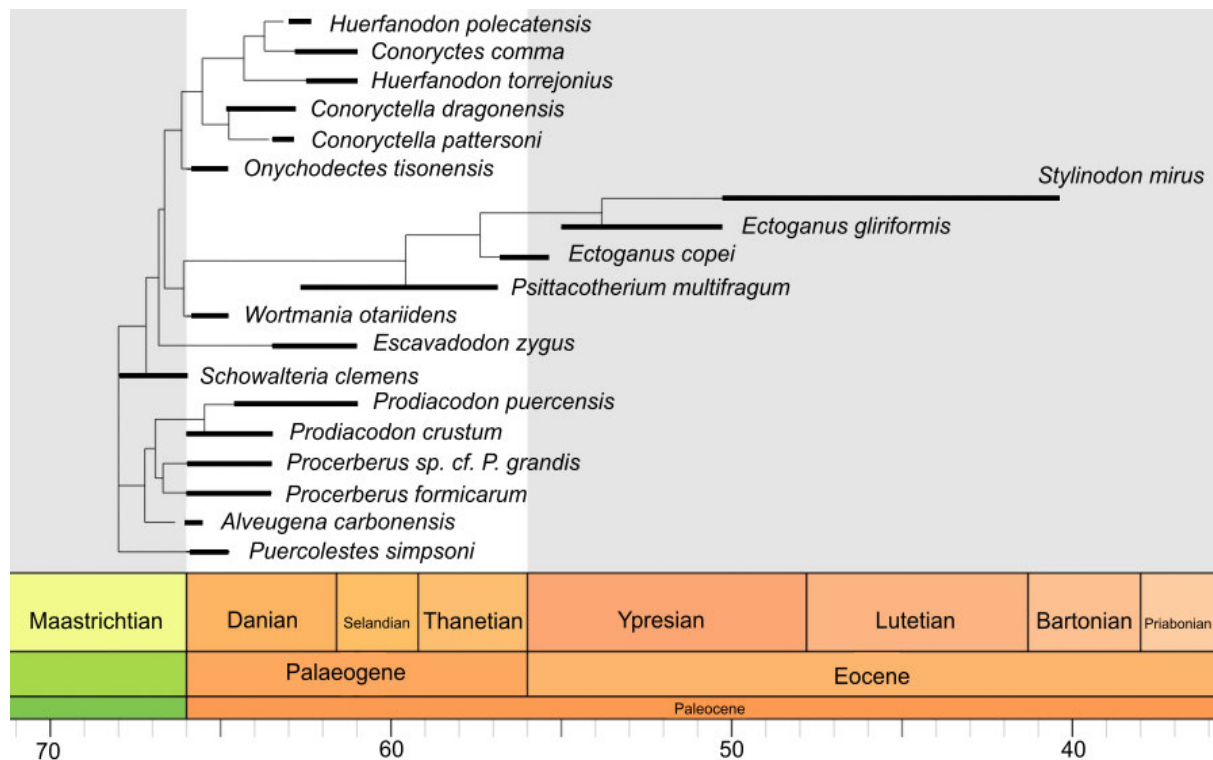


Figure 26: Time-calibrated tree of Taeniodonta. Mammal biochronology and NALMA intervals after Lofgren et al. (2004); San Juan Basin mammal biozones after Williamson (1996) and Flynn et al (2020).

With the age of *Schowalteria* at Lancian, and *Puercolestes* rooting the tree, as seen in the consensus tree from the analysis in TNT, the whole topology is placed in

the geological time. The results of this method propose that the diversification within taeniodonts happened just before the Cretaceous-Palaeogene mass extinction. Further tests need to be done to prove the origin of the Stylinodontidae and Conoryctidae, as well as the position of Taeniodonta in the mammalian tree, and their relation to *Escavadodon*, which is known from the middle Paleocene. If taeniodonts are found within placentals and the split of the two subgroups happened before the K-Pg extinction, then they will favour the Trans-KPg or the Long Fuse models.

Synapomorphies

The phylogenetic analysis shows the synapomorphies of some major clades. These are listed here based on the characters number found in the dataset (Supplementary material, S2) and the changes in the states will be mapped too. The first character is numbered 0. The number of the characters and the states that form the synapomorphies will be presented in bold format.

Theria Parker and Haswell 1897

Ch. 115: Upper molar M2 shape: as long as wide or longer square mesiodistal length mesial labiolingual width 1.0 (0) → **wider than long length more than 75 and less than 99 (1)**

Ch. 117: Upper molars styler shelf width: present and 50 or more of tooth width (0) → **present but less than 50 but more than 25 (1)**

Ch. 123: Upper second molar M2 parastylar lobe width measured to stylocone or stylocone position: more than 30 total width (0) → **less than 30 but more than 20 (1)**

Ch. 134: Upper molars preparacingulum presence: absent (1) → **present (0)**

Ch. 155: Development of postvallum wear extent: Present but only by the first rank postmetacrista (0) → **Present with second rank wear postprotocrista below postmetacrista but the second rank does not reach labially below the base of the metacone (1)**

Ch. 174: Upper molar protocone presence: absent (1) → **present (0)**

Ch. 205: Upper molar lingual root position: supporting paracone (0) → **supporting trigon (1)**

Ch. 236: Lower molar trigonid to talonid length: long more than 75% of total tooth length (0) → **some shortening 51% to 75% of total tooth length (1)**

Definition: All most recent common ancestor of marsupials, placentals, and all descendants (Rougier, Wible and Novacek, 1998)

METATHERIA Huxley 1880

Ch.29: Staggered lower third incisor i3: absent (0) turned → **present (1)**

Ch.158: Upper molar metaconule presence: absent (0) → **present (1)**

Ch. 214: Lower molar paraconid position: Paraconid on mesiodistal midline of the tooth (3) → **Paraconid positioned on lingual margin (0)**

Ch. 240: Ultimate lower molar hypoconulid form: short and erect (0) → **tall and sharply recurved (1)**

Ch. 241: Lower molar entoconid presence: absent (0) → **present (1)**

Ch. 260: Mandible posteriormost mental foramen: below ultimate premolar (2) → **at ultimate premolar and first molar junction or more posterior (3)**

Ch. 272: Mandible labial mandibular foramen: present (1) → **absent (0)**

Ch. 273: Mandible condyloid crest: present (1) → **absent (0)**

Ch. 288: Mandible coronoid facet presence: present (0) → **absent (1)**

Ch. 316: Lacrimal foramen exposed on face because lateral edge of the foramen is reduced or absent: absent (1) → **present (0)**

Ch. 321: Palatal process of premaxilla: does not reach to canine alveolus (0) → **does reach or nearly reach to canine alveolus (1)**

Ch. 409: Glenoid fossa shape: concave or concave posteriorly and flat anteriorly open anteriorly (0) → **anteroposteriorly elongate and concave with the major axis of fossa directed anteroposteriorly (1)**

Ch. 438: Course of internal carotid artery: lateral transpromontorial (0) → **medial perbullar or extrabullar (1)**

Ch. 442: Sulcus or canal for stapedial artery on promontorium: present (0) → **absent (1)**

Ch. 470: Foramen for superior ramus of the stapedial artery presence: present (0) → **absent (1)**

Ch. 473: Ascending canal passage for the superior ramus of the stapedial artery presence: present (0) → **absent (1)**

Ch. 490: Jugular foramen and inferior petrosal sinus: confluent (0) → **separated (1)**

Ch. 504: Position of sulcus for anterior distributary of transverse sinus to subarcuate fossa: anterolateral (0) → **posterolateral (1)**

Definition: All mammals more closely related to Marsupialia than placentals (Rougier, Wible and Novacek, 1998)

EUTHERIA Huxley 1880

Ch. 51: Penultimate upper premolar P4 protocone presence: absent (0) → **present (1)**

Ch. 63: Ultimate upper premolar P5 protocone presence: present (1) → **absent (0)**

Ch. 158: Upper molar metaconule presence: absent (0) → **present (1)**

Ch. 221: Lower molar trigonid configuration: open paracristid protocristid angle more than 50 degrees (0) → **more acute angle between 36 and 49 degrees (1)**

Ch. 236: Lower molar trigonid to talonid length: some shortening 51 75 of total length (1) → **anteroposterior compression of trigonid 50 or less of total length (2)**

Ch. 240: Ultimate lower molar hypoconulid form: short and erect (0) → **tall and sharply recurved (1)**

Ch. 241: Lower molar entoconid presence: absent (0) → **present (1)**

Definition: All mammals more closely related to Placentalia than metatherian (Rougier, Wible and Novacek, 1998)

PLACENTALIA Owen 1837

Ch. 66: Ultimate upper premolar P5 metacone size: swelling metacone connate to paracone (0) → **large metacone and paracone distinctly separate (1)**

Ch. 185: Upper molar postcingulum presence: absent (1) → **present (0)**

Ch. 297: Lateral margin of paracanine fossa: formed by maxilla (0) → **formed by maxilla and premaxilla (1)**

Ch. 321: Palatal process of premaxilla: does not reach to canine alveolus (0) → **does reach or nearly reach to canine alveolus (1)**

Ch. 331: Posterior nasal palatine spine: weak or absent (0) → **prominent (1)**

Ch. 340: Maxillary jugal contact bifurcated: absent (0) → **present (1)**

Ch. 348: Lacrimal contributes to maxillary foramen: present (0) → **absent (1)**

Ch. 387: Vomer contacts pterygoid: present (0) → **absent (1)**

Ch. 388: Pterygoids contact on midline in roof of basipharyngeal canal: present (0) → **absent (1)**

Ch. 390: Midline crest in basipharyngeal canal: present (1) → **absent (0)**

Ch. 395: Ectopterygoid process of alisphenoid extent: present approaches ear region posteriorly (1) → **present terminates at anterior basisphenoid (0)**

Ch. 400: Exit for maxillary nerve V2 via foramen rotundum relative to alisphenoid: within the alisphenoid (1) → **at anterior end of alisphenoid (2)**

Ch. 402: Foramen ovale composition: between alisphenoid and squamosal (3) → **in alisphenoid (2)**

Ch. 404: Alisphenoid canal: absent (0) → **present (1)**

Ch. 413: Glenoid process of jugal presence: present (1) → **absent (0)**

Ch. 424: Entoglenoid process of squamosal position 2: State one (1) → **State zero (0)**

Ch. 425: Posttympanic crest of squamosal: present (1) → **absent (0)**

Ch. 484: Crista interfenestralis and lateral caudal tympanic process connected by curved ridge: present (1) → **absent (0)**

Ch. 489: Size of jugular foramen relative to external aperture of fenestra cochleae: smaller or subequal (0) → **larger (1)**

Ch. 492: Hypoglossal foramen number of openings: two or more (0) → **one (1)**

Ch. 525: Atlas neural arch and intercentrum fused: absent (0) → **present (1)**

Ch. 526: Suture between atlantal and axial parts of the axis: present (0) → **absent (1)**

Ch. 561: Pelvis epipubic bone: present (0) → **absent (1)**

Definition: All extant placentals mammals and their most recent common ancestor (Rougier, Wible and Novacek, 1998; Archibald, 2012)

Schowalteria clemensi + *Escavadodon zygus* + Conoryctidae + Stylinodontidae

Ch. 262: Mandible retromolar space between ultimate molar and coronoid process: present (1) → **absent (0)**

Ch. 336: Posterior edge of anterior zygomatic root: aligned with last molar or more posterior (0) → **aligned between M1 and M2 (1)**

Escavadodon zygus + Conoryctidae + Stylinodontidae

Ch. 57: Penultimate upper premolar P4 parastylar lobe development: well developed and prominent lobe (0) → **expanded lobe but not prominent (1)**

Ch. 110: Size area of lower molars m1 vs. m3: teeth are subequal 80% -120% (1) → **m1 is much larger more than 120% larger (0)**

Ch. 123: Upper second molar M2 parastylar lobe width measured to stylocone or stylocone position: less than 30% but more than 20% (1) → **20% or less (2)**

Ch. 237: Lower molar talonid width to trigonid width: talonid narrower than trigonid (1) → **talonid subequal to wider than trigonid (2)**

Conoryctidae + Stylinodontidae

Ch. 109: Size area of lower m2 vs m3: both teeth are subequal 80 to 120 (1) → **m2 is much larger more than 120 (3)**

Ch. 136: Upper molar ectoflexus presence: present (0) → **absent (1)**

Ch. 564: Femur fovea for ligamentum teres on femur head: does not interrupt margin of articular surface (0) → **does interrupt margin of articular surface (1)**

Ch. 566: Femur size of lesser trochanter: small forms a small boney ridge (1) → **large forms a well defined prominent projecting flange (0)**

Ch.617: P5 stylocone: absent (0) → **present (1)**

Conoryctidae

Ch. 95: Ultimate lower premolar p5 metaconid presence: present (0) → **absent (1)**

Ch. 242: Lower molar entoconid size: subequal or larger than hypoconid and or hypoconulid (1) → **smaller than hypoconid and or hypoconulid (0)**

Ch. 255: Last lower molar length to penultimate lower molar: subequal or larger (0) → **smaller (1)**

Ch. 262: Mandible retromolar space between ultimate molar and coronoid process: absent (0) → **present (1)**

Huerfanodon torrejonus + Conoryctes comma

Ch. 100: Ultimate lower premolar p5 talonid width: narrower than anterior crown (0) → **as wide as anterior crown (1)**

Ch. 233: Lower molar cristid obliqua completeness: incomplete does not reach trigonid wall metacristid may be present (0) → **complete reaches trigonid wall (1)**

Stylinodontidae

Ch. 12: Number of lower incisors: 3 (1), 2 (2) → **1 (3)**

Ch. 46: First upper premolar P1 protocone presence: absent (0) → **present (1)**

Ch. 48: Second upper premolar P2 protocone presence: absent (0) → **present (1)**

Ch. 58: Penultimate upper premolar P4 metastylar lobe presence: present (1) → **absent (0)**

Ch.104: Ultimate lower premolar p5 width: narrow length width or 1.4 (1) → **wide length width or 1.4 (0)**

Ch. 261: Mandible depth of mandibular body: shallow and long (0) → **deep and short (1)**

Ch. 284: Mandible mandibular symphysis posterior extent: second premolar p2 or more anterior (1) → **penultimate premolar p4 or more posterior (2)**

Ch. 416: Postglenoid process presence: absent or highly reduced (1) → **present (0)**

*Stylinodon mirus + Ectoganus gliriformis + Ectoganus copei + Ectoganus
bighornensis + Ectoganus lobdelli*

Ch. 116: Upper molars stylar shelf presence: present (1) → **absent (0)**

Ch. 119: Upper molars parastylar lobe presence: present (0) → **absent (1)**

Ch. 125: Upper molar stylar cusp A parastyle presence: present (0) → **absent or vestigial (1)**

Ch. 132: Upper molar stylar cusp E metastyle presence: present (0) → **absent or vestigial (1)**

Ch. 139: Metacone position to paracone on M1 or M2: approximately at same level (1) → **metacone_lingual (2)**

Ch. 232: Lower molar cristid obliqua presence: present (0) → **absent (1)**

Ch. 619: Distolingual cusp on upper molars: absent (0) → **present (1)**

Discussion

One of the biggest challenges when studying Taeniodonta is their worn teeth, which lack valuable information, essential for the classification of fossil mammals. Studying the specimens in various museums, as well as the new specimens from NMMNH&S, led to understanding their dental morphology better and coming up with three major remarks.

The first important observation is the morphological diversity of the lower teeth in the Conoryctidae. The new specimens provided a closer look at the number of cuspids in the talonid. The lower molars of *Onychodectes* have a mesoconid and a large hypoconid buccally, a small hypoconulid, and lingually an entoconulid, while the presence of a pre-entoconulid varies within the specimens of the genus. *Conoryctella* has the same morphology, with a present pre-entoconulid and the hypoconulid appears to have smaller cuspids (specimen NMMNH P-53835). *Conoryctes* has similar morphology to *Conoryctella* with a present post-entoconulid, sometimes larger than the entoconulid (NMMNH P-47921), sometimes equal in size (NMMNH P-19381). These additions of cuspids distally and lingually happened within a few million years apart, pointing to the rapid evolution of Taeniodonta in the early Paleocene.

The second remark is the presence of a distolingual cusp, which has previously been proposed as a true hypocone. Here I argue that *Ectoganus* does not have a true hypocone since there is no postcingulum (Gregory, 1922; Butler, 2000). Therefore, this is a pseudohypocone as seen in other taxa, either deriving from the metaconule

or the protocone (de Muizon *et al.*, 2019). The former is the case for the pseudohypocone of Artiodactyla (Hunter and Jernvall, 1995), pleuraspidotheriid “condylarths” (Ladevèze *et al.*, 2010) and Paenungulatomorpha (Gheerbrant *et al.*, 2016). In the case of notharctine primates (e.g., Gregory 1920; 1922; Gazin, 1958; Butler, 2000; Anemone *et al.*, 2012), the pseudohypocone is formed on the post-protocone fold, called the *Nannopithec* fold. These are ways of creating *de novo* a hypocone and are due to convergence in the evolution of these taxa. Looking at the M2 of *Psittacotherium multifragum*, NMMNH P- 30630, the metaconule is prominent and so the pseudohypocone of *Ectoganus* could be due to the lingual shift of the metaconule and is better to be referred as a distolingual cusp.

Lastly, the third observation using known and new specimens is the use of the term “hypsodonty” for the taxa of Conoryctidae. Studying their teeth, I noticed that their level of hypsodonty should have a reference point. When looking at the upper molars in buccal view of *Conoryctes*, *Huerfanodon*, *Psittacotherium* and even *Ectoganus* buccally, the crown of the tooth is not higher than its root. This changes completely when looking at the same teeth in lingual view. The lower molars however have a more even distribution of the enamel around the tooth. This pattern, of the enamel extending more lingually on the upper teeth and more buccally on the lower teeth, is what Patterson (1949) mentioned as the “rolling eruption” for all taeniodonts. Tobien (1963) defined this as “partial hypsodonty” and it should be used for the taxa of *Conoryctes* (Figure 13 and 20 for the upper teeth, Figure 15 for the lower teeth) and *Huerfanodon*. This enamel distribution, higher lingually on the upper teeth, and the formation of the roots being smaller buccally, is usually seen in lagomorphs (Tobien 1963; Koenigswald *et al.* 2010) and rodents (Schmidt-Kittler and Vianey Liaud, 1987; Wang, 2001). Based on Koenigswald (2011) animals with partial hypsodonty show “sidewall

hypsodonty” in their lower molars. These features match perfectly with *Conoryctes* and *Huerfanodon* since if looked only at the buccal side of the upper teeth, the term “hypsodonty” does not apply. This might be the result of what has been previously described as the “rolling eruption” of their teeth (Patterson, 1949b). For the partial hypsodonty and the level of wear, I believe that the broad term “hypsodonty” does not adequately describe the teeth of taeniodonts, especially when trying to quantify the level of hypsodonty in *Conoryctes* and *Huerfanodon*.

Relationships within Taeniodonta

Schowalteria clemensi

One of the biggest challenges is understanding the affinities of the poorly known genus of *Schowalteria*. Previous studies (Rook and Hunter, 2011; 2013; Williamson and Brusatte, 2013) had indicated that, contrary to Fox and Naylor (2003), *Schowalteria* is not a member of Stylinodontidae. The current parsimonious analysis agrees with the previous studies in not finding *Schowalteria* within Stylinodontidae. The most parsimonious tree also finds *Escavadodon* as a sister taxon to Conoryctidae and Stylinodontidae, with high Bremer support and Jackknife values. *Schowalteria*, therefore, is not found within Taeniodonta.

Fox and Naylor (2003), when comparing *Schowalteria* with taeniodonts pointed out common characteristics, some of which were used to point to Stylinodontidae affinities. In order to better interpret the results of this study regarding *Schowalteria* the opinion of Fox and Naylor (2003) are addressed in the text below:

1. The second lower incisor is enlarged: this is not a character in the diagnosis of Taeniodonta, most genera of which have an unknown number of incisors.
2. The canines are robust and the enamel is restricted: This is a character that is seen in other taeniodonts and not only in Stylinodontidae. Moreover, even if this could be an argument of *Schowalteria* belonging to the Stylinodontidae, the wear pattern of the teeth is a dubious good phylogenetic character or a diagnostic feature since it is prone to misidentification of young individuals with less worn teeth.
3. The lower canine has an “anteroposteriorly compressed apex and a posteroventral grinding buttress”: This is mostly seen in the taxa *Psittacotherium*, *Ectoganus* and *Stylinodon* and not in *Wortmania*. The latter is so extreme that it even shows this transversely posterior area in the P1-p1. Therefore, *Schowalteria*, an older taxon, had this character of a sharp and flat area on the canines, that shifted to only the anterior sharp area in *Wortmania* and then changed again in the other Stylinodontidae. This scenario is not the most parsimonious one and does not comply with the stratigraphic origin of the taxa. Moreover, the current study finds very strong support for a close relationship between *Wortmania* and *Psittacotherium*. Lastly, the members of the Stylinodontidae that have this posterior flat compression, show it for the lower and the upper canines (*Psittacotherium* USNM 15411, *Stylinodon* PM 3895). The upper canine of *Schowalteria* is cylindrical and less robust than *Wortmania* (AMNH 3394).
4. The anterior side of the protoconid in p1-5 is worn: This is not mentioned in the diagnosis of Taeniodonta, and it is again a feature based on a wear pattern which is prone to preservation biases.
5. The distal lower premolars (p4-p5) and the lower last molar (m3) have thinner enamel on the anterior side compared to the labial or lingual side: This is not a

character in Taeniodonta, although Koenigswald *et al.* (2010) did propose that variation of the enamel of upper molars of *Stylinodon*. Even if this is visible in *Schowalteria* and it is not a matter of poor preservation, it raises again the question of how that character shifted twice over time and it was evident in a basal stylinodontid, *Schowalteria*, and then the most derived member, *Stylinodon*.

6. The upper ultimate premolar (P5) and the first upper molar (M1) have a narrow styler shelf: This is one interesting argument since I do not consider the styler shelf of *Schowalteria* narrow, or at least as narrow as in all taeniodonts. Also, later in the publication Fox and Naylor (2003), in a section about the differences between *Schowalteria* and Taeniodonta, point out the styler shelf width as a difference.
7. The parastylar lobe of the two first molars (M1, M2) is rounded instead of “hook-like”: This is not found as a common characteristic in the definition of Taeniodonta. The parastylar lobe is indeed rounded in taeniodonts, and it is not lost as in more derived forms, as in other Paleocene taxa, apart from *Ectoganus* and *Stylinodon*. What is very different though is that the parastylar lobe creates a strong ectoflexus in *Schowalteria*, something Fox and Naylor (2003) mention too as a difference with taeniodonts. The current study finds the absence of an ectoflexus (ch.136) as a common synapomorphy on the Conoryctidae and Stylinodontidae nodes.
8. The enamel of the lower postcanine teeth extends ventrally on the labial side: This is indeed true for most Taeniodonta and is not a factor of wear. This extension of the enamel can be observed only in the p4 and p5 of *Schowalteria*, while this is seen mostly on molars of taeniodonts. It is also less prominent in the taxa of *Onychodectes*, *Conoryctella* and *Wortmania*. It might reflect behavioural characteristics for *Schowalteria*, as hypsodonty or partial hypsodonty usually does, and not the “rolling eruption” of the premolars and molars of Taeniodonta.

9. The post canine teeth have “horizontal, planar wear” due to a transverse movement of the jaw and there are signs of the “cross-loph” on the trigonids of the lower molars: The jaw movement was described in Schoch (1986) similar to what is described for *Schowalteria*. This is not an apomorphic character, but a behavioural pattern, that could point to false affinities. Also, looking at the specimen of *Schowalteria*, only the trigonid of the m3 indicates “cross-loph” morphology on the trigonids but it is extremely worn. It is unclear if that is a “cross-loph” formed by high cristids, or just very worn down enamel and dentine. Moreover, as mentioned above the term “cross-bilophodont” needs further investigation for the derived taxa of Stylinodontidae.
10. The lower ultimate molar (m3) is shorter than the anterior ones, m2 and m1: This is indeed a diagnostic feature for Taeniodonta (Schoch, 1986). Interestingly though, Fox and Naylor (2003) later in the study pointed out that it is ambiguous if the lower and upper molars decrease in size.
11. The muzzle of *Schowalteria* is short and deep: This is a characteristic of Stylinodontidae, which is also captured in the matrix of the current study. However, *Schowalteria* is known only from an incomplete and damaged skull, so it is hard to quantify this robustness.
12. The zygomatic arch is robust in *Schowalteria* and the maxilla is meeting the jugal within the arch: This is not actually a diagnostic feature for Taeniodonta and I would argue that the zygomatic arch is relatively slender compared to the robustness of their skull. This might be the case for *Schowalteria* too, but unfortunately, it is not complete. As for the maxillary-jugal contact, this is a character in the current study (ch.377 and 340). It is true that in most basal Cretaceous eutherians, the maxilla is contacting the jugal in the most anterior part of the zygomatic arch, as Fox and

Naylor (2003) pointed out. In most taeniodonts that have preserved jugal, the maxillary extends further posteriorly, like in *Conoryctes* (AMNH 15939), *Ectoganus* (USNM 12714) and *Stylinodon* (PM 3895). However, this does not mean that *Schowalteria* is a member of Taeniodonta since other Paleocene mammals share this feature.

Fox (2016) when commenting on the study by Rook and Hunter (2011; 2013) made some interesting points which will be addressed here as well. Firstly, I agree with Rook and Hunter (2011; 2013) that the enamel does not look like it is restricted only to the upper canine of *Schowalteria*. The current study has many of the characters proposed by Fox (2016), that were missing in Rook and Hunter (2013). There are a few characters proposed by Fox (2016) that I disagree with, such as the jaw movement since this is a behavioural character. Similarly, the large size of *Schowalteria* should not be a phylogenetic feature, and the current dataset is capturing relative size differences of each taxon. Moreover, the size of *Schowalteria* is similar to *Cimolestes magnus* (now *Altacreodus magnus*, Fox, 2015) and *Didelphodon vorax* as pointed out by Rose (2006).

To summarize, the characteristics that could point to affinities with Taeniodonta are the buttress on the lower canine, which is not similar to derived members of taeniodonts. Moreover, the upper canine is cylindrical in *Schowalteria* and unlike stylinodontids. The thinner enamel mesially and distally could be possibly a feature but given the state of *Schowalteria*, it is hard to tell if it is not a preservation bias. The parastylar lobe is rounded in Taeniodonta and *Schowalteria*, however, it is protruding a lot buccally in the latter taxon creating an ectoflexus, the lack of which is a phylogenetic character uniting taeniodonts. As for the features that diagnose

Taeniodonta, *Schowalteria* only meets the criteria of subequal trigonids and talonids and the restricted hypoconulid area on m3. The rest of the features that define Taeniodonta are not present in *Schowalteria* either due to wear or lack of these features in the anatomy of the teeth.

However, there are major differences between *Schowalteria* and taeniodonts that were also captured in the present study. The present phylogenetic analysis agrees with the previous studies (Rook and Hunter, 2011; 2013; Williamson and Brusatte, 2013) and does not find *Schowalteria* in Stylinodontidae. The parsimonious analysis does not place *Schowalteria* in Taeniodonta either. Here are a few of the distinctive differences:

- The second upper premolar has a distinctive metastyle in *Schowalteria*, a feature missing in all taeniodonts that their P2 is known of, such as *Wortmania* (NMMNH P-64001), *Onychodectes* (AMNH 15628), *Psittacotherium* (USNM 15411), *Ectoganus copei* (USNM 12714).
- As pointed out by Fox and Naylor (2003), the upper molars of taeniodonts have a greater mesiodistal width, measured at the conular area position, approximately the middle of the buccolingual width, than in *Schowalteria*.
- All taeniodonts have upper and lower molars decreasing in size (see ch.105-107 and ch.108-110 discussed above), unlike *Schowalteria*.
- The upper molars of Taeniodonta lack ectoflexi, unlike the strong ectoflexus seen in *Schowalteria*.
- The lower premolars are transversely placed on the mandible in all Taeniodonta, even more so in Stylinodontidae, which is not seen in *Schowalteria*.

- The lower first premolar of *Schowalteria* is very small compared to the p1 of Stylinodontidae.
- The lower p4 of *Schowalteria*, looks more molariform and almost equal in size to the p5, opposite to older taeniodonts, *Onychodectes* and *Wortmania*.
- There is also space between the last lower molar of *Schowalteria* and the coronoid process as seen in Conoryctidae.

Moreover, Rose (2006) stated that the derived morphological characteristics seen in *Schowalteria* may be due to convergence with Taeniodonta. Clemens (2013) also mentions that although the Lancian localities in Wyoming and Montana are well sampled, only one specimen of *Schowalteria*, and no other taeniodont has been found. That study (Clemens, 2013) mentions also that the origin and the time of diversification of Taeniodonta are “best regarded as unresolved”.

To sum up, the results of this study find *Schowalteria* outside of Taeniodonta. The phylogenetic analysis led to defining the clades of Taeniodonta, Conoryctidae and Stylinodontidae as follows.

Systematic Palaeontology

MAMMALIA (Linnaeus 1758)

EUTHERIA (Gill 1872)

TAENIODONTA (Cope 1876)

Genera: *Onychodectes* (Cope, 1888); *Conoryctella* (Gazin, 1939); *Conoryctes* (Cope, 1881a); *Huerfanodon* (Schoch and Lucas, 1981b); *Wortmania* (Hay, 1899);

Psittacotherium (Cope, 1882a); *Ectoganus* (Cope, 1874); and *Stylinodon* (Marsh, 1874).

Distribution: Puercan to Uintan of western North America

Revised Diagnosis: Upper molars are relatively narrow, bearing paracones and metacones moderate in size, narrow styler shelf and no ectoflexus, the pre- or postcingula are minuscule or absent and there is no true hypocone; upper and lower molars decrease in size posteriorly; lower molars with minuscule or absent cingulids; trigonids and talonids of lower molars are subequal in both length and width; metaconid is subequal to protoconid; the talonid is not expanded posteriorly in the hypoconulid area on the m3; partial hypsodonty on cheek teeth (particularly on the lingual side of the upper and the buccal on the lower); the femur fovea interrupts the margin of the articular surface of the femoral head

Definition: The most inclusive clade including *Stylinodon* but not *Escavadodon*, *Prodiacodon*, *Procerberus*, *Leptictis*, *Gypsonictops*, *Deccanolestes*, *Alcidedorbignya*, *Harpyodus*, *Trogosus*, *Arctocyon*, *Periptychus*, *Carsinodon*, *Alticonus*, *Phenacodus*, *Meniscotherium*, *Macrauchenia*, *Colbertia*, *Carodnia*.

CONORYCTIDAE (Wortman 1896b)

Genera: *Onychodectes* (Cope, 1888); *Conoryctella* (Gazin, 1939); *Conoryctes* (Cope, 1881a); *Huerfanodon* (Schoch and Lucas, 1981b).

Distribution: Puercan to Torrejonian of western North America

Revised Diagnosis: ultimate lower premolar p5 with metaconid absent and small talonid heel; lower molar entoconid is smaller than hypoconid; last lower molar shorter

than penultimate lower molar; present of a mandibular retromolar space between the ultimate molar and the coronoid process

Definition: The most inclusive clade including *Conoryctes comma* but not *Stylinodon mirus*

STYLINODONTIDAE (Marsh, 1875)

Genera: *Wortmania* (Hay, 1899); *Psittacotherium* (Cope, 1882a); *Ectoganus* (Cope, 1874); and *Stylinodon* (Marsh, 1874).

Distribution: Puercan to Uintan of western North America

Revised Diagnosis: one lower incisor; upper P1 and P2 bear a protocone; P4 lacks a metastylar lobe; p5 is wider than long; skull and mandible deep and short

Definition: The most inclusive clade including *Stylinodon mirus* but not *Conoryctes comma*

Conoryctes and *Huerfanodon*

The genus *Huerfanodon* Schoch and Lucas, 1981b is known from a few specimens that are assigned to species, *H. torrejonius* and *H. polecatensis* (Figures A24, A25 in Appendix) and nomen dubium ?*Huerfanodon* "*heilprinianus*". The type of the first species is a partial skull and part of a mandible with the p5 and m1. The type of *H. polecatensis* is a partial mandible with p4-m2. As for the type of ?*Huerfanodon* "*heilprinianus*", previously assigned to *Conoryctes comma* (van Valen, 1978), is a damaged mandible with the m2, that I was unable to locate in the AMNH. Of the two species, only *H. polecatensis* has been found outside of the San Juan Basin. When

studying *H. torrejonus* and *H. polecatensis* there are noticeable differences that can be spotted. Firstly, there is a difference in size, with *H. polecatensis* being significantly bigger. There is a well-developed metaconid on the p5 of *H. polecatensis* which is missing in *H. torrejonus* and in all other Conoryctidae.

In his study, Schoch (1986) named a few specimens, previously thought to belong to *Conoryctes comma* as conoryctids, Indeterminate A (AMNH 832), Indeterminate B (USNM 9597, USNM 9816, USNM 9826) and Indeterminate C (AMNH 15939). I had a similar difficulty assigning new specimens of teeth from the San Juan Basin, between *C. comma* and *Huerfanodon torrejonus*.

The phylogenetic analysis by Williamson and Brusatte (2013) shows that when the characters were unordered, there is a polytomy between the genera of *Conoryctes*, *Conoryctella* and *Huerfanodon*. Similarly, in Rook and Hunter (2013) the Bremer support between *Conoryctes* and *Huerfanodon* is very low, easily collapsing and giving the same polytomy. When adding the species, the current analysis finds that the species of *H. torrejonus* is the sister taxon to *C. comma* and not to *H. polecatensis*. The clade of *H. torrejonus* and *C. comma* is also very well supported with absolute and relative Bremer support and Jackknife values.

To try and understand if the analysis lacks some phylogenetic features that distinguish *Huerfanodon torrejonus* from *Conoryctes comma* I investigated the previous diagnoses of the species by Schoch and Lucas (1981a) and Schoch (1986). Both genera are thought to have the same size, apart from *H. polecatensis* which is larger. Only the teeth of *C. comma* are described as having crown hypsodonty, which is something that applies also to the two species of *Huerfanodon*. The P5 is missing

in all known specimens of *Huerfanodon* so no differences with the P5 of *Conoryctes* can be spotted.

The differences in the upper dentition are regarding the P4 and the molars. In more detail, the P4 of *Conoryctes* is described as nonmolariform with a small metacone and a lingual cingulum. The P4 of *Huerfanodon* has a larger metacone and a “protocone and hypocone”. This is of course not a hypocone, there is no postcingulum, but it should be better referred to as a cuspidated lingual cingulum. This is also the way it was scored in the matrix (see the previous discussion on character sampling). Looking into the specimens of *Conoryctes* though, the size of the metacone and the lingual cingulum varies. The P4 of AMNH 3396 (*C. comma*) shows an incipient metacone, whereas the P4 of AMNH 3398 (*C. comma*) has a well-formed metacone, which seems to be the case also in AMNH 15939, described as Indeterminate C Conoryctid by Schoch (1986). The lingual cingulum is also variable in these specimens (Appendix, Figure A26, A27). Therefore, I argue that the size of the metacone and the lingual cingulum on P4 is a variable feature in *Conoryctes comma* and therefore not a strong difference with *H. torrejonius*. Because of this variation, the newfound specimen NMMNH P-61799 (Figures 12 and 13) was assigned to *C. comma*. The molars of that specimen also indicated the presence of conules which have been worn in the other specimens of *Conoryctes*. Another potential difference in the diagnoses is that *Conoryctes* shows variability in the presence and size of mesostyles. This is very true since specimen NMMNH P-16200 (Figure 20) shows this variability from the left to the right molars of the same individual. However, Schoch and Lucas (1981b) failed to report that and said this to be a major difference between the two genera.

In the lower dentition, one major difference is the “lack of internal grooves” on the canines in specimens of *Conoryctes*. The canines of USNM 15412 (*H. torrejonus*) indeed show enamel around the canines and there are grooves. However, I should strongly point out how, given the unworn teeth of the specimen, these may not have been found if the canines were worn. Which is the case in most known lower canines of *Conoryctes*, such as the type of *Conoryctes* (AMNH 3395). Similar grooves are found in the less worn lower canines of *Conoryctella* (NMMNH P-25056). Therefore, the presence of this diagnostic feature could be valid if unworn teeth were examined. This means that it is not a strong difference between *Conoryctes* and *Huerfanodon*. It is worth mentioning that there are signs of grooves in the enamel of the less worn upper canine of NMMNH P-61799 (*C. comma*) and the lower canines of *C. pattersoni* (NMMNH P-25056). Potentially this is a characteristic feature in other taeniodonts or conoryctids, but it can not be observed due to the level of wear on their canines.

The last lower premolar of *Conoryctes* has is only a protoconid, lacking a metaconid. The new specimen of *Conoryctes* NMMNH P- 19976, as well as the type of the genus AMNH 3395, show that the talonid is not “simple” as described in the diagnosis of Schoch (1986) but is cuspidated, resembling the many cuspids of the type of *Huerfanodon torrejonus*. This is very different from the molariformed p5 that bears a metaconid rather than of *H. polecatensis*. On the lower molars, paraconids and paracristids are prominent in *H. torrejonus* slightly more than in *C. comma*. However, both species (USNM 15412 *H. torrejonus* and AMNH 16029 *C. comma*) have the same anatomy in the talonid, a mesoconid, a large hypoconid, cuspidate hypoconulid area, a post-entoconulid, an entoconulid and a pre-entoconulid. The absence of a post-entoconulid is different for the other two genera of Conoryctidae, *Onychodectes* and *Conoryctella*. And since the upper teeth of *Conoryctes* are so polymorphic with

the size and presence of the mesostyle (see specimen NMMNH P-16200), I believe that the same could apply to the size of the paraconids.

To summarize, I find that the taxa *Conoryctes comma* and *Huerfanodon torrejonus* lack any significant dental anatomical differences. As seen in the specimens of *C. comma* the size and shape of the metacone and lingual cingulum on the P4 and the size of the mesostyle in the upper molar vary considerably. Therefore, the only small difference is in the size of the paraconid, which could also vary among individuals. Based on the synapomorphies seen in the most parsimonious tree, *Conoryctes* lacks a well-formed basin lingually on the P4, contrary to *H. torrejonus*. Also, there is a difference in the shape of the M2, with *Conoryctes* having a much longer than wide M2, while *H. torrejonus* is scored for having a wider than longer. Similarly, the trigonid of the lower molars is slightly longer than the talonid for *H. torrejonus* while it is found as intermediate for *C. comma*. These differences in size, don't seem to validate why these two species should belong to different genera or species. In the following chapter, the postcranial elements of *Conoryctes* show a small variation in size without having any anatomical differences. Also, other taeniodonts, like *Onychodectes* and *Wortmania* are known to have some variability in their morphology among the individuals of the same species.

For these reasons, I synonymize the species of *C. comma* and *H. torrejonus* and following nomenclature, I am keeping the name of the older known genus of the two. Therefore, specimen USNM 15412, the only specimen of *H. torrejonus*, now belongs to *Conoryctes comma*. Since the genus *Huerfanodon* is no longer valid, the species of *H. polecatensis* should belong to a new genus.

Relationships with other mammals

The current analysis, which primary goal is the in-group phylogeny of taeniodonts, is also providing evidence regarding their relationships with other mammalian taxa. Taeniodonta is a monophyletic clade, outside of Placentalia, close to a Cimolesta, Leptictida, and Palaeanodonta grouping. A bigger dataset, like the one PaIM, is building, will further address these relationships and test the position of leptictids and cimolestids.

Evolution of Taeniodonta

The current study helps to understand the timing and the evolution of Taeniodonta. The time-calibrated tree shows that that the two major subgroups, Conoryctidae and Stylinodontidae, are found after the Cretaceous-Palaeogene mass extinction. The current study demonstrates that *Schowalteria* is not a member of Stylinodontidae, as proposed before (Rook and Hunter, 2011; 2013; Williamson and Brusatte, 2013). Since *Escavadodon* is plotted outside of Taeniodonta the position of *Schowalteria* as a basal taeniodont, or even as a sister taxon to the group, is no longer valid. The current parsimony analysis has found polytomies for other groups such as leptictids and Zhelestidae. A further analysis to check these polytomies is required, since it can provide evidence of the taxonomic rank Taeniodonta belong to.

Conoryctidae includes the taxa *Onychodectes tisonensis*, *Conoryctella dragonensis*, *Conoryctella pattersoni*, *Conoryctes comma*, and the new genus of the

specimen USNM 15412, previously belonging to *Huerfanodon polecatensis*. Stylinodontidae includes the genera *Wortmania otariidens*, *Psittacotherium multifragum*, *Ectoganus copei*, *Ectoganus gliriformis*, *Ectoganus bighornensis*, *Ectoganus lobdelli* and *Stylinodon mirus*. As for the species of *Ectoganus*, they are forming a big polytomy probably due to the lack of scored characters in the matrix. This is because both species of *E. bighornensis* and *E. lobdelli* are known from a few worn teeth and their diagnoses are not too different from the other species of *Ectoganus*. Therefore, a closer look at the dentition of the genus is needed in a future study.

Some characters that are found in some of the genera are absent in others due to the lack of specimens. Therefore, potential characteristics that are found in both Conoryctidae and Stylinodontidae and could be diagnostic for the whole group are:

- the grooves on the enamel of the canines seen in *Conoryctella*, *Conoryctes*
- the recurved claws seen in all Stylinodontidae but based on chapter three, this is seen in *Conoryctes* too

As seen in other animals that developed a hypocone de novo, taeniodonts may have needed more occlusal areas and a square molar to process the tough vegetation. Most importantly though, derived Taeniodonta were not the only members of the group to have changed their dental anatomy. The presence of the shifted metaconule in *Psittacotherium* shows that they already started modifying their dentition. Also, the presence of the pre- entoconulid and post-entoconulid as well as the multicuspid hypoconulid as seen in *Conoryctes* shows that even Conoryctidae had changed their dentition to favour a course diet.

These new findings raise questions regarding the level of specialization in Conoryctidae. Williamson and Brusatte (2013) highlighted that there are morphological characteristics to support a level of fossoriality in *Onychodectes*. If this is true, then the ancestor of Taeniodonta may have already started relying on digging behaviours, probably essential for their survival after the Cretaceous-Palaeogene extinction. The following chapter investigates further this question, providing a detailed anatomical study of new postcranial elements, of the genus *Conoryctes comma*.

CHAPTER 3

The postcranial skeleton of *Conoryctes comma*



Sculpture of *Conoryctes comma*, at the USNM

“I have myself had a hand in nearly all the collecting done in Colorado, and a poor eye for a taeniodont is not one of my defects.”

Bryan Patterson (1909-1979)

Introduction

The robust postcranial elements of *Psittacotherium*, *Ectoganus* and *Stylinodon* show clear adaptations to fossoriality (Schoch, 1986; Turnbull, 2004). As for the earlier taeniodonts, *Onychodectes*, *Conoryctes*, and *Conoryctella* previous studies suggested that they had generalised postcranial skeletons (Patterson, 1949b; Schoch, 1986; Lucas *et al.*, 1998; Rose, 2006). Williamson and Brusatte (2013) described the new postcranial elements of *Wortmania* and thoroughly explained the anatomical features that point to digging adaptations for the genus. In that study, they also introduced the hypothesis that even the basal *Onychodectes* had anatomical characteristics indicative of digging behaviour. They also emphasised the need for new fossils to assess whether members of conoryctids were also able to dig at least to some degree. The present study is providing evidence for the skeleton of another Paleocene taeniodont, *Conoryctes*.

Conoryctes is known from the early Paleocene (Torrejonian, Tj4-Tj6) of the San Juan Basin in New Mexico, USA mainly from dental specimens. Only a partial humerus and a radius of the specimen AMNH 3396 are assigned to *Conoryctes* (Schoch, 1986). The lack of postcranial specimens led to unanswered questions regarding the anatomy of *Conoryctes*, and unsupported theories about its locomotion. Nine new specimens from the San Juan Basin consisting mostly of postcranial elements helped understand this enigmatic genus. This chapter includes a detailed description of the vertebrae, forelimb and hindlimb of *Conoryctes*, as well as comparisons with other Palaeogene mammals. Lastly, using the new specimens, and anatomical observations of the skeleton the locomotor behaviour of *Conoryctes* is evaluated. This helped answer the

debate about whether *Conoryctes* had any specialization in its mode of life, or if it was a “generalised” animal that lived after the Cretaceous-Palaeogene extinction.

Historical background of *Conoryctes comma*

The genus of *Conoryctes* was first diagnosed by Cope (1881a) based on a partial lower jaw (AMNH 3395) preserving damaged and worn p5, m1 and m2. In this publication Cope uses the term “allied to *Mesonyx*” when describing *Conoryctes comma*. During that time, he had already studied *Calamodon* (= *Ectoganus*) (Cope, 1874) and had already introduced the term Taeniodonta (Cope, 1876). He thought it was a suborder of the Bunotheria order and that they were intermediate between Edentata and Insectivora. Moreover, *Stylinodon* had been described by Marsh (1874). Therefore, when looking at *Conoryctes* Cope might not have seen the resemblances with the derived taeniodonts known at that time.

In 1884a, Cope described the specimen AMNH 3396 as a new genus named *Hexodon molestus*. This specimen consists of a partial skull, with left upper canine, right upper P4, left and right upper P5-M3, an almost complete mandible with lower canines, right p4, left p5, left and right m1, left m2, right and left m3, and a partial humerus and radius, which Cope thought was part of the tibia. The teeth are worn providing little information on the cusps and cuspids and the postcranial elements are damaged. Cope implied a relationship between the new genus, *Hexodon*, with *Periptychus*.

In the years that followed, Cope found and described *Onychodectes* (Cope, 1888) and *Hemiganus* (= *Wortmania*) (Cope, 1885). In that publication, Cope

synonymised the genus *Hexodon* with *Conoryctes* and assigned both specimens (AMNH 3395, AMNH 3396) to *Conoryctes*. He also said that *Conoryctes* might belong to Creodonta since it has few similarities with Condylarthra, but its dentition is very similar to *Onychodectes* and *Hemiganus*.

Later Wortman (1897) erected Ganodonta, including the then-known Taeniodonta (*Calamodon* and *Ectogonus*), *Psittacotherium* (that was placed then in Tillodontia) and Hemiganus (=Wortmania), *Onychodectes* and *Conoryctes* (placed by then with the Creodonta). Wortman also introduced the families Stylinodontidae and Conoryctidae, including *Onychodectes* and *Conoryctes*. In that study, he also introduced the idea that Ganodonta was a suborder of Edentata.

A more detailed description by Matthew (1937) followed, where he changed the name Ganodonta to Taeniodonta since it was introduced first. In his study, Matthew also gave interesting and important information about the anatomy of the teeth, skull, mandible and the limited postcranial of *Conoryctes*. Apart from his detailed description, he also pointed out anatomical features that showed *Conoryctes* was more specialised than *Onychodectes*. The similarities between *Conoryctes*, *Onychodectes* and *Wortmania* noticed by Cope (1888) were also discussed by Matthew (1937) and Patterson (1949b). The latter also proposed that *Conoryctes* is more closely related to *Onychodectes* than *Wortmania* and the Stylinodontidae.

A detailed study of Taeniodonta was published by Schoch (1986), including *Conoryctes*. Schoch reported the specimens that belong to *Conoryctes* and gave a detailed description of the dentition and postcranial elements while comparing *Conoryctes* to other taeniodonts. Schoch and Lucas (1981) introduced the genus *Huerfanodon* and compared the new skull with the skull of *Conoryctes*, AMNH 15939.

However, later in Schoch (1986), three specimens are referred to as “Conoryctid Genus Indeterminate” (AMNH 832, AMNH 15939, USNM 9597), among which is skull AMNH 15939, because they are very similar between *Conoryctes* and *Huerfanodon*.

The phylogenetic affinities of *Conoryctes* have been discussed in a few studies. The first attempts were by Patterson (1949b, figure 2, figure7) where he looked into the evolutionary rates of taeniodonts and illustrated the relationship between *Conoryctes* and *Conoryctella* and *Onychodectes*. Schoch (1986) wrote about the phylogeny and evolution of taeniodonts and was the first to create phylogenetic characters and plot them in a cladogram (figure 56), but this was not a numerical phylogenetic analysis. Recent phylogenetic analyses (Rook and Hunter, 2011; 2013, Williamson and Brusatte, 2013) and chapter two of the current thesis, find *Conoryctes* within Conoryctidae.

Geological setting

Conoryctes comma is known from the Torrejonian age deposits of the Nacimiento Formation of the San Juan Basin, New Mexico, USA. The Torrejonian is a North American land mammal age (NALMA) that extends from ~64 to 61.7 million years ago (Lofgren *et al.*, 2004). The Nacimiento Formation primarily consists of fluvial deposits of mudstones and sandstones, as well as moderately well-developed palaeosoils and carbonaceous shales (Williamson, 1996; Lofgren *et al.*, 2004). The flora of the formation indicates a subtropical climate, with warm and humid conditions, and dense vegetation (Tidwell *et al.*, 1981; Flynn and Peppe, 2019). There were also many endemic species in the studied flora of the San Juan Basin, especially right after the K-Pg extinction (Flynn and Peppe, 2019). The fauna of the Nacimiento Formation consists of a variety of mammals and reptiles, such as crocodiles and turtles, birds and fish (Matthew, 1937; Williamson and Lucas, 1992; Williamson, 1996). The abundance of turtles and crocodiles also indicates a warm and humid climate (Markwick, 1998). Based on the sediment and the fossils found, the San Juan Basin was a warm and humid forest in the early Paleocene.

The stratigraphy of the San Juan Basin is well-studied and many of the localities are dated based on magnetostratigraphy and biostratigraphy (Williamson and Lucas, 1992; Flynn *et al.*, 2020). Specimens were collected before this detailed understanding of the stratigraphy. For this reason, some of the specimens of *Conoryctes* collected by Cope cannot be accurately placed stratigraphically. Tables A6a and A6b (Appendix) states the localities and the biozones in which the specimens used in this study were found.

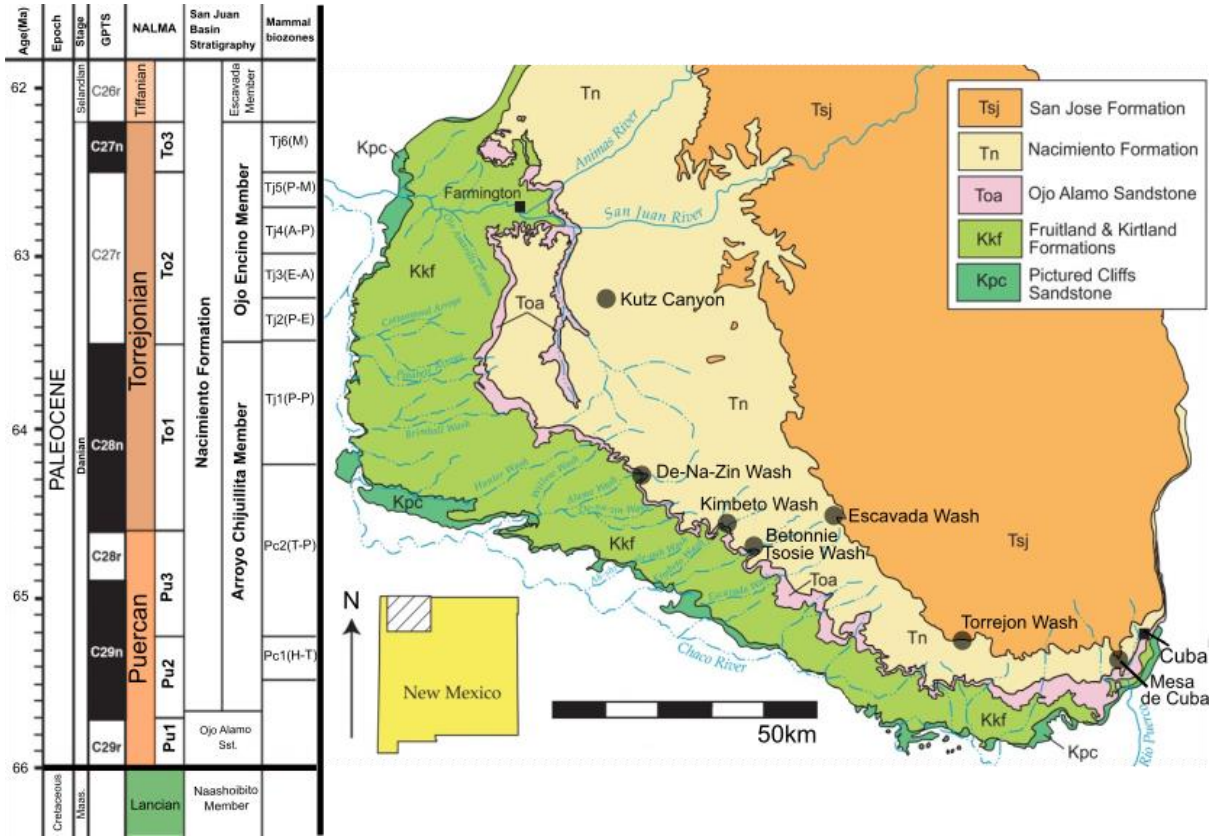


Figure 27: The stratigraphy of the San Juan Basin (GPTS, Gradstein et al., 2012; NALMA intervals, Lofgren *et al.*, 2004; Mammal biozones, Williamson, 1996), and the geological map with fossil localities of the basin (modified after Williamson, 1996).

Systematic Palaeontology

MAMMALIA (Linnaeus 1758)

EUTHERIA (Gill 1872)

TAENIODONTA (Cope 1876)

CONORYCTIDAE (Wortman 1896b)

(=*Conoryctes comma* Cope, 1881a)

Conoryctes comma Cope, 1881b

Hexodon molestus Cope, 1884a

Conoryctes comma Cope, 1884b

Conoryctes comma (= *Hexodon molestus*) Cope, 1888

Conoryctes comma Wortman, 1897

Conoryctes comma Matthew, 1937

Conoryctes comma R. W. Wilson, 1956

non *Conoryctes comma* Van Valen, 1978

non *Conoryctes comma* L. H. Taylor, 1981

Huerfanodon torrejonius Schoch and Lucas, 1981b)

Type species and only known species: *Conoryctes comma* (Cope 1881a)

Age and locality

Middle to late Torrejonian, early Paleocene. Known from the Nacimiento Formation, San Juan Basin, New Mexico, USA.

Etymology

Cope (1881a) did not provide an etymology for *Conoryctes comma*. The generic name *Conoryctes* derives from the ancient Greek words κώνος (=cone) and ὀρύσσω (=to dig). The “cone digger” is likely referring to the conical morphology of the teeth. However, it is unclear how Cope decided upon ‘-oryctes’ given the genus was known only from dental specimens. The species name derives from the ancient Greek word κόμμα (=a part of), which is today used as the word for the punctuation mark, comma. When looking at the p5 of the type AMNH 3395 in occlusal view, it resembles a comma.

Diagnosis: see Chapter 2

Differential diagnosis

Conoryctes is larger than *Onychodectes*, *Wortmania* and *Conoryctella* but smaller than the other taeniodonts. *Conoryctes* lacks an upper P1, unlike other taeniodonts. On the upper molars, the styler shelf is also less buccally extended in *Conoryctes* than in *Onychodectes* and *Conoryctella*. In *Conoryctes* the enamel of the upper teeth extends more towards the root of the tooth lingually than buccally. This uneven distribution of the enamel in the upper and lower teeth, partial hypsodonty, is not seen in *Wortmania*, *Onychodectes* and *Conoryctella*. As for the lower molars, *Conoryctes* has more cuspids on the talonid than *Onychodectes* and *Conoryctella*. These cuspids are a pre- and a post-entoconulid and more cuspids in the hypoconulid position. *Conoryctes* is different to *Psittacotherium* because the latter is bigger, lacks a continuous styler shelf on the upper molars, it has more cuspids in the talonid of lower molars, and it has a higher level of hypsodonty on lingual and buccal areas of the tooth. *Conoryctes* is different to *Ectoganus* because the latter has more

hypsodonty canines, has a distolingual cusp on the upper molars, lacks a continuous styler shelf and the lower molars are almost squared in shape. *Conoryctes* differs from *Stylinodon* since it does not have square-shaped ever-growing teeth and the most anterior premolars are not larger than the posterior premolars. *Conoryctes* differs from *Conoryctella* and *Onychodectes* in having relatively more robust fore-limb. The distal epiphysis of the radius extends anteriorly in *Conoryctes*, whereas it is less protruding in *Wortmania*.

Species

Conoryctes comma Cope 1881a (= *Hexodon molestus* Cope, 1884a)

Type

AMNH 3395, partial left mandible with worn p5, m1 and worn m2, alveolus for p1, roots for p4 and m3, isolated lower canine (Figure 28).

Type locality

Torrejonian strata of the Nacimiento Formation, San Juan Basin, New Mexico

Diagnosis

Same as for genus.

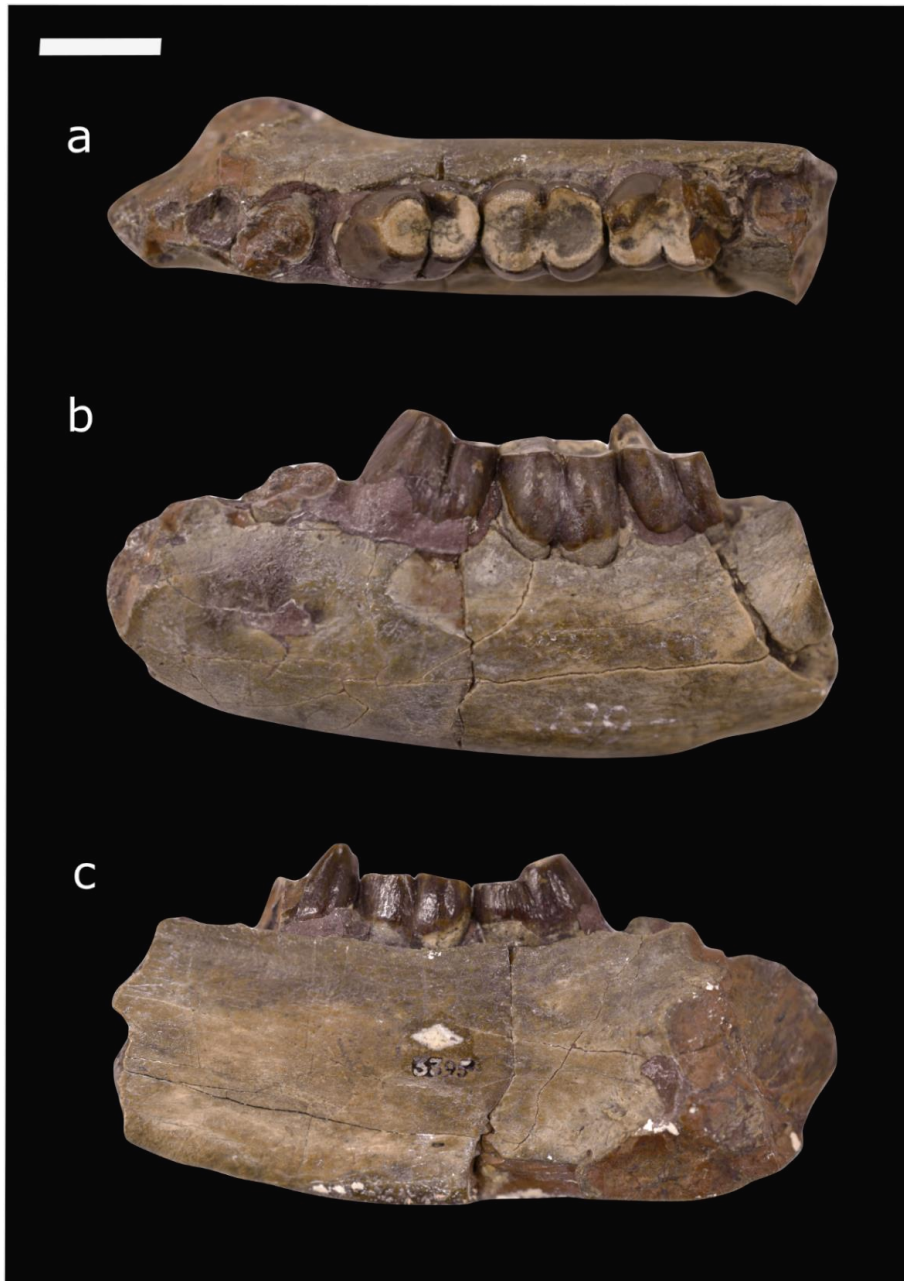


Figure 28: Type specimen of *Conoryctes comma*, AMNH 3395 partial left mandible with worn p5, m1 and m2, in occlusal (a), buccal (b) and lingual (c) views. The scale bar is 1 cm.

Materials and methods

The skull and mandible of *Conoryctes comma* have been described in detail by Matthew (1937, AMNH 15939) and Schoch (1986, USNM 22484). Using the method of Kirk *et al.* (2014) and the cranial length of these skulls, it was calculated that *Conoryctes comma* was a medium-sized animal, approximately 12-14kg, similar in weight as a beagle dog. The new postcranial elements from San Juan Basin are short and stout, indicate that *Conoryctes* was a robust animal.

To understand and compare the postcranial elements, specimens from the following museums were studied: the New Mexico Museum of Natural History and Science (NMMNHHandS), the American Museum of Natural History (AMNH), the Yale Peabody Museum (YPM), the Carnegie Museum of Natural History (CM) and the National Museum of Natural History, Smithsonian Institution (USNM). These specimens were of Taeniodonta and other comparative taxa of the study, such as *Escavadodon*, *Procerberus*, *Prodiacodon* and *Periptychus*.

The specimen USNM 22484 (Appendix, Figure A33) was assigned to *Conoryctes comma* by Schoch (1986) and preserves a complete ulna, radius and parts of the vertebrae and the manus. The postcranial elements were previously assigned to specimen USNM 22483 associated with a skull of *Triisodon*. Because both specimens were collected from the same site on the same day, Dr Bakker suggested to Dr Schoch that they are associated with the skull of *Conoryctes* USNM 22484 instead. They are not illustrated or described by Schoch (1986) apart from the manus.

The postcranial elements of *Conoryctes*, that were known before this study, are very few and are associated with specimen AMNH 3396. These include an incomplete

proximal humerus and a partial right radius with preserving the distal epiphysis. After studying the new postcranial elements from San Juan Basin, the postcranial elements of USNM 22484 are dissimilar from those of *Conoryctes*. The radius of USNM 22484 is straight whereas the distal part of the radius of *Conoryctes* (AMNH 3396) has a “notable expansion toward the end with a lower anterior crest” as Matthew (1937) described it. Similarly, the ulna of USNM 22484 is not posteriorly curved on the olecranon as in *Wortmania* and in *Onychodectes*. The cervical vertebrae are bigger and more anteroposteriorly elongated than those of taeniodonts and of *Conoryctes*. Similarly, the metacarpals of USNM 22484 are slender in the middle and have mediolaterally robust distal epiphyses. The manus of *Onychodectes* (AMNH 16528) and *Wortmania* (NMMNH P-19460) have uniformly robust metacarpals, something noticed also in the new specimens of *Conoryctes* (NMMNH P-79457 and NMMNH P-48052). Also, the metacarpals of USNM 22484 lack the flexor tubercles seen in *Wortmania* (NMMNH P-19460), *Onychodectes* (AMNH 16528) and *Conoryctes*. For all the above reasons the postcranial elements of USNM 22484 were excluded from this study. There are no known postcranial elements of *Triisodon* that could help point similarities to the postcranial in question. I support the former labelling of them, i.e. they are associated with the skull USNM 22483 of *Triisodon*.

Apart from describing the new material, I made anatomical comparisons with other taeniodonts and other taxa. The purpose was to understand the distribution of characters within the group. The other Palaeogene taxon that was used for comparison is *Procerberus* because it has been proposed as closely related to Taeniodonta in many studies (Schoch, 1986; Rook and Hunter, 2011; 2013; Williamson and Brusatte, 2013; Clemens, 2013). During this study, I also compared *Conoryctes* to other potential taxa that I saw similarities with *Conoryctes*, such as

Escavadodon, palaeonodonts and leptictids (Rose, 1999; Gunnell *et al.*, 2007; Gunnell and Rose, 2008; Rose, 2006b; Rose and Lucas, 2000; Szalay, 1977). These also have a typical “leptictimorph astragalocalcaneal morphology”, meaning that they exhibit features associated with extreme plantar flexion in the tibial-astragalar joint because of the increased astragalar trochlear arch and the lack of dorsal astragalar foramen (Figure 51, 52), increased lateral stability due to well-developed lateral border of the lateral astragalar facet on the distal tibia (Figure 48, 49, 50), expansion of the navicular facet of the astragalar head and reduced fibular facet in the calcaneum (Figure 53,54) (Szalay, 1977). Moreover, the analysis in chapter two of this thesis suggests affinities of taeniodonts with these groups.

To compare *Conoryctes* with other “archaic” mammals that are also found in the San Juan Basin at the same time I used *Periptychus*, a condylarth, and *Pantolambda*, a pantodont, which are well-known for their postcranial elements (Shelley *et al.*, 2018; Matthew, 1937; de Muizon *et al.*, 2015). These two outgroup genera are also compared to *Conoryctes* to assess character polarity.

Measurements are provided in the Appendix (tables A8-A20) and were made using digital callipers to the nearest two decimals. When needed, I also took digital measurements using the software ImageJ 1.6.0 (Schneider *et al.*, 2012). I coated the few teeth studied in this chapter with magnesium oxide before photographing the material. Photos of all the studied specimens were taken in the standard anatomical views using a Nikon D3500 camera and an 18-55mm lens or a 105mm macro lens when needed. I used a photo stacking technique to focus on different layers of the specimen and then I combined these using Helicon Focus 8.0.4 and exported a final image. The photos were later edited, cropped and scaled, using the software Inkscape

0.92.3. I also used photos and descriptions I found from the literature as stated in the text. When describing the new material, the Anatomy of the Dog (Evans and de Lahunta, 2013) and the PhD thesis of Shelley (2018) were used for the osteological and myological nomenclature.

New Specimens

Among the studied specimens, only one, NMMNH P-19494 has associated teeth (Figure 29) that can be firmly assigned to the *Conoryctes comma*. After comparing the associated postcranial elements of NMMNH P-19494 to the other specimens, I noticed many anatomical similarities, allowing the referral of additional specimens without associated dentition. Therefore, specimens NMMNH P-48198, NMMNH P- 48052, NMMNH P- 21509, NMMNH P- 79457, NMMNH P-47700 and NMMNH P- 47866 also are referred to *Conoryctes comma*. Two more specimens NMMNH P-61789 and NMMNH P-77896 include postcranial elements but were not associated with diagnostic bones. They resemble the postcranial fossils of *Onychodectes* but are bigger and more robust. They were found in strata that contain *Conoryctes* and *Psittacotherium* but are significantly smaller than the latter.

Most of the studied specimens have elements of the hindlimb and vertebrae, while there are four elements of the forelimb and phalanges. Some of them are exceptionally preserved, however, most of the elements are incomplete. Only specimen NMMNH P-19494 is found with associated teeth of *Conoryctes comma* and postcranial elements. Comparing the postcranial elements among the new specimens

lead to identify all of them as *Conoryctes*. Here is an overview of the elements included in each of the studied specimens. A more detailed anatomical analysis of each bone of *Conoryctes* will follow below.

Specimen NMMNH P-19494 is found in the Nacimiento Formation, Torrejonian, Tj6. It consists of three associated teeth and four bone fragments, the proximal part of a femoral diaphysis, and an almost complete left tibia that is broken proximally. One of the teeth is a lower premolar, with two roots, possibly a non-molariform right p4. The other two are upper molars, one right M1 and one right M2. Apart from the dentition that leads to associating the specimen with *Conoryctes*, the tibia of NMMNH P- 19494 resembles the distal tibia of *Onychodectes tisonensis*, AMNH 3405 (Cope, 1888, Matthew, 1937, Schoch, 1986). The tibia is slender with a minor tibial crest. On the distal epiphysis, the medial malleolus is very prominent on the anterior view, while the flexor sulci on the posterior view are well developed. In the distal view, the medial and lateral astragalar facets are subequal in size and depth. The size and anatomy of the teeth and the tibia, as well as the locality of NMMNH P-19494, point out to the genus *Conoryctes*.

Specimen NMMNH P-48198 was found in Nacimiento Formation, Tj6 and consists of 8 vertebrae, an almost complete left innominate, one almost complete left tibia, one left astragalus, and one left and one right calcaneum. Although, NMMNH P-48198 has no associated teeth, however, it has an almost complete tibia. When comparing the distal epiphysis of the tibia to the one of NMMNH P-19494 there are no anatomical differences, and both are the same size. Both tibiae have a prominent medial malleolus and flexor sulci and subequal medial and lateral astragalar facets.

For these reasons, it is reasonable to indirectly refer specimen NMMNH P-48198 to *Conoryctes comma*.

Specimen NMMNH P-48052 of the Nacimiento Formation, Tj6, includes numerous postcranial elements, most of which are fragmented. There is a left ulna with an almost complete proximal part, but it is broken distally. There is also a proximal right humerus that is damaged, but resembles the specimen AMNH 3396 of *Conoryctes*. Parts of the femur are preserved, such as a femoral head, with a well-distinguished fovea capitis, the most distal part of the left femur, with a prominent lateral epicondyle, as well as the lateral and medial epicondyles of the right femur and a patella. There are the proximal and distal parts of the left tibia, missing the diaphysis. NMMNH P-48052 has also parts of the right and left tarsals. The right tarsals are well preserved, whereas only the astragalar body of the left astragalus and the tuber calcanei of the left calcaneum are preserved. Although there are no associated teeth, there are many similarities in the tibia and the tarsals between specimens NMMNH P-19494 and NMMNH P-48198. The similarities in the tibia are as described previously for the other specimens. The calcaneum of NMMNH P-48052 and NMMNH P-48198 are identical and both are elongated and slender mediolaterally. They also have an elongated ectal facet extending medially, the cuboid facet is deep and inclined more plantarly, reaching a very robust plantar tubercle. There are also astragalar elements in both specimens (NMMNH P-48198, NMMNH P-48052), that are very similar. The trochlea rims are subequal in size and elevation leading to a narrow and slender neck. The astragalar head is wide and convex for articulation with the navicular and cuboid, and there is a small tibial facet medially. Medially, the medial tibial facet in the astragalar body is very prominent in both astragali; this is a feature seen in *Onychodectes* (AMNH 3405, AMNH 3576, AMNH 27679) too and could possibly be a

distinguishing feature for the astragalus of all taeniodonts. For these similarities in the tarsals and tibia, specimen NMMNH P-48052 belongs to *Conoryctes comma*.

Specimen NMMNH P-21509 was found in the Nacimiento Formation and consists of fragments of a left lower tooth, the proximal part of a left tibia, a left astragalus and one caudal vertebra. The lower tooth is deciduous, probably a dp5. The dp5 is very small and is not of a Taeniodont. I believe that this tooth is not associated with the rest of the elements of NMMNH P-21509. Since all the material was selected by surface collection, having more animals allocated to a specimen is very common. Both the astragalus and the proximal tibia share many morphological similarities in the shape, anatomical features and articulation surfaces with the other studied specimens (NMMNH P-19494, NMMNH P-48198 and NMMNH P-48052) as previously described. Therefore, NMMNH P-21509 is referred to *Conoryctes*.

Specimen NMMNH P-79457 was collected from Red Mesa, Nacimiento Formation, Tj5. It consists of two vertebrae, a sacrum, a complete right radius, two metacarpals and the distal end of a metacarpal, seven phalanges and three curved unguals as well as the proximal part of a right femur. The femoral head and the fovea capitis are exactly like those of specimen NMMNH P-48052. The proximal femur resembles the partial femur of specimen NMMNH P-19494. Moreover, the distal part of the radius resembles the distal radius of specimen AMNH 3396 *Conoryctes comma*. For these features and the curved and deep unguals, NMMNH P-79457 is also referred to *Conoryctes*.

Specimen NMMNH P-47700 from the Angel Peak, Tj4, consist of many postcranial elements, including seven almost complete vertebrae, a left innominate, metatarsals, phalanges and unguals, and a proximal left tibia. The proximal tibia is

damaged however the size and the anatomy of the epiphysis are similar to the proximal tibia of specimen NMMNH P-48052. The ischium and acetabular area of the pelvis are preserved in specimen NMMNH P-47700. In both specimens, NMMNH P-48052 and NMMNH P-47700, there is an acetabular notch underneath the lunate surface creating a deep groove, the ischium spine is prominent and transverse leading to the ischial tuberosity. Moreover, in both specimens, there is a prominent iliopectineal eminence. For these reasons, the specimen NMMNH P-47700 belongs to a slightly smaller individual of *Conoryctes comma*.

Similarly, specimen NMMNH P-47866 consist of only one small right calcaneum and was found in Nacimiento Formation, Angel Peak, Tj4. The calcaneum is identical to the calcanei that were described above. Therefore, NMMNH P-47866 is also referred to *Conoryctes comma*.

Specimens NMMNH P- 61789, and NMMNH P-77896, both have a partial distal humerus and a partial innominate. The humeri have a robust medial epicondyle similar to the humerus of *Onychodectes tisonensis* AMNH 16410 (Matthew, 1937; Schoch, 1986), further supporting a referral to Taeniodonta. Biostratigraphically they were collected from strata where only *Conoryctes* and *Psittacotherium* are found. Their innominate resembles those of specimens NMMNH P-48198 and NMMNH P-47700, having a prominent illiopubic eminence. Based on that and their size, they are referred to cf. *Conoryctes*.



Figure 29: Associated teeth of *Conoryctes comma*, specimen NMMNH P-19494. Upper M1 (a-d), upper M2 (e-h) in occlusal views (a, e), distal view (b, f), mesial view (c, g) and buccal view (d, h). On the third row is the lower p4 in occlusal (i), mesial (j), lingual (k) and distal (l) views. Scalebar is 1 cm.

Comparative description

Vertebrae

Many of the studied specimens have elements of vertebrae, but most of them are damaged and incomplete. Part of the vertebrae column of *Conoryctes* is described in the current study for the first time. Specimen NMMNH P- 48052 has four almost complete anterior cervical vertebrae, one of which is the axis, and one posterior cervical vertebra. The same specimen has numerous parts of the body and caudal

vertebrae and articular process of probably thoracic, lumbar and caudal vertebrae, as well as partial ribs. Specimen NMMNH P-79457 also has two partially complete cervical vertebrae, two thoracic vertebrae, an almost complete lumbar and a sacrum. It also has another lumbar vertebra that is more damaged and a few pieces of the body and caudal processes of other vertebrae, and a medial epiphysis of a rib. Similarly, specimen NMMNH P-47700 has two cervical vertebrae, two partial lumbar vertebrae and four anterior caudal and one posterior caudal, plus medial parts of a rib. Specimen NMMNH P-21509 has only one distal caudal vertebra and a few broken parts of the caudal processes of other vertebrae. Lastly, specimen NMMNH P-48198 has seven caudal vertebrae, from the most anterior to the more posterior, giving new insight into the tail of *Conoryctes*.

The axis as seen in specimen NMMNH P-48052 is short anteroposteriorly (Figure 30). Cranially, the two articular processes that connect the axis to the atlas are circular in shape and convex. Between these two processes is the dens extension, which is broken off in NMMNH P-48052. The transverse and spinous processes are also broken. In dorsal view, there is a pair of transverse foramina caudally.

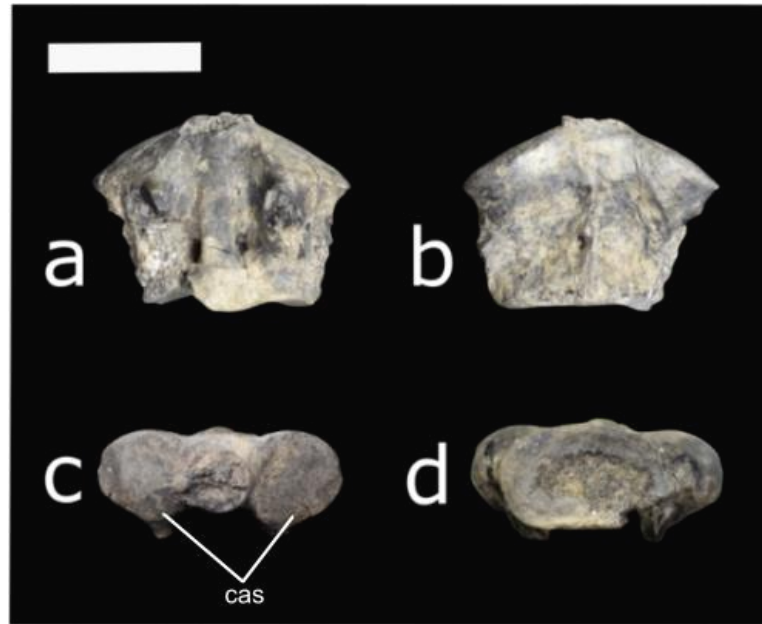


Figure 30: The axis of *Conoryctes comma* NMMNH P-48052 in dorsal (a), ventral (b), cranial (c) and caudal (d) views. cas: cranial articular surface. Scale bar is 1cm.

The posterior cervical vertebrae, as seen in figures 32 and 33, (NMMNH P-48052, NMMNH P-79457, NMMNH P-47700) have a shorter anteroposterior length compared to mediolateral width (table A9, in Appendix). The most posterior cervical is also anteroposteriorly longer compared to the most anterior and the axis (NMMNH P-48052). Mostly the body of the cervical vertebra is preserved, so all the dorsal information is missing. The morphology of the body is very similar to the morphology of the axis and is more mediolaterally elongated than dorsoventrally. The anterior epiphysis is convex and the posterior concave. Specimens NMMNH P- 47700 and NMMNH P-480552 have one cervical vertebra each, and both preserve the transverse process. In specimen NMMNH P-48052 this process is more complete extending laterally and ventrally. Specimen NMMNH P-48052 looks like it has a dorsoventrally larger body than any other cervical vertebrae, so it must belong to a more distal cervical vertebra. Based on these specimens, and particularly the individual NMMNH

P- 47700, *Conoryctes* had a short neck relative to the rest of its body (Figure 33). The anteroposterior length of the cervical vertebrae is almost half as long as the thoracic and lumbar.

The thoracic vertebrae are not well represented in the new specimens and only specimen NMMNH P-79457 has one, potentially two, thoracic vertebrae. Both of them have a well-distinguished saddle-shaped body, but only one of them is less damaged. In the cranial and caudal view, there is a small cranial and caudal costal fovea in the body. In the lateral view, there is a mamillary process with a circular transverse fovea ventrally, for attachments with the tubercle of the rib. Although the transverse process is missing, and these two thoracic vertebrae are not complete, there is no evidence of an extra articulation between the vertebrae. This extra bony interlocking of the posterior thoracic and lumbar vertebrae is seen in *Xenarthra* (Hautier *et al.*, 2018). Specimens NMMNH P- 79457 and NMMNH P-48052 have many parts of rib. Specimen NMMNH P- 48052 has also a partial body of the rib that was attached to the costal arch towards the sternum.

Specimen NMMNH P-47700 has a lumbar vertebra, with a less saddle-shaped body, and a large vertebral foramen and the base of the mamillary processes is extending more dorsally than mediolaterally. The base of the spinous process is also preserved while the transverse processes are incomplete. More distal lumbar vertebrae are known from specimen NMMNH P-79457 which has one almost complete and one very damaged vertebra. The lumbar vertebra of specimen NMMNH P-79457 has anterolaterally extended transverse processes, a distinction between the posterolaterally extended transverse processes of the caudal vertebrates. In the lateral view, the mamillary processes and the spinous process are broken, but there is the

caudal articular process. Partial caudal articular processes can be seen in specimens NMMNH P-21509, NMMNH P-48052 and NMMNH P-79457 too. The articular surface is convex and is ventrolaterally oriented compared to the body.

Specimen NMMNH P-79457 has an almost complete sacrum (Figure 31), composed of three fused sacral vertebrae. In dorsal aspect, the cranial articular process and the median and lateral sacral crests are broken. The medial part is missing from the second and third sacral. There is also concretion and some features cannot be observed.

In dorsal aspect, the two cranial articular processes, mediolateral to the sacral canal, are broken. Based on the size of the broken area there must have been quite robust and dorsomedially oriented. These processes would have joined with the posteriormost lumbar vertebra. The sacral canal is large and circular in shape. The medial and lateral sacral crests are broken. On the lateral side, there is a well-preserved dorsal sacral foramen. There are signs for at least other two sacral foramen on each side, that are covered with concretions or are missing due to breakage. Through these four dorsal sacral foramina passed the spinal nerves and vessels. More caudally, the intermediate sacral crests are preserved, both medially and laterally, on the third fused sacral vertebra. The caudal articular process is very well preserved, forming the apex of the sacrum, which is extending far more caudally than the body. This is where the sacrum is articulated with the first caudal vertebra.

In ventral aspect, the first sacral vertebra, the most cranial one, is more robust and shorter; the second and the third sacral are long and slender. Cranially, the first sacral has a robust transverse ridge; this is the promontory and is part of the base of the sacrum. Between the first two sacral, the wings of the sacrum are formed on the

lateral and the medial side. They are more noticeable in ventral view, than in dorsal, and are slightly expanding ventrally. Caudally to the fusion of the first and second is a pair of pelvic sacral foramina. Only the right one is not filled with matrix; it is subequal in size to the corresponding dorsal foramen. There is evidence of another pair of pelvic sacral foramina at the fusion of the second and third sacral. Through these two pairs of pelvic sacral foramina, blood vessels and nerves were passing.

In lateral and medial views, there are the wings of the sacrum, cranially, with enlarged articular surfaces for attachment with the ilium. Caudally, the lateral and medial sides of the specimen are broken. Using the innominate of specimen NMMNH P-48198. The two elements and the wing of the sacrum match perfectly with the signs of attachment in the ilium. The ilium has two areas for attachment, indicating that caudally to the wings of the sacrum, the lateral and medial sides that are broken in specimen NMMNH P-79457, would have been extended at the same level as the wings.

In cranial view, the base of the sacrum is almost flat and is more mediolaterally elongated than circular. Dorsally to the base is the sacral canal and ventrally the promontory. Caudally, there is the caudal body that has a more circular shape than the base of the sacrum. The apex of the sacrum extends further caudally.

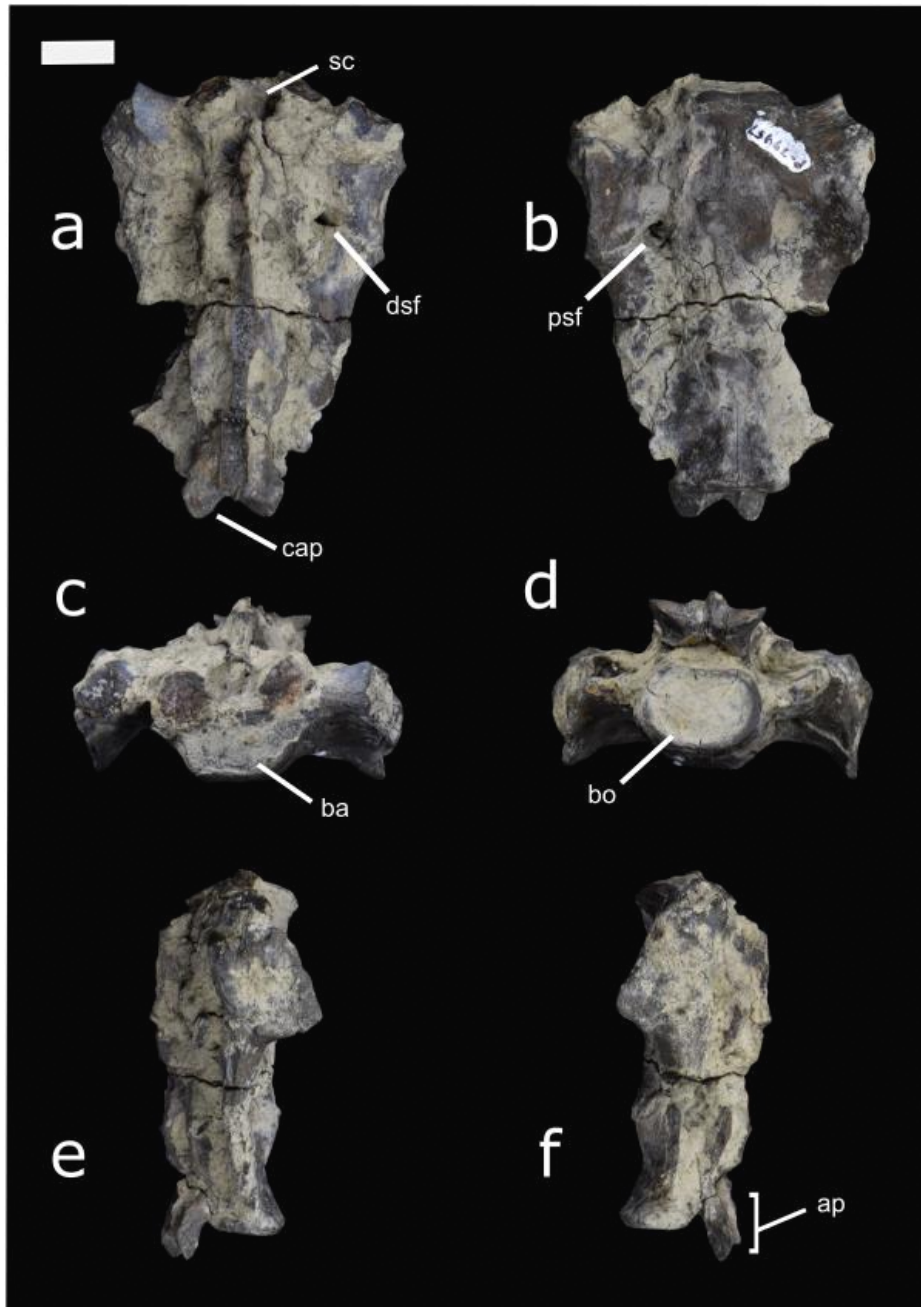


Figure 31: The sacrum of *Conoryctes comma*, NMMNH P-79457 in dorsal (a), ventral (b), cranial (c), caudal (d), medial (e) and lateral (f) views. ap: apex, ba: base, bo: body, cap: caudal articular process, dsf: dorsal sacral foramina, sc: sacral canal, psf: pelvic sacral foramina. Scale bar is 1cm.

The caudal vertebrae are known from specimens NMMNH P-48198, NMMNH P-47700, NMMNH P-48052 and NMMNH P-21509. Of them, the two former

specimens have almost a complete sequence of the most proximal caudal vertebrae, from the first caudal to the fourth and fifth. Specimen NMMNH P-47700 has better-preserved vertebrae with the dorsal processes being less broken. The body of the caudal vertebrae is more cylindrical, and the transverse processes extend posterolaterally. In dorsal view, there is a similar trigonid shape bulging near the caudal epiphysis of the body, as seen in the cervical vertebrae. The vertebral arch is becoming smaller posteriorly and in more distal caudal vertebrae the mamillary processes are becoming smaller. There are more distal caudal vertebrae, such as in specimens NMMNH P-48198 and NMMNH P-48052. These are more cylindrical and have a smaller foramen posteriorly for the nerves and blood vessels. Also, the more distal caudals have a cylindrical and slender shape in the middle, because the transverse process is divided into two mediolateral extensions of the body.

The number of vertebrae for *Conoryctes* remains unknown, however, based upon the morphology of the vertebrae (Figure 32, 33), it had a short and robust neck and probably a long tail (Figures 32 and 33). This structure has been proposed for *Onychodectes* too by Schoch (1986) and is also seen in the PM 3895 specimen of *Stylinodon*.

There are only two other sacral elements known for taeniodonts; the specimens of *Onychodectes* (AMNH 16410) and *Stylinodon* (PM 3895). Both specimens have partially preserved sacra, but the number of fused sacral vertebrae is unknown. The specimen of *Onychodectes* is incomplete; only part of the first sacral and part of the wings are preserved. It is smaller in size than *Conoryctes*, but it also had robust cranial articular processes and wide wings. The base of the sacrum is also not circular but mediolaterally elongated, similar to *Conoryctes*. Turnbull (2004) described the

incomplete sacrum of *Stylinodon* PM 3895 and hypothesised it consisted of three sacrals. Also, “segment 2” in Turnbull (2004), which is possibly the third sacral, is narrower and more elongated than in *Conoryctes*.

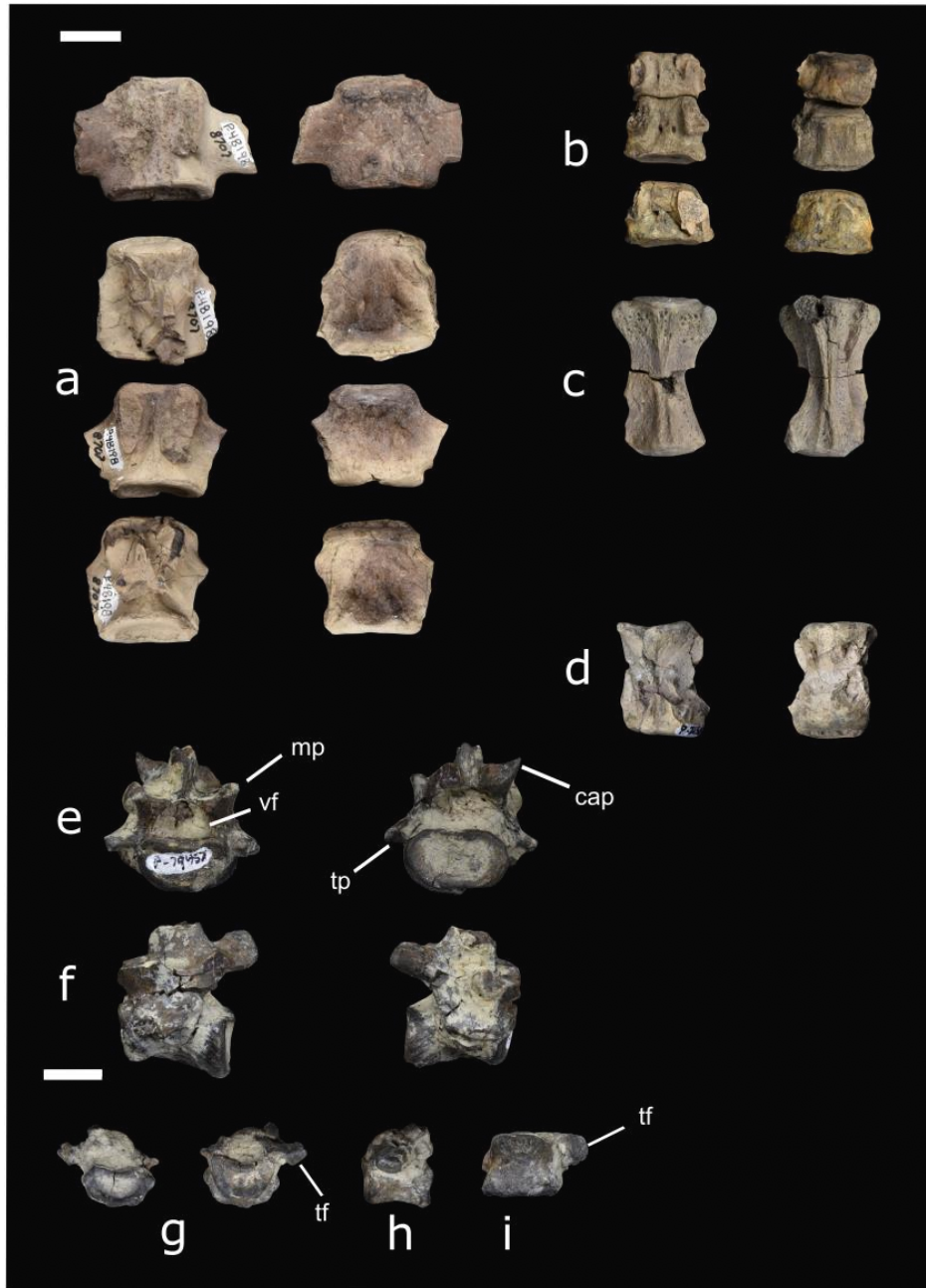


Figure 32: Vertebrae of specimens NMMNH P-48198 (a), NMMNH P-48052 (b, c), NMMNH P-21509 (d), NMMNH P-79457 (e-i). Part of the neck with cervical vertebrae (b), a thoracic vertebra in anterior and posterior views (g), in a side view (h) and distal view (i). A lumbar vertebra in posterior and anterior view (e) and side views (f). Proximal caudal vertebrae of *Conoryctes comma* (a), as well as distal caudal vertebrae (d, c). cap: caudal articular process,

mp: mamillary process, tf: transverse fovea, tp: transverse process, vf: vertebral foramen.
Scale bar is 1cm.

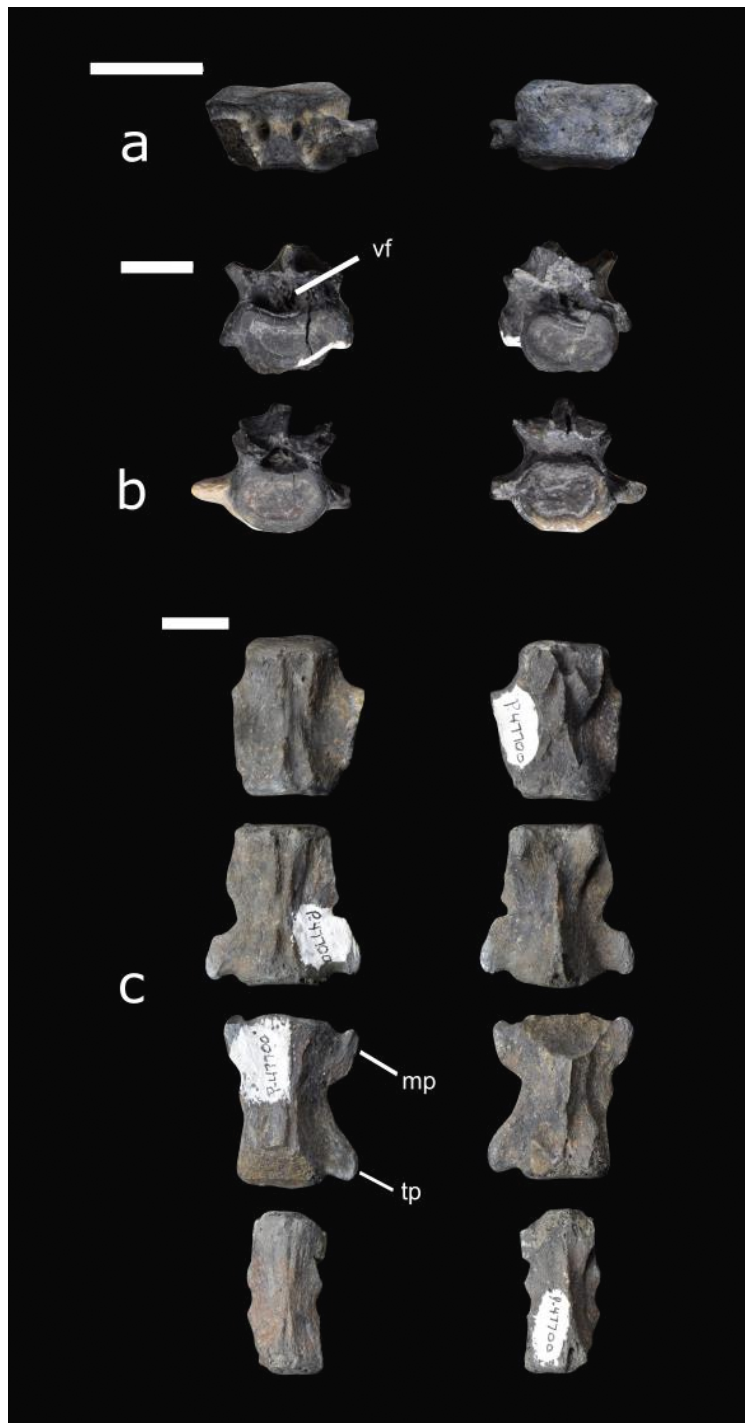


Figure 33: Vertebrae of *Conoryctes comma* NMMNH P-47700. Cervical vertebra (a), two lumbar vertebrae in cranial and caudal views (b) and caudal vertebrae (c) from the most proximal to the most distal. mp: mamillary process, tp: transverse process, vf: vertebral foramen. Scale bar is 1cm.

Humerus

Specimen AMNH 3396 consists of a partial mandible and upper dentition of *Conoryctes comma* as well as the proximal-most part of the humerus and the distal end of a radius (Figure 34). The right humerus is not complete, missing the distal end and part of the diaphysis is also missing and it is connected with plaster, so the total length cannot be estimated.

The new specimens NMMNH P-48052, NMMNH P-61789 and NMMNH P-77896 provide more information (Figure 35). NMMNH P-48052 preserves the proximal part of the right humerus. The humeral head is preserved; however, the specimen is mediolaterally compressed with the greater tubercle being crushed against the humeral head. Specimens NMMNH P-61789 preserves part of a broken diaphysis and only the distal end of the humerus is preserved in NMMNH P-77896. As mentioned, specimens NMMNH P-61789 and NMMNH P-77896 belong to cf. *Conoryctes* and based on them I studied the distal humerus. The partial left humerus of NMMNH P-61789 consists of part of the diaphysis and is similar in width to the proximal epiphysis of the specimen NMMNH P-48052.

The humeral head is oval in shape and has a deep bicipital groove next to it as seen in both AMNH 3396 (Figure 34c) and NMMNH P-48052 (Figure 35d). Another feature seen in the AMNH 3396 and the new specimens from the San Huan Basin is the robust deltopectoral crest. In the new specimens, deltopectoral crest extends further distally, near the entepicondylar foramen. Specimen AMNH 3396 is connected with plaster giving the illusion that the deltopectoral crest is not approximating the entepicondylar foramen. As Matthew (1937) pointed out for AMNH 3396 and can be

seen in NMMNH P-61789 and NMMNH P-77896, the deltopectoral crest is broad distally.

Proximally the humerus of *Conoryctes* has a distinguished greater tubercle. In anterior view, based on the AMNH 3396 humerus, the head is approximately at the same level as the greater tuberosity. There is a lip for the bicipital groove separating the head from the greater tubercle and extending anterodistally (Figure 36a).

The humeral head is complete, almost hemispherical being longer proximodistally than mediolaterally wider. In medial view, the apex of the humeral head is raised, the lesser tubercle is close to the anteromedial surface of the humeral head. In anterior view, the lesser tubercle is separated from the greater with a deep groove.

The shaft of the humerus, although not complete, is robust with prominent crests and flanges. Proximally, in anterior view, there is a well-defined deltopectoral crest that forms a prominent deltoid tuberosity. The edges of the crest are strong forming a U-shaped deltopectoral region. The deltopectoral tuberosity is very prominent as seen in NMMNH P-61789 and NMMNH P- 77896 and extends to the level of the epicondylar crest.

In anterior view, medial to the deltopectoral region, there is a very prominent crest on the humeral diaphysis terminating distally almost at the same level as the deltopectoral tuberosity. This is the area for the insertion of the teres major and the latissimus dorsi. The teres major muscles were attached to the lateral border of the scapula and were responsible for the extension and medial rotation of the humerus. The latissimus dorsi was also assisting in the rotation and extension of the shoulder. This prominent crest points to a strong shoulder joint.

The lateral epicondylar crest extends laterally, providing attachment for the extensor carpi radialis muscles. It is broken and it is undetermined where the proximal origin of it was. It is very lateromedially broad giving a more robust shape of the humerus.

Distally, on the medial side, the supracondylar crest is mediolaterally expanded and there is a large and robust entepicondylar crest (Figure 35j). The proximodistal distance between the deltopectoral tuberosity and the proximal border of the entepicondylar foramen is short.

The distal epiphysis of *Conoryctes* is mediolaterally broad with a well-defined humeral trochlea and capitulum. In anterior view, the mediolateral width of the trochlea is approximately equal to the width of the capitulum. The trochlea is deep, and more medially expanded and the trochlear keels are subequal as seen in posterior view. The capitulum is more spherical in anterior view and flatter in posterior view. The distal extent of the epicondylar crest extends laterally and it reaches distally near the distal level of the deltopectoral tuberosity. The large area of the epicondylar crest is where the extensor muscles, the radial collateral ligament and tendons were attaching, providing stability to the elbow joint. The olecranon fossa is deep but lacks an opening. In lateral view, the lateral epicondyle is damaged, but there are signs of a well-defined sulcus.

The humerus is known for other taeniodonts including *Onychodectes* (AMNH 16410, Figure A42), *Ectoganus* (FMNH P 26090), *Psittacotherium* (NMMNH P-48358) and *Stylinodon* (YPM 1196). There are many similarities between the humerus of *Onychodectes* and *Conoryctes*. Both have similarly broader distal than proximal epiphyses and the greater tubercle is more anteriorly extended in both. However,

Onychodectes has a slender diaphysis than *Conoryctes*. The deltopectoral region is broader in *Conoryctes* than in *Onychodectes* and the deltopectoral tuberosity is more robust. The deltoid crest extends more distally in *Conoryctes* than in *Onychodectes*. The more derived taeniodonts *Psittacotherium*, *Ectoganus* and *Stylinodon* have even mediolaterally broader humeri with more mediolaterally extending deltopectoral regions than *Conoryctes*. In addition to being almost six times larger, the humerus of *Stylinodon* has a more laterally expanding deltopectoral crest than in *Conoryctes*.

Escavadodon shares many similarities with the humerus of *Conoryctes*. The greater tuberosity is almost on the same level as the humeral head proximally and the deltopectoral crest and tuberosity are similar in both taxa, extending distally near the level of the epicondylar crest (Rose and Lucas, 2000). However, *Conoryctes* has a relatively more slender humerus than *Escavadodon*. The teres major tubercle is more prominent in *Escavadodon* compared to *Conoryctes* (AMNH 3396) and the humeral trochlea is equal in mediolateral width to the capitulum. The humeral trochlea is placed central to the mediolateral width of the distal epiphysis in *Conoryctes*, while it is more laterally placed in *Escavadodon*.

The humerus of *Periptychus* and *Pantolambda* share some similarities but also differences with *Conoryctes*. In all three taxa, the greater tubercle is on the same level as the humeral head. The humeral head is proximodistally longer relative to the humeral shaft in these two taxa than in *Conoryctes*. The deltopectoral region is more prominent in *Pantolambda* and *Conoryctes* than in *Periptychus* (Simons, 1960; Matthew, 1937; Shelley *et al.*, 2018). All three taxa have a moderately deep humeral trochlea that is medially expended in *Conoryctes* and *Periptychus* and less so in *Pantolambda*.



Figure 34: The humerus of *Conoryctes comma*, specimen AMNH 3396, in posterior (a), medial (b), anterior (c) and lateral (d) views. Scale bar is 1cm.

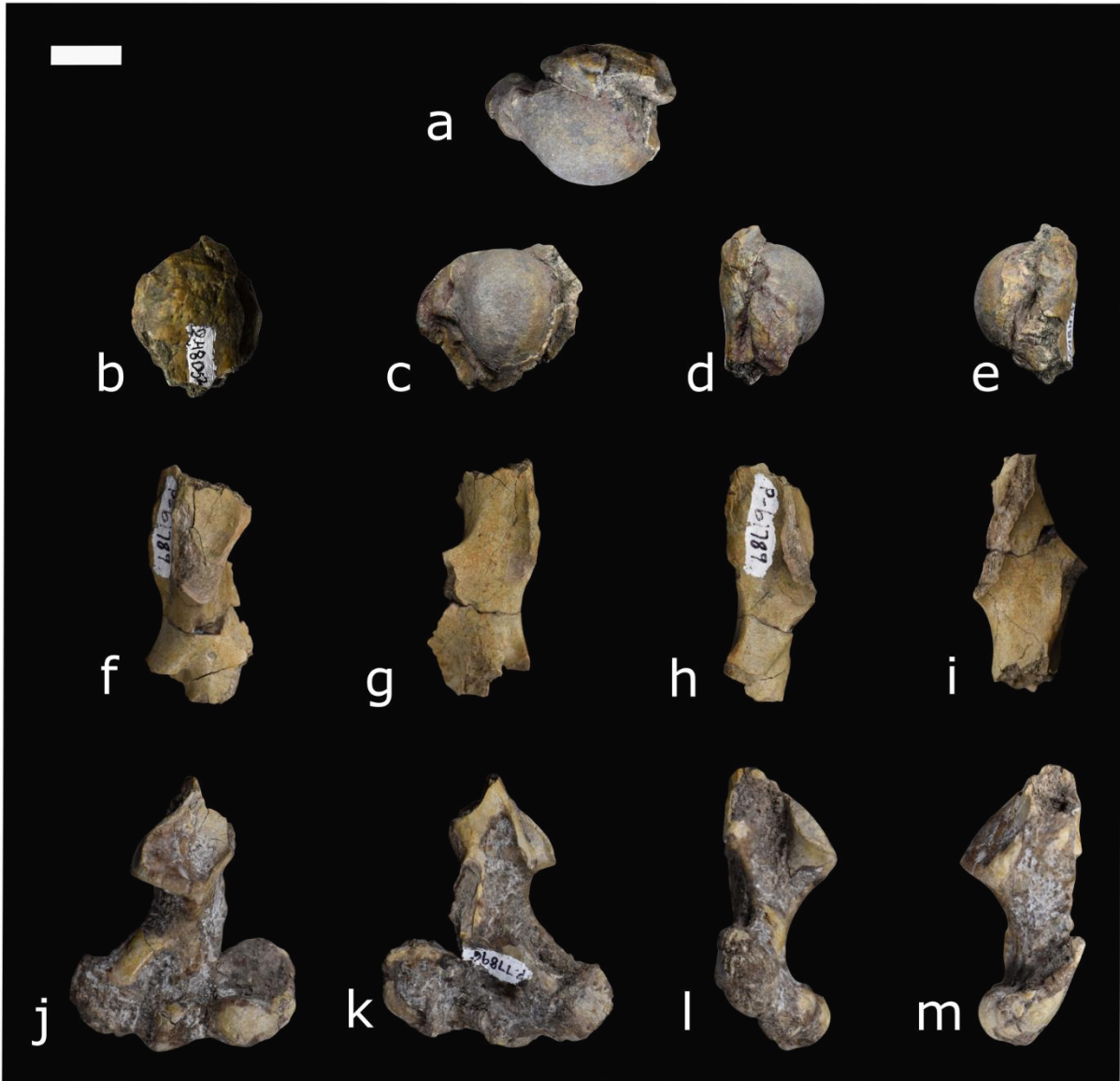


Figure 35: The new specimens of the humerus of *Conoryctes comma*, NMMNH P-48052 (a-e), NMMNH P-61789 (f-i) and NMMNH P-77896 (j-m) in proximal (a), anterior (b, f, j), posterior (c, g, k), medial (d, h, l) and lateral (e, i, m) views. Scale bar is 1cm.

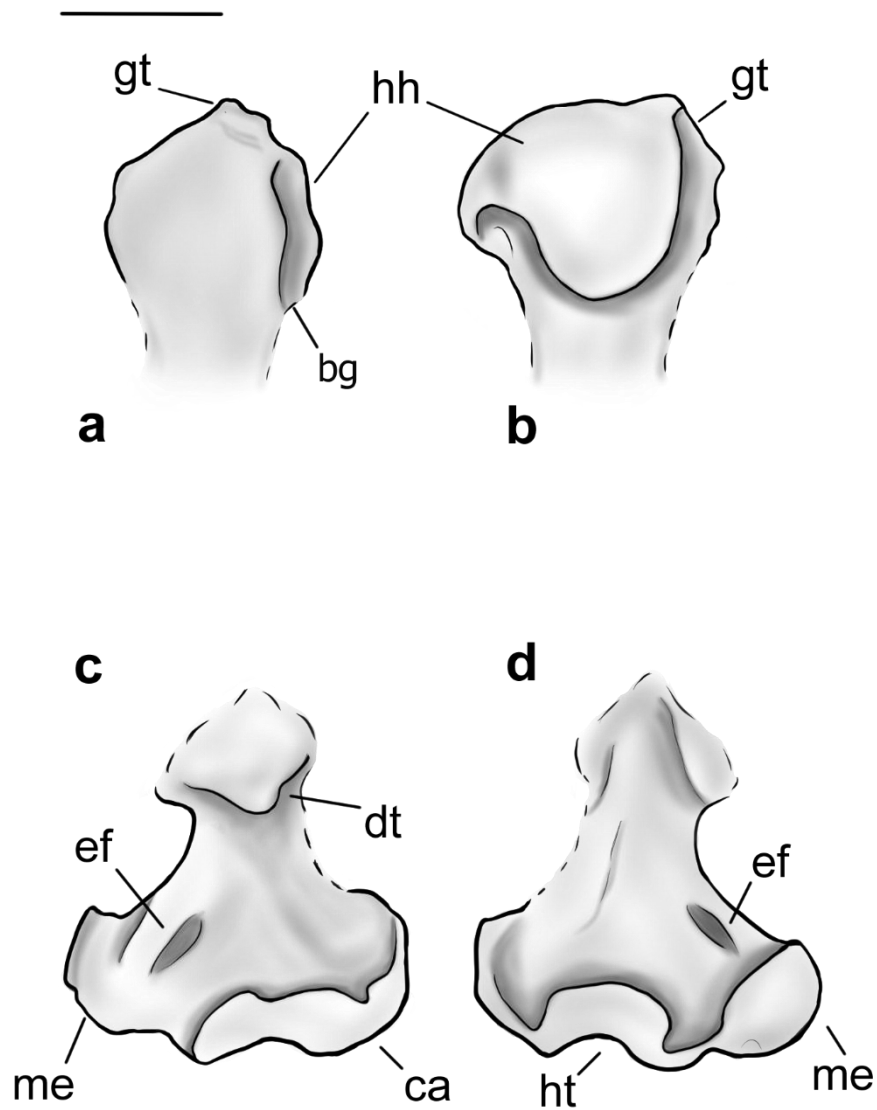


Figure 36: Drawing of the humerus of *Conoryctes comma* in anterior (a, c), posterior (b, d) views. bg: bicipital groove, ca: capitulum, dt: deltopectoral crest, ef: entepicondylar foramen, gt: greater tubercle, hh: humeral head, ht: humeral trochlea, me: medial epicondyle. Scale bar is 1cm.

Ulna

There are left and right proximal ulnae among the elements of specimen NMMNH P-48052 (Figures 37 and 38). The left ulna is broken distally at the diaphysis and is damaged on the articular region with the humerus and the radius. However, there are many features on the olecranon, as well as on the medial and lateral sides of the shaft that are well preserved. In general, the ulna is slender mediolaterally and broader anteroposteriorly. Due to damage, it is unclear how mediolaterally protruding the coronoid and the anconeal processes are. In lateral view, the ulna is strongly bent proximally, at the olecranon, and less curved distally, at the distal diaphysis.

The olecranon of *Conoryctes* is almost complete, missing only a small part of the anteromedial end. In anterior view, the olecranon is wider mediolaterally than the rest of the shaft and is oriented laterally (Figure 37). There is a longitudinal ridge dividing the olecranon in half. On the medial half, the olecranon is almost flat and protrudes medially forming a broad tuber, while the lateral half is less pronounced and inclined laterally. In proximal aspect, this division of the olecranon continues and there is a groove separating a medial and a lateral fossa on the most proximal end of the olecranon; the lateral fossa that is deeper than the medial. The lateral fossa has well-defined borders more so proximally, laterally and medially than distally. In this fossa, the anconeus muscle, the lateral flexor digitorum profundus and the lateral head of the triceps brachii were attached. The medial fossa is shallower but subequal in size to the lateral fossa. The proximomedial part of the medial surface is broken. In the medial fossa of the olecranon attached the medial head of the triceps brachii, the tensor fasciae antebrachii, the flexor carpi ulnaris muscle and the medial flexor digitorum profundus muscle. In posterior view, the olecranon process is connected to

a flat surface that continues distally until the ulnar diaphysis. In lateral view, distally to the olecranon process, there is the elongated anconeal fossa that extends distally, forming a ridge posteriorly (Figure 37a). Similarly, in medial view, there is an even deeper elongated flexor fossa. The posterior ridge of the flexor fossa is strong and continues distally until the proximodistal end of the humerus-ulna articular region, meeting the proximal ulnar diaphysis.

In specimen NMMNH P-48052, the ulnar trochlear and the articulation surfaces for the humerus and the radius are damaged. Part of the anconeal process is preserved, showing that it might have been asymmetrical and more elevated medially. The coronoid process, on the medial area, is damaged. The trochlear notch is concave. The radial notch is better preserved; it forms a concave and large area for articulation with the radius. The radial notch might have been adjacent to the coronoid process laterally. The radial notch forms a protuberance that extends laterally from the ulnar shaft. The proximodistal length of the articular surface is smaller than the olecranon's proximodistal length (see appendix).

Only the proximal diaphysis of *Conoryctes* is preserved and is more robust anterodistally than mediolaterally. In anterior view, the shaft is flat and medially twisted, while in posterior view, it is sharp. In medial view, this twist continues to the medial area of the proximal diaphysis and is almost flat. On the contrary, the lateral area, in lateral view, has a prominent longitudinal fossa starting almost at the distal end of the radial notch and continuing distally (Figure 38c). This fossa provided attachment for the flexor digitorum profundis and lateral triceps brachii. The anterior border of this fossa creates a ridge with the anterior crest of the proximal diaphysis. On the proximal border, the ridge is smooth proximally but extends distally to a more

prominent ridge. This ridge creates a second longitudinal fossa. This second fossa is very shallow and continues distally alongside the first one; it provided attachment for the abductor pollicis longus. Due to breakage, it is unclear where the two fossae ended distally.

There are many ulnae known for almost all the genera of Taeniodonta, i.e. *Onychodectes* (AMNH 16410, Figure A43), *Conoryctella* (UNM B-1258, new label NMMNH P-25056, Figure A45), *Wortmania* (NMMNH P-19460), *Psittacotherium* (AMNH 2453 and AMNH 16560, Figure A46), *Ectoganus* (USGS 3838 and FMNH P 26083) and *Stylinodon* (YPM 11096, USNM 18425, UW 2270 and PM 3895) (Schoch, 1986; Turnbull, 2004). *Onychodectes* has an almost straight ulna in lateral/medial view, whereas *Conoryctes*, *Conoryctella* and even *Wortmania* have more posteriorly curved ulnae. The olecranon protrudes medially and is posterolaterally inclined in *Onychodectes* and *Conoryctella*, similar to *Conoryctes*. These three genera also have a crest dividing the olecranon into lateral and medial areas, that continues to the lateral and medial fossae proximally. The olecranon of specimen AMNH 3394 of *Wortmania* is broken. The articular surface is subequal to the olecranon in *Onychodectes*, but the olecranon is longer proximodistally than the articular surface in *Conoryctes* and *Conoryctella*. Due to damage of specimen NMMNH P-48052 of *Conoryctes* the articular surfaces cannot be compared. However, the radial notch is flatter in *Conoryctes* and *Conoryctella* than in *Onychodectes*. In these three specimens, the radial notch is more laterally placed than in *Wortmania*, which has a more concave radial notch. In medial view, the flexor fossa on the olecranon is deep, yet the posterior ridge is not as prominent in *Onychodectes* as in *Conoryctes*, *Conoryctella* and *Wortmania*. In lateral view, the two longitudinal fossae in *Onychodectes* are similar to

those of *Conoryctes*, with the most anterior one starting from the middle of the articular region and the posterior one more distally.

The ulna of *Ectoganus* (USGS 3838) is similarly curved as in *Conoryctes* whereas in *Stylinodon* (YPM 11096) the ulna is even more curved posteriorly. The specimens of *Psittacotherium* (AMNH 2453) are damaged and it is uncertain how the olecranon was formed anatomically. *Psittacotherium* had an anteromedially prominent olecranon that was longer proximodistally than the articular surface, as in *Conoryctes*. *Stylinodon* also has a medially protruding proximal olecranon but less so than *Conoryctes*; in *Stylinodon* the olecranon anteriorly is also divided with a very strong crest. Unlike *Conoryctes*, *Conoryctella*, probably *Psittacotherium* and *Ectoganus* (due to damage of the specimens) have a longer olecranon than the articular surface, which is exactly the opposite in *Stylinodon*. In *Psittacotherium* the radial notch is less laterally than in *Conoryctes*, while in *Ectoganus* and *Stylinodon* it is almost completely anteriorly. In medial view, the flexor fossa is not as prominent in *Psittacotherium* as in *Conoryctes*, while the fossa and the posterior ridge are more robust in *Stylinodon*. In lateral aspect, in *Stylinodon* the two fossae for the muscle attachments are large and they are both subequal to each other anteroposteriorly, unlike in *Conoryctes*.

The ulna of *Conoryctes* has a different shape than *Escavadodon*, the olecranon of the latter is very medially inflected and oriented (Rose, 1999; Rose and Lucas, 2000; Rose, 2006). The olecranon of *Escavadodon* is longer proximodistally than in *Conoryctes* and even more than in leptictids. The radial notch of *Escavadodon* is not laterally placed like in palaeonodonts and *Conoryctes*. In lateral view, the most anterior fossa is very prominent in *Escavadodon*, leptictids and *Conoryctes*, while in medial

view, the flexor fossa is deep with a prominent ridge in *Escavadodon* similar to *Conoryctes*.

Compared to *Periptychus* and *Pantolambda* the ulna of *Conoryctes* is less robust (Simons, 1960; Matthew, 1937; Shelley *et al.*, 2018). Particularly in the proximal olecranon both *Periptychus* and *Pantolambda* have an anteromedially strong protruding eminence. In the olecranon, *Conoryctes* and *Periptychus* have a well-defined ridge anteriorly that continues proximally creating two fossae for muscle attachment; this is not that pronounced in *Pantolambda*. The olecranon of *Periptychus* is almost subequal in proximodistal length to the articular surface, similar to *Onychodectes* and unlike *Conoryctes*. *Periptychus* and *Pantolambda* have an anteromedially placed radial notch while in *Conoryctes* it is more laterally placed. In medial view, the flexor fossa of *Periptychus* is deep with a larger ridge than in *Conoryctes*, while the fossa is less excavated and the ridge is even larger in *Pantolambda*. In latera view, the two longitudinal fossae are similar in size and shape in *Periptychus* and *Conoryctes*. In *Pantolambda* the fossae are less defined and extend less distally.

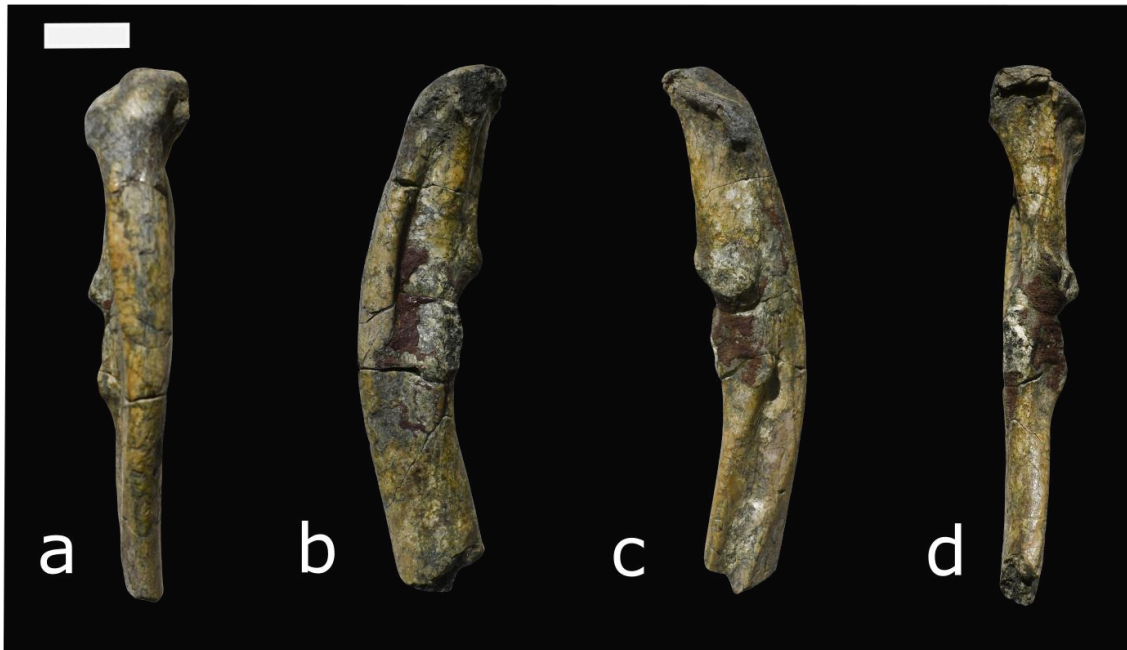


Figure 37: The ulna of *Conoryctes comma*, specimen NMMNH P-48052, in posterior (a), medial (b), lateral (c) and anterior (d) views. Scale bar is 1cm.

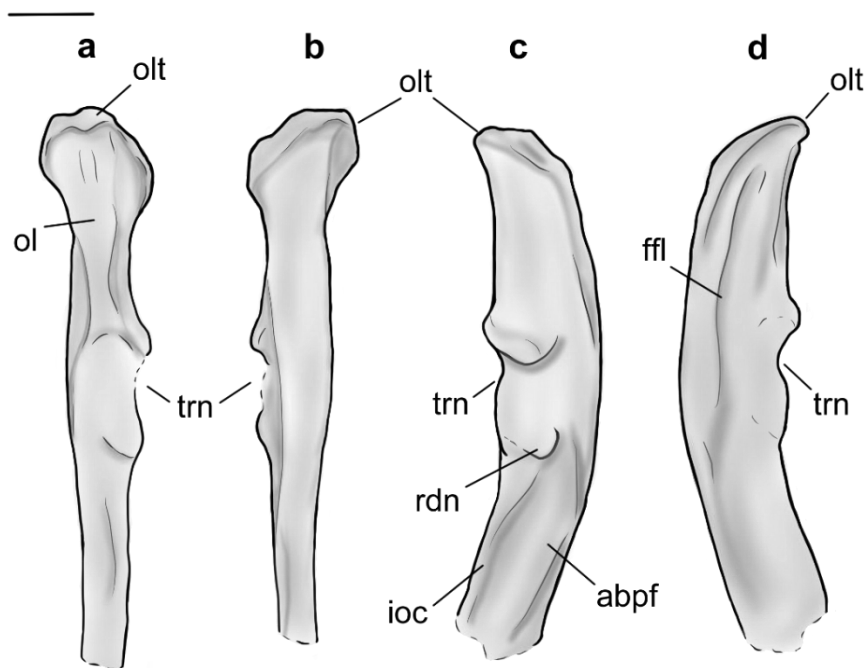


Figure 38: Drawing of the ulna of *Conoryctes comma* based on the NMMNH P-48052 specimen in anterior (a), posterior (b), lateral (c) and medial (d) views. adpf: abductor pollicis longus fossa, ffl: flexor fossa, ioc: interosseous crest, ol: olecranon, olt olecranon tuber, rdn: radial notch, trn: trochlear notch,. Scale bar 1cm.

Radius

Specimen NMMNH P-79457 has a complete left radius of *Conoryctes*. The element is well preserved, and many anatomical features can be observed (Figures 39 and 40). The radius is wider mediolaterally at the distal epiphysis than at the proximal end. The proximal diaphysis is also slender proximally and becomes more robust anteroposteriorly at the distal diaphysis. The capitular eminence proximally and the grooves at the distal end are very distinguished in *Conoryctes*.

The proximal diaphysis is broader mediolaterally than anteroposteriorly and is asymmetrical. In proximal view, the head of the radius is almost squared-shaped (Figure 39e). The mediolateral width of the proximal epiphysis is greater than the anteroposterior width (table A12, in Appendix). The deepest point of the capitulum is in the middle of the fossa and the rims of the capitulum are continuous. The rims of the radial fossa are more distally placed anterolaterally and extend more proximally posterolaterally. In anterior view, the radial head is bulging over the neck, while the posterior and lateral parts of the capitulum can be seen reaching more proximally than the rest of the circumference of the fossa. Therefore, the radial head of *Conoryctes* is medially inclined. The capitulum, in medial view, is oriented posteromedially creating a large lip over the radial neck. In posterior view, there is a flat ulnar facet that is broad both mediolaterally and proximodistally. Distal to this facet is the prominent bulging area of the bicipital tuberosity (Figure 40). The bicipital tuberosity is almost circular and was responsible for the insertion of the tendon of the biceps brachii. In lateral aspect, the radial head and neck are almost continuous.

The proximal radial diaphysis of *Conoryctes* is cylindrical and broadens more anteroposteriorly. In lateral aspect, there is a longitudinal large fossa for the abductor pollicis longus muscle (Figure 40c). The distal diaphysis is flattened mediolaterally and anteriorly forms a crest. This is the pronator crest and gives an anteriorly curved shape to the radius. In anterior view, the pronator crest is strong, sharp and slightly curved laterally, extending almost 40% of the total length of the radius. On this crest, there are areas evident in specimen NMMNH P-79457 for the attachment of the pronator teres and a broad area mesiodistally for the pronator quadratus. Distally the crest is raised into a very prominent tuberosity, proximodistally elongated, that is near the distal radial epiphysis. Lateral to that tuberosity, there is a broad and deep sulcus for the extensor digitorum communis and the digitorum lateralis. Medially to the tuberosity, the sulcus for the tendon of the extensor carpi radialis is smaller and shallower. In lateral view, on the posterodistal end of the diaphysis, there is a small protuberance possibly for the distal articulation with the ulna.

The distal radial epiphysis of *Conoryctes* is mediolaterally broader with a moderate styloid process (table A12). In distal view, there are two fossae that are poorly separated (Figure 39f). The lateral fossa is larger, more than half the distal radial epiphysis, deeper and almost circular. This is the area where the lunate articulated with the radius. The medial fossa is smaller and shallower but also circular in shape for articulation with the scaphoid.

There are other taxa of Taeniodonta that have complete, or almost complete radii, such as *Onychodectes* (AMNH 16410) *Wortmania* (AMNH 3394, NMMNH P-19460), *Psittacotherium* (AMNH 16560, Figure A46 and NMMNH P-77785), *Ectoganus* (USNM 1001) and *Stylinodon* (YPM 11096 and PM 3895) (Schoch, 1986;

Turnbull, 2004). Only the proximal epiphysis is preserved in *Onychodectes* (AMNH 16410) while *Wortmania* (AMNH 3394) has an almost complete radius, missing the distal epiphysis. The distal end of the radius is very similar between *Conoryctes* and *Onychodectes*. The capitulum, in proximal view, is mediolaterally more elongated in *Wortmania* than in *Onychodectes* and *Conoryctes*; the latter two genera, distally, have a slender neck relative to the capitulum. In all these three genera, the capitular eminence is more proximally protruding in the lateral area of the ridge. The bicipital tuberosity is more proximodistally elongated in *Onychodectes* and *Wortmania* while it is almost circular in *Conoryctes*. The ulnar facet in *Onychodectes* is very small yet it is strong and proximodistal broad in *Conoryctes* and *Wortmania*. On the lateral shaft of the radius, the fossa for the abductor pollicis longus in *Wortmania* is deeper and more longitudinal broad than in *Conoryctes*. Moreover, the pronator crest starts more proximally in *Wortmania* and ends more distally than in *Conoryctes*.

Compared to the radii of *Psittacotherium* (AMNH 16560), *Ectoganus* (YPM 39805) and *Stylinodon* (YPM 11096 and PM 3895), *Conoryctes* has a very slender radius. All these taxa though, and potentially all taeniodonts, are mediolaterally broader on the distal diaphysis. The capitulum in *Ectoganus* and *Stylinodon* is elongated mediolaterally unlike the almost circular capitulum of *Conoryctes*. The capitular eminence is more proximally extended in the lateral area of the ridge in *Onychodectes* and *Conoryctes* than in the more robust taeniodonts. In posterior view, *Ectoganus* and *Stylinodon* have a broad and long ulnar facet, almost semi-circular in shape, yet the bicipital tuberosity is large. In *Ectoganus* the tuberosity is proximodistally elongated and more laterally placed as in *Stylinodon*. In anterior aspect, the pronator crest of *Ectoganus* and *Stylinodon* is not as strong as in *Conoryctes* and starts more proximally like in *Wortmania*. Also, similar to *Wortmania*,

there are two sulci laterally and medially to that crest but are originating more proximally in *Ectoganus* than in *Conoryctes*. These sulci are very evident in *Stylinodon* (YPM 11096), where there are two elongated fossae distally to the crest, which is slightly twisted, starting laterally and continuing distally to the mediolateral middle of the shaft. Therefore, the lateral fossa for the abductor pollicis longus is deeper in *Stylinodon* than in *Conoryctes*. Due to damage, the distal epiphysis is only known from *Stylinodon*; it has a mediolaterally broad styloid process, more so than *Conoryctes*. In distal view, the epiphysis of *Stylinodon* is mediolaterally elongated like in *Conoryctes*, yet the two fossae are poorly defined. The lateral fossa for the articulation with the lunate is bigger, deeper and almost circular in shape, like in *Conoryctes*. The medial fossa is much smaller than the lateral in *Stylinodon*, unlike the medial fossa which is almost half in size as the lateral in *Conoryctes*.

The radius of *Conoryctes* is compared to *Escavadodon*, leptictids and palaeonodonts (Rose, 1999; Rose and Lucas, 2000; Rose, 2006). Leptictids, *Escavadodon* and *Conoryctes* have a relatively slender radius and less robust than in palaeonodonts. The radial head of *Escavadodon* has an elliptical capitulum, more mediolaterally broad than anteroposteriorly, unlike the almost circular capitulum in *Conoryctes*. *Escavadodon*, *Leptictis* and *Conoryctes* have a flat, gently curved ulnar facet. The distal shaft of *Conoryctes* is very similar to *Escavadodon* and primitive palaeonodonts; the pronator crest forms after half the proximodistal length ending in a tubercle. Distally, lateral and medial to the pronator crest are two fossae. The crest of *Conoryctes* is sharp and strong possibly like in palaeonodonts. *Escavadodon* and *Conoryctes* have a distinct styloid process and in distal view, these two genera, as well as leptictids and palaeonodonts, have two carpal facets that are not well defined.

All three genera of *Conoryctes*, *Periptychus* and *Pantolambda* (Simons, 1960; Matthew, 1937; Shelley *et al.*, 2018) have radii which are mediolaterally broader and more distally than proximally and the capitular eminence is expanding more laterally. The ulnar facet is more curved in *Periptychus* than in *Conoryctes*. The pronator crest is larger in *Periptychus* leading to a round tuberosity, whereas the crest and the tuberosity are stronger in *Pantolambda* and *Conoryctes*. In these three taxa, lateral and medial to the tuberosity are two fossae. Distally, *Periptychus* has a broader styloid process and in the distal aspect, the carpal facets are well distinguished and separated from each other, unlike in *Conoryctes*.



Figure 39: Radius of *Conoryctes comma* NMMN P-79457 in posterior (a), lateral (b), anterior (c), medial (d), proximal (e) and distal (f) views. Scale bar is 1 cm.

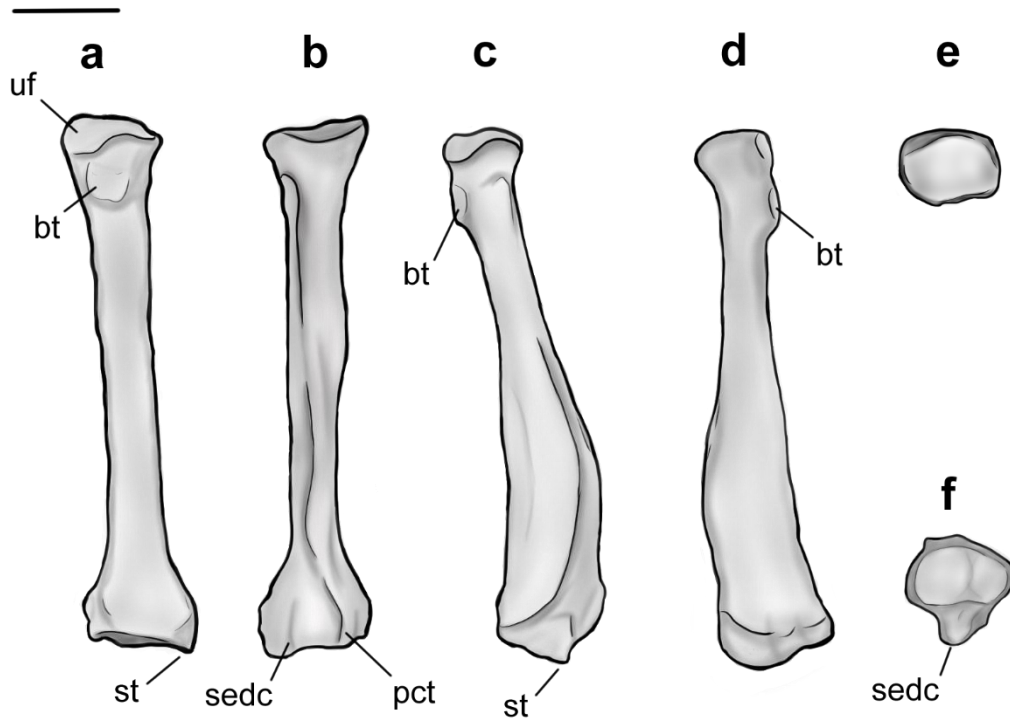


Figure 40: Drawing of the radius NMMN P-79457, *Conoryctes comma*, in posterior (a), anterior (b), lateral (c), medial (d), proximal (e) and distal (f) views. bt: bicipital tuberosity, pct: pronator crest, sedc: sulcus for the extensor digitorum communis, st: styloid process, uf: ulnar facet. Scale bar is 1 cm.

Metacarpals

Specimen NMMNH P-79457 has seven phalanges, three distal unguals and two metacarpals. The metacarpals and the phalanges are short, and their proximal articulations show that are the second and fifth metacarpals. The proximal end of the metacarpal II has a saddle shape while the IV has a more convex surface and a clear articular surface for metacarpal V. Since the phalanges are from the same specimen with the metacarpals, it is believed that these belong to the manus.

Specimen NMMNH P-48052 has one complete metacarpal, two complete phalanges, one complete distal phalanx, an ungual, and three incomplete phalanges, with only their proximal part remaining. There is also part of a small carpal bone, probably the cuneiform. The metacarpal is very similar to that of NMMNH P-79457 and based on the saddle-like proximal shape, it is metacarpal II.

Based on these specimens the proximal end of the metacarpal II has a distinctive mediolaterally concave and dorsoventrally convex articular process, giving it the saddle-like shape. This articular process is where the trapezoid and trapezium would be. The metacarpal IV is also short and stout (table A13) with a convex articular surface proximally for the articulation with the unciform. Posteriorly both metacarpals are more robust, and mediolaterally broad leading to a well-defined distal articulation for the phalanges. In dorsal aspect, there are extensor tubercles in the metacarpals of *Conoryctes*. As seen in Figure 41 (a and b), the distal end of the metacarpals is flat plantarly and convex dorsally. Distally the metacarpals have a dorsoventral ridge at the centre (Figure 42b). This ridge, or spine (Hildebrand, 1985), is forming a great

connection of the metacarpal with the first phalanx, which also has a small groove on the proximal end.

The phalanges are also relatively flat and wide with prominent articular surfaces. The terminal unguals are proximally having a deep curvature for the articulation with the proximal phalanges. Dorsally the unguals have a “bony stop” (Hildebrand, 1985) that prevented the dislocation with the phalanges, and plantarly there are large flexor tubercles preventing dislocations during flexion. Distally, the unguals are laterally compressed and well-curved. Functionally, the flat phalanges, the spine of the metacarpals providing internal stabilization between metacarpals and proximal phalanges, and the recurved unguals with the large flexor tubercle, show that *Conoryctes* was a plantigrade animal with digging adaptations.

Comparing specimen NMMNH P-79457 to the right manus of *Onychodectes* (AMNH 16528) there are similarities with *Conoryctes*. The metacarpals are long, wide proximal and distally and slender in the middle. The metacarpals of *Conoryctes* are more robust than *Onychodectes*, very similar to those of *Wortmania* (NMMNH P-19460). The phalanges of *Conoryctes* are longer and the unguals are shorter when compared to those of *Psittacotherium* (AMNH 2453, Figure A47) and *Stylinodon* (PM 3895). I was not able to identify sesamoid bones of the manus for *Conoryctes*, similar to those of *Stylinodon*.

The ungual of *Escavadodon* (Rose and Lucas, 2000) is not complete, but it is curved in lateral view. The metacarpal has a similar flexor tubercle as seen in *Conoryctes*, but it is less prominent. The manus of *Conoryctes* differs from that of *Periptychus* and *Pantolambda*. The metacarpals are concave on the plantar aspect in

Pantolambda, less so in *Conoryctes* and even less in *Periptychus* (Matthew, 1937; Shelley *et al.*, 2018).

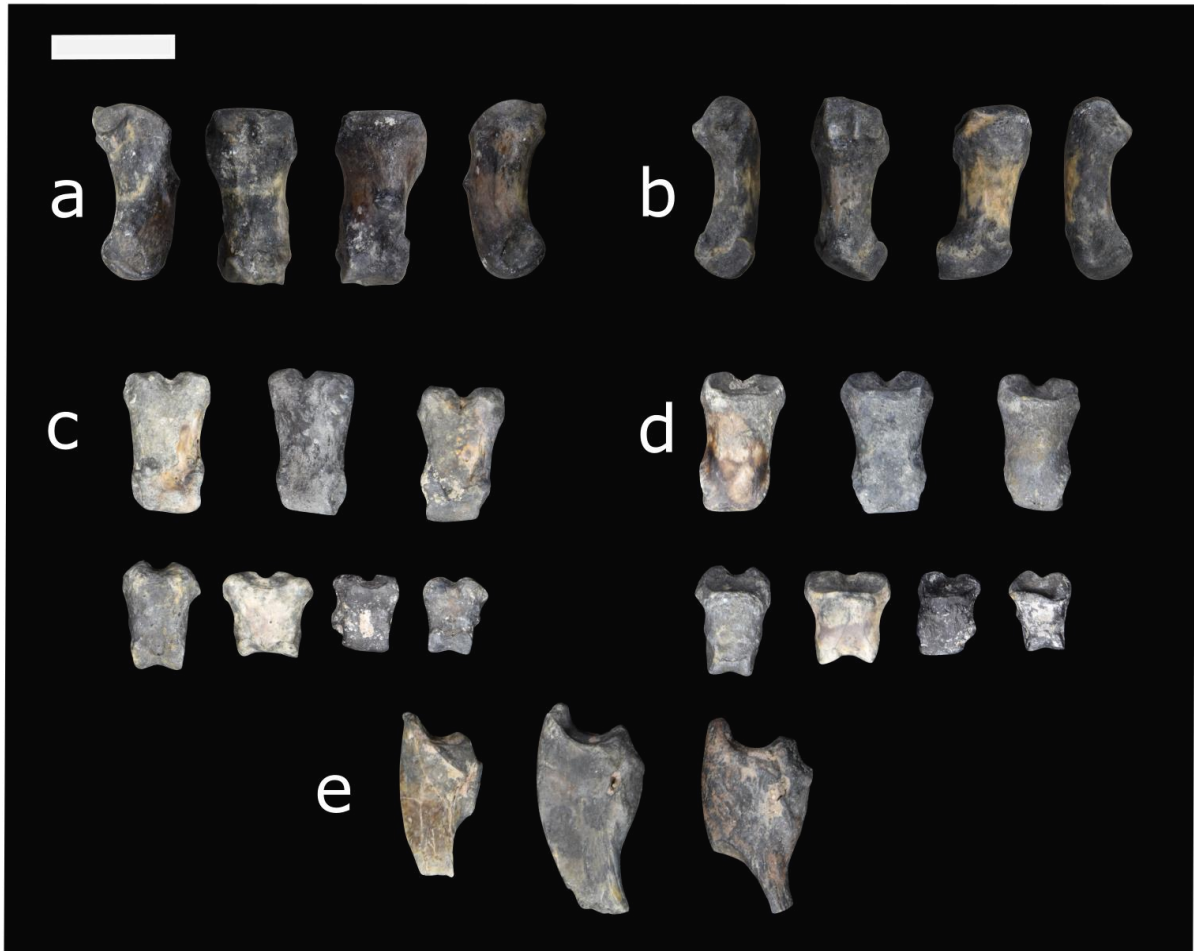


Figure 41: Part of the manus of *Conoryctes comma* NMMNH P-79457. Different views of the metacarpal II (a), metacarpal IV (b) and plantar (c) and dorsal (d) views of the phalanges and medial view (e) of unguals. Scale bar is 1cm.

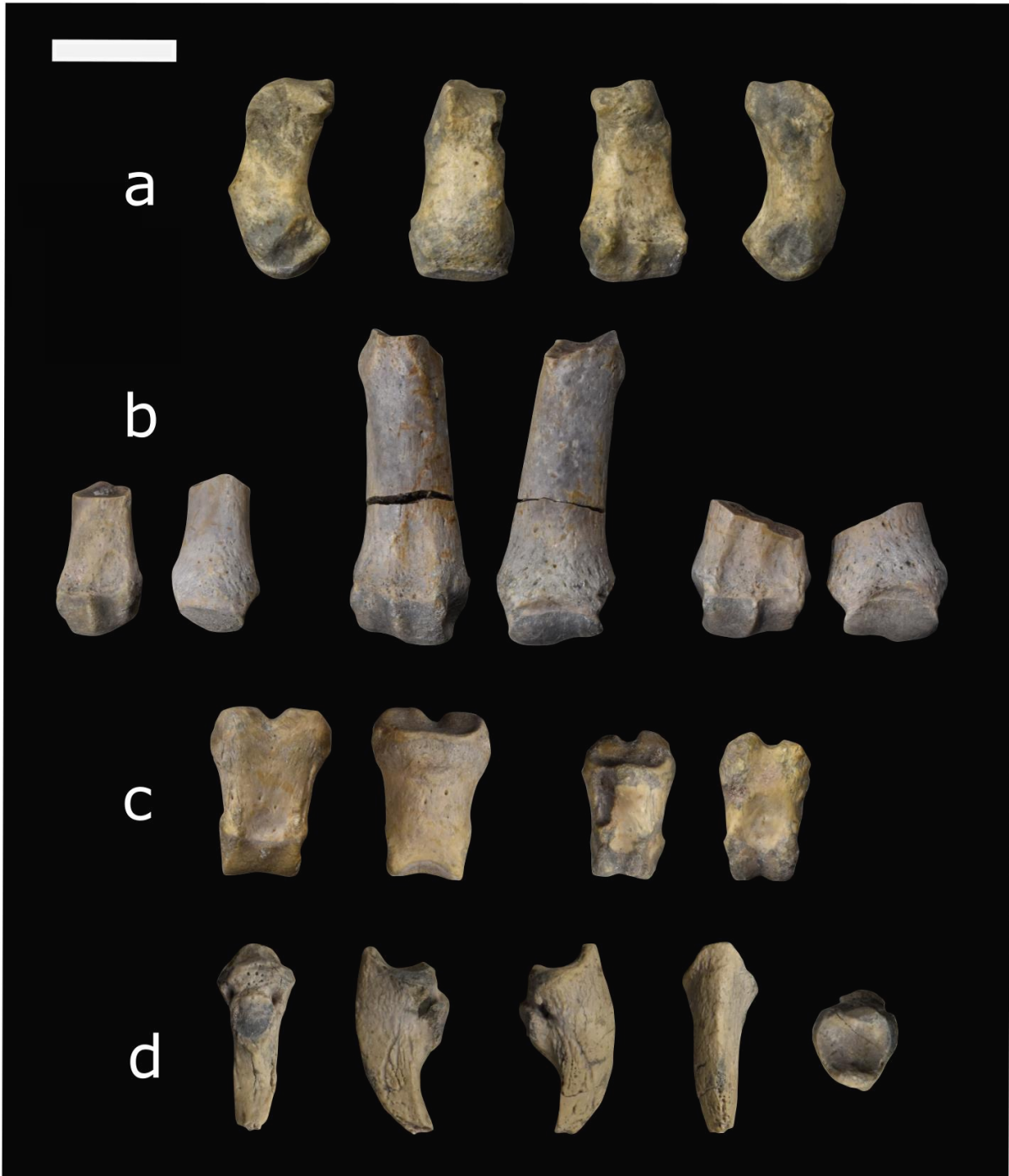


Figure 42: Part of the manus of *Conoryctes comma*, specimen NMMNH P-48052. Different views of the metacarpal II (a), plantar and dorsal views of phalanges (b, c) and ungual (d). Scale bar is 1cm.

Innominate

Specimens NMMNH P-48198, NMMNH P-47700, NMMNH P-61789, and NMMNH P-77896 have part of a left innominate and are the only well-preserved pelvises of any taeniodont. These specimens are incomplete; the anterior iliac spine is damaged from the ilium, and the ischiatic arch is missing as well as a part of the pubis and the pelvic symphysis. Generally, the innominate of *Conoryctes* is very slender and elongated (Figures 43 and 44).

The anterior part of the ilium is missing, however, based on the posterior end, it might have been dorsoventrally broad. In dorsal view, there is the posterior origin of the wing of the ilium. The iliac neck is slender and expands more mediolaterally towards the body of the ilium; there are no clear distinctions between these two features. The area is concave possibly forming cranially the gluteal fossa for the attachment of the gluteus maximus and gluteus medius muscles. There is no evidence of anterodorsal or anteroventral iliac spines due to breakage. In ventral aspect, there is the posterior origin of a smaller concave area, possibly of a narrow iliac fossa. In lateral view, the iliac fossa and the gluteal fossa are separated by the acetabular crest. In *Conoryctes* the acetabular crest is relatively sharp and prominent. Posteriorly to the acetabular crest, there is a protruding iliopectineal eminence. In medial view, there are two fossae on the ilium, that continue to one another. These were the attachment areas for the wings of the sacrum, forming the sacropelvic surface. *Conoryctes* has a very large eminence at the posterior end of this attachment area. This small notch is on the right end, near the end of the attachment surface and is the greater ischiatic notch.

The acetabulum where the ilium, ischium and pubis meet, is complete in most studied specimens. In dorsal aspect, the area of the acetabulum is expanding laterally and is robust. It is convex and the rim of the acetabular fossa is parallel to the ischium and at approximately 45° with the ilium. In ventral view, the acetabulum is very robust in the ilium-pelvis area. Medially, there is the illiopubic eminence, starting more anteriorly than the acetabulum and at the anterior border of the latter. The illiopubic eminence, which provided attachment for the psoas minor muscle of *Conoryctes*, is well defined yet does not protrude a lot ventromedially. In dorsal aspect, the acetabular fossa is consisting mainly of the lunate surface and the acetabular fossa. The rim of the acetabulum is continuous for at least three-fourths of the perimeter; it starts from the ischium and ends with a posterior opening, where the obturator foramen begins anteriorly. On the rim of the acetabulum, there would have been a ring of cartilage. On the walls of the acetabulum, there is a broad line along the rims that expands to the acetabular fossa. In *Conoryctes*, the lunate surface is continuous and only broader ventromedially, whereas the acetabulum extends more laterally from the ilium. Further deeper is a deep acetabular fossa, almost circular in shape. Posteriorly towards the ischium, the acetabular fossa opens forming the acetabular notch, which borders with the obturator foramen. The transverse acetabular ligament would have bridged this opening created by the acetabular notch. The lunate surface overhangs the acetabular fossa, creating a foramen, possibly for the obturator artery or nerves. In medial view, there is a well-defined large fossa with a very robust rim towards the dorsal aspect of the innominate (Figure 43d). That fossa was the attachment surface for the coccygeus muscle, which would have expanded to the lateral end of the tail. Near the illiopubic eminence, there is a narrow fossa that probably continued posteriorly for the attachment of the levator ani muscle.

Specimen NMMNH P-48198 is broken at the pecten of the pubic bone, so the pubis is missing. Based on what is preserved, it would have extended from the acetabulum with an almost 70° angle from the ischium-iliac plane. The symphysis of the pelvis is not preserved, so the pubis-ischium attachment remains unknown for *Conoryctes*. The presence or absence of an epipubic bone is also unclear.

The ischium is almost complete, missing the posteromedial end, i.e. the medial angle of the ischiatic tuberosity and the connection with the pubis. The ischium is potentially shorter than the ilium. It is also more dorsoventrally than mediolaterally robust. In dorsal view, the ramus of the ischium becomes slender posteriorly. The ischiatic spine is very prominent anteriorly and medially transverse. It flattens posteriorly and ends before the anterior border of the ischiatic tuberosity. In lateral aspect, the ischium has a well-defined crest. On the dorsal side of this crest, there is a narrow, anteroposteriorly elongated fossa, for the attachment of the quadratus femoris. Ventrally to that crest, there is a flat, much broader, posteromedially inclined area. In the posterior part of that area, there is a shallow broad fossa, where the quadratus femoris muscle originated. This muscle was responsible for the extension and lateral rotation of the joint between the femoral head and the acetabulum of the pelvis. Near the obturator foramen, the ischium of *Conoryctes* forms a continuous hemi-circular ridge. In medial view, the ischiatic spine is more prominent anteriorly, and it is not adjacent to the ischiatic tuberosity, which is dorsally inclined (Figure 43c).

There are other two specimens of taeniodonts with elements of the innominate that are purely studied; one belongs to *Onychodectes* (AMNH 3405) and the other to *Stylinodon* (USNM 16664). AMNH 3405 has part of the left ilium, missing the most anterior part and reaching to an almost complete acetabulum, that is filled with

sediments. In the same specimen, there is also part of the most posterior end of the ischium. *Stylinodon* has a right innominate consisting basically of the acetabulum and the anterior part of the ischium. *Onychodectes* has a slender ilium like *Conoryctes* and a well-defined gluteal fossa. The iliopectineal eminence is not as posteriorly placed as in *Conoryctes*. It is uncertain how prominent the eminence of *Onychodectes* is since it is partially broken in the AMNH 3405; in *Stylinodon* the eminence is completely broken. Dorsally, there are no signs of articulation with the sacrum in *Onychodectes*. The acetabulum is posteroanteriorly elongated in *Conoryctes* and *Onychodectes*, whereas it is more circular in *Stylinodon*. In all three taxa though, the anterior border of the acetabulum that extends from the ilium is protruding more laterally. The acetabulum is filled with sediments in AMNH 3405, however, the socket is very deep in *Stylinodon*. Also, *Stylinodon* similarly to *Conoryctes* has a continuous and subequal in broadness lunate surface. There is a foramen in the pubic area of the acetabular fossa in *Stylinodon* where the ligamentum teres attached; *Conoryctes* is lacking this foramen. The ischium of *Stylinodon* expands more posteriorly like in *Conoryctes*.

Comparing to *Escavadodon*, *Prodiacodon* and *Leptictis* (Rose, 1999; Rose and Lucas, 2000; Rose, 2006) the innominate of *Conoryctes* shows few differences. All these taxa have a relatively long and narrow ilium. The acetabular crest on the ilium in *Conoryctes* is similar to *Escavadodon* and a bit sharper like in leptictids. The iliopectineal eminence of *Conoryctes* is similar to leptictids and not as prominent as in palaeonodonts. The iliopectineal eminence is more anteriorly placed in *Escavadodon* than in *Conoryctes*. The shape of the acetabulum and the ischium of both *Escavadodon* and *Conoryctes* are very similar, however, the obturator foramen of the former is more elongated and oblique near the pubis-ilium connection.

Relative to *Periptychus* (NMMNH P-47693, Shelley *et al.*, 2018) and *Pantolambda* AMNH 16663 (Simons, 1960; Matthew, 1937; Shelley *et al.*, 2018) the innominate of *Conoryctes* shows more differences. In dorsal view, *Periptychus* is more concave medially than either *Pantolambda* or *Conoryctes* are. Both *Conoryctes* and *Pantolambda* have an acetabular crest that is relatively sharp and prominent, unlike the more rounded one in *Periptychus*. The illiopubic eminence is more anteriorly placed in *Periptychus* than in *Conoryctes*. The ilium and ischium in *Conoryctes* and *Pantolambda* are approximately on the same plane, whereas they are angled in *Periptychus*.



Figure 43: Innominate of *Conoryctes comma* specimens NMMNH P-48198 (a-d), NMMNH P-77896 (e) in lateral view, NMMNH P-47700 (f) in lateral and ventral views. Views of NMMNH P-48198 are lateral (a), dorsal (b), medial (c) and ventral (d). Scale bar is 1cm.

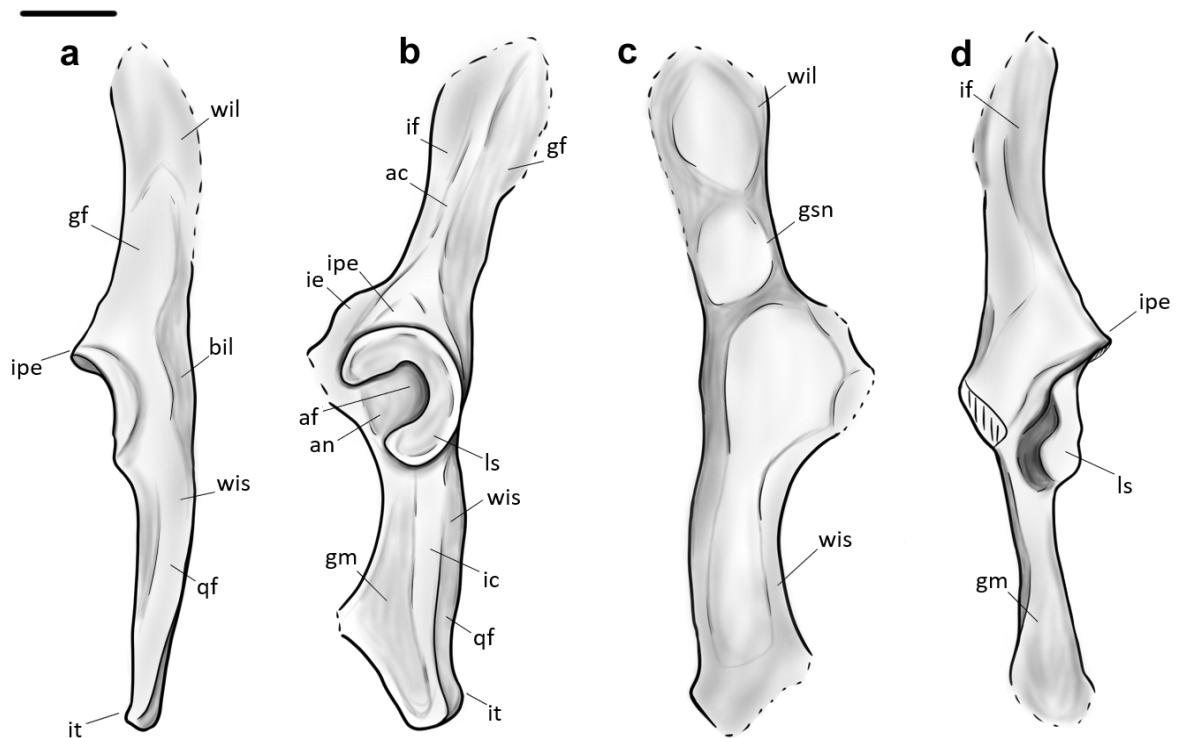


Figure 44: Drawing of *Conoryctes comma*, NMMNH P- 48198, in dorsal (a), lateral (b), medial (c) and ventral (d) views. ac: acetabular crest, af: acetabular fossa, an: acetabular notch, bil: body of the ilium, gm: attachment for gemelli muscle, gf: gluteal fossa, gsn: greater ischiatic notch, ie: illiopubic eminence, if: iliacus fossa, ipe: iliopectineal eminence, it: ischiatic tuberosity, ic: ischiatic crest, qf: quadratus femoris, ls: lunate surface, wis: wing of the ischium, wil: wing of the ilium. Scale bar is 1 cm

Femur

Three specimens have femoral elements of *Conoryctes* (Figures 45 and 46, table A15). Specimen NMMNH P-79457 has an almost complete right proximal femur, broken at the proximal end of the third trochanter. The epiphysis and metaphysis are well preserved, and it is damaged on the anterior aspect at the proximal diaphysis. Specimen NMMNH P- 19494 has the proximal diaphysis of a right femur, laterally it is broken at the proximal end of the third trochanter. The distal end of the femur is known from specimen NMMNH P-48052. A left distal diaphysis and epiphysis are preserved; however, it is anteroposteriorly compressed and broken medially with part of the medial epicondyle preserved separately. There is also a broken part of a lateral epicondyle, probably belonging to the distal epiphysis of the right femur of the same individual. In specimen NMMNH P-48052, there is also the femoral head, with a deep fovea capitis, potentially of the right femur.

The information on the diaphysis, of *Conoryctes*, is limited. Specimen NMMNH P-79457 is slightly smaller than the NMMNH P- 19494, the latter has a more mediolateral expanded proximal diaphysis, with potentially broader trochanteric fossa in the posterior aspect. Specimen NMMNH P-48052 is damaged, however, the femoral head of the right femur is very similar to the femoral of NMMNH P-79457, in size, shape as well as structure of the fovea capitis. Based on these specimens, the total length, of the femur cannot be calculated. Since specimen NMMNH P-19494 is damaged and the diaphysis of the femur is broken, the circumference of the femoral shaft can not be measured. Looking at the specimens it is evident that generally, the femur of *Conoryctes* is relatively robust and has well-developed areas for muscle attachments.

The proximal epiphysis as seen in specimen NMMNH P-79457 is broad mediolaterally, with well distinguished femoral head, also seen in specimen NMMNH P-48052, and a less protruding greater trochanter (Figure 45a-e). The femoral head is robust, hemispherical and extends medially. In anterior aspect, the articular surface of the femoral head is highly convex. The articular surface continues laterally and smoothly connects to the femoral neck, whereas it extends further medially than the femoral neck forming a distinct rim. In medial view, there is a deep fovea capitis starting almost from the top of the femoral head and continuing distally interrupting the posteromedial articular surface of the femoral head (Figure 45b). In the posterolateral view, the articular surface extends on the femoral neck. Generally, the femoral neck is slender and elongated. Medially the femoral neck extends less than the femoral head, forming an acute angle with the proximodistal long axis of the femur. In posterior aspect, the neck is more robust, coming in contact posterolaterally with the articular surface of the head and the intertrochanteric fossa.

On the lateral side of the proximal femoral epiphysis of *Conoryctes*, there is a moderate greater trochanter, well separated from the femoral head. In anterior aspect, the femoral head projects superior to the greater trochanter; the latter having a more robust circumference than the femoral neck. The head of the greater trochanter is anterolaterally inclined, laterally it continues smoothly to the proximal diaphysis, while on the medial side, it forms a rim. The great trochanter of *Conoryctes* has evidence for muscle attachments. In lateral aspect, there are two well-defined surfaces; the anterior was for the attachment of the gluteus profundus, and the posterior was for the pyriformis. The apex of the great trochanter is not prominent and has no marks for the attachment of the gluteus medius. In posterior view, the greater trochanter is smaller and forms a rim with the intertrochanteric fossa.

The intertrochanteric fossa of *Conoryctes* is on the posterior proximal end of the femur (Figure 45d). It is deeply excavated and forms a continuum with the femoral head medially and a well-developed intertrochanteric crest. Distally the lateral ridge ends, and the fossa becomes shallower. Approximately in the proximodistal middle of the fossa, there is the proximal end of the lesser trochanter on the medial side. In both specimens, NMMNH P-79457 and NMMNH P-19494, the distal end of the intertrochanteric fossa is well-defined and reaches approximately the middle of the third trochanter protuberance that is located on the later side. In the distal end of the fossa, the internal and external obturators and the superior and inferior gemelli muscles were attached.

On the proximal diaphysis of the femur, on the medial side, there is the eminence of the lesser trochanter. In *Conoryctes*, the lesser trochanter extends medially forming an almost triangular flange, for the attachment of the iliopsoas muscle. In anterior view, the proximal end extends almost vertically to the diaphysis, whereas the distal end forms a more acute angle with the shaft. The apex of the lesser trochanter protrudes almost as medially as the femoral head. In medial aspect, the lesser trochanter extends more posteriorly starting from the posterior part of the femoral shaft. In posterior view, the lesser trochanter comes in contact with the intertrochanteric fossa. However, due to damage, only specimen NMMNH P-19494 shows a large pectineal line for the attachment of the pectineus muscle.

On the lateral side of the proximal diaphysis is the third trochanter for the attachment of the gluteus superficialis muscle. In *Conoryctes* the third trochanter has a semi-circular shape and is less wide proximodistally than the lesser trochanter. In anterior view, the third trochanter extends more laterally from the femoral shaft than

the greater trochanter. In lateral aspect, the third trochanter is curved anteriorly. The apex is flat; less curved than the apex of the lesser trochanter. In posterior view, the third trochanter is not close to the intertrochanteric fossa.

The rest of the femoral diaphysis might have been slender anteroposteriorly, based on specimen NMMNH P-19494. Part of the distal diaphysis and the lateral epiphysis are preserved in specimen NMMNH P-48052. In anterior aspect, the femoral trochlea is relatively shallow, mediolaterally broad and does not extend proximally to the diaphysis. The femoral trochlea terminates proximally at approximately the same level as the proximal end of the femoral condyles. Distally the specimen is damaged. Medially to the femoral trochlea, the fossil is damaged and so the presence and the shape of the adductor tubercle of *Conoryctes* is still unclear. Specimen NMMNH P-48052 is compressed anteroposteriorly, so the fossa for the gastrocnemius internus, in posterior aspect, can not be studied.

The distal epiphysis of *Conoryctes* is studied based on the specimen NMMNH P-48052 (Figure 45h-l). The lateral epicondyle is damaged and compressed; however, it is moderately prominent in anterior view. In lateral aspect, there are three fossae. The largest fossa is shallow and anteroproximally positioned for the attachment of the lateral collateral ligament. Posterodistally, there is a large, deep and elongated fossa where the popliteus muscle originated. Anterior to this fossa, there is a small fossa, which is now damaged, possible for the insertion of the extensor digitorum longus muscle. In posterior view, there is a smooth and rounded lateral femoral condyle. Medially to the condyle, there is a depression that is damaged. This is the intercondyloid fossa that is deep in *Conoryctes* for the attachment of the anterior cruciate ligament (Figure 46).

The medial part of the femoral distal epiphysis is completely broken off the specimen NMMNH P-48052. The medial epicondyle is larger than the lateral and probably extended more posteriorly. In medial aspect, there is a large shallow fossa, where the medial collateral ligament was attached. In posterior view, the femoral medial condyle is smooth and more rounded than the lateral condyle. Due to damage, it is not possible to position the medial condyle to the rest of the distal femoral epiphysis. Moreover, the distal epiphysis is anteroposteriorly compressed and so no comparisons between the two epicondyles and condyles can be made.

The femur of *Conoryctes* shares resemblances with other genera of Taeniodonta. Compared to the partial femur of *Onychodectes* (AMNH 3405) and of the more robust *Wortmania* (AMNH 3394), the three genera have a slender femur, with robust lesser and third trochanter protruding from the shaft. The specimen AMNH 3405 of *Onychodectes* is broken proximally and distally and so no comparisons for the proximal epiphysis can be made. In anterior aspect, the femoral head of *Wortmania* expands proximally more than the greater trochanter, more so than in the proximal epiphysis of *Conoryctes*. The femoral neck of *Wortmania* is very robust, unlike *Conoryctes*. The lesser trochanter of *Onychodectes* is less triangular than *Conoryctes*, yet that may be due to damage to the former. The shape and robustness of the lesser and third trochanter are very similar between the *Conoryctes* and *Wortmania*; the lesser trochanter has a more trigonid shape protruding more from the shaft than the more semi-circular third trochanter. In these three genera of taeniodonts, the lesser trochanter ends distally, approximately at the proximodistal middle of the third trochanter. In lateral view, the third trochanter has a flat apex in all three studied specimens. In posterior aspect, the intertrochanteric fossa of *Onychodectes* is shallower than in *Conoryctes* and *Wortmania*. For the latter two genera, the greater

trochanter and the intertrochanteric fossa form a deep ridge. However, for all three genera, the intertrochanteric fossa continues distally until the proximodistal middle level of the third trochanter. Distally the femur of *Onychodectes* and *Wortmania* and *Conoryctes* are slender.

Compared with other taeniodonts like *Psittacotherium* (TMM 41364-1, Figure A48, AMNH 16560, NMMNH P-19713), *Ectoganus* (USNM 175531) and *Stylinodon* (USNM 18425, UW 2270), the femur of *Conoryctes* shows some differences. Proximally, in anterior view, the femoral head of *Psittacotherium* and *Stylinodon* is more robust and becomes even more spherical in the latter. The femoral neck is also more robust in *Psittacotherium* and *Stylinodon* than in *Conoryctes*. The femoral head extends more proximally than the greater trochanter in *Psittacotherium* and even more in *Stylinodon*, making that a character for all studied taeniodonts. The specimen of *Ectoganus* is missing the femoral head and neck and has a well-defined and robust greater trochanter. The lesser trochanter is very prominent, extending medially from the shaft and has a trigonal shape in *Ectoganus*, similar to *Conoryctes*. For *Psittacotherium* and *Stylinodon* the lesser trochanter is less prominent and more proximally placed. The third trochanter is large in *Ectoganus* and becomes robust in *Psittacotherium* and *Stylinodon*. In posterior view, the intertrochanteric fossa in *Psittacotherium* and *Ectoganus* is relatively shallow compared to *Conoryctes*, but that could be due to bad preservation of the fossils. In *Stylinodon* (UW 2270), the intertrochanteric fossa is deep and there is a well-defined ridge with the greater trochanter; however, unlike *Conoryctes*, the fossa does not extend so distally. The distal end of the intertrochanteric fossa is at approximately the level of the third trochanter. In *Psittacotherium*, *Ectoganus* and *Stylinodon* the lesser and third trochanter end approximately on the same level distally, meaning that the third

trochanter is more proximally positioned than in *Onychodectes*, *Conoryctes* and *Wortmania*. The femoral shaft of *Psittacotherium*, *Ectoganus* and *Stylinodon* are straight and more robust mediolaterally than anteroposteriorly. On the distal epiphysis, in anterior view, the femoral trochlea ends at the same level as the most posterior parts of the femoral condyles, as seen in *Psittacotherium* (TMM 41364-1), *Ectoganus* and *Stylinodon* similarly to *Conoryctes*, making that a possible common character for all taeniodonts. The femoral fossa is shallower in *Ectoganus*, similar to *Conoryctes*, whereas it is deeper in *Psittacotherium* and *Stylinodon*. For *Psittacotherium*, *Ectoganus* and *Stylinodon* the femoral fossa is more laterally placed on the distal epiphysis; this cannot be studied in the NMMNH P-48052 specimen of *Conoryctes*. In posterior aspect, the femoral condyles are robust and the medial is bigger extending more distally for *Psittacotherium* and *Ectoganus*, while the two condyles are subequal in *Stylinodon*. The lateral and medial fossae for the attachment of the collateral ligaments are well excavated in *Psittacotherium* and *Ectoganus* as in *Conoryctes*. However, the other fossae on the lateral and medial aspects of the distal epiphysis are not clear on the specimens of *Psittacotherium*, *Ectoganus* and *Stylinodon*.

The femur of *Conoryctes* when compared with *Escavadodon*, *Prodiacodon* and *Leptictis* (Rose, 1999; Rose and Lucas, 2000; Rose, 2006) shares few similarities. The femoral head of *Escavadodon* has a “mushroom” shape as described by Rose and Lucas (2000) which could also apply to the femoral head of *Conoryctes*. *Escavadodon* and leptictids have a small fovea capitis, whereas palaeonodonts, similar to *Conoryctes*, have a large fovea that continues with a groove posteromedially. The greater trochanter is less projecting proximally like in *Conoryctes*, whereas in *Prodiacodon* the femoral head and the greater trochanter are almost on the same level, with the later extending more proximally. The lesser trochanter of *Escavadodon*,

leptictids and palaeanodonts is extended posteromedially, less than in *Conoryctes*. The third trochanter of *Escavadodon* has a crest-like shape as in *Conoryctes*, however, does not protrude as much laterally as in *Conoryctes* and palaeanodonts. On the distal epiphysis, the femoral trochlea of *Prodiacodon* (UM 88105) extends proximally more than the proximal end of the distal condyles, unlike *Conoryctes* and potentially all taeniodonts.

Comparing *Conoryctes* to *Periptychus* (NMMNH P-47693 Shelley *et al.*, 2018) and *Pantolambda* AMNH 16663 (Simons, 1960; Matthew, 1937; Shelley *et al.*, 2018) shows the following. The three genera have a robust femoral head with a deep fovea capitis. However, only in *Conoryctes* and *Periptychus*, the fovea has a groove that excavates posteromedially the articular surface of the femoral head. The greater trochanter is extending more proximally in *Periptychus*, even more so in *Pantolambda*, opposite to *Conoryctes*. In posterior view, the intertrochanteric fossa is deep in all three genera, with the intertrochanteric crest being more prominent in *Conoryctes* than in *Periptychus* and *Pantolambda*. The lesser trochanter is triangular in shape protruding posteromedially in *Periptychus*, similar to *Conoryctes*. The third trochanter of *Pantolambda* and *Conoryctes* is less prominent than of *Periptychus*. In *Periptychus* and *Pantolambda* the third trochanter is more distally placed on the femoral shaft, whereas in *Conoryctes* it is more proximal and near the lesser trochanter. Distally, the femoral trochlea of *Pantolambda* resembles that of *Conoryctes*, since it ends approximately at the most proximal end of the condyles. For *Periptychus*, the femoral trochlea continues more proximally than the femoral condyles. In lateral aspect, the lateral epicondyle of *Periptychus* has three well-defined fossae for muscle attachments, similar to *Conoryctes*.

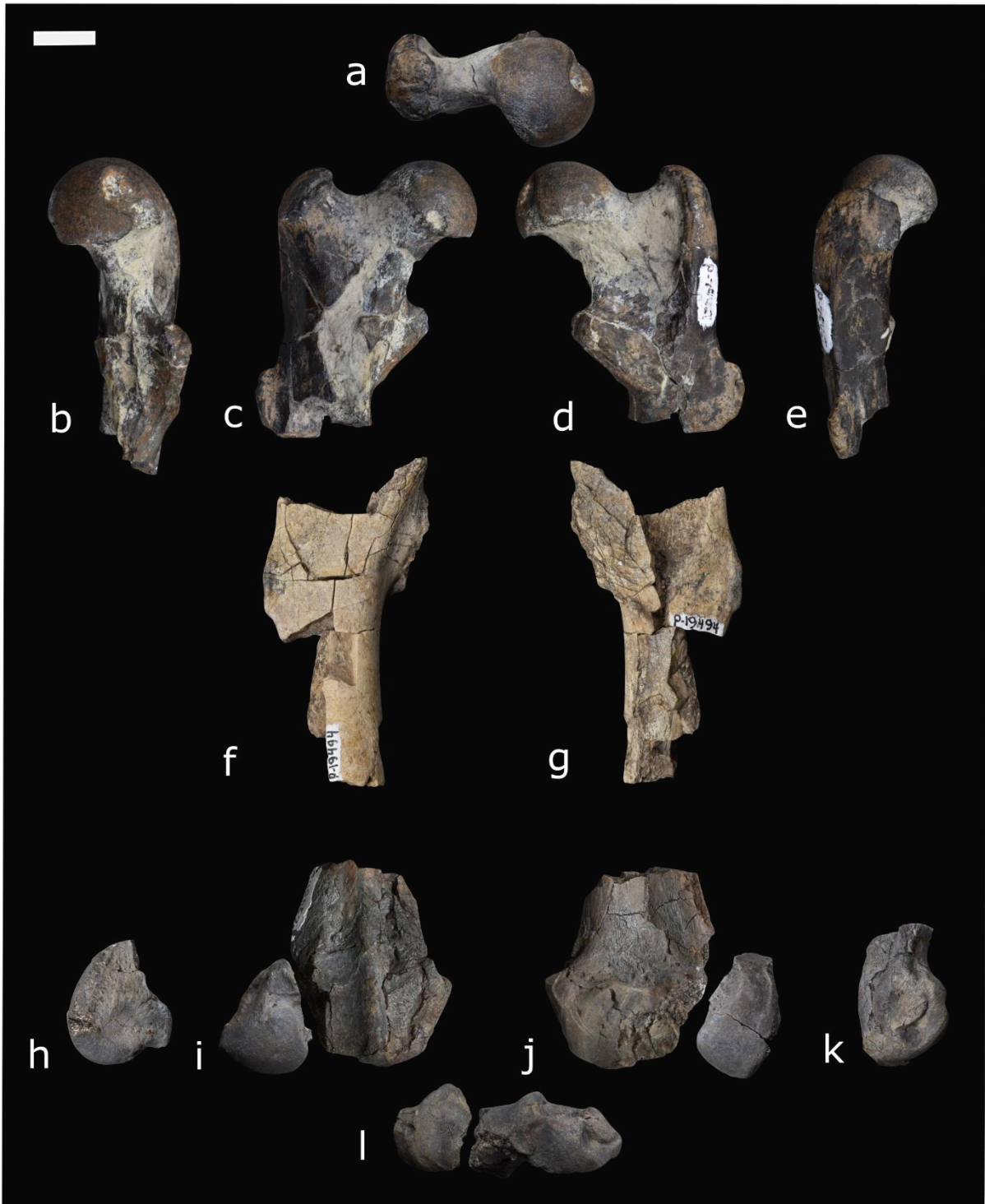


Figure 45: Femur of *Conoryctes comma* specimens NMMNH P-79457 (a-e), NMMNH P-19494 (f, g) and NMMNH P-48052 (h-l) in proximal (a), medial (b, h), anterior (c, f, i), posterior (d, g, j), lateral (e, k) and distal (l) views. Scale bar is 1 cm.

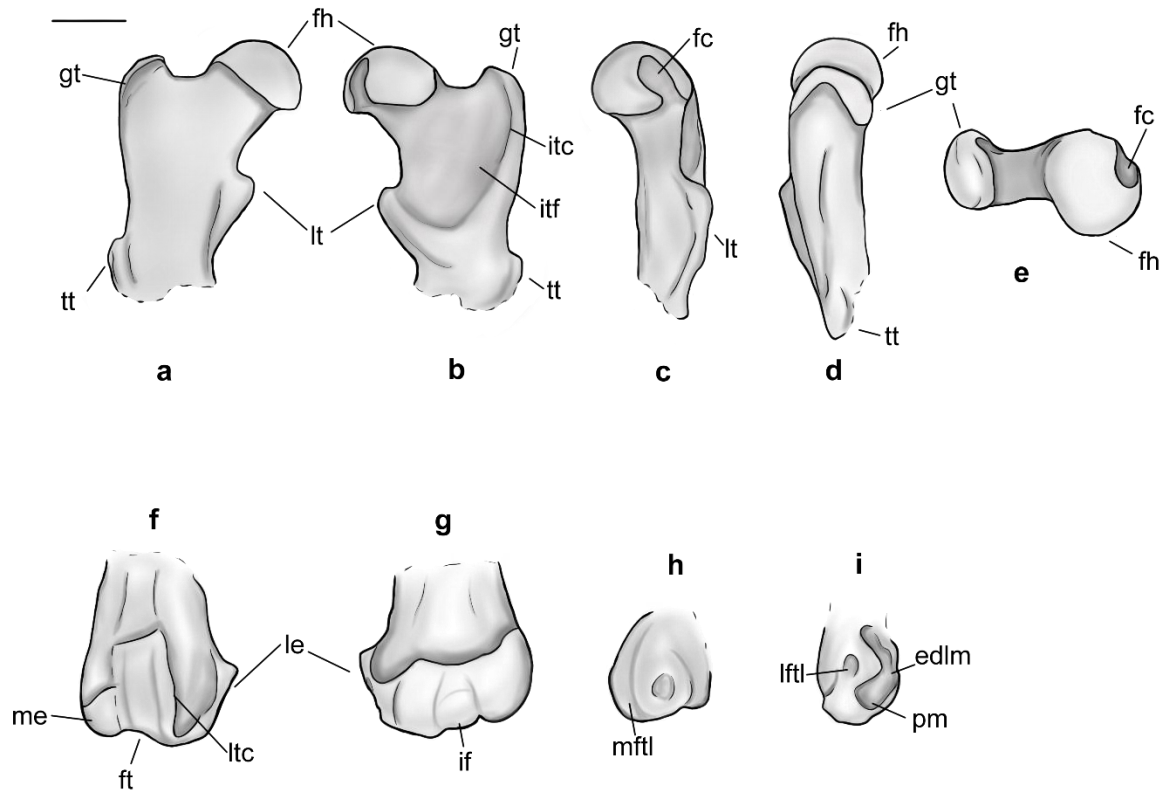


Figure 46: Drawing of the femur using specimens NMMNH P-79457 and NMMNH P-48052, *Conoryctes comma*, in anterior (a,f), posterior (b,g), medial (c,h), lateral (d, i) and proximal (e) views. edlm: fossa for attachment of extensor digitorum longus muscle, fc: fovea capitis, fh: femoral head, ft: femoral trochlea, gt: greater trochanter, if: intercondylar fossa, itc: intertrochanteric crest, ift: trochanteric fossa, ltc: lateral trochlear crest, le: lateral epicondyle, lt: lesser trochanter, lftl: fossa for attachment of lateral femorotibial ligament, me: medial epicondyle, mftl: fossa for attachment of the medial femorotibial ligament, pm: fossa for attachment of popliteus muscle, tt: third trochanter. Scale bar is 1 cm.

Patella

The patella of *Conoryctes* is described based on the left and right patella of specimen NMMNH P- 48052 (Figure 47). In anterior aspect, the patella is almost circular in profile, with a small distal apex for attachment of the patellar tendon. Proximally, the base of the patella extends from the medial to the lateral side, for the insertion of the quadriceps tendon. Distally, there is an elevation of the patella forming a slope marked with many proximodistally oriented striations. In this area the patellar tendon originated, connecting the patella with the tibia. The most distal part, the apex of the patella, is not prominent in *Conoryctes*. In medial aspect, the shape of the patella is convex anteriorly and concave posteriorly. In posterior view, there are two facets, one medially and the other laterally placed, divided by a weak ridge that is proximodistally oriented. Both facets are smooth, and the lateral facet is larger than the medial. In the medial-distal area of the medial facet, there is a smaller secondary facet.

Specimen AMNH 3576a of *Onychodectes* and USNM 16664 of *Stylinodon* are very similar to those of NMMNH P-48052. They are almost circular having two facets in posterior view.



Figure 47: Patella of *Conoryctes comma*, specimen NMMNH P- 48052 in anterior (a) and posterior (b) views. Scale bar is 1 cm.

Tibia

There are five elements of the tibia from the specimens NMMNH P-48198, NMMNH P-19494, NMMNH P-48052, NMMNH P-47700 and NMMNH P-21509 (Figures 48, 49 and 50). Specimen NMMNH P-48198 has a left tibia that is almost complete with few breakages on the proximal epiphysis. The epiphysis is broken and glued on the shaft; however, the element is very well preserved. Specimen NMMNH P-19494 has a left tibia that is missing the proximal end of the diaphysis and the proximal epiphysis. It is well preserved with few signs of erosion on the distal epiphysis. Specimen NMMNH P-48052 includes the proximal end of a right tibia, part of the proximal and the distal end of a left tibia. The right tibia has only the lateral part of the proximal epiphysis and diaphysis and is damaged, missing the medial condyle, while the left tibia is better preserved. Only the proximal part of the tibia is preserved in specimen NMMNH P-47700. There is sediment separating the distal epiphysis from the diaphysis and the medial and lateral condyles are also separated. Potentially there was breakage that was filled with sediments damaging these parts of the tibia. Lastly, only the proximal part of the tibia is preserved in specimen NMMNH P-21509; it is mediolaterally compressed and hence the lateral metaphysis is distorted.

Specimen NMMNH P-19494 when compared with specimens NMMNH P-48198 and NMMNH P-48052 is anteroposteriorly broader and more robust on the distal end (table A17). All three specimens share a similar extension of the medial malleolus and have a flatter distal diaphysis anteriorly than posteriorly. On the proximal part of the tibia, specimens NMMNH P-48198, right NMMNH P-48052 and NMMNH P-21509 have the same size and the medial and lateral condyles are equally elevated, with the lateral extending more proximally. The tibial tuberosity is only preserved in the

right NMMNH P-48052 and NMMNH P-21509. It is not complete in either, however, it does not project anteriorly.

In general, the tibia of *Conoryctes* is slender and extends mediolaterally more on the proximal end rather than the distal end (table A17). The proximal epiphysis of NMMNH P-48198 is damaged on the anterior and medial part of the condyles and specimen NMMNH P-21509 is compressed. However, the two condyles are subequal in anteroposterior length. In proximal view, the medial condyle is more concave than the lateral and they are divided by a mediolaterally wide intercondylar eminence. The tibial shaft is slender and straight with a large tibial crest, as seen in the lateral or medial view. The distal epiphysis features a very prominent medial malleolus and very concave medial and lateral astragalar facets. The medial astragalar facet is larger than the lateral. There are fibular facets on the proximal and distal epiphyses. There is also no evidence to support a tibiofibular attachment along the shafts of the two bones. Therefore, in *Conoryctes* the tibia and fibula are separated in the shafts and are not fused.

In proximal aspect, there are two round prominences divided by a prolonged area (Figures 48e and 49e). These are the lateral and medial condyles of the tibia, separated by the cranial intercondyloid area. The medial condyle is wider mediolaterally than the lateral condyle. The medial condyle is oval in shape, more anteroposteriorly elongated, and strongly concave. In medial view, it slopes posteriorly. In proximal view, the lateral condyle has a circular shape. It is less concave than the medial condyle, almost flat with a convex medial border leading to the lateral intercondylar eminence. In posterior view, the lateral condyle continues, however, due to breakage in the studied specimens, it is not certain how posteriorly it is expanding.

In proximal aspect, the intercondyloid area is generally wide and elongated, defined by two protuberances, the medial and lateral intercondylar eminence. Medially, the medial condyle is almost flat and there is a thick neck around the condyle for the medial collateral ligament. Laterally, the medial condyle rises more steeply and leads to the medial intercondylar eminence for attachment of the medial meniscus. On the lateral side, there is a lateral eminence for the attachment of the lateral meniscus. The lateral intercondylar eminence is flatter, less prominent and more posteriorly placed than the medial.

The proximal diaphysis of the tibia is partially damaged in all the studied specimens. In anterior aspect, there is the tibial tuberosity, which is better preserved in specimens NMMNH P-21509 and NMMNH P-48052 (Figure 49). Although damaged in the specimens, the tibial tuberosity is prominent, mediolaterally extending providing attachment for the patellar tendon. In anterior view, the tibial tuberosity extends mediolaterally as far as the middle of the medial and lateral condyle. The tuberosity originates proximally at the level of the lateral and medial condyles, not coming in contact with them, and continues distally. In posterior view, there are signs of the popliteus crest in specimen NMMNH P-21509. However, because this part of the tibia is compressed, no clear observations can be made. In lateral aspect, the extension of the lateral condyle leads to a facet on the posterolateral edge. That is the proximal fibular facet which in *Conoryctes* is flat and circular. The proximal tibiofibular joint shows that in *Conoryctes* the tibia and fibula were not fused proximally.

The shaft of the tibia, as seen in specimens NMMNH P-19494 and NMMNH P-48198, is slender (Figure 48). In anterior view, it is straight medially and concave laterally. In anterior view, the tibial crest is large and there is almost no tuberosity. The

crest originates proximally and continues distally being present for almost 70% of the tibial shaft. Lateral to the tibial crest the tibialis anterior muscle passed following the crest. Distally, the diaphysis extends laterally where the crest of the tibiofibular ligament originates. In lateral view, the proximal tibial fossa is large and elongates distally continuing down 30% of the tibial shaft. It forms part of the area where the tibialis cranialis muscle originated. In posterior aspect, the popliteal line extends from the proximal diaphysis to almost the middle of the shaft. The proximal diaphysis is broader mediolaterally than the distal diaphysis.

The distal diaphysis of *Conoryctes* has a concave area in anterior view and a groove for the crural extensor retinaculum ligament (Figure 50). In posterior aspect, two noticeable grooves extend more distally to the epiphysis of the tibia. The lateral groove is next to the crest of the tibiofibular ligaments and is deep and narrow. The short lateral collateral ligaments were passing through that groove, connecting the tibia with the proximal calcaneum, as well as the lateral digital flexor muscle. More medially, there is a very deep and narrow groove for the medial digital flexor muscle, following the malleolus distally. The medial collateral ligaments were attached to the flexor sulci, connecting the tibia with the distal calcaneum. In lateral view, there is a small and shallow facet, with a semi-circular shape. This is the distal fibular facet, the boundaries of which demarcate next to the lateral astragalar facet, angled with the distal epiphysis of the tibia. Therefore, in *Conoryctes* the tibia and fibula are unfused distally and form a synovial joint both proximally and distally.

The distal epiphysis is mediolaterally broad and strongly concave. A robust medial malleolus, with a deep flexor sulcus seen in posterior view, expands distally. In anterior aspect, the malleolus is curved medially taking part in forming the articulation

surface of the distal epiphysis of the tibia. The articular surface consists of the medial and lateral astragalar facets, which are almost continuous in *Conoryctes*. In distal view, the medial astragalar facet is deeper than the lateral (Figure 48k and 49m). The anterior and posterior borders of the epiphysis are very strong. Along with the medial malleolus, they fit perfectly into the astragalar trochlea and the medial tibial facet of the astragalus, especially using the tibia and tarsals of specimen NMMNH P-48198. Moreover, the posterior border of the distal epiphysis ends more distally than the anterior border. This was probably to prevent disconnection of the astragalus and the tibia in extreme dorsiflexion of the pes of *Conoryctes*.

Comparing the tibia of *Conoryctes* with other genera of Taeniodonta, *Onychodectes tisonensis* (AMNH 3405), *Wortmania otariidens* (AMNH 3394), *Psittacotherium multifragum* (TMM 41364-1, Figure A49, AMNH 15938, and NMMNH P-19713) and cf *Stylinodon mirus* (USNM 18425), there are many resemblances. Apart from *Onychodectes* which is known only from the distal end of the tibia, in all the other studied genera the tibia is slenderer in the posterior diaphysis, with a less prominent tibial crest and no tuberosity. Another common feature is the prominent medial malleolus extending distally even in more robust taxa like *Stylinodon mirus* USNM 18425. In all specimens, the distal epiphysis extends noticeably more on the posterior aspect than the anterior. The presence of a well-distinguished flexor sulcus on the medial malleolus can be seen in the specimens of *Conoryctes* and *Wortmania*. The other specimens, however, are not as well preserved to study the flexor sulcus. Moreover, another similarity within Taeniodonta, based on the studied specimens, is the unfused tibia and fibula both proximally and distally. Particularly the distal fibular articulation that is adjacent to the epiphysis laterally, is a feature seen in the smaller taxa like *Onychodectes* and *Conoryctes* and the bigger taxa like *Psittacotherium* and

Stylinodon. Moreover, even the smaller taxa have a well-defined crest of the tibiofibular ligament, which is even more prominent in bigger taxa.

There are a few differences regarding their anatomical structures. *Stylinodon* and *Wortmania* have a wider mediolateral proximal than distal part, something not so evident in *Psittacotherium*, and even less so in *Conoryctes*. All four taxa have a large proximal tibial fossa. In posterior aspect, *Stylinodon*, *Wortmania* and *Psittacotherium* have a deep posterior tibial fossa, deeper in the two former genera. *Conoryctes* does not have a prominent popliteus crest and since the specimens are damaged it is unsure how deep the posterior tibial fossa is. Also, in posterior view, there is a protuberance medially, almost near the distal borders of the posterior tibial fossa, on the medial side of the shaft. This can be seen more in *Stylinodon* and less in *Wortmania*, while *Psittacotherium* is broken at that point. The tibia of *Conoryctes* though does not have this protuberance. Lastly, the proximal fibular facet is well distinguished at the lateral-distal end of the proximal epiphysis in *Conoryctes*. For the other three genera, the facet is not as eminent and is placed more on the lateral aspect of the epiphysis than distally.

The tibia of *Escavadodon*, *Prodiacodon* and *Leptictis* (Rose, 1999; Rose and Lucas, 2000; Rose, 2006) were compared with *Conoryctes*. Generally, in all these taxa the shaft of the tibia is slender; apart from *Conoryctes* that has a straight shaft, in the other three genera, it is more curved, and concave posteriorly. The tibial crest is very large and flat in *Conoryctes* in comparison to the other three taxa; in *Escavadodon* and leptictids the crest is sharp, and in palaeonodons more rounded. The tibia and fibula are unfused both proximally and distally in *Conoryctes*, while the two bones are fused only distally in *Escavadodon* and *Prodiacodon*. In leptictids, the tibia and fibula

are also fused distally and continue to almost half the length of the shaft. Proximally there is a fibular facet; in leptictids, the facet is small, and oriented laterally, whereas in *Escavadodon* and *Conoryctes* it is bigger and more distally oriented (Rose and Lucas, 2000). The medial malleolus of *Escavadodon* and palaeonodonts is not as prominent as in leptictids and *Conoryctes*, yet all four taxa have a well-developed flexor sulcus posteriorly (Rose, 1999; Rose and Lucas, 2000). On the distal epiphysis, the medial and lateral astragalar facets in *Conoryctes* are subequal mediolaterally and anteroposteriorly and the medial facet is deeper. On the contrary, *Escavadodon* and leptictids have a deeper groove for the lateral astragalar rim.

Relative to *Periptychus* (NMMNH P- 47693 Shelley *et al.*, 2018) and especially *Pantolambda bathmodon* (AMNH 16663) (Simons, 1960; Matthew, 1937; Shelley *et al.*, 2018) the tibia of *Conoryctes* is more slender and the shaft is less curved. The feature that distinguishes *Conoryctes* is the large tibial crest and tuberosity of the tibial crest relative to the other two taxa; particularly in *Pantolambda* the crest and the tuberosity are very prominent, and the former extends rather distally. In proximal view, the medial condyle is oval, wider mediolaterally and more concave than the lateral condyle, both in *Conoryctes* and *Periptychus*. Distally, *Pantolambda* and *Conoryctes* have a more prominent medial malleolus than *Periptychus*; the medial flexor sulcus is not noticeable in either *Periptychus* or *Pantolambda*. In all three genera, the tibia and fibula are unfused both posteriorly and distally. The distal fibular facet is very close to the lateral astragalar facet and laterally oriented both in *Periptychus* and *Conoryctes*. In distal view, both *Conoryctes* and *Periptychus* have a deeper medial astragalar than lateral astragalar facet. The medial facet is larger in *Periptychus* whereas in *Conoryctes* these two facets are subequal.



Figure 48: Tibiae of *Conoryctes comma* specimens NMMNH P-48198 (a-f) and NMMNH P-19494 (g-k) in posterior (a, g), lateral (b, h), anterior (c, i), medial (d, j), proximal (e) and distal (f, k) views. Scale bar is 1cm.

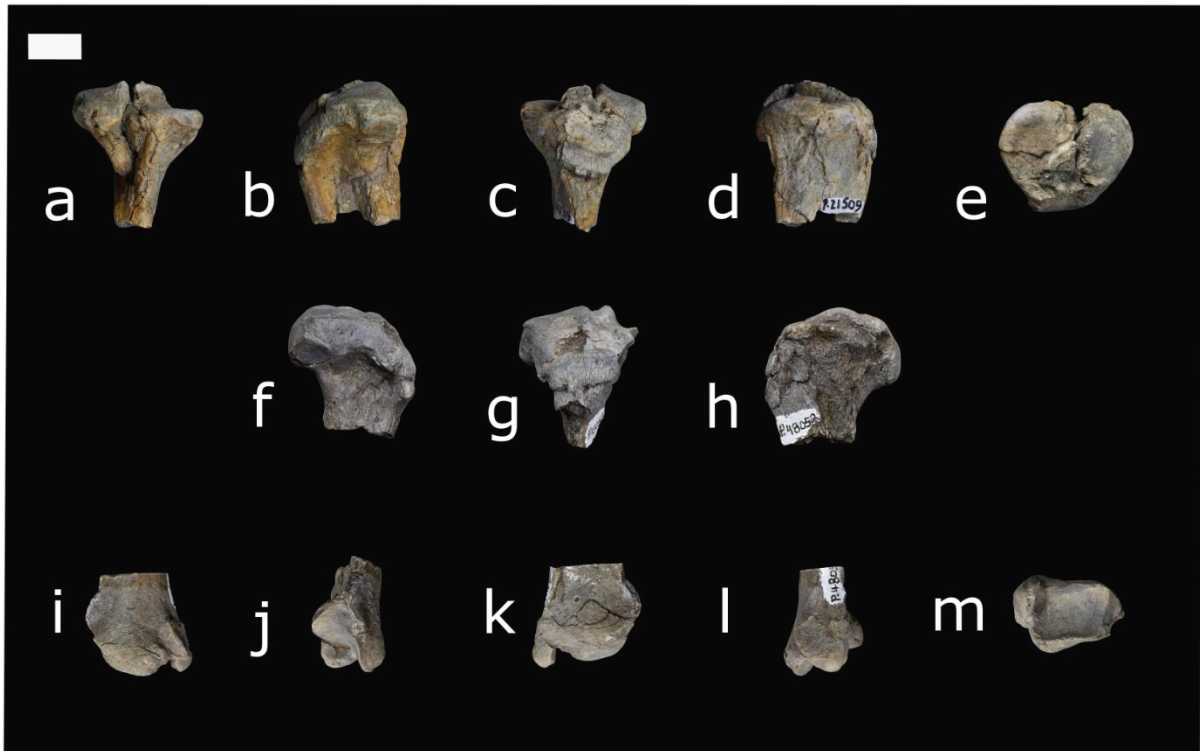


Figure 49: Tibiae of *Conoryctes comma* specimens NMMNH P-21509 (a-e) and NMMNH P-48052 (f-m) in posterior (a, i), lateral (b, f, j), anterior (c, g, k), medial (d, h, l), proximal (e) and distal (m) views. Scale bar is 1cm.

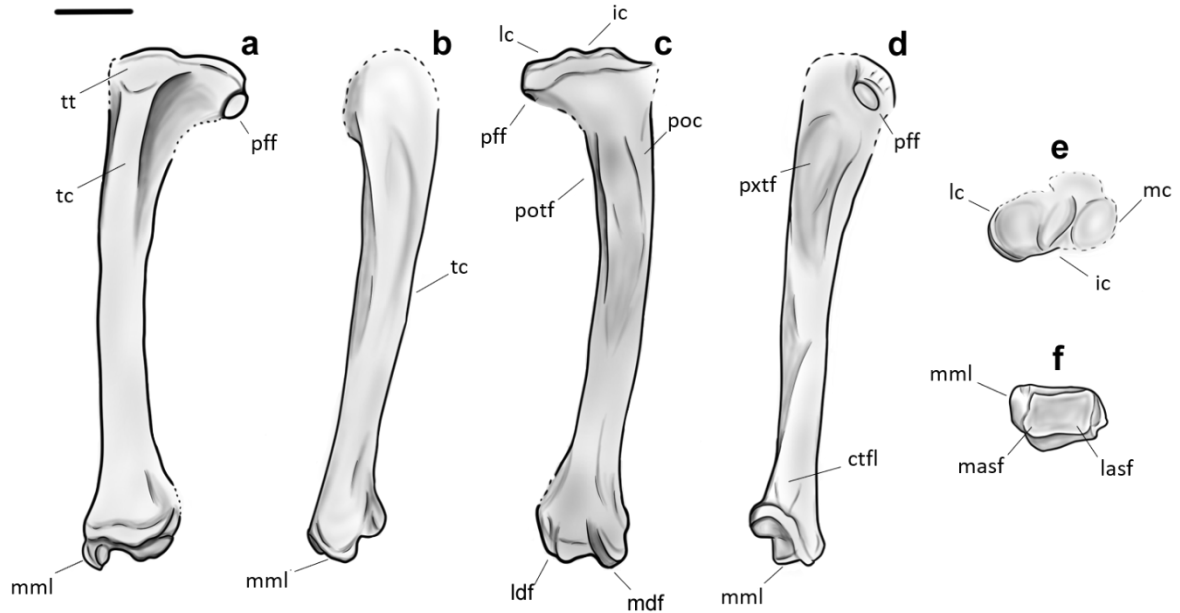


Figure 50: Drawing of *Conoryctes comma* tibia based on NMMNH P-48198 specimen, in anterior (a), medial (b), posterior (c) lateral (d), proximal (e) and distal (f) views. ctfl: crest of the tibiofibular ligament, ic: intercondyloid eminence, lc: lateral condyle, ldf: lateral digital flexor, lasf: lateral astragalar facet, masf: medial astragalar facet, mc: medial condyle, mdf: medial digital flexor, mml: medial malleolus, pff: proximal fibular facet, poc: popliteus crest, potf: posterior tibial fossa, pxtf: proximal tibial fossa, tc: tibial crest, tt: tibial tuberosity. Scale bar 1cm.

Astragalus

There are four astragalar elements among the specimens NMMNH P-48052, NMMNH P-21509, and NMMNH P-48198 (Figures 51 and 52). Specimen NMMNH P-48052 consists of two astragali, one almost complete right astragalus and partial astragalar body and the astragalar head of the left astragalus. The right astragalus of NMMNH P-48052 is missing the central part of the astragalar trochlea and the astragalar head is damaged in plantar view. There is a left astragalus in specimen NMMNH P-21509; it is dorsoplantarly compressed and the astragalar head is damaged in the plantar aspect. There is a left astragalus in specimen NMMNH P-48198 that is well preserved with very well-distinguished articular surfaces. Specimen NMMNH P-48198 is more robust, anteroposteriorly and mediolaterally than NMMNH P-48052 and NMMNH P-21509. Taking into account all of these elements, the astragalus of *Conoryctes* can be described as follows.

In general, the astragalus of *Conoryctes* is anteroposteriorly elongated with a rectangular body, a moderately long and slender neck, and a broad head. The γ angle is defined by the most anterior part of the astragalar head and the line formed by the most anterior points of the astragalar body, measured medially to laterally. In *Conoryctes* the astragalar neck and head are medially offset relative to the body by an angle of approximately 66° . The astragalar body is wider anteroposteriorly than the neck and body (table A18, Appendix). In the dorsal view, the rims of the astragalar trochlea are wider anteriorly than posteriorly. In plantar aspect, the ectal facet is longer anteroposteriorly than the mediolaterally, making the ectal facet relatively elongated.

The body of the astragalus, in dorsal view, is mediolaterally wide and anteroposteriorly short. The trochlea of *Conoryctes* is broad and moderately grooved (U shaped) with subequal lateral and medial rims in length. The medial tibial facet is larger and more prominent than the lateral tibial facet. Distally, the trochlea does not extend to the astragalar neck, with no pit for the anterior process of the tibia. On the most medial part of the astragalar head, plantarly than the astragalar trochlea, there is a medially protruding tibial facet. This facet must have been interlocking well with the prominent medial malleolus of the distal tibia (Figures 51 and 52). On the most lateral part, the fibular facet extends less than the medial tibial facet. In medial aspect, the astragalar body has a protruding tibial facet that is separated from the medial rim of the trochlea by a deep groove. In lateral view of the astragalar body, there is a flatter and smaller fibular facet. Anteriorly the fibular facet is adjacent to the anterior border of the ectal facet.

In posterior view, the medial and lateral rims are strong and the lateral rim of the astragalar trochlea is less elevated than the medial rim of the medial tibial facet. That would have provided *Conoryctes* with a degree of stability of the ankle joint during flexion and extension of the foot. The posterior border of the trochlea expands plantarly allowing more movement of the tibia during flexion of the foot. None of the specimens of *Conoryctes* has a dorsal foramen of the astragalar canal. In plantar view, there is a small round ventral foramen that leads to a wide and long canal anterolaterally. This canal creates a broad and deep sulcus; that is the sulcus astragali where the tendons of the tibialis posterior would have attached. Adjacent to the sulcus astragali are the ectal facet, laterally, and the sustentacular facets, medially, for the articulation of the astragalus with the calcaneum. In *Conoryctes* the ectal facet is broader posteriorly with a narrower ending anteriorly. Both borders of the ectal facet are almost equally

elevated, forming a deep U-shaped facet. The anterior border is part of the lateral tibial facet. Anteromedially to the sulcus astragali is the sustentacular facet; it has an oval shape and is elongated in the anteroposterior direction. The sustentacular facet originates posteriorly on the body of the astragalus and extends anteriorly towards the head of the astragalus where it is almost in contact with the cuboid facet.

In *Conoryctes* the astragalar neck is long (28% of the total anteroposterior length) and medially inclined (76°) relative to the astragalar body. In dorsal view, it joins with the astragalar body posteriorly. The most medial edge of the astragalar neck is near the anteromedial border of the medial astragalar trochlea. Similarly, the most lateral edge of the astragalar neck originates from the mediolateral half of the lateral astragalar trochlea. Anteriorly, the neck is slender and it becomes broader as it reached the astragalar head. In plantar view, the well-defined oval sustentacular facet is present as described above, making the neck dorsoplantarly broad. Medially and laterally, there are grooves next to the sustentacular facet, where the deltoid and talofibular ligaments continued, respectively.

The astragalar head of *Conoryctes* is robust, almost equally broad mediolaterally as dorsoplantarly (table A18). The navicular facet is convex and comes smoothly in contact with the groove of the talofibular ligament laterally. In medial view, the navicular facet is narrow mediolaterally with a sharp medial point, well-separated from the dorsal deltoid groove. In plantar view, the cuboid facet is in contact with the navicular facet anteriorly and very close to the sustentacular facet posteriorly. In anterior aspect, the cuboid and navicular facets meet.

The astragalus of *Conoryctes* was compared to that of *Onychodectes* using the specimens AMNH 3405 (Figure A44), AMNH 3576 and AMNH 27679 of *Onychodectes*

tisonensis, *Psittacotherium* (NMMNH P-19713, TMM 41364-1, Schoch, 1986) and of *Stylinodon* (USNM 18425). The astragali of *Conoryctes* and *Onychodectes* are similar in size, while *Psittacotherium* and *Stylinodon* are more robust.

Regardless of the size difference, they share many similarities, i.e. a U-shaped astragalar trochlea, with subequal astragalar trochlear rims, and a very distinct neck from the head and the body of the astragalus. The trochlea of the astragalar body in *Psittacotherium*, is not so deep in the middle, making the rims less prominent. The trochlea is more concave for *Onychodectes* and *Stylinodon*, and even more so in *Conoryctes*. On the trochlea, the rims are mostly anteroposteriorly subequal in all the studied taeniodonts apart from *Stylinodon*; the lateral trochlear rim is anteroposteriorly longer and dorsoplantarly taller. The medial tibial facet extends anteriorly towards the medial end of the navicular facet, which expands posteriorly, as seen in *Conoryctes* and *Onychodectes*. In *Conoryctes*, the medial facet is more prominent than the lateral; the opposite condition is seen in *Psittacotherium*, whereas in *Stylinodon* both facets are almost vertical. All studied taeniodonts have a deep plantar sulcus astragali and no dorsal foramen of the astragalar canal. In plantar view, the ectal facet of *Conoryctes*, *Onychodectes* and *Psittacotherium* is almost triangular in shape; broader posteriorly, ending to almost a point anteriorly. The specimen USNM 18425 of *Stylinodon*, is articulated with the calcaneum and observations on the plantar aspect could not be made. *Onychodectes* has a wider neck mediolaterally that is more laterally inclined. The neck of *Psittacotherium* (TMM 41364-1, NMMNH P-19713) is short and the tibial facet extends more medially than in *Conoryctes*. In *Stylinodon* the neck is almost vertical to the mediolateral plane of the astragalar body. In plantar view, *Onychodectes* and *Conoryctes* have a similarly elongated sustentacular facet reaching the astragalar head. The astragalar head, for all studied taeniodont, has

facets for the cuboid and the navicular. The cuboid facet is not as posteriorly extended as in *Conoryctes* and the astragalar neck of *Onychodectes* is more robust dorsoplantarily. In dorsal view, *Conoryctes*, *Onychodectes* and potentially *Stylinodon* have a tibial facet as well. Both *Conoryctes* and *Stylinodon* have shallow sulcus for the talonavicular ligaments on the astragalar head.

The tarsal bones of *Procerberus* have been well-studied by Szalay and Decker (1974). Using that description and the specimen AMNH 117454, which is a cast of *Procerberus* sp. (Figure A41), the astragali of *Procerberus* and *Conoryctes* were compared. Regardless of their size, there are basic differences in their shape. *Procerberus* has less extrusive trochlear rims, meaning that the astragalar trochlea is flatter. The anterior part of the trochlea is wider mediolaterally than the posterior part, as seen in *Conoryctes*. The astragalar neck of *Procerberus* is wider and is not so medially inclined as in *Conoryctes*, yet it resembles more *Onychodectes*. Contrary to both taeniodonts, the medial tibial facet and the navicular facet of *Procerberus* are not extended towards each other and the latter is not very noticeable. There is a groove where the calcaneonavicular ligament passed through the astragalar head in dorsal view, similarly, shaped as in *Conoryctes*. In plantar view, *Procerberus* has a more shallow sulcus astragali, and the sustentacular facet is more circular than elongated. This facet is also very robust, making the astragalar neck wider dorsoplantarily, almost as much as in *Onychodectes*. The astragalar head is also dorsoplantarily wider in the medial aspect. A dorsal foramen of the astragalar canal is not present similarly to *Conoryctes*, and as suggested by Szalay and Decker (1974) *Procerberus* had no astragalar canal. In posterior view, the trochlear rims of *Procerberus* are more laterally inclined to the body of the astragalus. This feature is characteristic of *Procerberus* and is not seen in any of the taeniodonts studied.

The astragalus of *Conoryctes* is similar to the astragali of *Escavadodon*, leptictids and palaeonodonts (Rose, 1999; Rose and Lucas, 2000) as they are more anteroposteriorly elongated than mediolaterally wide. *Conoryctes*, *Escavadodon* and *Palaeonodon* have no evidence of a dorsal foramen on the astragalar head. Leptictida astragali are more elongated and less wide mediolaterally than *Escavadodon*, while in *Conoryctes* it is wider than both of these two taxa. *Escavadodon* and *Conoryctes* have subequal trochlear rims in anteroposterior length and elevation and in both taxa the neck is shorter than the mediolateral width of the medial trochlea. On the contrary, in leptictids, the lateral trochlear rim is longer than the medial rim and the astragalar neck is longer than the mediolateral width of the medial trochlea. *Conoryctes* and leptictids have extended medial tibial facets and fibular facets, whereas only the fibular facet of *Escavadodon* is moderately noticeable. Rose and Lucas (2000) described in *Escavadodon* and leptictids an extension of the navicular surface medially of the astragalar neck. However, based on the figures in the publication, *Escavadodon* has a more rounded astragalar head and less posteromedially extended navicular facet than leptictids. The astragalar head of leptictids is less mediolaterally wide yet resembles more the head of *Conoryctes*. In *Escavadodon* and leptictids the sustentacular facet is separated from the navicular and cuboid facets. Similarly, these facets are not connected, yet are closer together in *Conoryctes*.

When compared to *Periptychus* (NMMNH P-47693 Shelley *et al.*, 2018) and *Pantolambda* (AMNH 16663, Simons, 1960; Matthew, 1937; Shelley *et al.*, 2018) the astragalus of *Conoryctes* is more similar to the former. *Pantolambda* has a unique and distinguished astragalus. The astragalar head of *Periptychus* and *Conoryctes* are similar since, the rims are subequal in size and parallel, whereas *Pantolambda* has oblique rims, with the lateral being longer anteroposteriorly. The fibular facet is more

prominent in *Periptychus* than in the other two genera. Similarly, among these three genera, *Conoryctes* has the more prominent medial tibial facet. In plantar aspect, the ectal facet is almost triangularly shaped in *Pantolambda* and *Conoryctes*, while it is more rectangular in *Periptychus*. Both *Periptychus* and *Pantolambda* have a deep sulcus astragali, that leads to the dorsal foramen of the astragalar canal; this is missing from *Conoryctes*. The neck is more slender in *Conoryctes* than in *Periptychus*, while it has a very unique shape in *Pantolambda*. In plantar aspect, the sustentacular facet is almost circular in *Periptychus* and *Pantolambda* and more anteroposteriorly elongated in *Conoryctes*. The head of *Periptychus* and *Conoryctes* is similarly convex, with facets for the cuboid and the navicular, with the latter expanding posteriorly in medial aspect.



Figure 51: Astragali of *Conoryctes comma* of specimens NMMNH P-48198 (a-c), NMMNH P-21509, NMMNH P-48052 (g-i) in dorsal and plantar (a, d, g), anterior and posterior (b, e, h) and medial and lateral (c, f, i) views. Scale bar is 1cm.

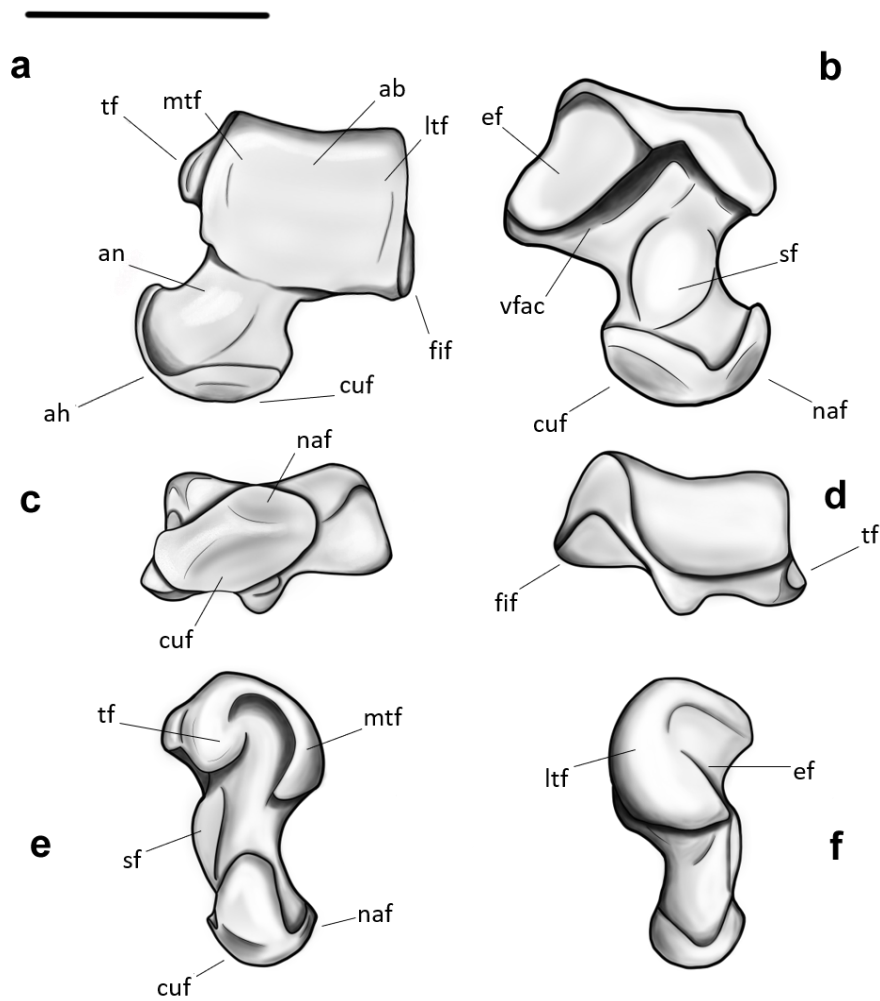


Figure 52: Drawing of the astragalus, *Conoryctes comma*, using specimen NMMNH P-48198 in dorsal (a), plantar (b), anterior (c), posterior (d), medial (e) and lateral (f) views. ab: astragalar body, ah: astragalar head, an: astragalar neck, cuf: cuboid facet, ef: ectal facet, fif: fibular facet, mtf: medial tibial facet, naf: navicular facet, ltf: lateral tibial facet, sf: sustentacular facet, tf: tibial facet, vfac: ventral foramen of the astragalar canal (sulcus astragali), .. Scale bar is 1cm.

Calcaneum

There are four elements of calcaneum from specimens NMMNH P-48198, NMMNH P-48052 and NMMNH P-47866 (Figures 53 and 54). Specimen NMMNH P-48198 has two calcanei, one left and one right, that are associated with the astragalus described above. Both calcanei are well preserved with the peroneal process broken and the cuboid facet damaged. The left calcaneum is also damaged in the ectal facet. Specimen NMMNH P-48052 has a right almost complete calcaneum and part of a left calcaneum. The right calcaneum of this specimen is missing part of the tuber calcanei and the sustentaculum. However, the peroneal process and the cuboid facets are in great condition. The right calcaneum is also associated with the right astragalus of the same specimen, NMMNH P-48052. The left calcaneum of NMMNH P-48052 has part of the ectal and cuboid facets and the posterior part of the calcaneal tuber. Specimen NMMNH P-47866 has a complete calcaneum.

The calcaneum of *Conoryctes* is generally elongated and slender, with prominent facets anteriorly for articulation with the astragalus, fibula and cuboid. In *Conoryctes* the tuber calcanei is elongated, representing approximately 56% of the maximum anteroposterior calcaneal length. One distinguishing feature is the anteriorly extended anterior plantar tubercle, which is almost on the same level as the cuboid facet. There is also a robust posterior plantar tubercle.

On the anterior part of the calcaneum, the articular facets are extended mediolaterally in *Conoryctes*. The ectal facet is anterolaterally to posteromedially oriented, forming a 145° angle with the anteroposterior calcaneal length; the facet is also mediolaterally elongated and rather convex (table A19). In dorsal aspect, the ectal

facet reaches the medial border of the calcaneum; there it flares medially and is thus separated by the tuber calcanei. Laterally it reaches the lateral border of the peroneal process, however, the two facets are not adjacent. The most anterior border of the ectal facet extends at the same level as the posterior borders of the sustentaculum and peroneal process. In medial aspect, there is a groove between the ectal facet and the sustentaculum. This groove and the plantar groove of the astragalus (ventral foramen of the astragalar canal) form the calcaneal sulcus, a canal through which the interosseous astragalocalcaneal ligament and nerves passed. In lateral view, the ectal facet is separated from the peroneal process by a narrow canal, possibly for the medial collateral ligament, the extensor digitorum lateralis and the fibularis (peroneus) brevis muscles. There is a small, convex facet close to the ectal facet dorsolaterally; this is the fibular facet which due to damage is only evident in the right calcaneum of specimen NMMNH P-48198. The fibular facet is circular and is located almost vertically to the anterolateral border of the ectal facet.

The sustentaculum of *Conoryctes*, in dorsal view, extends medially, it is oval in shape and mediolaterally elongated. It is well separated from the ectal facet by the deep calcaneal sulcus. Dorsally, there is the ovoid and shallowly concave sustentacular facet which connects with the plantar-medial part of the astragalar sustentacular facet. In anterior view, the sustentaculum is thick dorsoplantarly and is demarcated distally from the cuboid facet by a narrow groove which continues plantarly. The flexor hallucis longus tendon passed through this groove and was involved in the flexion of the pedal digit I.

The peroneal process of *Conoryctes* is situated off the lateral edge and originates more anteriorly than the sustentacular process and it does not protrude

laterally. In dorsal aspect the peroneal process extends to the same level as the most anterolateral boundary of the cuboid facet. As mentioned before, there is a wide and narrow groove that separates the peroneal process and the ectal facet. In anterior view, the peroneal process is next to the cuboid facet, but the two features do not meet. Plantarly, the peroneal process and the anterior plantar tubercle are separated by a wide and shallow canal. Through this groove passed the abductor digit V muscle, responsible for the abduction of the fifth metatarsal, and other ligaments, i.e., the calcaneoquartal and the lateral collateral ligaments.

The cuboid facet is concave and is on the most anterior part of the calcaneum, articulating with the cuboid. In dorsal view, *Conoryctes* exhibits a convex structure that originates from the cuboid facet and extends distally. This facet is medioplantarly oblique relative to the calcaneal long axis. In anterior view, as described before, the cuboid is separated from other calcaneal facets and is surrounded by a shallow groove laterally and a deeper one medially. There is also another smaller sulcus to separate the cuboid facet and the anterior plantar tubercle.

The most distinctive calcaneal feature of *Conoryctes* is the protruding anterior plantar tubercle, which is long and cylindrical on the anterior plantar area. In anterior aspect, it is medially placed, closer to the sustentacular than the peroneal process, separated from these two processes by two grooves for the passing muscles, nerves and ligaments, as mentioned above. In medial view, the anterior plantar tubercle extends straight anteriorly and is not medioplantarly oblique like the cuboid facet. The anterior plantar tubercle and the cuboid facet are separated by a small fissure. The plantar border of the cuboid facet extends on the same level anteriorly as the anterior

plantar tubercle. Due to the inclination of the cuboid facet, the dorsal border of the cuboid facet extends more anteriorly than the anterior plantar tubercle.

In *Conoryctes* the elongated tuber calcanei forms a posterior apex, that is inclined medially. In lateral aspect, the apex has a bulging shape anteriorly, and the posterior plantar tubercle leads to an almost flat surface posteriorly. The gastrocnemius muscle was attached to the calcaneum tuber and was responsible for the extension and flexion of the pes. The flexor digitorum superficialis muscle, which flexes the II, III, IV and V digits, passed by the tuber calcanei making the galea calcanea cap. All specimens have a more flat and textured lateral side of the tuber calcanei. This could be due to the connection of the calcaneoquartal ligament that starts from the plantar-lateral surface of the calcaneum and attaches to the IV tarsal and the base of V metatarsal (Evans and de Lahunta, 2013). In distal aspect, the tuber calcanei have a groove, swallow and are almost mediolaterally oriented for the calcaneal tendon.

Conoryctes has a very similar calcaneum to *Onychodectes* (AMNH 27679), and less so to *Ectoganus* (USGS 3838, Schoch, 1986) and *Stylinodon* (USNM 18425). In *Onychodectes* the tuber calcanei are also wider dorsoplantarly than mediolaterally, yet it is not as slender and elongated mediolaterally as *Conoryctes*. For *Onychodectes*, *Conoryctes* and *Stylinodon* the tuber calcanei shaft is almost 50% of the maximum anteroposterior calcaneal length (see appendix). In medial aspect, *Onychodectes* has a more prominent posterior plantar tubercle at the distal end of the tuber calcanei than *Conoryctes*. Specimen USNM 18425 of *Stylinodon* also has a “hook” shape (Schoch, 1986) probably for the attachment of the gastrocnemius and the superficial digital flexor. Proximally, the ectal facet is large and concave in all studied specimens. It is

more anteroposteriorly oriented in *Ectoganus* and *Stylinodon*, whereas more mediolateral in the other two studied genera. Also, the ectal facet extends along the medial and lateral borders of the calcaneal shaft having an oval shape in *Onychodectes* and *Conoryctes*. The sustentacular facet is elongated mediolaterally and extends substantially from the calcaneal tuber medially in all studied taeniodonts. The peroneal process is broken in *Onychodectes* (AMNH 27679), while the cuboid facet is complete and is shallower than in *Conoryctes*. *Onychodectes* has also a more dorsally bulging cuboid facet and, along with the anterior plantar tubercle, is medioplantarly oblique to the calcaneal long axis. Szalay and Decker (1974) considered this as a primitive eutherian condition and is to some degree evident in *Procerberus* as well. This is different to *Conoryctes*, where only the cuboid facet is medioplantarly inclined. *Stylinodon* also has an anterior plantar tubercle that does not reach the level of the cuboid and is transversely elongated. The peroneal process reaches the cuboid facet anteriorly, yet it is not as prominent as in *Conoryctes*. Specimen AMNH 27679 of *Onychodectes* has evidence of a wide calcaneal sulcus, and a groove for the flexor hallucis longus tendon. It is unclear if there is a small groove or pit between the cuboid facet and the peroneal process anteriorly.

The calcaneum of *Procerberus* (AMNH 117455) shares few similarities with both *Conoryctes* and *Onychodectes*. In *Procerberus* the ectal facet is the largest, most prominent feature, whereas in the studied taeniodonts, especially in *Conoryctes*, the sustentaculum and peroneal processes form equally large areas. *Procerberus* has a slender tuber calcaneus in all aspects, which is less than 50% of the total calcaneal length. The most posterior apex of the tuber calcanei in dorsal view is similarly inclined medially like *Conoryctes*. In plantar aspect, it has a bulging posterior plantar tubercle like *Onychodectes*. In *Procerberus* this tubercle is almost equally protruding as the

anterior plantar tubercle. All three genera have an ectal facet that reaches the medial and lateral borders of the calcaneum in dorsal view. The sustentaculum of *Procerberus* is less pronounced and has a more circular shape than the oval-shaped sustentaculum of *Conoryctes*, and the peroneal process is proportionally larger (Szalay and Decker, 1974). In dorsal view, there is also a wide and deep calcaneal sulcus. The cuboid facet is shallowly concave, almost circular in profile and more anteriorly placed than in taeniodonts. The cuboid facet and the anterior plantar tubercle are also medioplantarly oriented to some extent, similar to *Conoryctes*. The peroneal tubercle of *Procerberus* is less prominent and does not reach the same level anteriorly as the cuboid facet, and there is a very small pit between them. The peroneal tubercle is closer to the sustentaculum in the anterior view, with grooves on each side.

In dorsal aspect, the posterior apex of the tuber calcanei in *Escavadodon*, leptictids and *Conoryctes* is inclined medially (Rose and Lucas, 2000). The tuber calcanei in *Escavadodon* and leptictids is less than half the total calcaneal length, like *Procerberus*, and unlike taeniodonts. In *Escavadodon* and leptictids, the ectal facet is oblique and oval, almost reaching both the medial and lateral sides of the calcaneum (Rose, 1999). The calcaneum of *Escavadodon* is similar to *Conoryctes* with a thick and prominent sustentacular facet that is closer to the cuboid facet anteroposteriorly (Rose and Lucas, 2000). Leptictids, however, have a less medially protruding sustentacular facet, almost circularly shaped, more posteriorly located relative to the cuboid facet, and a less pronounced anterior plantar tubercle (Rose, 1999). In leptictids, the cuboid facet is tapering medioplantarly towards the planter tubercle more so than in the specimens of *Conoryctes*.

Comparing the calcaneum of *Conoryctes* to *Periptychus* (NMMNH P-47693 Shelley *et al.*, 2018) and *Pantolambda* (AMNH 16663, Simons, 1960; Matthew, 1937; Shelley *et al.*, 2018) there are some similarities and differences. All three taxa have a well-developed and elongated tuber calcanei shaft, almost half as long as the calcaneus. The posterior plantar tubercle is more prominent in *Conoryctes* and *Periptychus*. Anteriorly, the ectal facet is more elongated in *Conoryctes*, less so in *Periptychus* and more oval in *Pantolambda*. In all three genera though, the ectal facet is more mediolaterally oriented than anteroposteriorly. The sustentacular facet extends more medially in *Pantolambda* than in the other two genera. The cuboid facet is bulging anterodorsally and is tapering medioplantarly in both genera of *Conoryctes* and *Periptychus*. The anterior plantar tubercle is not reaching the cuboid facet anteriorly in *Periptychus*, as opposed to *Conoryctes*. However, the peroneal process is more robust in *Pantolambda* than in *Periptychus*, while it is larger in *Conoryctes*.

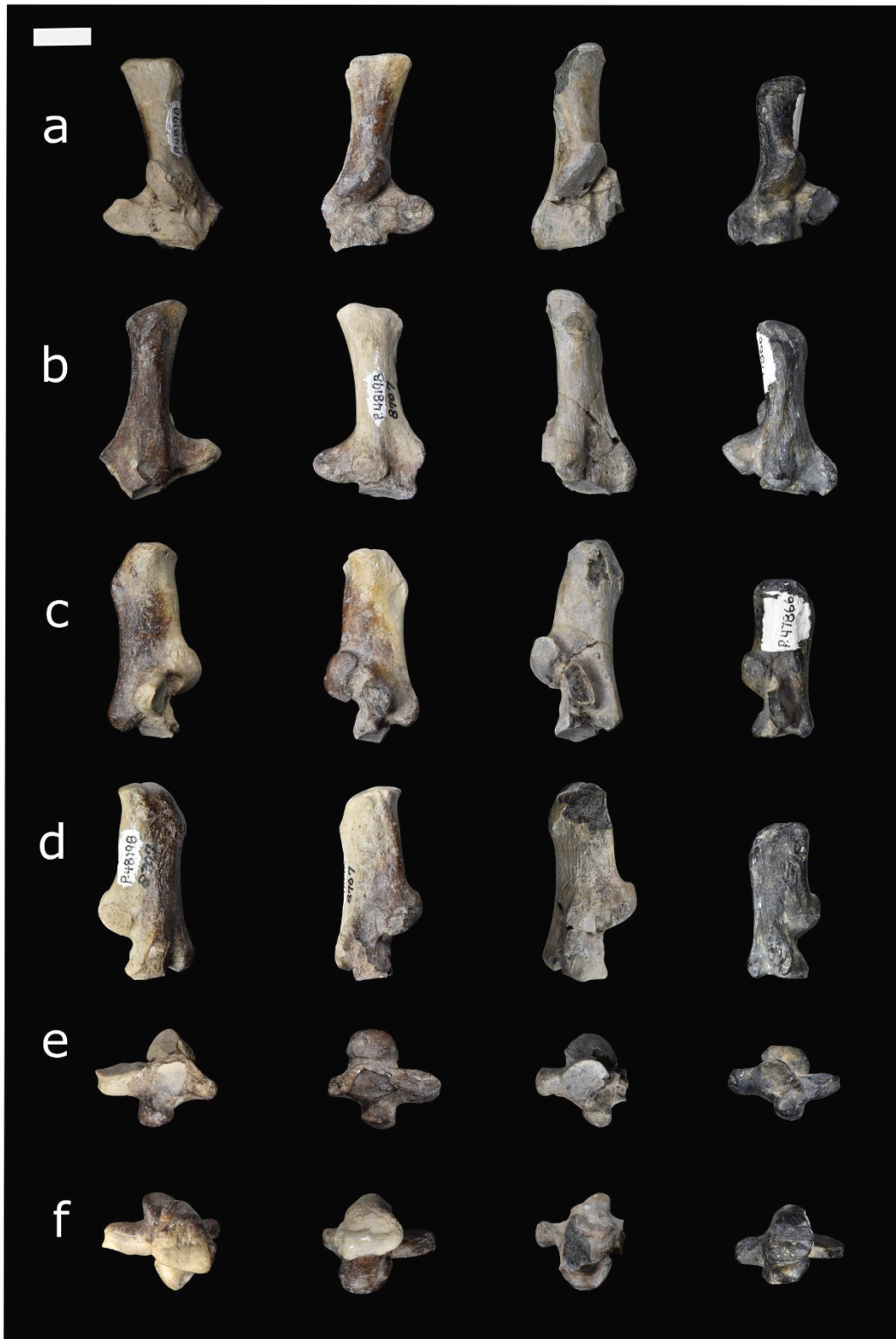


Figure 53: Calcanei of *Conoryctes comma* of specimens NMMNH P- 48198 (first two), NMMH P-48052 and NMMNH P-47866 (on the right) in dorsal (a), plantar (b), medial (c), lateral (d), anterior (e) and posterior (f) views. Scale bar is 1cm.

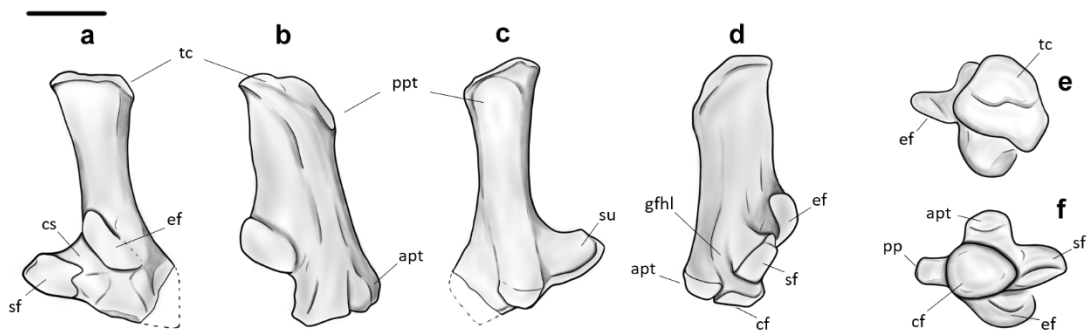


Figure 54: Drawing of the calcaneum, *Conoryctes comma*, NMMNH P- 48198 and NMMNH P-47866, in dorsal (a), lateral (b), plantar (c), medial (d), distal (e) and anterior (f) views. apt: anterior plantar tubercle, cf: cuboid facet, cs: calcaneal sulcus, ef: ectal facet, gfhl: groove for the flexor hallucis longus tendon, pp: peroneal process, ppt: posterior plantar tubercle, sf: sustentacular facet, su: sustentaculum, tc: tuber calcanei. Scale bar is 1cm.

Metatarsals

Part of the pes of *Conoryctes* is known from specimen NMMNH P-47700. In that specimen there are the parts of the tarsals, with ectocuneiform and navicular the proximal part of metatarsal III, complete metatarsal IV and V and a broken metatarsal with the proximal end missing, as well as two distal phalanges. This is the metatarsal III because it is longer than the other metatarsals.

In general, the metatarsals of *Conoryctes* are more slender than the elements of the manus and have less prominent flexor tubercles (table A20). The ectocuneiform (Figure 55a) and the navicular (Figure 55b) are complete. The navicular is proximodistally short with a deeply concave navicular facet. Distally there are three distinct facets for the articulation with the cuneiforms. The ectocuneiform is longer plantar dorsally than mediolaterally. It has two facets where it articulates with the navicular and there is a lateral facet for the cuboid. Distally it is curved, and it articulates with a concave proximal facet of the metatarsal III.

The metatarsals are proximodistally long and are concave on the plantar aspect. Distally the metatarsals have a similar ridge dorsoplantarly as the metacarpals. There is a groove on the proximal end of the first phalanges of the pes as well (27 d, e). This provided extra stability to the metatarsal-phalanges joint (Hildebrand, 1985). The terminal phalanges are the almost same size as the ones of the manus. The manual unguals are morphologically very similar to the unguals of the pes, having a deep curvature proximally with a “bony stop” and plantar flexor tubercles and being recurved, laterally compressed.

Compared with other taeniodonts the pes of *Conoryctes* is similar to *Onychodectes* (AMNH 16528) in shape and size. The dorsoplantar ridges on the distal articulation of the metatarsals are less prominent in *Onychodectes*. The pes of *Psittacotherium* and *Stylinodon* have more robust and mediolaterally wide metatarsals, with more long and more curved terminal phalanges.

The metatarsals of *Conoryctes* resemble those of *Escavadodon* (Rose and Lucas, 2000) in being concave on the plantar aspect. *Escavadodon*, as well as *Periptychus* and *Pantolambda*, differ from *Conoryctes* because they lack the dorsoplantar ridges on the distal articulation of the metatarsals. Lastly, *Conoryctes* has laterally compressed, curved unguals compared to the hoof-like rounded unguals with a median fissure of *Periptychus* (Shelley, 2018) and the mediolaterally broad unguals of *Pantolambda*.

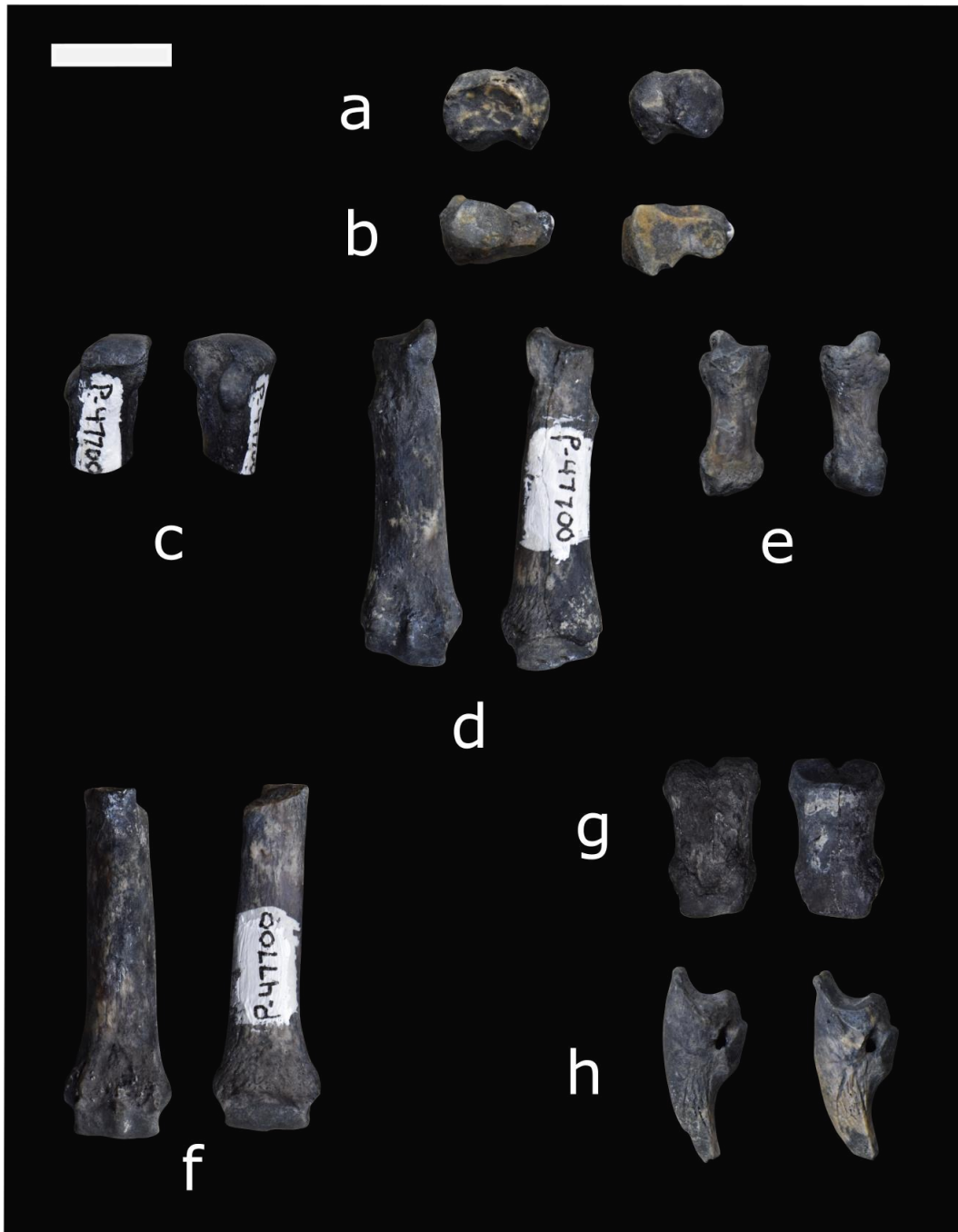


Figure 55: Part of the pes of *Conoryctes comma*, specimen NMMNH P-47700. Different views of the navicular (a), ectocuneiform (b), dorsal and plantar views of the proximal metatarsal III (c), complete metatarsal IV (d) and V (e), partial metatarsal (f), phalanges (g) and medial views of unguals (h). Scale bar is 1cm.

Results and Discussion

Many taeniodonts have anatomical adaptations that point to fossoriality and scratch-digging behaviours (Coombs, 1983; Schoch, 1986; Turnbull, 2004, Williamson and Brusatte, 2013). There are also many studies of the osteological specializations seen in fossorial animals (Shimer, 1903; Lehmann, 1963; Coombs, 1983; Hildebrand, 1982; 1985; Thewissen and Badoux, 1986; Rose, 1993; 1999; Salton *et al.*, 2008; Chen and Wilson, 2015; Dunn, 2018; Shelley *et al.*, 2021; Mao *et al.*, 2021) which related to digging adaptations to loosen the substrate, powerful limbs to move the soil, mechanisms to stabilize the body and prevent hyperextension of the joints while digging. The new specimens from the San Juan Basin provide information to understand the mode of life of *Conoryctes*.

Functional anatomy

Based on the new specimens, *Conoryctes* also had a short neck since the cervical vertebrae are much shorter anteroposteriorly than the rest of the vertebrae (Appendix, table A9). Many fossorial animals like hedgehogs, have short necks to strengthen their vertebrae column (Shimer, 1903), making their body stouter and more robust. The tail is very robust cranially; the first caudal vertebra is mediolaterally robust, and the most caudal vertebrae are craniocaudally long. Therefore, *Conoryctes* had a long tail that helped stabilize its hind body. Hildebrand (1985) suggests that mammals that dig with their forelimb use their tail as another way to stabilize their hind body. Although a short tail is usually seen in digging animals, there are other great diggers, such as armadillo, that have long tails (Shimer, 1903). Similarly, the sacrum

of digging animals usually consists of more than four sacral vertebrae fused, since a longer sacrum assists in the stability of the pelvis (Hildebrand, 1985; Tague, 2020). The sacrum of *Conoryctes* consists only of three fused vertebrae, but it is elongated.

Fossorial animals have robust limbs that are usually short and stout (Shimer, 1903; Chen and Wilson, 2015). The forelimb of *Conoryctes*, known from the humerus, the radius, and the proximal ulna, is robust. The humeral head is hemispherical, and the humeral index (Humeral head mediolateral width/ proximodistal length) is high (91.9%), indicating a more mobile glenohumeral joint (Dunn, 2018). The humeral shaft has a long distally extended and mediolaterally broad deltopectoral area where powerful deltoid and pectoral muscles were attached. The distal end of the humerus is broad, and the medial epicondyle is very prominent indicating strong digital and carpal flexor (medially) and extensors (laterally) muscles. The robust deltopectoral area and the distally broad humerus are also seen in modern fossorial animals, such as pangolins (Chen and Wilson, 2015). The anteriorly projecting deltopectoral crest, the mediolaterally broad distal epiphysis with a moderate entepicondylar foramen of *Conoryctes* matches the description of the “primitive fossorial type” proposed by Gregory (1910). These humeral features of *Conoryctes* are also seen in more derived taeniodonts, such as *Psittacotherium*, *Ectoganus* and *Stylinodon*, that were adapted for digging, similar to aardvarks and wombats (Schoch, 1986; Turnbull, 2004).

The olecranon of the ulna is usually enlarged in fossorial animals (Chen and Wilson, 2015; Dunn, 2018). The ulna is not complete so the length of the olecranon relative to the ulna is unknown for *Conoryctes*. The olecranon of *Conoryctes* is medially curved and a deep flexor fossa indicates powerful digital flexors, such as the flexor digitorum profundus. On the lateral side, the ulna of *Conoryctes* has a deep

fossa for well-developed abductors. The flat ulnar facet on the radius of *Conoryctes* allowed limited supination of the forelimb and is a feature seen in other taeniodonts too, *Onychodectes*, and *Wortmania*. A flat ulnar facet has been associated with terrestrial or digging behaviours (Rose, 1999). The radius is very stout and is anteriorly curved with a strong pronator crest, a moderate styloid process and separated facets distally for the lunar and scaphoid facets. The curvature of the radius has been seen in fossorial animals while the styloid process is robust providing additional support in the wrist joint (Lehmann, 1963).

All diggers have powerful muscles that originate and insert far from the joints, therefore the distal bones of the forelimb are short (Hildebrand, 1985; Dunn, 2018). This is seen in *Conoryctes* with the radius and particularly the metacarpals being short. Figures 41 and 42 show that the most proximal and the intermediate phalanges are short while the unguals are elongated, very common for fossorial animals (Chen and Wilson, 2015). The metacarpals of *Conoryctes* are curved posteriorly and have large extensor tubercles on dorsal surfaces and a prominent ridge at the distal end for the stabilization of the metacarpal-phalanges joint. This ridge prevents the dislocation and hyperextension of the phalanges in fossorial animals (Hildebrand, 1985). This anatomy of the metacarpals and the phalanges is also seen in other palpigrade animals, as well as in *Prodiacodon*, *Escavadodon* and all taeniodonts, apart from *Conoryctella* which is known from a few postcranial elements (Williamson and Brusatte, 2013). The unguals of *Conoryctes* are also indicative of a digging animal because they are enlarged, laterally compressed, bearing large flexor tubercles and a curved articular surface with the phalange. The dorsoventral depth and the curvature of the unguals are also similar to those of fossorial animals (MacLeod and Rose, 1993).

The innominate of *Conoryctes* has a long ischium, the ilium is parallel to the sacrum and the acetabulum creates an angle with the long axis of the innominate. Moreover, there are at least two points on the medial side of the ilium where the sacrum was attached. All these interesting features also helped stabilise the body of *Conoryctes* while digging (Chapman, 1919; Hildebrand, 1985).

The tibial crest of *Conoryctes* is long (Figure 48-50) relative to the total length of the tibia, indicative of powerful knee flexion seen in digging animals (Dunn, 2018). The anteroposteriorly short astragalar neck relative to the total length of the astragalus (table A18), and the elongated tuber calcanei (measurement 10 of Figure A39, in the Appendix) are anatomical features seen in many taeniodonts, including *Conoryctes* and in digging animals (Chen and Wilson, 2015). The metatarsals of *Conoryctes* are very similar to the metacarpals, having flexor tubercles and being curved posteriorly. The unguals of the pes are very similar to the unguals of the manus having enlarged flexor tubercles.

The study of Hildebrand (1985) shows that the level and ways of fossoriality are a complex combination of the way animals use different parts of their body to loosen soil, flex their limbs against the resistance of the substrate, and move the soil. Based on the muscle structure and the osteological characteristics, Hildebrand (1985) proposed six categories of digging: scratch-digging, chisel-tooth digging, head-lift digging, hook-and-pull digging, humeral-rotation digging, hind-feet-first digging. Following this organization, *Conoryctes* was a scratch-digging animal with powerful forearm muscles for the flexion and extension of the humerus and the elbow and strong and well-stabilised digits.

As mentioned above, there are many similarities between the postcranial skeleton of *Conoryctes* and *Onychodectes*. Among these are the modifications in the forelimb i.e. the robust deltopectoral area, the medial extension of the distal humerus, the medially oriented and long olecranon of the ulna and the laterally compressed recurved unguals, that point to digging adaptations for *Onychodectes* too. Therefore, this study agrees with Williamson and Brusatte (2013) that more taeniodonts had at least some level of digging adaptations. Based on their study and the new material, *Conoryctes* and *Wortmania* were powerful scratch-digging animals.

CHAPTER 4

Conclusions



San Juan Basin, New Mexico, fieldwork May 2019

“Ἐν οἶδα ὅτι οὐδὲν οἶδα”

ΑΠΟΛΟΓΙΑ ΣΩΚΡΑΤΟΥΣ, Πλάτων

“I know one thing, that I know nothing”

APOLOGY, Plato (428/427 or 424/423 BC)

Summary

The study of Paleocene mammals is challenging and there needs to be a multi-multifactorial approach to understanding the placentals that lived right after the Cretaceous mass extinction. The present study has focused on the dental and postcranial anatomy of the enigmatic group of Taeniodonta. Looking into many specimens of taeniodonts and other Paleocene taxa many anatomical features were observed, and they were then developed into phylogenetic characters. Understanding the anatomy helped to better evaluate the characters and the way they were scored. Using the species-level phylogeny for taeniodonts, elucidated their evolution and their relationship with other taxa. The second aim of this study was to describe the anatomy and the functional morphology of the skeleton of *Conoryctes comma*. Combining the results of the study, it is demonstrated that Taeniodonta originated from an ancestor that was well adapted for digging.

The insights on the dental morphology and the phylogeny of Taeniodonta

The new specimens of taeniodonts proved to be very helpful in understanding their dental anatomy. For example, the specimens of *Conoryctes*, particularly the upper dentition of NMMNH P-61799 and lower of NMMNH P-19976, confirm the typical taeniodont feature of the outrolling eruption of the cheek teeth, but also give an insight into the occlusion of conoryctids. There is a large protocone, slightly recurved buccally, and moderately large conules that are wearing out. In the lower dentition, the trigonid has approximately the same height as the talonid and lingually the teeth are wearing more rapidly than buccally. These indicate that during mastication, there was a

chewing mediolateral stroke similar to what Schoch (1986) described for *Onychodectes*. The enamel wear even in Paleocene taeniodonts indicates that they were moving their jaw transversely and wearing mostly the upper lingual margins and the lower buccal margins of their tooth. The protocone must have first occluded with the talonid basin in a mortar-and-pestle style and then followed a movement of the jaw lingually (Schoch, 1986). Over time, the lingual cusps and cuspids were worn out creating a shearing-grinding area, similar to what is described as secondary occlusal surfaces by Schultz *et al.* (2021).

The new specimens also led to understanding the upper molars of derived *Psittacotherium* and *Ectoganus*. The distolingual cusp on the upper molars of *Ectoganus* is derived from the lingual shift of the metaconule. This cusp has increased the occlusal area of the molars, making them square-shaped. For the derived Taeniodonta the distolingual cusp, although functionally serving as a hypocone, should not be considered a true hypocone, but a distolingual cusp that is derived from the metaconule. The idea of the formation of a distolingual cusp has been proposed before for Perissodactyla (Holdbrook, 2015) and examples of the “metaconular hypocone” have been seen also in the middle Paleocene Afrotheria, *Ocepeia* (Gheerbrant *et al.*, 2014; 2016). The hypocone has evolved more than twenty times among mammals in the Cenozoic, mostly to increase the occlusal area of the molars (Thesleff and Jernval, 1997; Hunter and Jernvall, 1995).

Understanding these important changes in the dental anatomy within the group, helped score taeniodonts and modify the Shelley_2020 matrix. Adding all the valid species of Taeniodonta and more Palaeogene taxa produced interesting results. The three most important findings of this study are: placing Taeniodonta outside of

placentals, excluding *Schowalteria* from taeniodonts and synonymizing *Conoryctes comma* and *Huerfanodon torrejonus*.

As mentioned, an important finding from chapter two is the position of *Schowalteria* in relation to Taeniodonta. The few unworn teeth of *Schowalteria* share unambiguous features with Taeniodonta but show a more cimolestid-like morphology. The anatomical characteristics that *Schowalteria* has, which are different to taeniodonts, are:

- the size and shape of the anterior upper premolars
- the strong ectoflexus on the upper molars
- the narrower upper molars measured on the middle buccal-lingually
- the upper and lower molars do not decrease in size (m2 and M2 are relatively bigger than the other molars)
- the distinctive metastyle on p2
- the lower p4 is almost equal in size to the p5
- the lower premolars are not transversely placed in the mandible

The results of the phylogenetic analysis captured these differences and so *Schowalteria* is not found within Taeniodonta. The current study defined the clades of Taeniodonta, Conoryctidae and Stylinodontidae based on these results.

Looking into the previous work done on Taeniodonta, the fragmentary nature of specimens has led many researchers to name new taxa, only to be later synonymised with previously studied taxa. After naming the new genus of *Huerfanodon* Schoch (1986) recognized a few specimens, that were previously

belonging to *Conoryctes*, as indeterminate. It is also worth noting that when Schoch (1986) described the skull of *Conoryctes comma* he mentioned how it is identical to that of *Huerfanodon torrejonus* and used both taxa in his description. The phylogenetic results of the current study found the two species as sister taxa, with *Huerfanodon polecatensis* (PU 14178) outside of that clade. Studying the new specimens of *Conoryctes* and looking into the previous definitions of *Huerfanodon torrejonus* I was able to observe major similarities. The only significant difference is the level of development of the lingual cingulum on the P4, which is very variable in all the specimens of *Conoryctes*. Considering all these and the results of the phylogenetic analysis, I synonymize *Huerfanodon torrejonus*, with *Conoryctes comma*. Therefore, the genus of *Huerfanodon* is no longer valid and since the species of *Huerfanodon polecatensis* (PU 14178) is not the type species, it should belong to a new genus. A detailed description of the specimen PU 14178 should follow and there should be a new genus named for that specimen.

The current analysis finds Taeniodonta outside of Placentalia and their sister taxon is *Escavadodon*. This connection with Palaeodonta has been proposed by previous analyses too (Matthew, 1937; Halliday *et al.*, 2019). Taeniodonts and *Escavadodon* share similarities in the dental (e.g. absence of strong ectoflexus and pre- and post-cingula on the upper molars, the talonid subequal to wider than the trigonid on the lower molars), and postcranial characters (e.g. strong deltopectoral crests of the humerus, distal tubercle of the radius, lack of a dorsal foramen on the astragalar head). The Cimolesta and Leptictida are still orders that need further investigation, and future work on these groups might help place taeniodonts better on the mammalian phylogenetic tree.

The anatomy and functional morphology of *Conoryctes comma*

The new specimens of *Conoryctes* from the San Juan Basin include elements of the vertebrae, such as the axis and sacrum, ribs, and of the humerus, the ulna, the radius, and part of the manus, the pelvis, the femur, the tibia, and part of the pes, including the tarsals. *Conoryctes* was a medium-sized mammal (Figure A40, Appendix), with a robust humerus, radius, and femur. The neck of *Conoryctes* was relatively short compared to the long tail. In the manus and the pes, the phalanges were short distally, leading to recurved unguals. The studied specimens referred to *Conoryctes comma* showed a small difference in size without any anatomical differences, which is interpreted as an interspecific variation.

When compared to other taeniodonts, there are many similarities with the other conoryctids, such as *Onychodectes*. Postcranial elements are rare for taeniodonts. However, this study showed that there are a few anatomical features that have been noted in all members of the group, of which postcranial elements have been found. These common features are:

- The greater tubercle of the humerus reaches almost at the same level as the head.
- The distally deltopectoral region of the humerus is broad.
- The radial distal diaphysis is mediolaterally broad.
- The femoral head extends more proximally than the greater trochanter.
- The femoral trochlea reaches at the same level as the posterior part of the femoral condyles.

- The medial malleolus of the tibia is prominent expanding distally and has a deep groove for a well-distinguished flexor sulcus.
- The astragalus has no dorsal astragalar foramen on the body; the astragalar trochlea is U-shaped, with subequal astragalar trochlear rims; the astragalar neck is a mediolaterally narrow.
- The sustentacular facet of the calcaneum is elongated mediolaterally and extends from the calcaneal tuber medially.
- The unguals of the manus and pes, are laterally compressed and have large flexor tubercles.

Conoryctes has a skeleton that is most similar to *Procerberus*, *Escavadodon* and leptictids. However, there are still many differences. The humerus is robust with a strong deltopectoral region for both *Conoryctes* and *Escavadodon*. The olecranon of the ulna is longer and more medially inclined in *Escavadodon* than in *Conoryctes*. The fovea capitis of the femur is large and continues posteromedially on the femoral head in *Conoryctes*, whereas it is smaller in *Escavadodon* and leptictids. Moreover, the femoral lesser trochanter of *Escavadodon*, leptictids and palaeonodonts extends more posteromedially, less so than in *Conoryctes*. On the distal femur, the femoral trochlea of *Prodiacodon*, unlike *Conoryctes*, extends more proximally than the proximal end of the distal condyles. *Escavadodon* and leptictids have a sharper tibial crest than *Conoryctes*. The tibia and fibula are proximally and distally unfused in *Conoryctes*, while these are fused only distally in *Escavadodon* and *Prodiacodon*. All taeniodonts lack a dorsal foramen on the astragalar head, which is also absent in *Escavadodon*, *Palaeonodon*, and *Procerberus* and is one of the anatomical features of the “leptictimorph astragalocalcaneal morphology” (Szalay, 1977). *Conoryctes* and

leptictids have extended medial tibial and fibular facets, whereas these are less protruding in *Escavadodon* and less so in *Procerberus*. In the calcaneum, the tuber calcanei is large in *Conoryctes*, while it is much anteroposteriorly shorter in *Escavadodon* leptictids and *Procerberus*.

The new fossils provided new anatomical information about the postcranial skeleton of *Conoryctes*. Looking at the functional morphology, there are many indications that *Conoryctes* was not an animal with a generalised body plan, as previously thought for all conoryctids (Patterson, 1949b). On the contrary, *Conoryctes* was bigger in size than other conoryctids and had potentially a high level of fossoriality.

Conoryctes had a short neck compared to the rest of the vertebrae and a long and strong tail. The forelimb of *Conoryctes* also exhibits anatomical features that are seen in other digging animals. The broad and mediolaterally expanding deltopectoral crest of the humerus suggest that the deltoid and pectoral muscles were large. Moreover, the broad distal humerus with the prominent medial epicondyle and the long and medially curved olecranon of the ulna indicates strong carpal and digital flexor muscles. These features also helped in the extension of the elbow, an important feature in animals that favour digging behaviours (Hildebrand, 1985). The wrist joint was also well supported by the prominent styloid process of the radius (Lehmann, 1961). The proximodistally short radius and metacarpals also resemble fossorial animals (Chen and Wilson, 2015). The unguals apart from being curved and laterally compressed, have large flexor tubercles that increased the area that the digital flexors were attaching. Also, both the phalanges and the unguals have a “bony stop” (Hildebrand, 1985, figure 6-3) that prevented dislocation due to extreme digit flexion.

The hindlimb of *Conoryctes* shows powerful knee flexion seen in diggers (Dunn, 2018). There are also similarities in the tarsals with other derived taeniodonts, known for their digging abilities. These are the anteroposteriorly short astragalar neck and the elongated tuber calcanei, characteristic also of a high level of fossoriality (Chen and Wilson, 2015). The metatarsals of *Conoryctes* have flexor tubercles as the metacarpals, and the unguals of the pes also have enlarged flexor tubercles.

All these anatomical features indicate that *Conoryctes* was a scratch-digging animal (Hilderbrand, 1985), similar to pangolins, with powerful forearm muscles and well-stabilized digits to dig and survive in the tropical forest of the San Juan Basin, approximately 63 million years ago. This adds to the study by Williamson and Brusatte (2013) which suggests that digging adaptations are seen in all members of Taeniodonta for which the postcranial elements are known.

Combining the results of the study, conoryctids show specializations in the functional morphology of the postcranial skeleton, and do not have a primitive body plan (Gregory 1910; Matthew 1937; Patterson, 1949b; Schoch, 1986). Since all members of taeniodonts show adaptations for a digging lifestyle, it is possible that this is an ancestral trait originating from the most recent common ancestor of the group. This agrees with Shelley *et al.* (2021) study on the tarsals, which found that mammals in the Paleocene had different locomotion abilities. It is still unclear though if that diversification of locomotor modes happened gradually or rapidly after the Cretaceous-Palaeogene extinction.

Future work

The current study shows that the dental anatomy of taeniodonts is complex. The presence of more molariform premolars, higher levels of hypsodonty, and more squared-shaped teeth point to a more abrasive diet for the late Paleocene-Eocene Stylinodontidae. Similarly, some members of Conoryctidae have more cuspids on their lower molars, pre- and post-entoconulid, and there is unevenly distributed enamel around the teeth. Following the analysis of the microstructure of the enamel and dentine that Koenigswald *et al.* (2010) did on *Stylinodon*, a study on the new less worn teeth could identify the diet and type of mastication for Conoryctidae. Specimens such as NMMNH P-47450, NMMNH P-81239 (lower molars of *Onychodectes*) or NMMNH P-61799 (upper teeth of *Conoryctes*) have less worn occlusal surfaces and so they can be important for studying the microstructure of the enamel. Moreover, non-destructive analyses on the dental microwear texture and could provide insights into their diet.

Another interesting project is to expand the phylogenetic analysis of the current study. As brought to my knowledge by Dr Eberle, there is also a taeniodont, a partial skull, from either late Puercan or Torrejonian strata in the Denver Basin. It would be interesting to visit DMNS and have a look at the specimen. Moreover, more species of leptictids, palaeonodonts and cimolestids could be scored to understand the relationships of these groups with taeniodonts. Moreover, the dataset was used to find the maximum parsimony but other methods such as Bayesian techniques could be used to infer the robustness of the tree. It would also be interesting to add molecular constraints to the analysis to understand the mammalian diversification.

Lastly, a quantitatively multivariate analysis that includes many taxa, found before and after the extinction, including taeniodonts, could help understand the locomotion of Paleocene animals. This analysis could include a variety of postcranial elements. Moreover, to exclude the difference in size, studying the shape of the skeletons will be helpful. The dataset of Shelley *et al.* (2021) of the tarsals, could be used for 2D geometric morphometric analysis. This could firstly be tested to infer if 2D morphological observations are better than linear measurements to answer the locomotion questions of Paleocene mammals. Secondly, after building a large dataset of postcranial measurements and shapes of the Cretaceous and Paleocene mammals, a multivariate analysis using different postcranial elements could be performed. This large dataset might provide a better understanding of the locomotion and the ecological diversity of mammals that lived right after the late Cretaceous- Palaeogene mass extinction.

References

- Álvarez-Carretero, S., Tamuri, A.U., Battini, M., Nascimento, F.F., Carlisle, E., Asher, R.J., Yang, Z., Donoghue, P.C.J., dos Reis, M., 2022. A species-level timeline of mammal evolution integrating phylogenomic data. *Nature* 602, 263–267. <https://doi.org/10.1038/s41586-021-04341-1>
- Amaral, A., 1935. Contribuicao ao conhecimento dos ophidios do Brazil. VII. Novos generos e especies de Colubrideos opisthoglyphos. *Mem. Inst. Butantan, Sao Paulo* 9: 203-6
- Ameghino, F., 1906a. Les edentes fossiles de France et d'Allemagne. *An. Mus. Nac. Hist. Nat., Buenos Aires* 6: 175-250
- Ameghino, F., 1906b. Les formations sedimentaires du cretace superieur et du tertiare de Patagonie. *An. Mus. Nac. Hist. Nat., Buenos Aires* 8: 1-568
- Ameghino, F., 1902. Premiere contribution a la connaissance de la faune mammalogique des couches a Colpodon. *Bol. Acad. Nac. Cienc. Cordoba, Argent.* 17: 71-141
- Ameghino, F., 1897. Mammiferes cretaces de l'Argentine. Deuxieme contribution a la connaissance de la faune mammalogique des couches a Pyrotherium. *Bol. Inst. Geogr. Argent., Buenos Aires* 18: 1 — 117
- Anemone, R. L., Skinner, M. M., & Dirks, W., 2012. Are there two distinct types of hypocone in Eocene primates? The 'pseudohypocone' of notharctines revisited. *Palaeontologia electronica*, 15(15.3)
- Archibald, J. D., and Deutschman, D. H. (2001). Quantitative analysis of the timing of the origin and diversification of extant placental orders. *J. Mamm. Evol.* 8, 107–124. [doi:10.1023/A:1011317930838](https://doi.org/10.1023/A:1011317930838)
- Archibald, J.D., 1993. The Importance of Phylogenetic Analysis for the Assessment of Species Turnover: A Case History of Paleocene Mammals in North America. *Paleobiology*, 19(1), pp.1–27
- Asher, R.J., 2018. 7. Diversity and relationships within crown Mammalia, in: Zachos, F., Asher, R. (Eds.), *Mammalian Evolution, Diversity and Systematics*. De Gruyter, pp. 301–352. <https://doi.org/10.1515/9783110341553-007>
- Bapst, D. W., 2014. Assessing the effect of time-scaling methods on phylogeny-based analyses in the fossil record, TIME-SCALING AND PHYLOGENETIC COMPARATIVE METHODS. *Paleobiology*, 40(3), 331-351
- Bertrand, O.C., Shelley, S.L., Williamson, T.E., Wible, J.R., Chester, S.G.B., Flynn, J.J., Holbrook, L.T., Lyson, T.R., Meng, J., Miller, I.M., Püschel, H.P., Smith, T., Spaulding, M., Tseng, Z.J., Brusatte, S.L., 2022. Brawn before brains in placental mammals after the end-Cretaceous extinction. *Science* 376, 80–85. <https://doi.org/10.1126/science.abl5584>
- Bertrand, O. C., Püschel, H. P., Schwab, J. A., Silcox, M. T., & Brusatte, S. L., 2021. The impact of locomotion on the brain evolution of squirrels and close relatives. *Communications biology*, 4(1), 1-15

- Bininda-Emonds, O.R.P., Cardillo, M., Jones, K.E., MacPhee, R.D.E., Beck, R.M.D., Grenyer, R., Price, S.A., Vos, R.A., Gittleman, J.L. and Purvis, A., 2007. The delayed rise of present-day mammals. *Nature*, 446(7135), pp.507–512
- Bloch, J. I., Secord, R., & Gingerich, P. D., 2004. Systematics and phylogeny of late Paleocene and early Eocene Palaeoryctinae (Mammalia, Insectivora) from the Clarks Fork and Bighorn basins, Wyoming
- Butler, P. 2000. The evolution of tooth shape and toothfunction in primates, p 201-211. In Teaford M., Smith, M., and Ferguson, M., (eds.), *Development, Function and Evolution of Teeth*. Cambridge: Cambridge University Press
- Chapman, R. N., 1919. A study of the correlation of the pelvic structure and the habits of certain burrowing mammals. *Am J Anat* 25:185–219. <https://doi.org/10.1002/aja.1000250204>
- Chen, M., Wilson, G.P., 2015. A multivariate approach to infer locomotor modes in Mesozoic mammals. *Paleobiology* 41, 280–312. <https://doi.org/10.1017/pab.2014.14>
- Chow, M., 1963. A xenarthran-like mammal from the Eocene of Honan. *Sci. Sin.* 12: 1889-1893
- Clemens, W.A., Jr., and Russell, L.S., 1965. Mammalian fossils from the upper Edmonton Formation. *University of Alberta Geology Bulletin*, 2: 32–40
- Clemens, W.A., 2019. *Puercolestes* and *Betonna* (Cimolestidae, Mammalia) from the early Paleocene (Puerco 3 Interval Zone) of northeastern Montana, U.S.A. *PaleoBios* 36. <https://doi.org/10.5070/P9361042705>
- Clemens, W.A., 2017. *Procerberus* (Cimolestidae, Mammalia) from the Latest Cretaceous and Earliest Paleocene of the Northern Western Interior, USA. *PaleoBios* 34. <https://doi.org/10.5070/P9341034494>
- Clemens, W.A., 2015. *Prodiacodon crustulum* (Leptictidae, Mammalia) from the Tullock Member of the Fort Union Formation, Garfield and McCone Counties, Montana, USA. *PaleoBios* 32. <https://doi.org/10.5070/P9321025382>
- Clemens, W.A., 2013. Cf. *Wortmania* from the early Paleocene of Montana and an evaluation of the fossil record of the initial diversification of the Taeniodonta (Mammalia). *Can. J. Earth Sci.* 50, 341–354. <https://doi.org/10.1139/e2012-055>
- Constantino, P.J., Bush, M.B., Barani, A., Lawn, B.R., 2016. On the evolutionary advantage of multi-cusped teeth. *J. R. Soc. Interface* 13, 20160374. <https://doi.org/10.1098/rsif.2016.0374>
- Coombs, M.C., 1983. Large Mammalian Clawed Herbivores: A Comparative Study. *Trans. Am. Philos. Soc.* 73, 1. <https://doi.org/10.2307/3137420>
- Cope, E.D., 1894. Schlosser on American Eocene Vertebrata in Switzerland. *Am. Nat.* 28: 585-94
- Cope, E.D., 1888. Synopsis of the vertebrate fauna of the Puerco series. *Trans. Am. Philos. Soc*, n.s., 16: 298-361
- Cope, E.D., 1887. Some new Taeniodonta of the Puerco. *Am. Nat.* 21: 469
- Cope, E.D., 1885. The mammalian genus *Hemiganus*. *Am. Nat.* 19: 492-93

- Cope, E.D., 1884a. The Condylarthra. *Am. Nat.* 18: 892-906
- Cope, E.D., 1884b. The Vertebrata of the Tertiary formations of the West. *Rep. U.S. Geol. Surv. Territories* (F.V. Hayden, in charge), vol. 3, p. 1-1009
- Cope, E.D., 1882a. A new genus of Tillodonta [sic]. *Am. Nat.* 16: 156-57
- Cope, E.D., 1882b. Contributions to the history of the Vertebrata of the lower Eocene of Wyoming and New Mexico made during 1881. *Proc. Am. Philos. Soc.* 20: 139-97
- Cope, E.D., 1882c. A new form of Taenidonta. *Am. Nat.* 16: 831-32
- Cope, E.D., 1881a. Mammalia of the lowest Eocene. *Am. Nat.* 15: 829-31
- Cope, E.D., 1881b. On some Mammalia of the lowest Eocene beds of New Mexico. *Proc. Am. Phil. Soc.* 19. 484-95
- Cope, E.D., 1881c. On the Vertebrata of the Wind River Eocene beds of Wyoming. *Bull. U.S. Geol. Geogr. Surv. Territories* 6: 183-202
- Cope, E.D., 1877. The extinct Vertebrata obtained in New Mexico by parties of the Expedition of 1874. Fossils of the Eocene period. *Rep. U.S. Geogr. Surv. west of the one hundredth meridian* (G. M. Wheeler, in charge), vol. 4 (Paleontology), part 2, chap. 12, p. 37-282
- Cope, E.D., 1876. On the Taeniodonta, a new group of Eocene Mammalia. *Proc. Acad. Nat. Sci. Philadelphia* 28: 39
- Cope, E. D., 1874. Notes on the Eocene and Pliocene lacustrine formations of New Mexico, including descriptions of new species of vertebrates. *Ann. Rep. Chief Eng., Appendix FF3* (43rd Congress, 2nd Session, House Executive Doc. 1, part 2, vol. 2, part 2), p. 561-606
- Cope, E. D., 1872. Second account of new Vertebrata from the Bridger Eocene. *Proceedings of the American Philosophical Society* 12:466–468
- Cuvier, G. L., 1798. *Tableau Élémentaire de l'Histoire Naturelle des Ani-maux*. Paris: J. B. Baillièrre
- Damuth, J., Janis, C.M., 2014. A Comparison of Observed Molar Wear Rates in Extant Herbivorous Mammals. *Ann. Zool. Fenn.* 51, 188–200. <https://doi.org/10.5735/086.051.0219>
- Davis, B.M., 2011. Evolution of the Tribosphenic Molar Pattern in Early Mammals, with Comments on the “Dual-Origin” Hypothesis. *J. Mamm. Evol.* 18, 227–244. <https://doi.org/10.1007/s10914-011-9168-8>
- de Muizon, C., Billet, G., Ladevèze, S., 2019. New remains of kollpaniine “condylarths” (Panameriungulata) from the early Palaeocene of Bolivia shed light on hypocone origins and molar proportions among ungulate-like placentals. *Geodiversitas* 41, 841. <https://doi.org/10.5252/geodiversitas2019v41a25>
- de Muizon, C.D., Billet, G., Argot, C., Ladevèze, S., Goussard, F., 2015. *Alcidedorbignya inopinata*, a basal pantodont (Placentalia, Mammalia) from the early Palaeocene of Bolivia: anatomy, phylogeny and palaeobiology. *Geodiversitas* 37, 397. <https://doi.org/10.5252/g2015n4a1>
- Dorr, J. A., 1977. Partial skull of *Paleosinopa simpsoni* (Mammalia, Insectivora), latest Paleocene Hoback Formation, central western Wyoming, with some general remarks on the

- family Pantolestidae. University of Michigan Contributions from the Museum of Paleontology 24:281–307
- Dunn, R.H., Rose, K.D., 2015. Evolution of early Eocene *Palaeosinopa* (Mammalia, Pantolestidae) in the Willwood Formation of the Bighorn Basin, Wyoming. *J. Paleontol.* 89, 665–694. <https://doi.org/10.1017/jpa.2015.31>
- Dunn, R.H., Townsend, K.E.B., 2019. New pantolestids from the Uinta Formation, Utah. *J. Vertebr. Paleontol.* 39, e1652622. <https://doi.org/10.1080/02724634.2019.1652622>
- Dunn, R. H., 2018. Functional morphology of the postcranial skeleton. In *Methods in paleoecology* (pp. 23-36). Springer, Cham
- Eberle, J.J., 1999. Bridging the transition between Didelphodonts and Taeniodonts. *J. Paleontol.* 73, 936–944. <https://doi.org/10.1017/S0022336000040762>
- Estravis, C., & Russell, D., 1992. The presence of Taeniodonta (Mammalia) in the early Eocene of Europe. *Ciências da Terra/Earth Sciences Journal*, 11
- Evans, H.E., and de Lahunta, A., 2013. Miller's anatomy of the dog, Fourth edition. ed. Elsevier, St. Louis, Missouri
- Flynn, A.G., Davis, A.J., Williamson, T.E., Heizler, M., Fenley, C.W., Leslie, C.E., Secord, R., Brusatte, S.L., Peppe, D.J., 2020. Early Paleocene Magnetostratigraphy and Revised Biostratigraphy of the Ojo Alamo Sandstone and Lower Nacimiento Formation, San Juan Basin, New Mexico, USA. *GSA Bull.* 132, 2154–2174. <https://doi.org/10.1130/B35481.1>
- Flynn, A.G., Peppe, D.J., 2019. Early Paleocene tropical forest from the Ojo Alamo Sandstone, San Juan Basin, New Mexico, USA. *Paleobiology* 45, 612–635. <https://doi.org/10.1017/pab.2019.24>
- Foley, N.M., Mason, V.C., Harris, A.J., Bredemeyer, K.R., Damas, J., Lewin, H.A., Eizirik, E., Gatesy, J., Zoonomia Consortium, Springer, M.S., Murphy, W.J., 2022. A genomic timescale for placental mammal evolution (preprint). *Evolutionary Biology*. <https://doi.org/10.1101/2022.08.10.503388>
- Foley, N.M., Springer, M.S., Teeling, E.C., 2016. Mammal madness: is the mammal tree of life not yet resolved? *Philos. Trans. R. Soc. B Biol. Sci.* 371, 20150140. <https://doi.org/10.1098/rstb.2015.0140>
- Foote, M., 1997. Estimating taxonomic durations and preservation probability. *Paleobiology*, 23(3), 278-300
- Fox, R.C., 2016. The status of *Schowalteria clemensi*, the Late Cretaceous taeniodont (Mammalia). *J. Vertebr. Paleontol.* 36, e1211666. <https://doi.org/10.1080/02724634.2016.1211666>
- Fox, R.C., 2015. A revision of the Late Cretaceous–Paleocene eutherian mammal *Cimolestes* Marsh, 1889. *Can. J. Earth Sci.* 52, 1137–1149. <https://doi.org/10.1139/cjes-2015-0113>
- Fox, R.C., Naylor, B.G., 2003. A Late Cretaceous taeniodont (Eutheria, Mammalia) from Alberta, Canada. *Neues Jahrb. Für Geol. Paläontol. - Abh.* 229, 393–420. <https://doi.org/10.1127/njgpa/229/2003/393>

- Fox, R.C., Scott, C.S., Bryant, H.N., 2007. A new, unusual therian mammal from the Upper Cretaceous of Saskatchewan, Canada. *Cretac. Res.* 28, 821–829. <https://doi.org/10.1016/j.cretres.2006.12.005>
- Funston, G.F., dePolo, P.E., Sliwinski, J.T., Dumont, M., Shelley, S.L., Pichevin, L.E., Cayzer, N.J., Wible, J.R., Williamson, T.E., Rae, J.W.B., Brusatte, S.L., 2022. The origin of placental mammal life histories. *Nature* 610, 107–111. <https://doi.org/10.1038/s41586-022-05150-w>
- Gaudin, T.J., Emry, R.J., Pogue, B., 2006. A new genus and species of pangolin (Mammalia, Pholidota) from the late Eocene of Inner Mongolia, China. *J. Vertebr. Paleontol.* 26, 146–159. <https://doi.org/10.1671/0272-4634>
- Gazin, C. L., 1958. A review of the middle and upper Eocene primates of North America. *Smithsonian Miscellaneous Collections*
- Gazin, C. L., 1941. The mammalian faunas of the Paleocene of central Utah, with notes on the geology. *Proc. U.S. Nat. Mus.* 91: 1-53
- Gazin, C. L., 1939. A further contribution to the Dragon Paleocene fauna of central Utah. *J. Wash. Acad. Sci. (Washington, D.C.)* 29: 273-86
- Gazin, C. L., 1936. A taeniodont skull from the lower Eocene of Wyoming. *Proc. Am. Philos. Soc.* 76: 597-612
- Gheerbrant, E., Filippo, A., Schmitt, A., 2016. Convergence of Afrotherian and Laurasiatherian Ungulate-Like Mammals: First Morphological Evidence from the Paleocene of Morocco. *PLOS ONE* 11, e0157556. <https://doi.org/10.1371/journal.pone.0157556>
- Gheerbrant, E., Amaghzaz, M., Bouya, B., Goussard, F., Letenneur, C., 2014. Ocepeia (Middle Paleocene of Morocco): The Oldest Skull of an Afrotherian Mammal. *PLoS ONE* 9, e89739. <https://doi.org/10.1371/journal.pone.0089739>
- Gheerbrant, E., Khaldoune, F., Schmitt, A., Tabuce, R., 2020. Earliest Embriothopod Mammals (Afrotheria, Tethytheria) from the Early Eocene of Morocco: Anatomy, Systematics and Phylogenetic Significance. *J. Mamm. Evol.* 28, 245–283. <https://doi.org/10.1007/s10914-020-09509-6>
- Gingerich, P. D., 1989. New earliest Wasatchian mammalian fauna from the Eocene of northwestern Wyoming: composition and diversity in a rarely sampled high-floodplain assemblage
- Gradstein, F.M., Ogg, J.G. and Hilgen, F.J., 2012. On The Geologic Time Scale. *Newsletters on Stratigraphy*, 45(2), pp.171–188
- Gregory, W. K., 1922. The origin and evolution of the human dentition. Williams and Wilkins Co., Baltimore. pp. 548
- Gregory, W. K., 1920. Studies of comparative myology and osteology: Number 4, a review of the evolution of the lacrymal bone of vertebrates with special reference to that of mammals. *Bull. Am. Mus. Nat. Hist.* 42: 95-203
- Gregory, W. K., 1910. The orders of mammals. *Bull. Am. Mus. Nat. Hist.* 27:1–524

- Grossnickle, D.M., Newham, E., 2016. Therian mammals experience an ecomorphological radiation during the Late Cretaceous and selective extinction at the K–Pg boundary. *Proc. R. Soc. B Biol. Sci.* 283, 20160256. <https://doi.org/10.1098/rspb.2016.0256>
- Grossnickle, D.M., Smith, S.M., Wilson, G.P., 2019. Untangling the Multiple Ecological Radiations of Early Mammals. *Trends Ecol. Evol.* 34, 936–949. <https://doi.org/10.1016/j.tree.2019.05.008>
- Goloboff, P.A., Farris, J.S. and Nixon, K.C., 2008. TNT, a free program for phylogenetic analysis. *Cladistics*, 24(5), pp.774–786
- Goloboff, P.A., 1999. Analyzing large data sets in reasonable times: solutions for composite optima. *Cladistics*, 15(4), pp.415–428
- Gunnell, G.F., Bown, T.M., Bloch, J.I., 2007. Leptictida, in: Janis, C.M., Gunnell, G.F., Uhen, M.D. (Eds.), *Evolution of Tertiary Mammals of North America*. Cambridge University Press, pp. 82–88. <https://doi.org/10.1017/CBO9780511541438.007>
- Gunnell, G.F., Rose, K.D., 2008. “Edentata” summary, in: Janis, C.M., Gunnell, G.F., Uhen, M.D. (Eds.), *Evolution of Tertiary Mammals of North America*. Cambridge University Press, pp. 127–134. <https://doi.org/10.1017/CBO9780511541438.009>
- Guthrie, D. A., 1971. The mammalian fauna of the Lost Cabin Member, Wind River Formation (early Eocene) of Wyoming. *Ann. Carnegie Mus.* 43: 47-113
- Guthrie, D. A., 1967. The mammalian fauna of the Lysite Member, Wind River Formation (early Eocene) of Wyoming. *Mem. South. Calif. Acad. Sci.* 5: 1-53
- Halliday, T.J.D., dos Reis, M., Tamuri, A.U., Ferguson-Gow, H., Yang, Z., Goswami, A., 2019. Rapid morphological evolution in placental mammals post-dates the origin of the crown group. *Proc. R. Soc. B Biol. Sci.* 286, 20182418. <https://doi.org/10.1098/rspb.2018.2418>
- Halliday, T.J.D., Goswami, A., 2016. The impact of phylogenetic dating method on interpreting trait evolution: a case study of Cretaceous–Palaeogene eutherian body-size evolution. *Biol. Lett.* 12, 20160051. <https://doi.org/10.1098/rsbl.2016.0051>
- Hautier, L., Oliver, J. D., Pierce, S. E., 2018. An overview of xenarthran developmental studies with a focus on the development of the xenarthrous vertebrae. *Journal of Mammalian Evolution*, 25(4), 507-523
- Hay, O. P., 1899. On the names of certain North American fossil vertebrates. *Science* 9: 593-94
- Hildebrand, M., 1982. *Analysis of Vertebrate Structure*, 2nd edn. John Wiley and Sons, New York
- Hildebrand, M., 1985. Digging of quadrupeds. In: M HildebrandDM BrambleKL LiemDB Wake. *Functional Vertebrate Morphology*. Cambridge. Harvard: University (Belknap) Press. pp. 89-109
- Holbrook, L., 2015. The Identity and Homology of the Postprotocrista and its Role in Molarization of Upper Premolars of Perissodactyla (Mammalia). *J. Mamm. Evol.* 22, 259–269. <https://doi.org/10.1007/s10914-014-9276-3>

- Hooker, J. J., 1979. Two new “condylarths” (Mammalia) from the early Eocene of southern England. *Bull. Brit. Mus. Nat. Hist. (Geol.)*, 32 (1): pp. 43-56
- Hunter, J.P., Jernvall, J., 1995. The hypocone as a key innovation in mammalian evolution. *Proc. Natl. Acad. Sci.* 92, 10718–10722. <https://doi.org/10.1073/pnas.92.23.10718>
- Inglis, G.N., Bragg, F., Burls, N.J., Cramwinckel, M.J., Evans, D., Foster, G.L., Huber, M., Lunt, D.J., Siler, N., Steinig, S., Tierney, J.E., Wilkinson, R., Anagnostou, E., de Boer, A.M., Dunkley Jones, T., Edgar, K.M., Hollis, C.J., Hutchinson, D.K., Pancost, R.D., 2020. Global mean surface temperature and climate sensitivity of the early Eocene Climatic Optimum (EECO), Paleocene–Eocene Thermal Maximum (PETM), and latest Paleocene. *Clim. Past* 16, 1953–1968. <https://doi.org/10.5194/cp-16-1953-2020>
- Kaiser, T.M., Müller, D.W.H., Fortelius, M., Schulz, E., Codron, D., Clauss, M., 2013. Hypsodonty and tooth facet development in relation to diet and habitat in herbivorous ungulates: implications for understanding tooth wear: Hypsodonty, mesowear, tooth wear. *Mammal Rev.* 43, 34–46. <https://doi.org/10.1111/j.1365-2907.2011.00203.x>
- Kielan-Jaworowska, Z., Cifelli, R., Luo, Z.-X., 2004. Mammals from the age of dinosaurs: origins, evolution, and structure. Columbia University Press, New York
- Kielan-Jaworowska, Z., Bown, T. M., 1979. Jason A. Lillegraven. Mesozoic Mammals: The First Two-thirds of Mammalian History, 234: 221
- Ladevèze, S., Missiaen, P. and Smith, T., 2010. First skull of *Orthaspidotherium edwardsi* (Mammalia, ‘Condylarthra’) from the late Paleocene of Berru (France) and phylogenetic affinities of the enigmatic European family Pleuraspidotheriidae. *Journal of Vertebrate Paleontology*, 30(5), pp.1559–1578
- Lehmann, W. H., 1963. The forelimb architecture of some fossorial rodents. University of Illinois at Urbana-Champaign
- Lillegraven, J. A., 1969. Latest Cretaceous mammals of upper part of Edmonton Formation of Alberta, Canada, and review of marsupial-placental dichotomy in mammalian evolution. *Univ. Kans. Paleontol. Contrib., Art. 50 (Vertebrata 12)*: 1-122
- Linnaeus, C., 1758. *Systema naturæ per regna tria naturæ, secundum classes, ordines, genera, species, cum characteribus, differentiis, synonymis, locis*. Vol. 1 (10th ed.). Stockholm: Laurentius Salvius. pp. 1–824
- Liu, L., Zhang, J., Rheindt, F.E., Lei, F., Qu, Y., Wang, Y., Zhang, Y., Sullivan, C., Nie, W., Wang, J., Yang, F., Chen, J., Edwards, S.V., Meng, J., Wu, S., 2017. Genomic evidence reveals a radiation of placental mammals uninterrupted by the KPg boundary. *Proc. Natl. Acad. Sci.* 114. <https://doi.org/10.1073/pnas.1616744114>
- Lofgren, D.L., Lillegraven, J.A., Clemens, W.A., Gingerich, P.D., and Williamson, T.E., 2004. Paleocene Biochronology: The Puercan Through Clarkforkian Land Mammal Ages, in Woodburne, M.O. ed., *Late Cretaceous and Cenozoic Mammals of North America*, New York, Columbia University Press, p. 43–105
- Lucas, S.G., 2011. *Robertschochia*, a new name for the Paleocene mammal *Schochia* Lucas and Williamson, 1993. *J. Paleontol.* 85, 1216–1217. <https://doi.org/10.1666/11-006.1>
- Lucas, S.G., Williamson, T.E., 1993. A new taeniodont from the Paleocene of the San Juan Basin, New Mexico and the phylogeny of the Taeniodonta. *J Mammal* 74: 175-179. doi:10.2307/1381918

- Luo, Z.-X., 2007. Transformation and diversification in early mammal evolution. *Nature* 450, 1011–1019. <https://doi.org/10.1038/nature06277>
- Luo, Z.-X., Ji, Q., Yuan, C.-X., 2007. Convergent dental adaptations in pseudo-tribosphenic and tribosphenic mammals. *Nature* 450, 93–97. <https://doi.org/10.1038/nature06221>
- MacLeod N, Rose KD, 1993. Inferring locomotor behavior in Paleogene mammals via eigenshape analysis. *Am J Sci* 293A:300–355
- Mao, F., Zhang, C., Liu, C., & Meng, J., 2021. Fossoriality and evolutionary development in two Cretaceous mammaliamorphs. *Nature*, 592(7855), 577-582
- Markwick, P. J., 1998. Crocodylian diversity in space and time: the role of climate in paleoecology and its implication for understanding K/T extinctions. *Paleobiology*, 24(4), 470-497
- Marsh, O. C., 1897. The Stylinodontia, a suborder of Eocene edentates. *Am. J. Sci.* 3: 137-46
- Marsh, O.C., 1877. Introduction and succession of vertebrate life in America. *Am. J. Sci.* 14: 337-78
- Marsh, O.C., 1876. Recent discoveries of extinct animals. *Am. J. Sci.* 12: 59-61. 1876b
- Marsh, O.C., 1875. New order of Eocene mammals. *Am. J. Sci.* 9: 221
- Marsh, O. C. 1874. Notice of new Tertiary mammals, III. *Am. J. Sci.* 7: 531-34
- Matthew, W.D., 1937. Paleocene faunas of the San Juan Basin, New Mexico. *Transactions of the American Philosophical Society*, 30, pp.1–510
- Matthew, W.D., 1929. Preoccupied names. *Journal of Mammalogy* 10:171
- Matthew, W.D., 1918. A revision of the Lower Eocene Wasatch and Wind River faunas. Insectivora (continued), Glires, Edentata. *Bull. Am. Mus. Nat. Hist.*, 38: 565-657
- Matthew, W.D., 1913. A aalambdodont insectivore from the basal Eocene. *Bulletin of the American Museum of Natural History*, 32: 307-314
- McKenna, M.C., Bell, S.K., Simpson, G.G., 1997. *Classification of mammals above the species level*. Columbia University Press, New York
- Matthew, W. D., & Granger, W., 1918. A revision of the Lower Eocene Wasatch and Wind River faunas. *Bulletin of the AMNH*; v. 38, article 16
- McKenna, M.C., 1975. Toward a Phylogenetic Classification of the Mammalia. In: W.P. Luckett and F.S. Szalay, eds., *Phylogeny of the Primates*. Boston, Springer, pp.21–46
- McKenna, M.C., 1969. The origin and early differentiation of the therian mammals. *Ann. N.Y. Acad. Sci.* 167: 217-40
- Middleton, M.D., and Dewar, E.W., 2004. New mammals from the Early Paleocene Littleton fauna (Denver Formation, Colorado). In S.G. Lucas, K.E. Zeigler, and P.E. Kondrashov (eds.), *Paleogene Mammals*. *Bulletin, New Mexico Museum of Natural History and Science* 26:59–80

- Napoli, J.G., Williamson, T.E., Shelley, S.L., Brusatte, S.L., 2018. A Digital Endocranial Cast of the Early Paleocene (Puercan) 'Archaic' Mammal *Onychodectes tisonensis* (Eutheria: Taeniodonta). *J. Mamm. Evol.* 25, 179–195. <https://doi.org/10.1007/s10914-017-9381-1>
- Nixon, K.C., 1999. The parsimony ratchet, a new method for rapid parsimony analysis. *Cladistics*, 15, pp.407–414
- Novacek, M. J., 1992. Mammalian phylogeny: Shaking the tree. *Nature*, 356, 121–5
- Novacek, M. J., 1986. The skull of leptictid insectivorans and the higher-level classification of eutherian mammals. *Bulletin of the American Museum of Natural History*, 183, 1–112
- Novacek, M.J., 1977. A review of Paleocene and Eocene Leptictidae (Eutheria: Mammalia) from North America. *PaleoBios* 24:1–42
- Novacek, M. J. and Wyss, A., 1986. Higher-level relationships of the recent eutherian orders: morphological evidence. *Cladistics*, 2, 257–87
- O'Leary, M.A., Bloch, J.I., Flynn, J.J., Gaudin, T.J., Giallombardo, A., Giannini, N.P., Goldberg, S.L., Kraatz, B.P., Luo, Z.-X., Meng, J., Ni, X., Novacek, M.J., Perini, F.A., Randall, Z.S., Rougier, G.W., Sargis, E.J., Silcox, M.T., Simmons, N.B., Spaulding, M., Velazco, P.M., Weksler, M., Wible, J.R., Cirranello, A.L., 2013. The Placental Mammal Ancestor and the Post-K-Pg Radiation of Placentals. *Science* 339, 662–667. <https://doi.org/10.1126/science.1229237>
- O'Leary, M. A., & Kaufman, S. G., 2012. MorphoBank 3.0: Web application for morphological phylogenetics and taxonomy
- Olivier, G. A., 1789. *Entomologie, ou histoire naturelle des insectes, avec leurs caracteres generiques et specifiques*, 1(7): 1-4
- Osborn, H. D., and Earle, C., 1895. Fossil mammals of the Puerco beds, collection of 1892. *Bull. Am. Mus. Nat. Hist.* 7: 1-70
- Patterson B., 1949a. A new genus of taeniodonts from the late Paleocene. *Fieldiana, Geol.*, 10: 41-42
- Patterson B., 1949b. Rates of evolution in taeniodonts. In: GL JepsenGG SimpsonE Mayr. *Genetics, Paleontology, and Evolution*. Princeton: Princeton University Press. pp. 243-278
- Patterson, B., 1936. Mounted skeleton of *Titanoides*, with notes on the associated fauna. *Proc. Geol. Soc. Am.* 1935, p. 397-98
- Phillips, M.J., 2016. Geomolecular Dating and the Origin of Placental Mammals. *Syst. Biol.* 65, 546–557. <https://doi.org/10.1093/sysbio/syv115>
- Reynolds, T.E., 1936. Two New Insectivores from the Lower Paleocene of New Mexico. *Journal of Paleontology* 10:202–209
- Rigby, J. K., Jr., 1980. Swain Quarry of the Fort Union Formation, middle Paleocene (Torrejonian), Carbon County, Wyoming: geological setting and mammalian fauna. *Evol. Monogr.* 3: 1- 179
- Robinson, P., 1966. Fossil Mammalia of the Huerfano Formation, Eocene, of Colorado. *Peabody Mus. Nat. Hist. Yale Univ. Bull.* 21: 1-95

- Robison, S., and Lucas, S. G., 1980. The early Paleocene Wagonroad local fauna, North Horn Formation, Utah: a case for early Paleocene provinciality in the western interior. *Geol. Soc. Am. Abstr. Progr.* 12: 302
- Rook, D.L., Hunter, J.P., 2013. Rooting Around the Eutherian Family Tree: the Origin and Relations of the Taeniodonta. *J. Mamm. Evol.* 21, 75–91. <https://doi.org/10.1007/s10914-013-9230-9>
- Rook, D.L., Hunter, J.P., 2011. Phylogeny of the Taeniodonta: evidence from dental characters and stratigraphy. *J. Vertebr. Paleontol.* 31, 422–427. <https://doi.org/10.1080/02724634.2011.550364>
- Rook, D.L., Hunter, J.P., 2013b. Erratum to: Rooting Around the Eutherian Family Tree: the Origin and Relations of the Taeniodonta. *J. Mamm. Evol.* 21, 93–93. <https://doi.org/10.1007/s10914-013-9241-6>
- Rook, D.L., Hunter, J.P., Pearson, D.A., Bercovici, A., 2010. Lower jaw of the Early Paleocene mammal *Alveugena* and its interpretation as a transitional fossil. *J. Paleontol.* 84, 1217–1225. <https://doi.org/10.1666/10-054.1>
- Rose, K.D., 2008. *Evolution of Tertiary Mammals of North America*, 1st ed. Cambridge University Press. <https://doi.org/10.1017/CBO9780511541438>
- Rose, K.D., 2006. *The beginning of the age of mammals*. Johns Hopkins university press, Baltimore (Md.)
- Rose, K.D., 2006b. The postcranial skeleton of early Oligocene Leptictis Mammalia: Leptictida), with a preliminary comparison to Leptictidium from the middle Eocene of Messel. In *Palaeontographica, Abteilung A: Palaozoologie-Stratigraphie* (pp. 37-56). E. Schweizerbart'sche Verlagsbuchhandlung
- Rose, K. D., 1999. Postcranial skeleton of Eocene Leptictidae (Mammalia), and its implications for behavior and relationships. *Journal of Vertebrate Paleontology*, 19(2), 355-372
- Rose, K. D., 1981. The Glarkforkian land-mammal age and mammalian faunal composition across the Paleocene-Eocene boundary. *Univ. Mich. Pap. Paleontol.* 26, pp. 197
- Rose, K. D., Chew, A. E., Dunn, R. H., Kraus, M. J., Fricke, H. C., & Zack, S. P., 2012. Earliest Eocene mammalian fauna from the Paleocene-Eocene thermal maximum at sand creek divide, southern Bighorn Basin, Wyoming
- Rose, K.D., Eberle, J.J., McKenna, M.C., 2004. *Arcticanodon dawsonae*, a primitive new palaeoanodont from the lower Eocene of Ellesmere Island, Canadian High Arctic. *Can. J. Earth Sci.* 41, 757–763. <https://doi.org/10.1139/e04-019>
- Rose, K.D., Lucas, S.G., 2000. An early Paleocene palaeoanodont (Mammalia, ?Pholidota) from New Mexico, and the origin of Palaeoanodonta. *J. Vertebr. Paleontol.* 20, 139–156. [https://doi.org/10.1671/0272-4634\(2000\)](https://doi.org/10.1671/0272-4634(2000))
- Rougier, G.W., Wible, J.R., Novacek, M.J., 1998. Implications of Deltatheridium specimens for early marsupial history. *Nature* 396, 459–463. <https://doi.org/10.1038/24856>
- Ruf, I., Volpato, V., Rose, K.D., Billet, G., de Muizon, C., Lehmann, T., 2016. Digital reconstruction of the inner ear of *Leptictidium auderiense* (Leptictida, Mammalia) and North

- American leptictids reveals new insight into leptictidan locomotor agility. *Paläontol. Z.* 90, 153–171. <https://doi.org/10.1007/s12542-015-0276-2>
- Salton, J. A. & Sargis, E. J., 2008. in *Mammalian Evolutionary Morphology: A Tribute to Frederick S. Szalay* (eds Sargis, E. J. & Dagosto, M.) 51–71
- Sargis, E.J., Dagosto, M. (Eds.), 2008. *Mammalian evolutionary morphology: a tribute to Frederick S. Szalay*, Vertebrate paleobiology and paleoanthropology series. Springer, Dordrecht, The Netherlands
- Schankler, D. M., 1980. Faunal zonation of the Willwood Formation, Wyoming: preliminary results, p. 99-110. In P. D. Gingerich [ed.]. *Early Cenozoic paleontology and stratigraphy of the Bighorn Basin, Wyoming*. Univ. Mich. Pap. Paleontol. , 24
- Schmidt-Kittler, N. & Vianey-Liaud, M., 1987: Morphometric analysis and evolution of the dental pattern of the genus *Issiodoromys* (Theridomyidae, Rodentia) of the European Oligocene: a key to its evolution. – *Proc. Koninklijke Nederl. Akad. van Wetenschappen, ser. B, Palaeontol., Geol., Phys., Chem., Anthropol.* 90: 281–306
- Schneider, C. A., Rasband, W. S., & Eliceiri, K. W., 2012. NIH Image to ImageJ: 25 years of image analysis. *Nature methods*, 9(7), 671-675
- Schoch, R.M., 1986. Systematics, functional morphology, and macroevolution of the extinct mammalian order Taeniodonta. *Yale Univ Peabody Museums Nat Hist Bulletins* 42: 1-307
- Schoch, R.M., 1985. Preliminary description of a new Late Paleocene land-mammal fauna from South Carolina, U.S.A. *Postilla (Peabody Mus. Nat. Hist., Yale Univ.)* 196, pp. 13
- Schoch, R. M., 1981a. Revision of the middle Paleocene (Torrejonian) taeniodont (Mammalia) *Psittacotherium* Cope, 1882, p. 177-85. In S. G. Lucas, J. K. Rigby, Jr., and B. S. Kues [eds.]. *Advances in San Juan Basin paleontology*. Univ. N.M. Press, Albuquerque
- Schoch, R. M., 1981b. Taxonomy and biostratigraphy of the early Tertiary Taeniodonta (Mammalia: Eutheria): summary. *Geol. Soc. Am. Bull.* 92: part 1, p. 933-41; part 2, p. 1982-2267
- Schoch, R. M., and Lucas, S. G., 1981a. The biostratigraphic and geographic distribution of the mammalian order Taeniodonta. *Geol. Soc. Am. Abstr. Progr.* 13: 225
- Schoch, R. M., and Lucas, S. G., 1981b. New conoryctines (Mammalia; Taeniodonta) from the middle Paleocene (Torrejonian) of western North America. *J. Mammal.* 62: 683-91
- Schoch, R. M., and Lucas, S. G., 1981c. A new species of *Conoryctella* (Mammalia: Taeniodonta) from the Paleocene of the San Juan Basin, New Mexico, and a revision of the genus. *Postilla (Peabody Mus. Nat. Hist. Yale Univ.)*, 185, pp. 23
- Schoch, R. M., and Lucas, S. G., 1981d. The systematics of *Stylinodon*, a middle to late Eocene taeniodont (Mammalia) from western North America. *J. Vertebr. Paleontol.* 1: 175-83
- Schultz, J. A., Engels, S., Schwermann, L. C., & v Koenigswald, W., 2020. Evolutionary trends in the mastication patterns in some perissodactyls, cetartiodactyls, and proboscideans. In: *Mammalian Teeth – Form and Function*, T. Martin & W. v. Koenigswald, München (Pfeil), ISBN 978-3-89937-266-3, pp. 215-230
- Scott, W. B., 1905. *Mammalia of the Santa Cruz beds*. Princeton Univ. Exped. Patagonia. pp 499

- Shelley, S.L., Brusatte, S.L., Williamson, T.E., 2021. Quantitative assessment of tarsal morphology illuminates locomotor behaviour in Palaeocene mammals following the end-Cretaceous mass extinction. *Proc. R. Soc. B Biol. Sci.* 288, 20210393. <https://doi.org/10.1098/rspb.2021.0393>
- Shelley, S.L., Williamson, T.E., Brusatte, S.L., 2018. The osteology of *Periptychus carinidens*: A robust, ungulate-like placental mammal (Mammalia: Periptychidae) from the Paleocene of North America. *PLOS ONE* 13, e0200132. <https://doi.org/10.1371/journal.pone.0200132>
- Shelley, S. L., 2018. Rise of placental mammals: the anatomy, palaeobiology and phylogeny of *Periptychus* and the Periptychidae. Doctoral Thesis, University of Edinburgh, <http://hdl.handle.net/1842/29539>
- Shimer, H., 1903. Adaptations to aquatic, arboreal, fossorial and cursorial habits in mammals. III. Fossorial adaptations. *Am. Nat.* 37, 819–825
- Simons, E. L., 1960. The Paleocene Pantodonta. *Transactions of the American Philosophical Society*, 50(6), 3-99
- Simpson, G. G., 1959. Fossil mammals from the type area of the Puerco and Nacimiento strata, Paleocene of New Mexico. *Am. Mus. Novitates* 1957, pp. 22
- Simpson, G. G., 1945. The principles of classification and a classification of mammals. *Bull. Am. Mus. Nat. Hist.* 85: 1-350
- Simpson, G. G., 1937. The Fort Union of the Crazy Mountain Field, Montana and its mammalian faunas. *U.S. Nat. Mus. Bull.* 169: 1-287
- Simpson, G. G., 1931. *Metacheiromys* and the Edentata. *Bull. Am. Mus. Nat. Hist.* 59: 259-381
- Simpson, G. G., 1929a. A collection of Paleocene mammals from Bear Creek, Montana. *Ann. Carnegie Mus.* 19: 115-22
- Simpson, G. G., 1929b. Third contribution to the Fort Union fauna at Bear Creek, Montana. *Am. Mus. Novitates* 345, pp. 12
- Sloan, R.E., and Van Valen, L., 1965. Cretaceous mammals from Montana. *Science* 148:220–227
- Springer, M.S., Foley, N.M., Brady, P.L., Gatesy, J., Murphy, W.J., 2019. Evolutionary Models for the Diversification of Placental Mammals Across the KPg Boundary. *Front. Genet.* 10, 1241. <https://doi.org/10.3389/fgene.2019.01241>
- Springer, M. S., Murphy, W. J., Eizirik, E., and O'Brien, S. J., 2003. Placental mammal diversification and the Cretaceous-Tertiary boundary. *Proc. Natl. Acad. Sci. U.S.A.* 100, 1056–1061. doi: 10.1073/pnas.0334222100
- Szalay, F. S., Decker, R. L., 1974. Origins, evolution, and function of the tarsus in Late Cretaceous Eutheria and Paleocene primates. *Primate locomotion*, 1, 223-259
- Szalay, F.S., 1977. Phylogenetic relationships and a classification of the eutherian Mammalia. In: Major patterns in vertebrate evolution. Springer, pp.315–374
- Szalay, F. S., 1969. Mixodectidae, Microsypodidae, and the insectivore-primate transition. *Bulletin of the AMNH*; v. 140, article 4

- Tague, R. G., 2020. Commonality in pelvic anatomy among three fossorial, scratch-digging, mammalian species. *Journal of Mammalian Evolution*, 27(2), 315-327
- Taylor, L. H., 1981. The Kutz Canyon local fauna, Torrejonian (middle Paleocene) of the San Juan Basin, New Mexico, p. 242-63. In S. G. Lucas, J. K. Rigby, Jr., and B. S. Kues [eds.]. *Advances in San Juan Basin paleontology*. Univ. N.M. Press, Albuquerque
- Thesleff, I., Jernvall, J., 1997. The enamel knot: a putative signaling center regulating tooth development, in: *Cold Spring Harbor Symposia on Quantitative Biology*. Cold Spring Harbor Laboratory Press, pp. 257–267
- Thewissen J.G.M., Badoux D.M., 1986. The descriptive and functional myology of the fore-limb of the aardvark (*Orycteropus afer*, Pallas 1766). *Anat Anz* 162: 109-123. PubMed: 3789409
- Tidwell, W.D., Ash, S.R., and Parker, L.R., 1981. Cretaceous and Tertiary floras of the San Juan Basin, in Lucas, S.G., Rigby, J.K., and Kues, B.S. eds., *Advances in San Juan Paleontology*, Albuquerque, New Mexico, University of New Mexico Press, p. 307–332
- Tobien, H., 1963: Zur Gebiß-Entwicklung tertiärer Lagomorphen (Mamm.) Europas. – *Notizbl. hess. L.-Amt Bodenforsch.* 91: 16–35
- Turnbull, W.D., 2004. Taeniodonta of the Washakie Formation, Southwestern Wyoming. *Bull. Carnegie Mus. Nat. Hist.* 36, 303–333. [https://doi.org/10.2992/0145-9058\(2004\)36:303:1-0](https://doi.org/10.2992/0145-9058(2004)36:303:1-0)
- Upham, N.S., Esselstyn, J.A., Jetz, W., 2021. Molecules and fossils tell distinct yet complementary stories of mammal diversification. *Curr. Biol.* 31, 4195-4206.e3. <https://doi.org/10.1016/j.cub.2021.07.012>
- van Valen, L.M., 1994 Serial homology: the crests and cusps of mammalian teeth. *Acta Palaeontologica Polonica*, 38.3-4: 145-158
- van Valen, L.M., 1978. The beginning of the age of mammals. *Evol. Theory* 4: 45-80
- von Koenigswald, W., 2018. Specialized wear facets and late ontogeny in mammalian dentitions. *Hist. Biol.* 30, 7–29. <https://doi.org/10.1080/08912963.2016.1256399>
- von Koenigswald, W., 2011. Diversity of hypsodont teeth in mammalian dentitions—construction and classification. *Palaeontographica Abteilung A*, 294.1–3: 63-94
- von Koenigswald, W., Kalthoff, D.C., Semprebon, G.M., 2010. The microstructure of enamel, dentine and cementum in advanced Taeniodonta (Mammalia) with comments on their dietary adaptations. *J. Vertebr. Paleontol.* 30, 1797–1804. <https://doi.org/10.1080/02724634.2010.521931>
- Wang, B., 2001: On Tsaganomyidae (Rodentia, Mammalia) of Asia. – *Amer. Mus. Nov.* 3317: 1–50
- White, T. E., 1959. The endocrine glands and evolution, no. 3: os cementum, hypsodonty, and diet.
- White, T. E., 1952. Preliminary analysis of the vertebrate fossil fauna of the Boysen Reservoir area. *Proc. U.S. Nat. Mus.* 102: 185-207
- Wible, J.R., Rougier, G.W., Novacek, M.J., Asher, R.J., 2009. The Eutherian Mammal *Maelestes gobiensis* from the Late Cretaceous of Mongolia and the phylogeny of cretaceous eutheria. *Bull. Am. Mus. Nat. Hist.* 2009, 1. <https://doi.org/10.1206/623.1>

- Wible, J.R., Rougier, G.W., Novacek, M.J., Asher, R.J., 2007. Cretaceous eutherians and Laurasian origin for placental mammals near the K/T boundary. *Nature* 447, 1003–1006. <https://doi.org/10.1038/nature05854>
- Winge, H., 1923. *Pattedyr-Slaegter, I. Monotremata, Marsupialia, Insectivora, Chiroptera, Edentata*. Copenhagen. pp. 360
- Winge, H., 1917. Udsigt over Insektaedernes indbyrdes Slaeggtskab. *Vidensk. Medd. Dan. Naturhist. Foren. Kbhbenhavn* 68: pp. 82-203
- Winge, H., 1915. Jordfunde og nulevende Gumlere (Edentata) fra Lagoa Santa, Minas Gerais, Brasilien. *E Mus. Lundii* 3: pp. 1-321
- Williams, S.H., Kay, R.F., 2001. A comparative test of adaptive explanations for hypsodonty in ungulates and rodents. *J. Mamm. Evol.* 8, 207–229. <https://doi.org/10.1023/A:1012231829141>
- Williamson, T.E., Brusatte, S.L., Wilson, G.P., 2014. The origin and early evolution of metatherian mammals: the Cretaceous record. *ZooKeys* 465, 1–76. <https://doi.org/10.3897/zookeys.465.8178>
- Williamson, T.E., Weil, A., Standhardt, B., 2011. Cimolestids (Mammalia) from the early Paleocene (Puercan) of New Mexico. *J. Vertebr. Paleontol.* 31, 162–180. <https://doi.org/10.1080/02724634.2011.539649>
- Williamson, T.E., Brusatte, S.L., 2013. New Specimens of the Rare Taeniodont *Wortmania* (Mammalia: Eutheria) from the San Juan Basin of New Mexico and Comments on the Phylogeny and Functional Morphology of “Archaic” Mammals. *PLoS ONE* 8, e75886. <https://doi.org/10.1371/journal.pone.0075886>
- Williamson, T.E., and Lucas, S.G., 1992. Stratigraphy and mammalian biostratigraphy of the Paleocene Nacimiento Formation, southern San Juan Basin, New Mexico: *New Mexico Geological Society Guidebook*, v. 43, p. 265–296
- Williamson, T.E., 1996. The beginning of the age of mammals in the San Juan Basin, New Mexico; biostratigraphy and evolution of Paleocene mammals of the Nacimiento Formation. *New Mex Museums Nat Hist Science Bulletins* 8: 1-141
- Wilson, J. A., 1967. Early Tertiary mammals, p. 157-69. In R. A. Maxwell, J. T. Lonsdale, R. T. Hazzard, and J. A. Wilson [eds.]. *Geology of Big Bend National Park, Brewster County, Texas*. Univ. Tex. Bur. Econ. Geol. Publ. 6711
- Wilson, J.A., 1956. A new multituberculate from the Paleocene Torrejon fauna of New Mexico. *Trans. Kans. Acad. Sci.* 59: 76-84
- Wortman, J.L., 1897. The Ganodontia and their relationship to the Edentata. *Bull Am Museum Nat Hist* 9: 59-110
- Wortman, J.L., 1896a. *Psittachotherium*, a member of a new and primitive suborder of Edentata. *Bull. Am. Mus. Nat. Hist.* 8: 259-62
- Wortman, J.L., 1896b. The North American origin of the edentates. *Science* 4: 865-66

Appendix

Appendix to Chapter 2

Table A1. A list of the new specimens studied from San Juan Basin, the taxa they are assigned to, the localities they were found and their proposed age.

Specimen number	Elements	Locality	Biozone
<i>Onychodectes tisonensis</i>			
NMMNH P-47450	lower molars	Taeniolabis zone De-na-zin Wash	Pc2
NMMNH P-63948	partial jaw with lower premolars and molars	Taeniolabis zone De-na-zin Wash	Pc2
NMMNH P-46299	partial jaw with lower premolars and molars	Taeniolabis zone De-na-zin Wash	Pc2
NMMNH P-81239	partial jaw with lower premolars and molars	Taeniolabis zone De-na-zin Wash	Pc2
<i>Conoryctella pattersoni</i>			
NMMNH P-53990	upper molar	Nacimiento Formation	Tj3
NMMNH P-21380	lower molar	Kutz Canyon	(Tj3 or Tj2?)
NMMNH P-53835	lower molar	Kutz Canyon	Tj3
<i>Conoryctes comma</i>			

NMMNH P-16200	upper premolars and molars, lower premolars, cranial elements	Torreón Wash of Nacimiento Formation	Tj6
NMMNH P-47943	upper last premolar	Angel Peak, Kutz Canyon	Tj4
NMMNH P-61799	upper premolars and molars, cranial elements	West Flank, Torreón Wash	Tj4
NMMNH P-54419	upper and lower canines, lower premolars and molars and incisor	West Flank, Torreón Wash	Tj6
NMMNH P-54106	partial jaw with lower premolars and molars	East Flank, Torreón Wash	Tj6
NMMNH P-19976	partial jaw with lower premolars and molars	West Flank, Torreón Wash	Tj6
NMMNH P-47921	lower molar	Angel Peak, Kutz Canyon	Tj4
NMMNH P-48434	lower molar	Angel Peak, Kutz Canyon	Tj4
NMMNH P-16182	lower premolar and lower molar	Angel Peak, Kutz Canyon	Tj4
NMMNH P-19381	lower molar	Angel Peak, Kutz Canyon	Tj4

NMMNH P-41519	deciduous lower premolar and molars	East Flank, Torreon Wash	Tj6
NMMNH P-02705	deciduous lower premolar	Head of Kimbeto and Blanco Washes	Tj4
NMMNH P-77882	lower premolar	Nacimiento Formation	Tj6
NMMNH P-51827	lower premolar p5	Nacimiento Formation	Tj6
NMMNH P-51828	lower premolar p5	Nacimiento Formation	Tj6
Conoryctidae			
NMMNH P-25014	partial jaw with lower premolars and molars	Kutz Canyon	Tj2
<i>Psittacotherium multifragum</i>			
NMMNH P-30630	upper molars	Kutz Canyon indet.	Tj5 or Tj6
NMMNH P-19381	lower molar	Angel Peak, Kutz Canyon	Tj4
NMMNH P-30628	upper incisor	Kutz Canyon	Tj6
NMMNH P-47826	lower incisors and canines	Kutz Canyon	Tj5
NMMNH P-44908	partial jaw and lower teeth	AMNH locality 14 ("cliffs at the head of Escavada Wash")	TJ5
NMMNH P-19800	lower molar	Kutz Canyon indet	
NMMNH P-57845	lower canines, incisor, premolars and molars	East Branch, Torreon Arroyo	Tj4

NMMNH P-16230	partial jaw with lower molars	Kutz Canyon	Tj3
---------------	----------------------------------	-------------	-----

Table A2. Measurements of the new specimens from San Juan Basin, upper dentition.
L: mesiodistal length, W: buccal-lingual width.

Specimen	P1	P2	P4	P5	M1	M2	M3
(in mm)	L	L	L	L	L	L	L
	W	W	W	W	W	W	W
NMMNH P-53990						7.5 9.4	
NMMNH P-16200 (left)					8.8 12.2*	7.5 11.8	
NMMNH P-16200 (right)			7.4 7.5	7.9 11.9	8.9 12.7	7.4 11.6	
NMMNH P-47943				8.1 11.2			
NMMNH P-61799 (left)		3.9 3.5		7.5 11.5	7.8 10.4	7 9.6	
NMMNH P-61799 (right)			7.3 7.4	7.6 11.6	7.8 10.6	7.1 9.6	5.6 8.2

NMMNH P-30630 (left)						10.4	14.7	
NMMNH P-30630 (right)						10.3	14.1*	

Table A3. Measurements of the new specimens from San Juan Basin, lower premolars. L: mesiodistal length, W: buccal lingual width, MW: mesial(trigonid) buccal lingual width, DW: distal (talonid) buccal lingual width.

Specimen (in mm)	p1 L	W	p2 L	W	p4 L	W	p5 L	MW DW
NMMNH P-63948	2.2	2			5.1	3.7		
NMMNH P-46299					5.4	3.7	6.1	4.7
NMMNH P-19976							9.9	8.1 8
NMMNH P-54106 (left)							9.6*	7.9* 7*
NMMNH P-16182								7.3
NMMNH P-41519							12*	7.7*

NMMNH P-02705							9.7*	5.4*
NMMNH P-77882							10.8	6.9
NMMNH P-51827							10.9	8.1 7.1
NMMNH P-54419			5.2	4.1			9.4	6.9
NMMNH P-16200							10.9	7.7 6.9
NMMNH P-25014							7.7	6.1 5.3

Table A4. Measurements of the new specimens from San Juan Basin, lower premolars. L: mesiodistal length, MW: mesial(trigonid) buccal lingual width, DW: distal (taloid) buccal lingual width.

Specimen (in mm)	m1			m2			m3		
	L	MW	DW	L	MW	DW	L	MW	DW
NMMNH P-47450	6.8	4.4	4.2	6.3	4.7	4.6			
NMMNH P-63948				6.6	5.4	5.3			
NMMNH P-46299		5.6			5.7	5.5			
NMMNH P-81239	6.8	5.1	4.9	6.1	5.3	5.0			

NMMNH P-53835			7.3	5.1 4.8		
NMMNH P-21380					7.3	3.8 4.2
NMMNH P-19976		8.8 8.3	9.5	7.9 7.6	8.4	6.2 5.7
NMMNH P-54106 (left)	10.9	8.8* 8.2*	9.5*	8* 7.4*	8.2*	6.3* 5.5*
NMMNH P-54106 (right)	10.6*	8.7* 8.2*	8.9*	8* 7.5*	8.1*	6.1* 5.5*
NMMNH P-48434	9.1	7.4 7.1				
NMMNH P-25014	9	6.6 6.4	8	6.3 6.1	6.6	5.2 4.9
NMMNH P-19381	9.8	7.3 6.8				
NMMNH P-16182	9.8	8.5 8.1				
NMMNH P-41519	11.3	9.2 10.1				
NMMNH P-54419	9.7	7.8 8.5	9.0	7.7 7.8		
NMMNH P-16230					10.6	10.9 8.2

NMMNH P-19383	13.7	14.2 9.4	13	13.9 11.5	12.3	11.4 8.9
NMMNH P-19800					10.2	9.6 8.2
NMMNH P-57845			10.5	11.2 10.3		

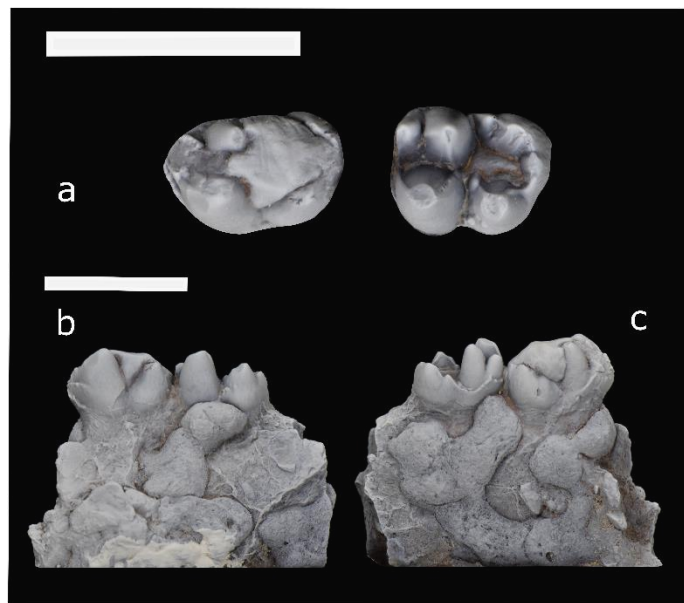


Figure A1: Specimen NMMNH P-47450, m1 and m2, in occlusal (a), buccal (b) and lingual (c) views. Scale bar is 1cm.

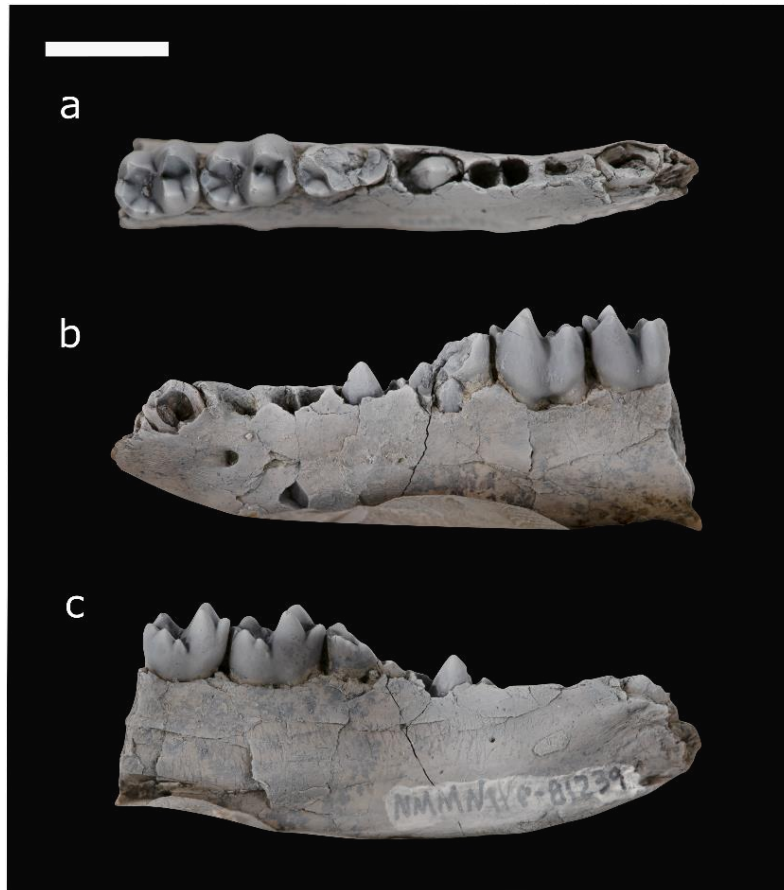


Figure A2: Specimen NMMNH P-81239 in occlusal (a), buccal (b) and lingual (c) views, with dp5, m1 and m2. Photos were taken by Thomas Williamson, edited by me. Scale bar is 1cm.

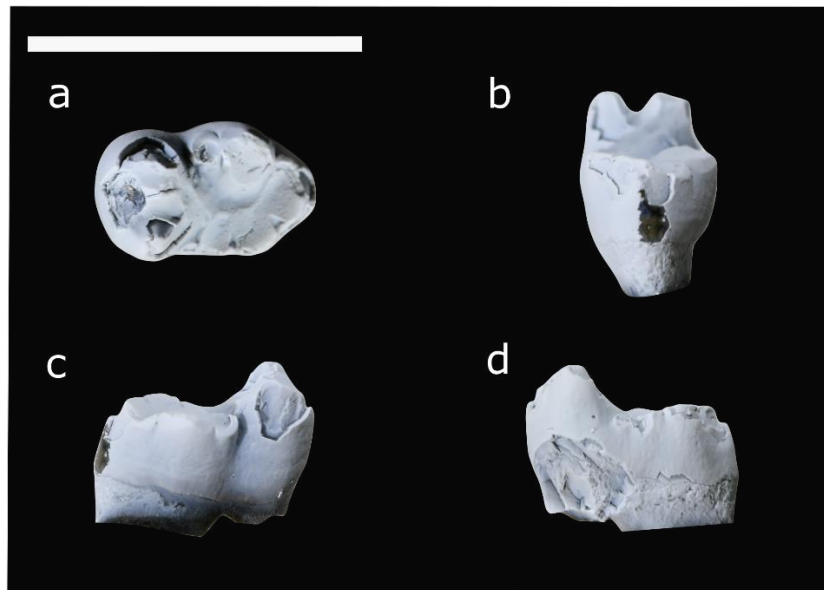


Figure A3: Specimen NMMNH P-21380, m3, in occlusal (a), distal (b), buccal (c) and lingual (d) views. Photos were taken by Thomas Williamson, edited by me. Scale bar is 1 cm.

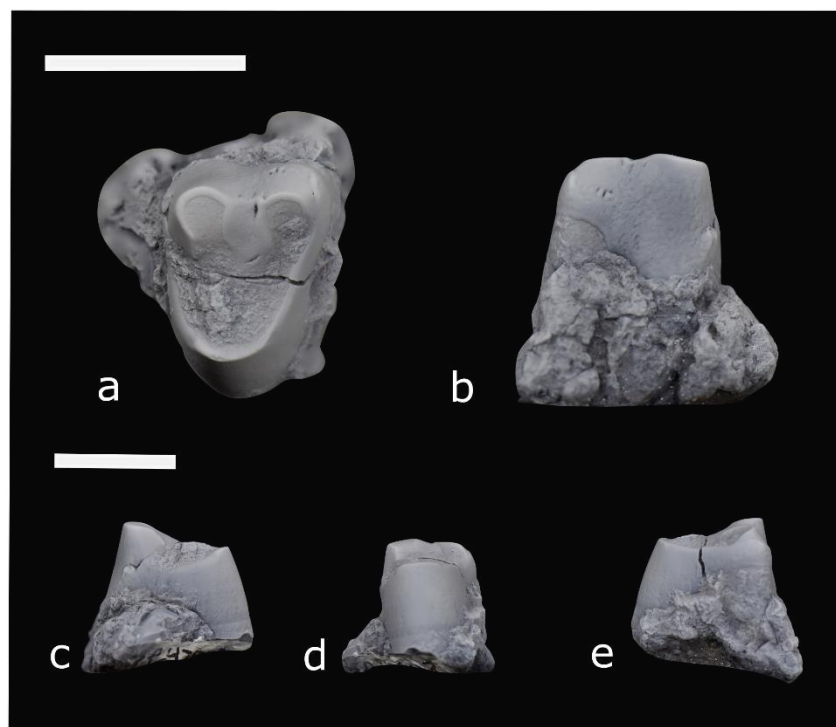


Figure A4: Specimen NMMNH P-47943 in occlusal (a), buccal (b), mesial (c), lingual (d), and distal (e) views. Scale bar is 1cm.

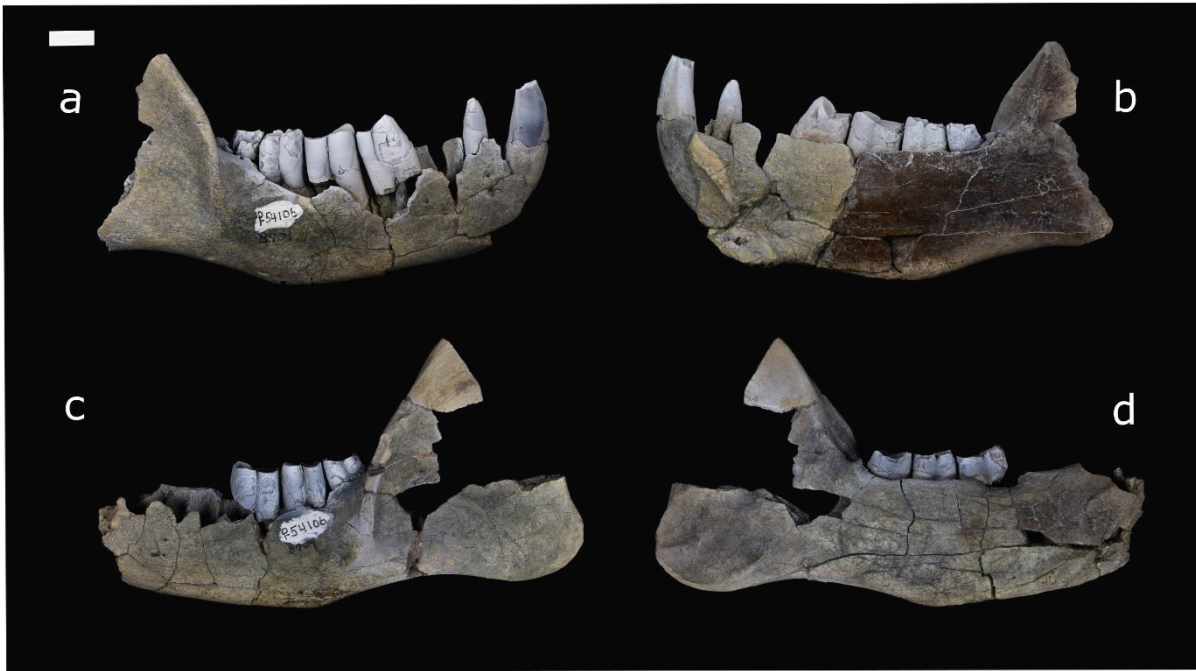


Figure A5: Specimen NMMNH P-54106 of the right (a, b) and left mandible (c, d) in buccal and lingual views. Scale bar is 1cm.



Figure A6: Articulated mandibles of specimen NMMNH P-54106 in occlusal view of *Conoryctes comma*. Scalebar is 1cm.

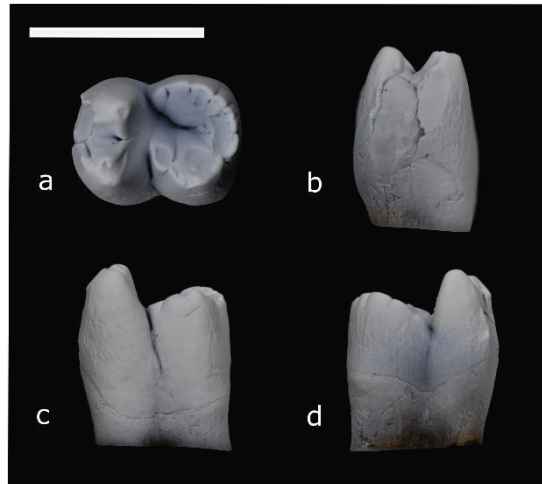


Figure A7: Specimen NMMNH P-48434 in occlusal (a), mesial (b), buccal (c) and lingual (d) views. Scale bar is 1cm.



Figure A8: Specimen NMMNH P-54419 with different views (anterior, medial, posterior, lingual) of the incisor (a), upper canine (b) and lower canine (c). Scale bar is 1 cm.

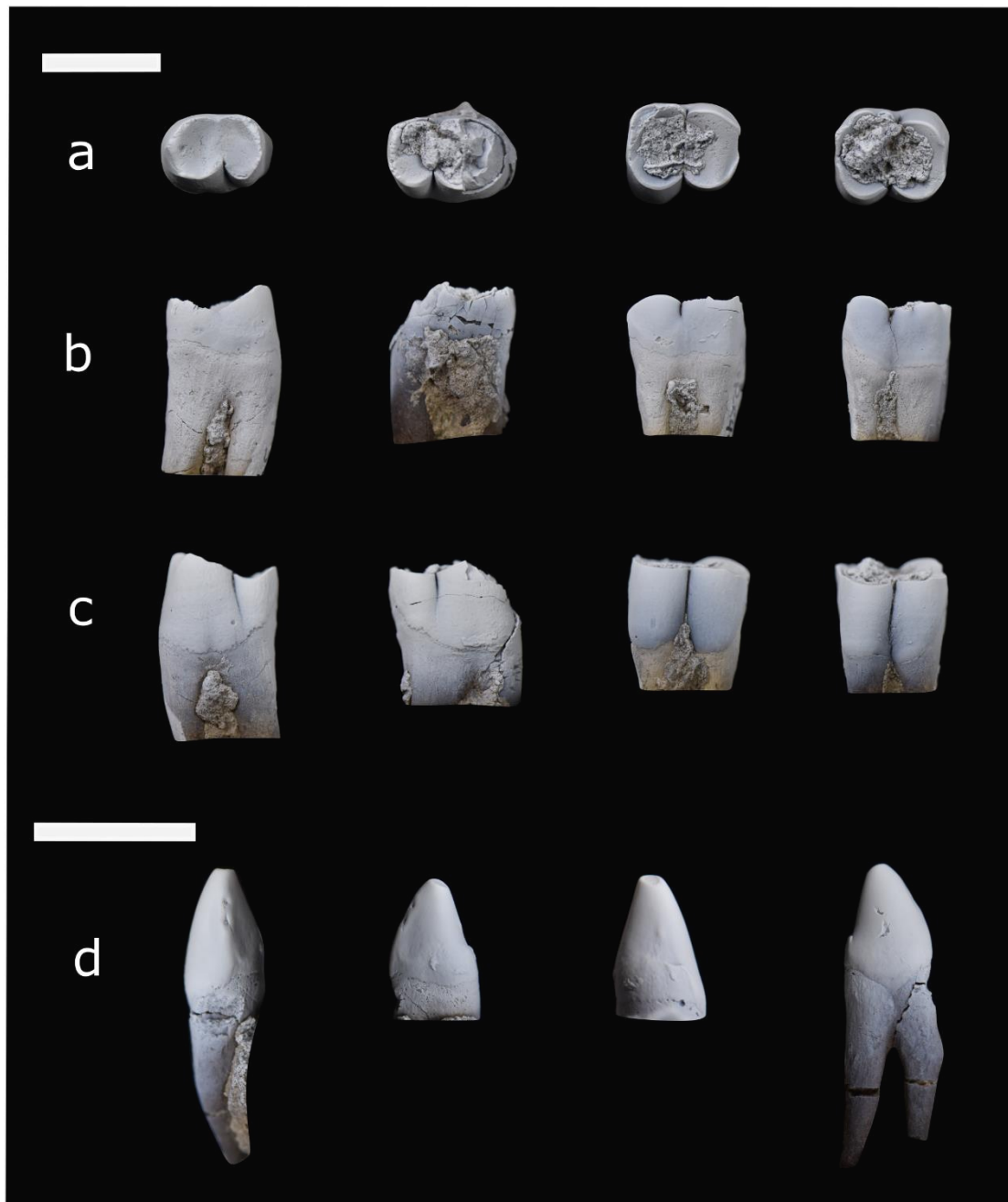


Figure A9: Specimen NMMNH P-54419 with the premolars (two teeth on the left) and the molars (two teeth on the right) in different views occlusal (a), lingual (b), buccal (c). The same views of the premolar (d). Scale bar is 1 cm.

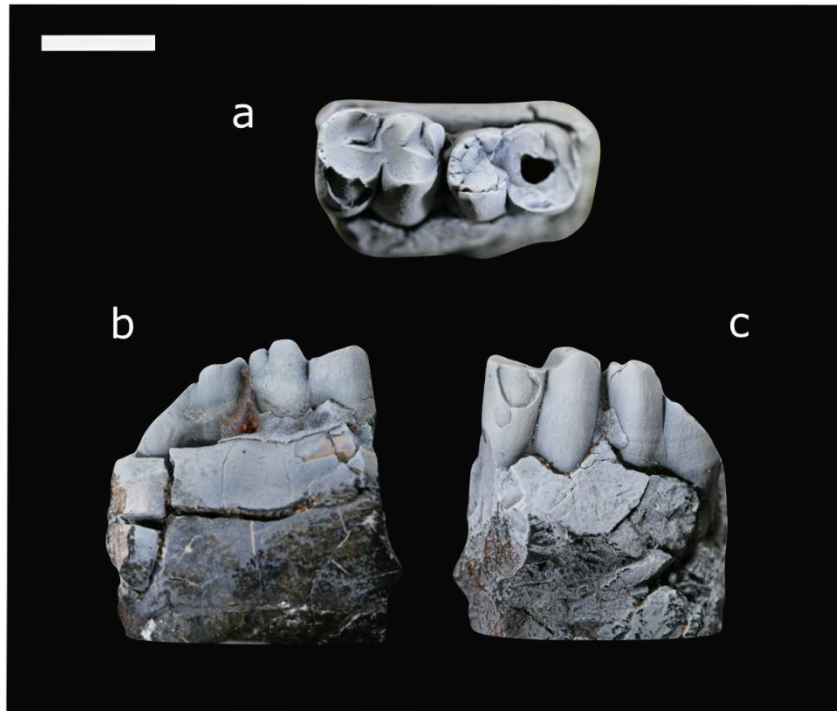


Figure A10: Specimen NMMNH P-16182 in occlusal (a), lingual (b) and buccal (c) views. Photos were taken by Thomas Williamson, edited by me. Scale bar 1 cm.

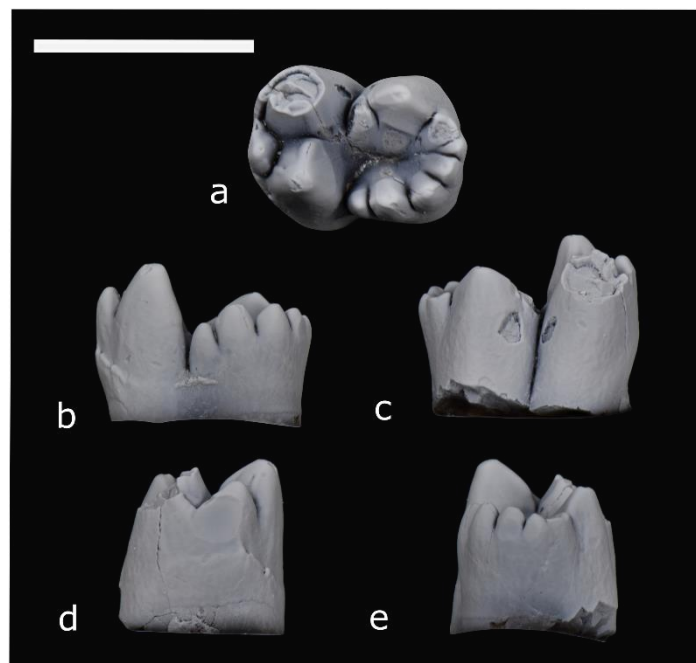


Figure A11: Specimen NMMNH P- 19381 in occlusal (a), lingual (b), buccal (c), mesial (d) and distal (e) views. Scale bar is 1cm.

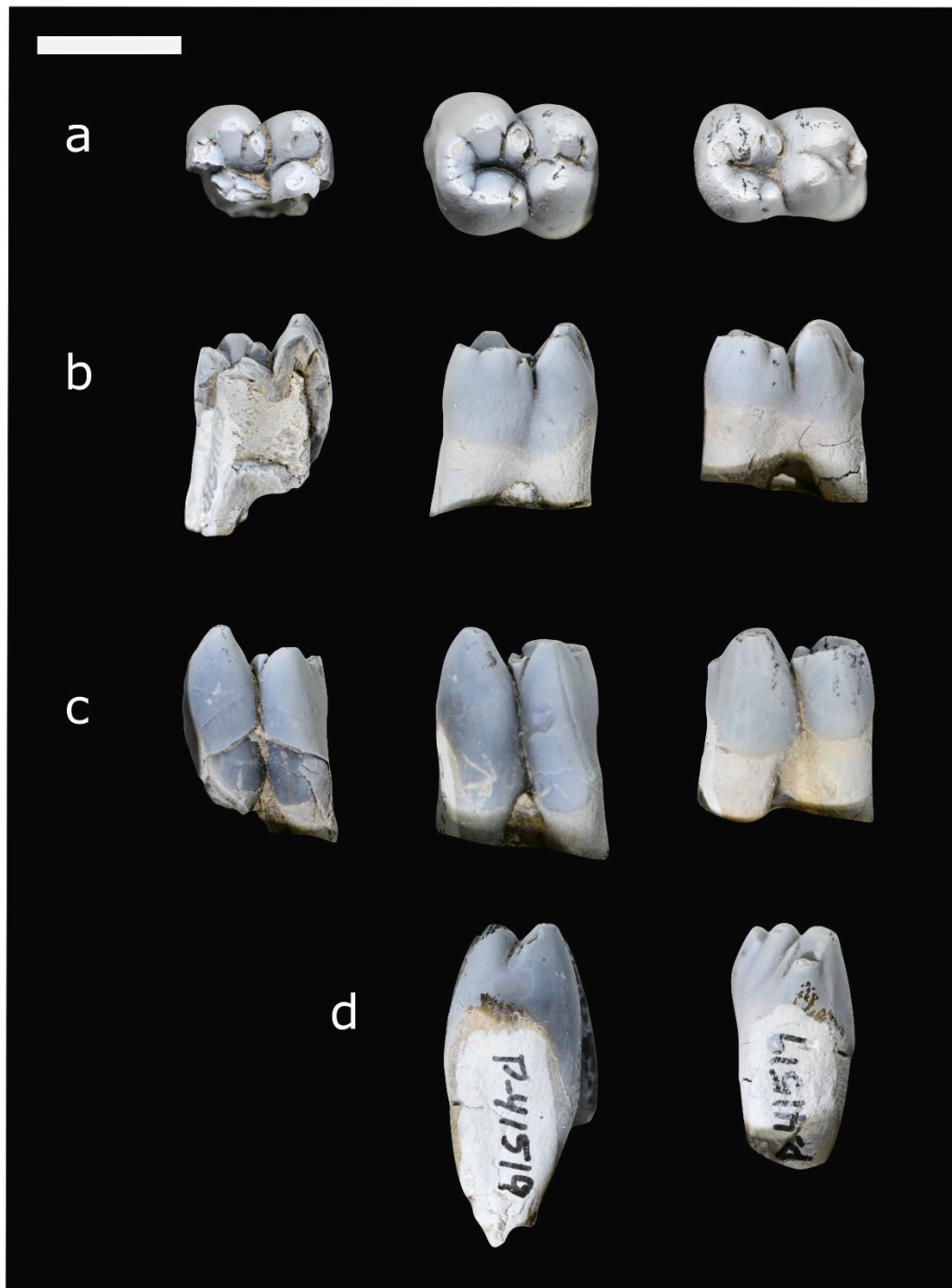


Figure A12: Specimen NMMNH P-41519 in occlusal (a), lingual (b), buccal (c) and mesial (d) views. The teeth are m2, m1 and dp5 in each row. Since m2 is damaged, there is no photo in the mesial view. Photos were taken by Thomas Williamson, edited by me. Scale bar 1cm.

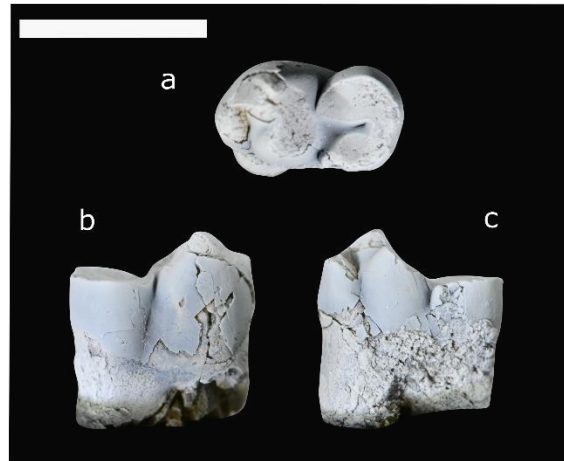


Figure A13: Specimen NMMNH P-02705 in occlusal (a), buccal (b) and lingual (c) views. Photos were taken by Thomas Williamson, edited by me. Scale bar 1cm.

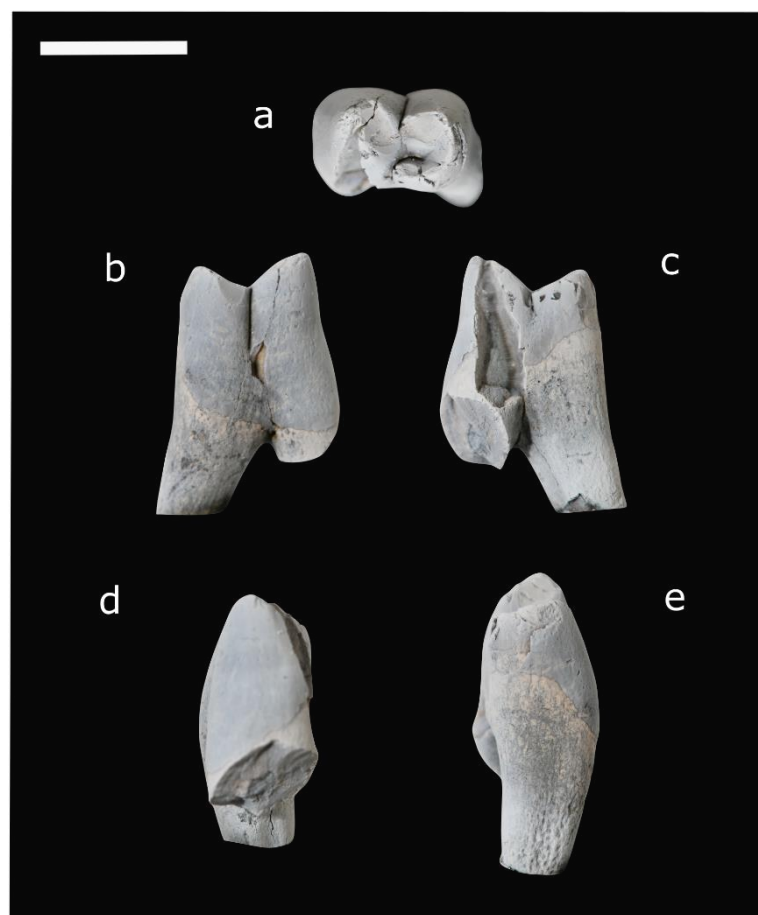


Figure A14: Specimen NMMNH P-77882 in occlusal (a), buccal (b), lingual (c), mesial (d) and distal (e) views. Photos were taken by Thomas Williamson, edited by me. Scale bar 1cm.

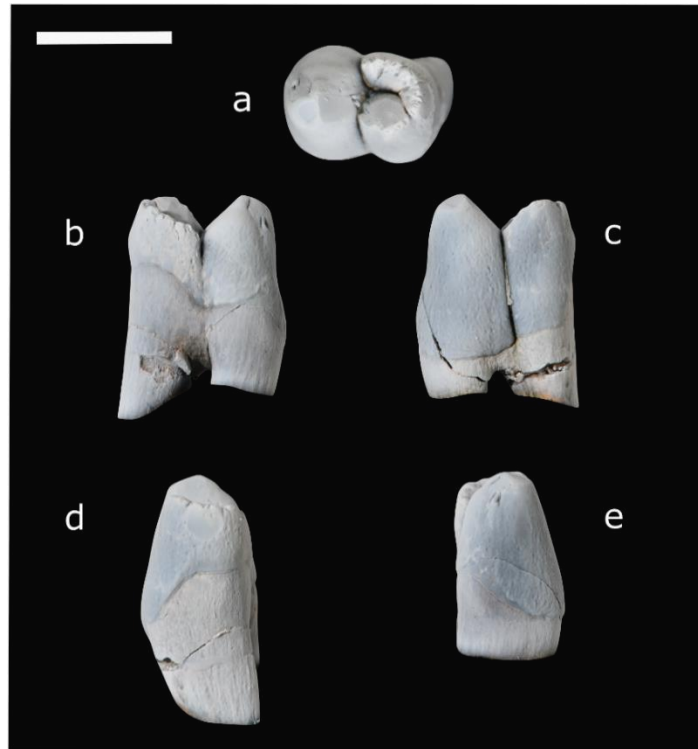


Figure A15: Specimen NMMNH P-51827 in occlusal (a), lingual (b), buccal (c), distal (d) and medial (e) views. Photos were taken by Thomas Williamson, edited by me. Scale bar 1cm.

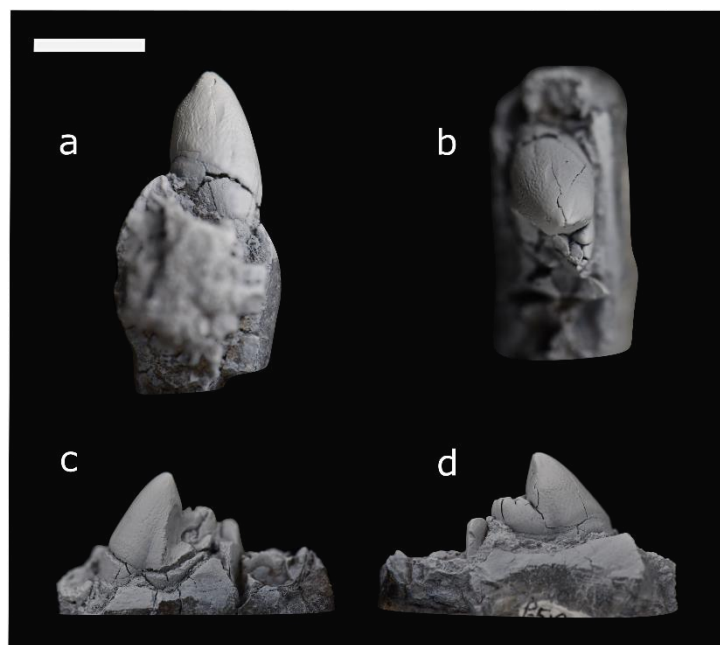


Figure A16: Specimen NMMNH P-51828 in mesial (a), occlusal (b), buccal (c) and lingual (d) views. Photos were taken by Thomas Williamson, edited by me. Scale bar 1cm.

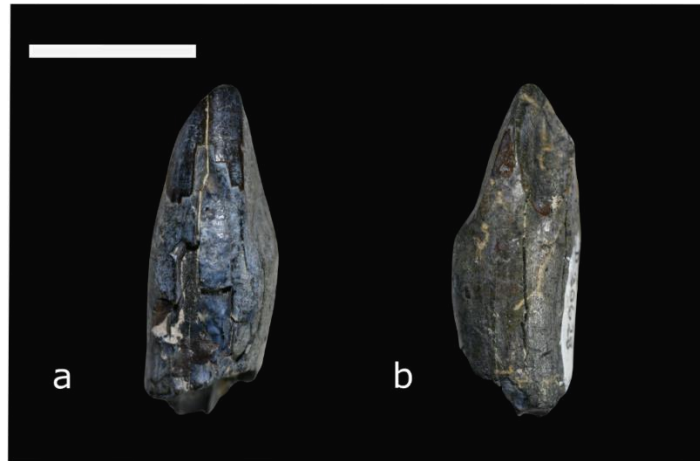


Figure A17: Specimen NMMNH P-30628, upper incisor, in anterior (a) and posterior (b) views. Photos were taken by Thomas Williamson, edited by me. Scale bar is 1cm.



Figure A18: Specimen NMMNH P-47826 of left and right lower canines in anterior (a), posterior (b), lateral (c) and medial (d) views. Photos were taken by Thomas Williamson, edited by me. Scale bar is 1cm.

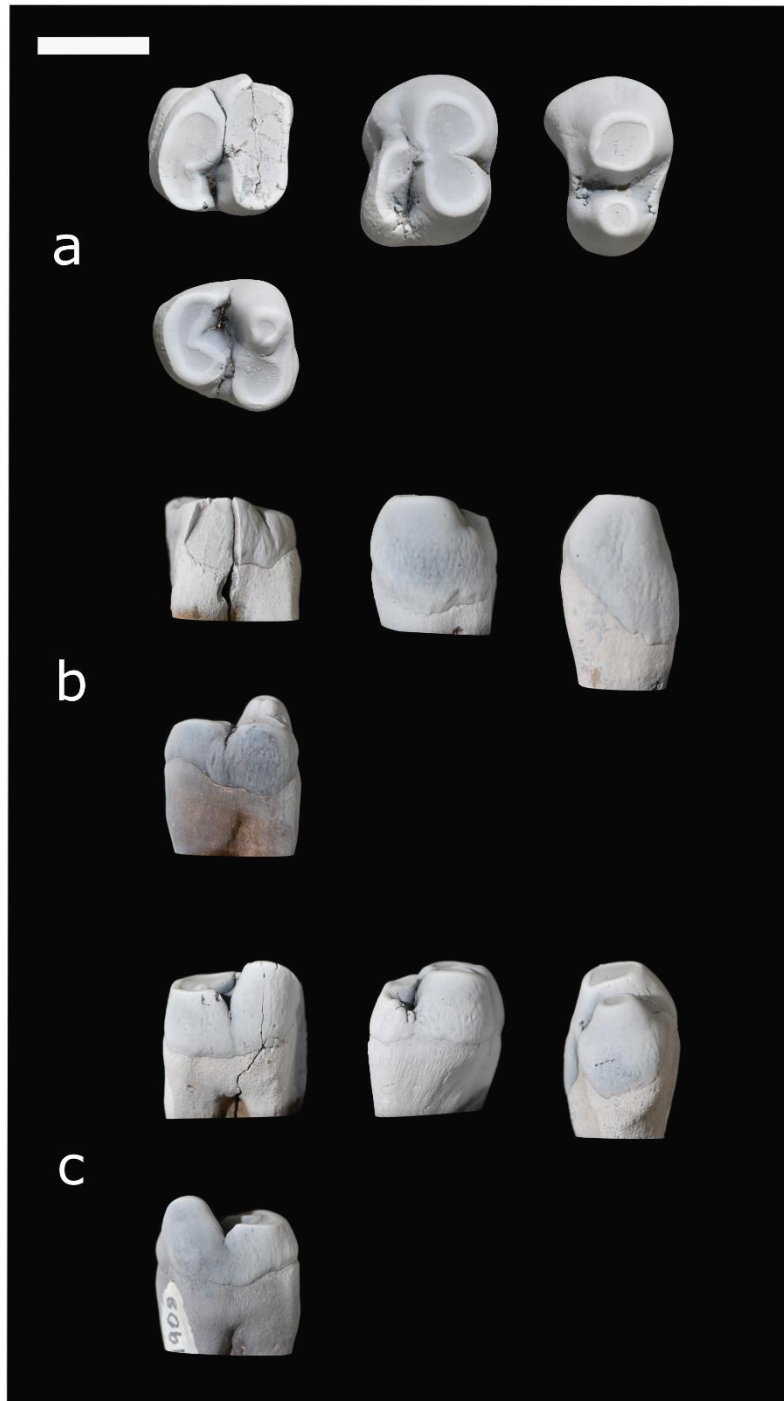


Figure A19: Photos of the lower teeth of specimen NMMNH P-44908, left and right p5 (left), p4 (centre), p2 (right), in occlusal (a), lingual (b) and buccal (c) views. Photos were taken by Thomas Williamson, edited by me. Scale bar is 1cm.

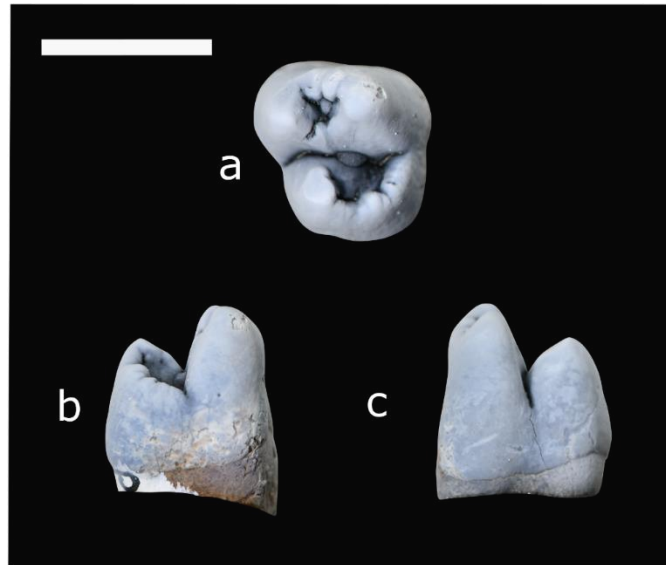


Figure A20: Specimen NMMNH P-19800 in occlusal (a), lingual (b) and buccal (c) views. Photos were taken by Thomas Williamson, edited by me. Scale bar is 1 cm.

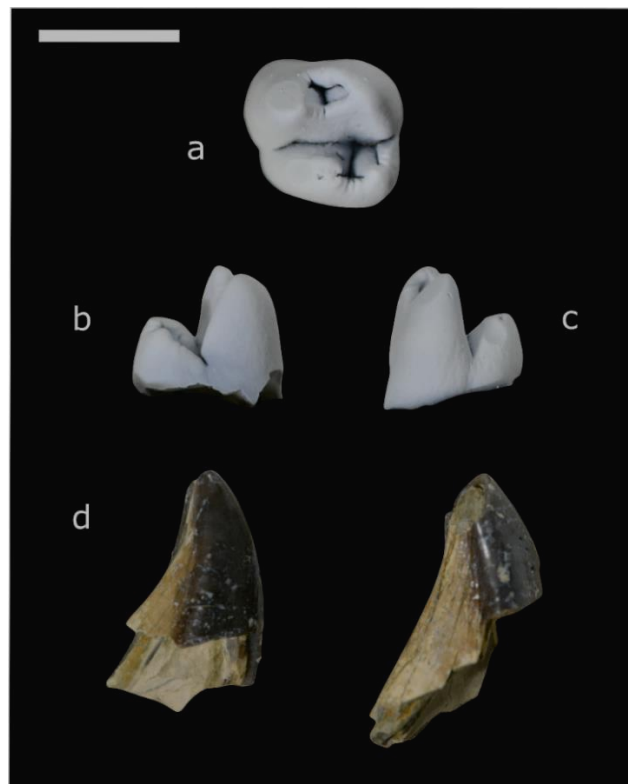


Figure A21: Specimen P-57845 in occlusal (a), lingual (b) and buccal (c) views of the p5 and the posterior and anterior views of the canine (d). Photos were taken by Thomas Williamson, edited by me. Scale bar is 1 cm.

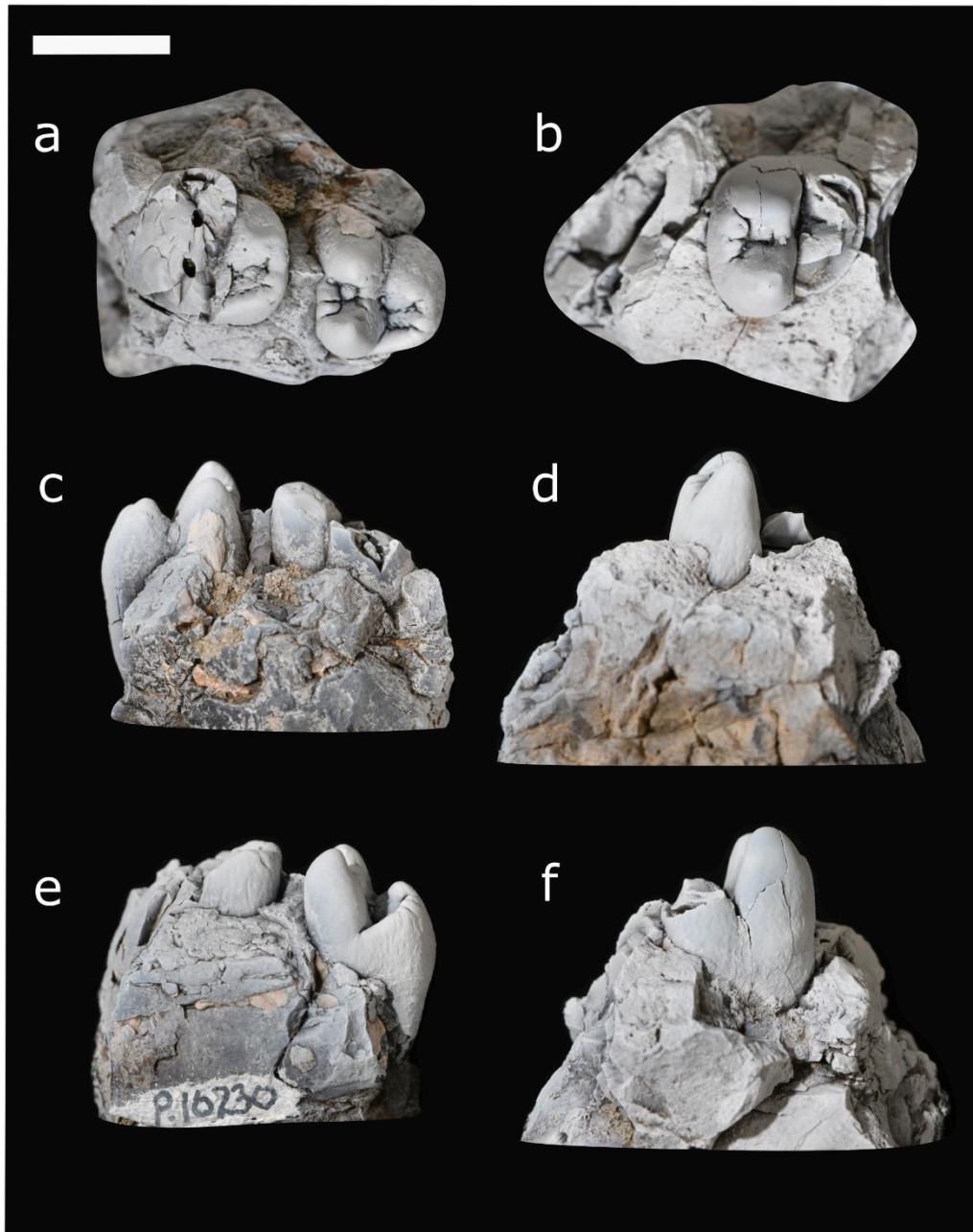


Figure A22: Specimen NMMNH P-16230 in occlusal (a, b), buccal (c,d) and lingual (e, f) views. Photos were taken by Thomas Williamson, edited by me. Scale bar is 1cm.



Figure A23: Skull and mandible of specimen PM 3895, *Stylinodon mirus*. Notice the elongated first premolar of the upper and lower dentition. Photos were taken by Paige dePolo, edited by me. Scale bar is 1cm.



Figure A24: Skull and partial mandible of specimen USNM 15412, previously known as the type of *H. torrejonus*. The skull consists of left M1 and M2, and the right P4, M1, M2 and M3. The lower teeth are a canine and the right p5, m1 and m3. Scale bar is 1cm.



Figure A25: The partial right mandible of specimen YPM PU 14718 in buccal (top), occlusal (middle) and lingual (bottom) views. It consists of p4, p5, m1 and m2, and belongs to the species of *polecatensis*, a new genus to be erected. Scale bar is 1cm.

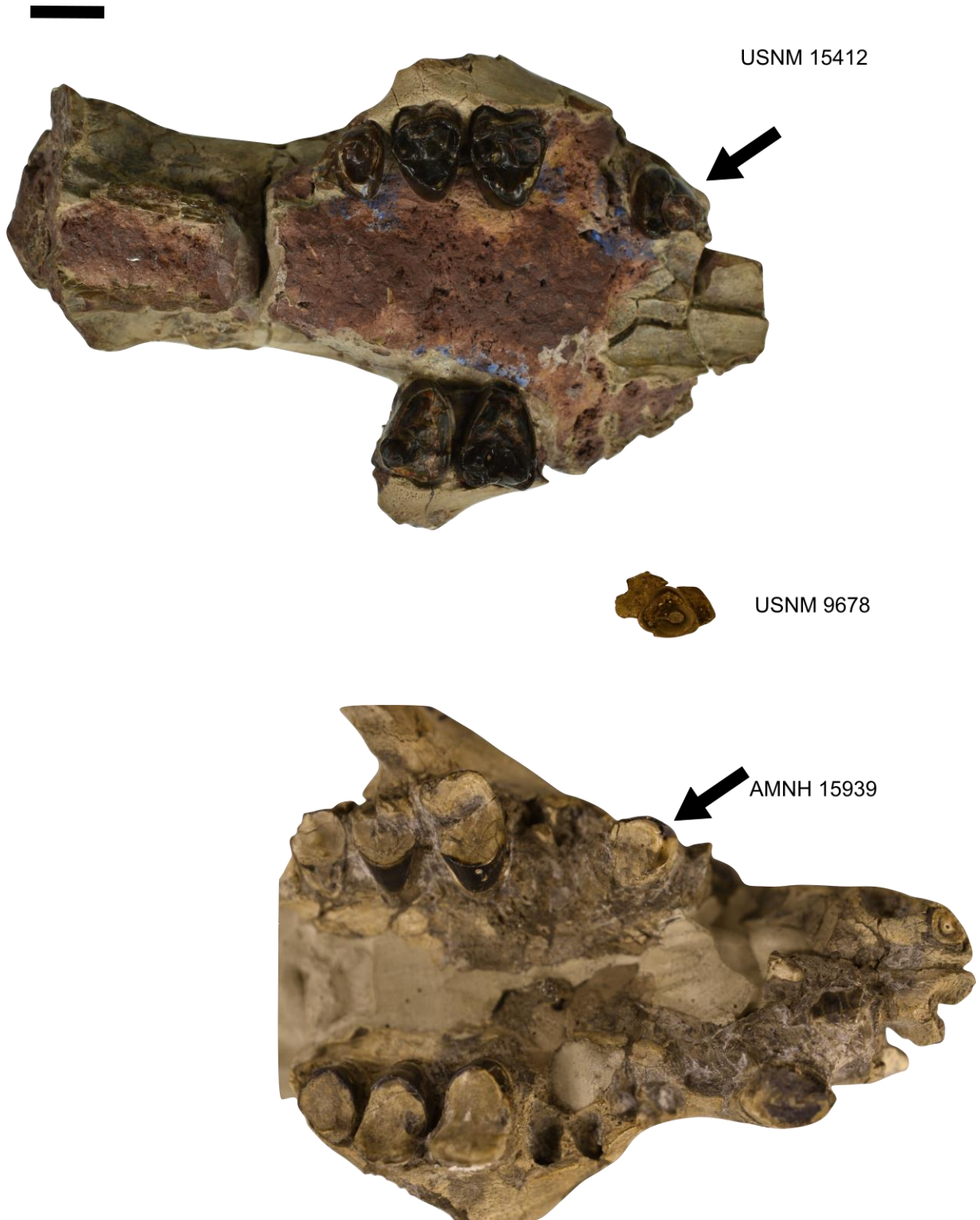


Figure A26: Skull of USNM 15412 (top) previously assigned to *H. torrejoni*, isolated P4 of USNM 9678 previously labelled as cf. *Huerfanodon* sp. And the skull of AMNH 15939, characterized as an undetermined conoryctid by Schoch (1986). Scale bar is 1cm, and arrows point at the P4 of each specimen.

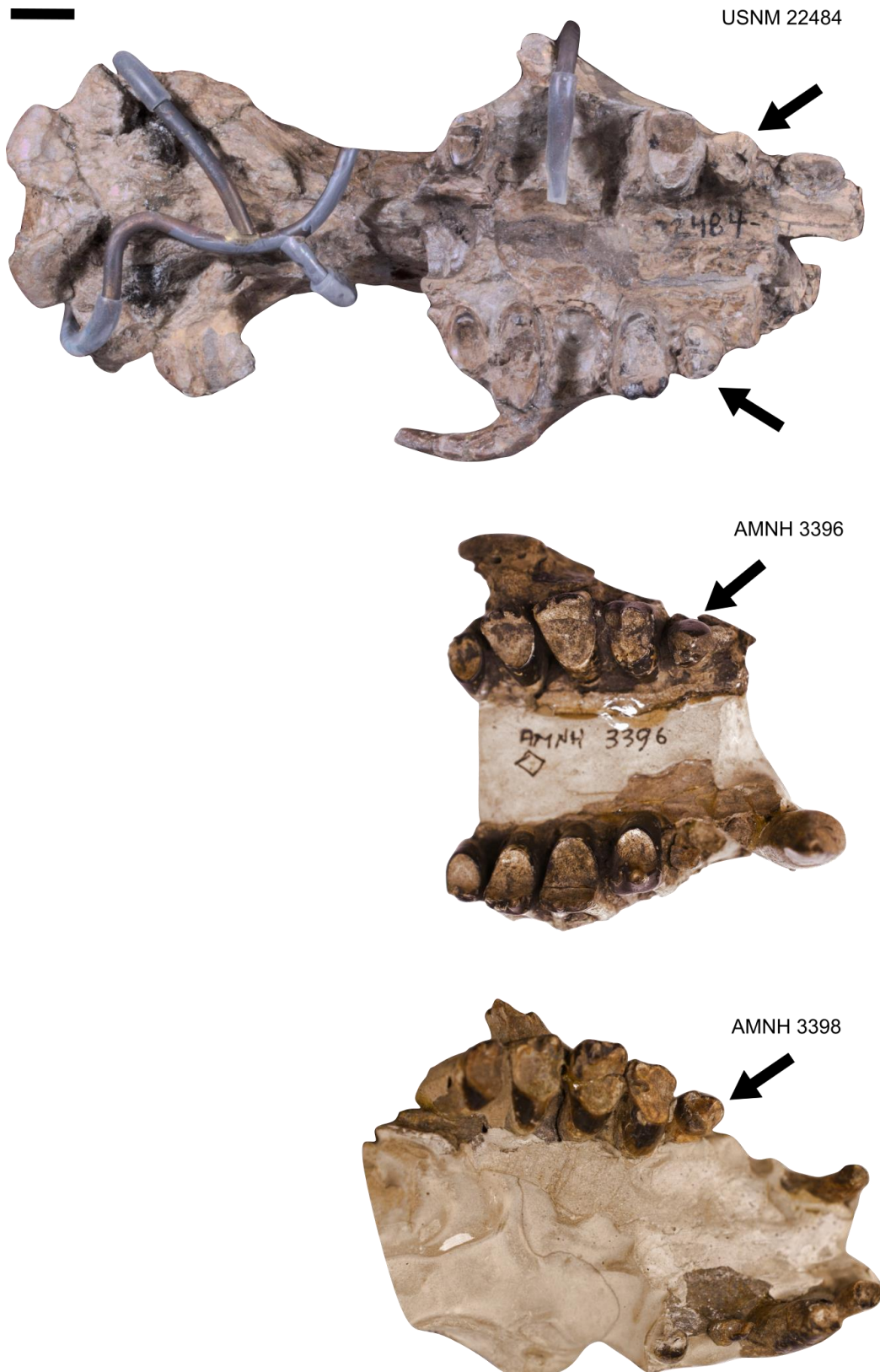


Figure A27: Skulls of *Conoryctes comma*, AMNH 3396 (top), AMNH 3398 (middle), USNM 22484 (bottom). Scale bar is 1cm, arrows point at the P4 of each specimen.



Figure A28: Skulls of *Schowalteria clemensi* (type, RTMP 93.90.01) in lateral view (top), and occlusal view (bellow). Photos provided to me by my supervisor, Steve Brusatte. Scalebar is 1cm.



Figure A29: Right part of the mandible of *Schowalteria clemensi* (type, RTMP 93.90.01) in buccal view (top), and occlusal view (middle) and lingual view (bottom). Photos provided to me by my supervisor, Steve Brusatte. Scalebar is 1cm.



Figure A30: Left part of the mandible of *Schowalteria clemensi* (type, RTMP 93.90.01) in buccal view (top), and occlusal view (middle) and lingual view (bottom). Photos provided to me by my supervisor, Steve Brusatte. Scalebar is 1cm.

Supplementary (S.1) material is the .tnt file from Morphobank, including the scored taxa with the ones excluded a priori for the analysis, and the characters of the analysis. Note that two characters should be excluded, ch.551 and ch.617) and that there were three analyses for the study:

- all species of *Ectoganus*
- only the two species *E. copei* and *E. gliriformis*
- only the two species *E. copei* and *E. gliriformis* and the new specimen NMMNH P-25014

Supplementary (S.2) material is a .png file of the synapomorphies of the analysis.

10000100?002122100100??00?001101000000?10?0010?1?000 - 01100021 - 10
00?01000?011001?000101000?00001000011001010?0011010000101112?1?00?1
010011110011002011100??10??10000110100000110020?1?0010000??2?10?001
???10?????0??1010?????1?00001001??00000111100

Astrapotherium

10??11??01051 - - - - - - - - - 041000 - 1000100110?3?0 - - - -
?????1110?00?????011 - 0011100?????0 - - - ??? - - - ?? - - 0[01]?01
??00?1 - ???????1?2?0?????????????01?01011?12 - 11 - 00101011??? - ??
?????????????????01?0?????0[01]?01?????????????????0?????11??????????????
10?????????01[12]22201?????????????100?????????0110?000?000?02101020 - 11
?121?0 - 10? - 0[01][12]01010?0?1?100?????????00?0100?100???010000001[01]
0????0?????????0[01]01?00?????????11?0?11011011??100000? - ? - 0?1110 -
0100??00?0010 - - - 01?00?1?00010?1?000?10101011 - 1100?00??0?????
0?????????100?00??0??[12]1?010010?????01??0??12?0?00?01?001?11101
??02?1?100??11??02?101100000?0?000?0?0??10000??2?01?11????0?????1?
?1010?????????112?????????????1111??

Bemalambda

00??0 - ???002?00000000?0000?10?00100110?1?0 - 000?????1100?00??2??0
11?001110100??0?00??? - - 1?01000?01??00000?[12]222?21?2?211?0?00200
11?01?1?1?010000011?1110121?100?0???? - ??????????010001?01?01?????
?????????????102??00?0?00?01??2?10?????????01002100010?????????0000????0
01??00011000?000?02011101111?1?1?1101010100000000?10000?0?1?001?0?0?
00?11001?00?00100101?????????????1?00000?????????010?10??1011??1000
0101?0??122??1100??00?00010?0?00?0?10?0010?1?000 - ???100??????????00
????????0?????????????????001?????1100[01]010?????010?????????????????000
111????1001011100??11??10000110100?????10011?1?001?000??2?1??100????1
?????????10??????1?00??2?????????????????00

Carodnia

00??1????00?1??????0?041000?1000100110?1?0 - 000?????1100?1???2??011
?001110000??0100??? - - 0?0001??01?000011?2?22?21?2?1??????????????0
1?1??1?????????1???????????? - ??????????????????????????0[01]?02?????????
?????????00????0?1?? - ?? - - ??? - ?11????????? - 1211?011??????????
01?????????003110010000?021010212[01]1?121?????????????????????????????
?????????0?????????1??????1???
?1?????????????????????????????????01?????????????????????????????????
???01?1?????????????????????
????0111100??0??1??????11??1001011110001??100??1??01?000??1?00?11
1????01?????2??1110??????0100120?????????0111100

Colbertia

00??0 - ???00210000?00000100010001101101?1?0 - 000?????1110?00??2??0
11?001110000??0100??? - - 0?0101??01??01110?[12]112?21?2?112?0?01200
01?01?01011?12111 - 001010101?? - 0?0???? - ??????????010021??01?01?
?????????????????002??11?1?? - ?? - 0??? - ?10?????????01122200011????????
?0110??0?3?????110000?0?0?02101021111??11?1110? - 01000000101??0????

?????0?0000[12]00001?0[01]000?001100?????????????01?00?????????0?0?
01??1011??10??0101?1??1110 - 0104??1??00110 - ??????0?1??00010??00??
??100?????????????????????1?????????????????????????01?0?02??11??????
??[12]?????????1?????????????????????????????100011100?????????0021?1?0????
?0??2?01?011??10?????????1010?????1??10101?????????111100

Coryphodon

00??1????00211100400004100011000100110?1?0 - 000?????1100?00??2??011
?001110100??0100??? - - 1?01001?01??00110?2312?21?2?012?0?00201?1?1
1?1?011?2201111?1110120112100??10?????????011011??01?00??????????
?????102??00?0??00?01??2?10?????????0122201010?????????0001??010??0
0111010?000?02001111?11?121?101121010000000011010??0110001??0000111
?01?00000?00101?????????????1?[01]1000?????????101?01??10110110000??
?????122??1100??00?001?????0000?1??0?????????????????????????????
?????????????????????00?????????01?10?????01?????????????????10?001?110?
1110?011100??11??10010110100010110110?1?0110000??2?10?011??10?????
??1110?????1?0011120?????000111100

Cynodontis

00??0 - ?????2?0003?0?0 - ??????0??001?????1?10000?????0 - 0111??1?
?000100310?000??0??0??? - - 0?0001?00?????000?0 - - 0 - - 2?0?212?0
?00201?0001?1?011?1201110010101101110?0??10?????????011001??00?00
?????????????????102??0?0??10?00??1?00?????????01101101?10?????????000
0??0?0[01]??00010000?010?0101110?101?111?1101220110200010111000?1110
001??0000200101?01000101001110100000000 - 1?00001101001??01?0?10??10
110010000101?002122111101??00?000100001?10?1111000?1?000 - 11?010?1
- 1100?1100?[01]011001?0?????000?000010000110010011?????01?00000??0?0
?1 - ?10?0???
???1????000111100

Dasypus

01?? - - ??10 - 54 - - - - - - - - - ? - - - - - - - 1 - - ? - - - - ? - ?0
- - - - ????? - - - ? - ? - ?? - ?? - - - - - - - ? - - - - ?? - - - - ?? - - - ? - -
- - - ?? - ??? - - - - ? - - - - - - ? - ? - ? - ??? - - - - ? - ? - - ? - ? - ? - - -
- - - - - - - - - - ? - ? - - - ? - ??? - ????????????? - - - - ??? - ?? - ??????
???????????? - - - ?? - - ? - ?? - ?? - - ??? - ? - - ?????????? - - - - ? - ? - ??????
??? - - - - ???003??0100?010?010?01110220 - 01?121?1 - 1? - - 01 - 110000111
01010101000 - ??0101 - 000? - ? - - 0000002000010[01]100[01]111 - 1?1? - ?0100
200101201?011?10111110010?? - ? - 121210 - 1102??10?001100010000?10?001
0?1?1 - 0 - 11110021 - 1200?00100?011101?01? - 1?000?001?001? - 11001100?0
011011000101102?1?01?0010011110100112111100??10??100001100000111101
20?1?0010110??2?00?000??01?????2??1010?????1?0010110???????????????

Diacodexis

00??10????0021?000000?040000100001011?0?1?0 - 011?????1100?1??2??011?
110110000??0101??? - - 0?1?001?1??01010?[12]11[12]221?1?112?0?00201?1?
01?1?011?1111110012101001111110?11?????????2011021??01?02??????????
??????0021000?0??00?0???2?1010?????01022201111?????????00010??02[12]

0100010000?00030200102010?????11100? - 01000???00110100?011000??????
?01001?00000000200??00[012]00100111000000010100010?100010011011??1?0
00100?0021210 - 1100??0110001000??0?10?0000?1?000 - ??1?1??1 - ??0?01
10?????????????????????0?01?????????110[01]0?1002??010?00?????10?1?1 - ?10?
?????????1??010?????????10??02?1??11?100101???21?1??110001??2?10?001??
?11?????1??1010?????1?0110110101000001111??

Dichobune

00??????0??1?????????0?10001100?101101?1???000??????110111???2??0100
110110000??0100??? - - 0?1?000?00??01101?1111111?1?103?0?00201?1?01?1
?011?111110012101001111011??10????????????010021??01?01?????????????
??002??00?1?00?01???2?11?????????01122200011?????????0001??011?0101
0000?000?02001020101?121?????0? - 01001??011110?01001000??????001[12]11
01?000000??20?1010010010111000000?1010?0??1100?01??1010??11??0?????
02121??0100??0??000100000000?1111000?1?000 - ???100??1101?1100?[01]01
0001?0001??000?000010000311011010?????11??????1110????00?10??????????
??
????????????????????????????000001111??

Harpyodus

00??0 - ?????????1100?00??2??011?
001110100??0????????????????????????????????????111??1?2?111?0010?0011?01?1?
1?010100011?1110121?10????????????????????????????011001??00?00??????????????
?002?00??
??0??????2??0????????????????1?01?
00?00?00000????????????????????0000????????????????0?10??1??0??1??????????????
??????0??00??
??
??
??
??1111??

Macrauchenia

00??0 - ??01210000200?02000010001101100?1?0 - 010????????00?00??2??010
1001110011??0000??? - - 0?0010[01]?01?01101?????????1?2?0??0010?00??1
??01001??1?1??01101002?? - ?????????????????????????????????01??????????
?????0 - - ??00?0??10?01??1?10?????????01022201010??????????0101??023??
0100?000?000?02100221011?1111?????0? - ??20?010?0??10?????????0??1000?1
?001?10000001100 - ???????????110[01]00?11?????????????1?011?1?0?0?1100?0
? - ? - ??1220 - 1100??1??0011000?00?0?1??0010?1??00??010101??1100?000?
??01?101?0?????000?0000101? - [12]10011010????01??????????2?0?00??0????
????????????011??1??10?02?10110011011100111?1?01??111??2?10?000?????
????2??1010?????2?011021[01]?????????1111??

Miguelsoria

00??01?00?1?0 - ??????????0?????????011?
001110000??0100??? - - 0?1?100?01??00100?231[12]221?1?112?0?0120001?01
?01001?02111 - 0010100001101111??10????????????010011??01?01????????????
?????002??00?0??03?01??1?10?????????01012200011?????????0001??0?3?????

???000?0?0?020????0111??21??11?
01?00000???1??1??0?0??1?????????????????
??0?00000 - 0010?011 - 1000?000???1??
1?1?000101000?0000101? - 1????????????????????????????12?1?00??0?????????????
??2??2?10?101???0?????2??
1010?????????101?1???????????????????

Notostylops

00??11??000[23][12]1111101020?00?2??[01]11[01]1100?[12]?0 - 000?????1110?0
0??2??011?003110000??0100??? - - 0?0111??01??00100?1111221?2?112?0?01
20001?01?01011?1[12]111 - 0010100100? - 0?0???? - ??????????011021??0[01]
?01?????????????????002??11?1?? - ?? - 0??? - ?10????????01122200011?????
??0110????0[01][23]??011100010000?02001020[12][01]1?121?1100? - 0110000000
110000?111001 - ??0?00111101?010000001100?10[012]01??????1?01?0010????
??1020?011?1011??10000101?00?1[12]10 - 0104??10?00110 - 1?1??0?1??00010
1??00?101110??1?????????0?????1?????????0??00????????20?01?01002??11
??10????12?1?00?00?1???
???

Plesiotypotherium

00??11??1[01]4200 - - 211 - 1211 - 0 - - - 1 - - 1 - - - - ?3?0 - - - - ???????10
?00?? - ?????1??????0????0 - - - ??? - - - ?? - - 1??01??01?? - ???????1?2?0
?????????????????????011?????????????01[12]??? - ??????????????????????????
?????????????????????????? - ???1????????????????????????????010222??????????
??????????0[12]3??0010?000?000?02101020211?1?1?111? - ?012110000011010
1001[01]001 - ??1100000001?00000000210 - 111[01]0011011100000001111[01]01
11110?011?10111110000101?1021110 - 0104??11100111 - 0000?0?1??00010??
00????11??????????????0?????1?????????????0??0??21?0[01]?01002??11?
?101??02??00?00?[01]111?????????????????11??100011100000??00011?1
??0?000??2?01?111??10?????1??1010?????1?0110110??????????????????

Protypotherium

00??1??10?210001201002100011001101101?1?0 - 000?????1110?00?? - ?????1
????????0?????0100??? - - ??01?0[01]?01??00??0?????????1?2?0?????????????????
?????011??2?1????????012??? - ??
??????? - ???1??1?? - ?? - 1??? - ?10?????????010222?????????????????1?????003?
??10?000?000?02101020111?111?1110? - 01[12]1100010110100?01[01][01]010?
?1000100001?11001000210 - 000[012]10000??00000001011??101110?01011011
1110000101?1?21110 - 0104??11100110 - 001??0?1??000101??00?11?1002??11
??101?0?????1?????????101?00??0?? - 21001?01002??11??10?????12?1?00?0
1?111110??????01?111??10??0000[01]1100?0??0?00021?1?00?011??2?10?0
1[01]??01?????1??1010?????1?0110101??????????????????

Pyrotherium

00??11????10330110111 - ?011112 - - 1 - - 1 - - - - ?[23]?0 - - - - ???????0??1
??[23]?01011101100????0 - - - ??? - - 0?01?1??01??01?01?2?22?21?2?1??
??????????01?1??1?????????1???????????? - ?????????????????????????0[01]
?02????????????????[01]13??00?1?? - ?? - - ??? - ?11?????????? - 222?????????

????????1?????3??1 - 1110010000?02?01020211??21????? - - 001[01]???????
??0????11??1 - ??0?0000001?01????001000??0?111??????????0010????0??1?
????????1??1??10000??1?1??1110 - ??00??1??011[01] - ??1??0?1??00?????????
????????????????????????????????1????????????????????????????????01?0??02??11?????
????????????????0111111??????11?????01??10010111010????00101?0?001?
000??1?10?101????11????1??1111??????0110 - - 0?????????1111??

Tenrec

00??11??1003111002000021000[12]1000100100?2?0?011?????0?0111??2??01
1?001110000?0001??? - - 0?00000?01??010?1?1111221?0?210??02?20011?00
01?011? - - 0 - 111?101? - - ? - 100?0???? - ??????????01 - 10 - ??00?00?????
?????????001??0?0?00?00??2??1????????? - 0120100?????????0000??02
3??0010?000?000?01111210201?121?11010201211101101111010[01]010001??0
001[12]01100?0101 - - 1?10 - 111000110010 - 1?1? - - - 100200101100?[01]2011
01100100010? - ? - 02122101110?0? - 01?100?00100?1111?10?1?000 - 01?1001
1 - 1010?0[01]?0?[01]0110000001101000?001?10010[12]100100110110010001101
110?1?1 - ?10? - 011111011102011101??11??10000110000011110001?1?001000
0??2?00?111??11????2??1010?????1?0001221?????????1111??

Tribosphenomys

00??11????11430001221 - 121131 - - 01 - - 1 - - - ?3?0? - - - ??????0?00?1???
0?????????????0????? - - - ??? - - - ?????1??01??0100 - ?1301111?1?212?0?00
20? - 1?01?1?011?1201111?12 - 012001111110?10?????????2011021??1??02?0
?????????????? - 021110?1?? - ?? - - ??? - ?11??????01212200011?????????10
000??1 - 2100?10?001000?2??0??10201?121?1??? - - 0101?????????????????
????????????????????10????????1?????????????????????????????????????
???
???
???
??000??2?10?00
1??01????2??1010?????1?00111?0???000001111??

Trigonostylops

00??11????10?[12]?????????0?100??1000100110?1?0??01?????111101??2??01
01001110000?0101??? - - 0?01100?01??01200?[12]222?21?2?112?0?0120001?
01?01011?12111 - 0110101000100?0???? - ??????????011011?01?01?????????
????????002??10?1?? - ?? - 0??? - ?10????????01122201011?????????0100??00
??01110000?000?0??01020[01]11?121????????0000??0??1?00?101000?????
?00111101?01?0????100?111[01]00110?1??0100?10101?111?10?11011011??1
00000? - ? - 021110 - 0100??0??0010 - - - 01??0?1??00?????????????????????
?????????????0?????????????????????????????????01001002??01??00?????????????
?0???
??0001111??

Adapis

00??0 - ???0032000040000400001000[01]1011000100?000?????1[01]?0?1??1??
0101110110?00??0100?????0?1?001?01??01100?????????1?1?212?0?[01]020? - 1
?01?1?011?2[12]?1110012101?0011??0? - ?10?????????20??01?????????1????
?????????0?2100??1?????????????1011?????0112221?011?????????00?10??01

210001101?0?0003001010?1[12]11?1311110??10[01]1?2?1?10110001110110?10
?0000?111???00000[01]00???01100011011??1?0001100??0110?02000?011010?
11000011???0112?0??110??0110??10?001?00?1110000?01010??1110211?1?10
10??0?1011????00[01]101?1?1111?00??0211010?0?100?110?0010??0????1???
0????????????????????????????????00???10?00???1????????????????0??2?10?1?
???0?????????1011????2?0111121????0?0001111??

Alostera

00??0????????????????????????
??0?112?001?201?1?01?1?
011?21?1110012101?0111????0?11?????????20??10????????????????????
?0??1????0??3??0??1?010?????01212202?11????????00?0????????????
??
??
??
??
??
??
????????????????0??0001111??

Asioryctes

00??10???000000000001000?00?0000000000?1?11010?????11?0?1???2?0001
00200??00??0001?????1?1?000?1???01001??????1?0?211?0?0010001?01?1?
010001?0110010101?0111??0?0?11?????????10??011??1??1????????????
???2100??0??03?00??2?0110?????01002100110????????00?00??0010100210
010?0102000100?0101?1111100?0011?0??0010?10??11100?00?000??110??[1
2]00000101???10?10000000????1???000110010?00000?011011?01100011???01
1300??100??0110??11?01011??0?000101?1?00011100?1?100000?000??11?1
?1???0[01]00?1001?11000?00011?0?01?000?00?0??????1??101?11001?01??
????????????????????????000????????????????00??1??????0????1?????????
?10????0?1?000?0???????????????

Aspanlestes

00??????0?[012]????????????????????????????0?11?0?????110??????1??0
000001110?00??0010??000?0001?01?01010??????1?0?212?0021211?1?01
?1?010021?1110012101?0111????0?11?????????20??10????????????????
????0?21????0??13??0??1?1110?????0112202011????????00?10??0[12]101
??110010?1?????????????1?111????????????????????????????????????
??
??
?????00[01]?00?0?000?001?2????????????????000??110?11??0?0????????
??
??
??101?1?0?1011???02100100??????

Avitotherium

?0????????????????????????0????????001????1????????????????????
?????????????0?0?????0?1?0????????????????????????0?112?001?201?1?01?1?
010021?1110012101?0111????0?11?????????20??101????????????????
?0??1????0?00?00??2?100?????01212200?11????????00?1????????????

????003100120?0?100100000012?1 - 11?1311001??01???1?1?[01]01100011101
00?02?0001?1001??0?00001????011000110011?1?1??000020110?10100?0111
?011100100????021[23]00??112?00?0?0?0?01?00?1110000?1?1?01101100?1
?110000??1?[012]0121?1?01??1?00?1001?001??2000[01]0?0?021?01101010100
2?1??01101?011110101112110110??0?00010110?00011111?01?0?0010000??
2?00?0?0?0?01??????0?10?????1?1?01000???????????????

Bulaklestes

00????????????????????0??0??000??1?11????????10?0?1???1?????
????????????000?????0?1?000?1??00010??????1?0?111?0021111?1?01?1?
010001?0110010101?0111??1?0?11?????????10??011??1??1?????????????
???21?0??0??03??0??1?0010?????01002100210????????00?00??002?1?????
????1?????????0101??11???
???
???
???
???
???
????????????????1????????1111??

Chaetophractus

01??0 - ???0054 - - - - - 0 - - - - - - - - 011011 - - ? - ??????????????
??? - ????
???
???
??000000120?1?0?0103001001?0 - 01?1311101??101??1?0?01010101000100?10
?0101?0001??0?000000??0110[01]0011011?1?010?000020011??0100?0110111
1100100????121200??103??10?0??11?110100?111000101?1?0111110121?1100
00??0?[012]1?21?1?01??1?00?1001?001??01011?0?021?11100010110001??10
001?01111011112111100??0??10000110?10011100120?1?0010110??2?00?0?
1??01??????1010????1?0010010?????????????????

Daulestes

00????????????????????0??0??000??1?11????????10?0?1???1??0000
00200??00??0000?????0?1?000?1??01011??????1?0?111?001[01]10000001?
1?010001?0110010101?0111??1?0?11?????????10??001??1??1?????????????
???0??1????0??03??0??2?0010?????01002100?10????????00?0??0?2?????
??????1?????????????1?????????01?????????????????????????????????
???
???
???
???
???
????????????????????????00001111??

Deltatheridium

00??10????001100??0000000?0??010010010012110000?????0?0?1???1??1?1?
11000??00??0011?????0?1?01??1??00000??????0?0?111?001010000001?1?
0101?1?0010011001?0111??1?0?10?????????10??00??1??1??????????????
???1110??0??20?00??0?0010?????00?01000110?????????0?01??0130100110

000?0001000101?0101?1?11100??0001?0???0010?001100000?10?0?00?100???
01000000???0000??10????????????00????????????????0111?1????????????????
????????1???1[01]0??10?0????????11???101?1?0?1011?0?02110000???0????0?
1?01??1?00?00001001??01????????????1?10??011??0??0?0????????????????
??0??10
00????????00??0?????????1111??

Eomaia

00??1????00000000000?000?00?0000100100?0?11011????110?0?1???1?001?
001?????????0?1???001?1?000?1???0?0?0????????1?0?[12]11?0?0?1?00??01?
1????[01]01?00?0010????0111??100?10????????????10??0??????1????????????
????????21?1?0??13?0??1?0?0?????????02??010?????????00?00??021010
1110010?1102000100?000000?01100??0011?0????010?10??1?0?????????????
?????0?00001????????????????????????????????????1?0?0?????????????????
????????????????????????????????1????????????????????????1????????????????
??
????00?0?0??0?0??110?000?0????1??0?11?0????????????????0????????
??10??????1?0????1?0?0001111??

Eozhelestes

00?????????0????????????????0????????011????????????????????????????
?????????????000???[01]?1????????????????????????????1?0????????????????
??
?????????????0?03?00??1?0010?????01002202011????????00?1??0?2?????
?????????????????0[12]0??
??
??
??
??
??
??0001111??

Erinaceus

00??10??000221001000[01]101000210010011010[23]010????????[01]0?0?1???[1
2]??001?110010?00?0?????????0?1?001?01??00000????????1?0?112?0?0020? -
1?01?00011?22?11?00121??0011? - 0? - ?????????????20??10?????????1??
?????????0?1110??0?00?00???2?1111?????0121221??11????????00?11??[0
1]3[23]01012101?0?0003001110?0201?1311120??001??1?1?111111?0[01]100?
12?0010?011??01001001??11?1[01]01110[01]0?1?1???000101010?12000?011
011111000010??021200??104??00?0??11??10000?011?100?00000?01110021?
101010??0?[01]0100?1?00010100?1000010000210?10?11010?0[01]0000101101?
1??10?01?01111?011001011101??0?02?10110?00111101?01?1?0010010??2?
10?1?0??11??????1010?????1?1?10110?????00?1111??

Gallolestes

00??
????????????????????????????1?000?01?????????????????0????????????????
????????????????????????????1?0?11????????????0??10????????????????
?0??1????0?03?00???2?100?????01202202111????????00?10????2??????

??0?????3??1?0101????1110??1011?0?0?0010?001000000?10??000?011???
00000000??000?000000?0?1?010?0????0?10?10000?01101100100000????011
1?0??101??0101??10?011?00?011000101?1?1?10110001?100000??1?[012]0100
?1?01??1?00?00001001????11000?0??0??10?00?0????????????01?1101000???
0?011100??1??10000110?00??100020?0?000?000?0?0??111????0?????????
000????1?0000000????????1111??

Meniscotherium

00??1????00210000400004000010001101100?100?011?????11?0?1???2??0101
110110?11??0101?????0?1?001?01??01100??????1?1?112?0?0020? - 1?11?1?
011?21?111011211??1?10??110?11????????20??01????????1?????????????
?1?2110??0??00?00??1?1010?????0102221??10????????0 - ?10?0021101210
1?0?0000010011?0211?111110??101[01]?0?0?[01]0110101101100?12??00?21
000?00?00000??01?0001000??1?000000?100?0??00001?011010??1000010??
??212011?100??0?0??10?000000?10?0010?1?000?01101011?100100??00?011
0?1?01?????0??001?1000020?011?10?????01??00?0??1??????0??011110111
002011111??0?02?01111?10010110121?1?0010000??2?00?001??00???????
1000????1?0011020??001001111??

Miacis

00??10????00210000000000000010?00100100?1?10101?????0??0?1???1??0001
00300??00??110??????0?1?000?1??00000??????1?0?212?0?00201?1?01?1?
011??0?1110012101?0111? - 0? - ?????????????20??001??1??1??????????????
??1?2110??0??10?00??1?0010?????01011001?10????????00?01??[01]?10100
?101?0?00?????111?????1?1?1??????01??2??10?10????????????????00?
???0?????????10?100000011?1?0000?00??0110?110?1?0110111?1000010???
?21[23]011?101??0??0??10?000010?1110000?1?000?011010?1?1?000??1?[012
]0110?1?0?????00?0000010000210000?11????01??00????????????0???????
???0010????????0??0000????000????????1?????000?????????????????
????????????????1????????????????

Vincelestes

00??10????00110000000000000010000000100?3010????????0??0?1???1??1?1?
11000??00??1????????0?1?01??1??????00??????1?1?010?0?00101?0000000
1?1?21??1100101????0010? - 0????????????000?00??1??1??????????????
???0110??0??13?00??0?00??????00?1000000??????????01??0321100110
010?1100010110?0001?0?10000?0001?0?0?0000?00?01000?00?0000?10000?
00000000??000000000000?1?00000??100010?10000?0000000001??00????000
000?000??01001?0??0?1?00?0100000?1?000?000000?00000000??00?0000?1?
00000000?00000001??000000?0??0?0000000100000??00000?000?0100?0000
0010????0??00000000?00000000000?0?0?0?000??0????0?1??00????0??1000
????1?1?000001110 - 00?1111??

Zhelestes

00??1????0????????????????001001?0?0?11?00????010?0?1???1??0000
001110????0010??100?0001??01??01????????1?0?212?002121011?01?1?
0[01]1?21?1110012101?0111????????????????20??101?????????????????
???0?2100??0??03?00??1?1110?????01112202011????????00?10??0120?0?1

0010?0002000010?0101?1311120??001??2?0?00111001110100?10?0000?111??
?01000101??111100100011?1?000110011000??11110?011010111000010??02
12010?100??0100??10?010000?1110000?1?010??1110211?1?1010??0?[01]0111
?1?00[01]101?0?0001?001??201010?0?101?0110001011111?1??01?01111?11[
01]101011111??0??10000110?00001110000?1?0010000??2?10?1?0??01?????
??1011????2?0011100???????????????

Pucadelphys

00??10??00000000000000000010100100100?2?10110????0?0?1??1??1?1?
11000??00??001[01]????0?1?01??1??00000??????0?0?111?0010100101000
1?000122?1010110101?0111??1?0?10??????20??101??1??1??????????
?????2110??0??00?10??1?1110?????01201202111??????00?10??01301002
10000?0011000111?0101?1?111[01]0??0011?0?0?0011000110[01]000?10??0000
011??00000001??100100000001?1?010?0??020110?100?0?0111?100100000?
???0111?0??101??0101??10?011?00?011000101?1?1?101100002100000??10?0
100?1?01??1?0?00000001??11000?0?000??10100?0110?01????01?1100000
10000011100??0??10000110??0??0000020?0?0001000??????11??00?????
??1000????1?00100001100000?1111??

Purgatorius

00?0????00?1????300?0?1?0??0????00100?1????????????????????010[0
1]002[01]0??000?0100?? - - 0?1?00111?0?001100?????1?00212000[12]0201?
1?01?1?011?2[12]?11100101011011110100011????????101?12??0100110000
? - ? - - - 0?0 - 0021?0020?0001020????10100?00?01012200110??????000000
??03200????????????????????0??1????????????????????????????????
??
??
??
??
??0??1100?110?00
????01??1?1001100011?11100000[01]01111??

Rhombomylus

00??11??011430001221 - 121131 - - 01 - - 1 - - - ?3?0????????11?111?????
?01[01]0001011?00??0??????0?00101?01?00200??????1?1?203?1??????
??0????1?1??2?01?1?12?1??0011? - 1?0??????????20??02??1????1?????
????????????111??1????????????110?????01212100111??????00?00??03[1
2]100011001100002100000?0201?1111120??011?2?0?0011000111110??0??00
0?200??01000000??1110[01]0110010?1?000010011010??02000?01101111110
1011??02120[01]0?102??10?01?11?001?01??[01]1000101?????11110[12]11?1?
100??0?10120?0101??1??0?1001?001??2100[01]0?11021?11000000110101?1?
??01????1??1??0?1?1?101??0??00001110??0??110021?1?0110000??2?10?0
?0??01??????1110????1?0010120??????????????

Rhynchocyon

00??1??10051 - ?? - - - 1031000?10000010000100?011?????10?101??2??0
001002011?00??1001?????1?00[01]01?01??01200??????2??003?1?????????
01?011?1??2?11?0012?01?0011? - 0? - ???????????20??011??1??1?????????
??????????1????0??03?01??1?10??????0112221??11??????00?0??0120

00?0020100110000?010200011[01]00[12]01?111?11012101000000001101010011
00002?0000111001?[01]10001001011110000000?0 - 1?010 - 010???0100010012?
?10110010000100?00212?110101??00?000100000000?1111000?1??00?01?1?0?
??110??00000?011001?0?????000?00001000010?011111???001??00?0??????
01?1??00111100?0?0?011100??11??100001101100?1100000?1?0010000??[12]1
100011??110000?2110?10100111000011110100000111100

Baioconodon_nordicum

00?01?????????????????????????0????00100100?[12]?0???????? - 1100?001120000
00001110000000?????? - - 111?[01]01101[01]001[01]0012?02?21?11212000[01]0
20001?01?01011?11?101001010100112101000110????????00110210001001000
011121?00?0 - 0021100200000[01]0001011110?100100111[12]20001000010??000
0100?0110100110000?000?02001010101?121?11????01000?0000????0??11?00
??????0??11?01?010001??0001??0?00?00??000010 - ?11??????0?0?11??1011
??1?000??????120111100??0??001100010100?10?0010?1?000 - 0110?0??110
??00000?????01?0001??0?0?0000100001100[01]000?????01?00?0??1?????
10?0??
??0????1111??

Oxyprimus_erikseni

00?0??1?0???????? - ??????????????
???????????????????? - - 1?1?0????????????????????1?1111200010201?1?01?1
?011?11?1010010101101??111000100????????001102100000000000110?1000?
0 - 0021?0??0??00?00??1?1010?????01012201110????????0001?0?????????
??
??
??
??
??
??
??
??
??

Protungulatum_donnae

0000?????????????????????????010?001001?0?1?0????????1000?0011200011?
00111000002010010? - - 111?0011010?0000012312?21?112120001020001?01?1
?011?11?101001010110112111000100????????0010021000000000010001?00?
0 - 002110010000010000?1110101000?01[01]1[12]20211011010??0000100?0[12][
12]0100210010?0102010010?0101?111????????????????????????????????
??01?01??????
??0?1?000?0111?0?1?10??0??
????11??001?0100?1001?10000????????????????1?000??110111?1??0??????
??0??2110?011??11000
0?2100?10?001000010120101?????1111??

Pantolambda_bathmodon

00?010????0021100[03]200002000010000100110?1?0?000???? - 1100?00??2??01
1?001110100?010[01]?? - - 1?01001?01??00110?1111111?20112?00[01]0201?
[01]011?1?011?01010101101012011210100?11????????0011011??01?01????
????????????0021000?0?00?00??2?10????????01012[12]01110????????000100

?00[01]1100311000?010202001011111?121?1001110100000000110100?0110000
??0000111001?000001001010110??0?00??001? - - 010??00??0010001??1011?
110000100?002122101100??00?001101000000?10?0010?1?000 - 0??100[12]1 - 1
101?01000?0110002000101000?00001000011001010?0211010000?011?2??00?
00?00?1110????01011100??01??10000110100001110010?1?0110000??2110?01
1??01000002101010?000000000020?????????1111??

Carcinodon_olearyi

00?0???10????????? - 1000?001120000[0
1]000100?000020?????? - - ??????0011?0?0101?12?02?01?101120001020001?0
1?01011?11?1010010101001??111100110?????????0010011000000110001[01]02
1?00?0 - 0021100300000000000?11010?0?00?011120001000010??0000110?????
???
???
???
???
???
???
???
??000001111??

Triisodon_quivirensis

00?011???? - ????????? - ??????????00100100?1?0?001???? - 10011001120000
1?00100?000010101??? - - 111?10011?0?011111301111?102120001020001?01
?01011?01?1010010101001??111001110?????????0020011000000[01]00011?021
?00?0 - 00211103000?010000?0100100000?01112000100?010??0000110?0?211
00??0000?0??0??0??0?1201??1??101??0011???
???
????????????????01???
???
?????????????????1??100??11????????????????????????????0??0??210?????????????????
????????????????????????????????????0001111??

Dissacus_navajovius

00?0?????01????????00??1000010?00100100?1?0??01??0 - - 100100011200010
100[12]00?0010[12]0101??? - - 101?10001?0?0131111302311?101120001020001
?01?01001?01?1010010100000?0?0? - ?? - - ???????002100110[01]00[01]000
0?0? - ? - - 0?0 - 002111030?00310000?01010?0?00?0121121??0?????????000
0010?0??0001???
???
????????????????????????????01???
???
????????????????????????????????10????0?000011101?0??1100????????????00??2010?010?
?111000?0100?111100100010121?????????1111??

Alticonus_gazini

00?1???1????????????1000?0110210001?
00[12]00?0110201001????11?000200110010102??1111?11?120001020001?01?
1?001?11?1010010101001??111110111?????????001101?000000[01]0000110?10
00?0 - 00?1?0200001100011101111110?0111220[01][01]1000010?0000100?0?

1?1????????????????????0101??
??
??
??
??
??
??1111??

Ampliconus_browni

00?1??1??????1?0??00?????1000?0110200001?
003110000020?????? - - 011?1001[01]0100011102?01111?112120001020001?01
?1?011?12?11 - 001010100111111101111????????00110210000?0000?01200100
101?002110020000310001101010?0?00?0111100[01]1010000?0000010?0???1
??210??0??
??
??
??
??
??
??
??
??

Anisonchus_sectorius

00?[12]??1?0????????? - 1100?010?20001
1?002110000030??000? - - 12[01]0001200110001101301111?1121200?0120001?
[01]1?1?011?12?101001010000011[01]1[01]110111????????00210211101102101
112001100?0 - 00211002010030000110101101[01]0100111120101010000??00001
00????01??
??
??
??
??
??
??0??21110110??1
10000??

Conacodon_entoconus

000210??1?0?00??0 - - 0?00?1?10200001
?00311000003110010? - - 0?1?01??1?11001[01]101301111?112120001120001?[
01]1?01011?12?1110010101001??[01]11111110????????00100222101002000013
000210?0 - 102110000100200001111010?1[01]0100111220111[01]210?1??000010
0?0110????10??0????????????????011????????????011????????????????
????????????????01?00100??0??
????????????????????00????????10????????????????????????????????
??
??
??
??000?0?11??

Ectoconus_ditrigonus

00?310?????0210??[03]0000??0001??00101100?1?0?0011011 - 1100?011021101
1?0011100[01][01]020100110 - - 0?01100101100[01][12]1101301111?1121200010
20001?10101010112?101001010100112111110110????????00210210001002100
11210[12]001121002100000000200001001[01]0[01]1111101111201010000?1??0

101110010?0102000011?0?01?1211100??1012?1?0?11110101101100?10?00002
111???00000101???011000000001?1?1???00?101011?10100?011011111001010
???1212010?110??00?0??10?010000?011?00101?000001110021?100001?0?[01
2]??10?1?001?0100?1001?101??11010?0?001?01100010111101?1??01??111?
???00020111110??0??00001110?00010100021?1?00?0010??2?0??0?00??01??
????1010?????1?001121010100100111100

Deccanolestes

00????????????????????????????????0????????001??1?11????????10?0?00??2?????
????????????001?????0?1?0??01??010?0?????????0?21?00010101?0?01?1?
010[01]21?1110010101?0111101?021001?0?0?1?10??11?01??1??0 - 0?????00
??? - ?21?00?0??00??0??1?00100????01012[12]00110??000??00000??012???
????????????????????010??
??
??
??
??
??
1010?????0?0011100??1000011110?

Kennalestes

00??10??00[012]1?0000001000?0?00000000001011010?????10?0?1???2??0
000002110?00??0001?????0?1?01??1??01001??????1?0?2110002021000001
?1?010001?0110010101?0111??1?0?11?????????10??011????????????????
??????2100??0?03?00??1?0110?????01002100110?????????00?00??0120100
210010?01020001??0101?1111100??0011?0??0?10?101111100?0??00?110
??[12]00?00001??10?10000000??1??001100?????000?011011?01?01?11?
???11300??100??0??0??1?01011??0?000101?1?00011100?1?100000??00??
1??1?1??0[01]00?1001?11000?00011?0??1??000000?0111111?1??0??110??
??
????????????????????????????00??0111100

Maelestes

00??10??00?1?????????0?100??1?00[01]00100?0?11000?????010?111??2??00
00002110?00?0101??110?1?01??1??00001?130??110?2120002120001?01?
1?000001?011001010??0111110??1??1?1?????10??101??00?01??0?[01]?0??
?0??0021000?0??03?000??2?1110?????01002101111[01]10?0??000000??0230
100210010?1102000110?0101?1??100??0011?????0??10??1000??????1??
210??[12]00100001??1101[01]0000001??0[01]000?????0??01??011011?01
101111?????[23]????110??0??0??10?011?10?00?000101?000?011100?021100
00??00?0010?1?101?0100?10000110012000[01]1?0?0?0??000??10111111??100
01?100010??????0010????0??00001110??????????????????????????????
??1010 - 000111100

Prokennalestes

00????????00?0????????0?????0??0????000??0?11????????10?0?1??1?00[01
]000100?00??0000??00[01]?1?010?1??0000[01]?130111110?[12]11000001100
0000000010001?0000010001?01111?100?10??[01]?[01]??10?00??0[01]??[01]
???0?0?????00?? - 021000?0?003?00??1?00100????00?02100110??0?0??000

000??0110101110010?110200011??0100000??????0011?????????????????
?????????????????????0?0???0110[01
]???101?000?0011?0?0111
0000?????0110?1?00010000?00000?01??00?????????????????1?000??11???1???0?
??
???1[01]0000011110?

Zalambdalestes

00??10???00[23]1100110?212112121000001101?[12]?11010?????11?1100??2??
000000200??00??1000?????0?1?000?01??01000?130???1?0?212?000020001?0
1?1?001??1?1100121???01111?1??1?01?1?1?1?20??01??01??1??0?0?????
00??? - ?21100?0??00?000??2?21100?????01212202111??????000000??011010
1110010?[01]102000110?0101?1311100??0011?0?0?0110?10??01001?01?000??
1[01]0??[12]01000001??1101[012]0011010?1?0000000110011?11[01]00?011011
001100111???011300??100??0110??11?010110?00?000101?1?0001110011?100
000?00?0010?0010110[01]00?1001?11001200000?0?011?010000?111???1??00
101????00?11?????11??????0??0??0?????????????01?????1?00?0??[12]?2?0??
??0??01???????101???????1?112?011101000111100

Characters in the matrix of the current study. Underlined are the characters I added to the Shelley_2020 matrix.

Ch. 0 Teeth present absent

Ch. 1 Teeth types differentiated into morphological types incisors canines premolars molars with enamel homodont simple peg like teeth without enamel

Ch. 2 Tooth enamel presence of Hunter Shreger bands absent present

Ch. 3 Tooth enamel crenulations enamel textured but lacks regular crenulated pattern enamel features fine crenulations enamel crenulated with regular apicobasally aligned ridges enamel very strongly crenulated with deep regular apicobasally aligned ridges

Ch. 4 Upper diastema between ultimate incisor and canine presence absent present

Ch. 5 Upper diastema between incisor and canine size narrow between incisor and canine enlarged

Ch. 6 Upper diastema between canine and premolar presence absent present

Ch. 7 Upper diastema between canine and premolar size narrow wide more than one tooth length

Ch. 8 Dental eruption timing vs. cranial growth early late

Ch. 9 Diastema behind lower incisors absent or narrow enlarged

Ch. 10 Incisor shape root and crown are straight and continuous in length root and crown forms a continuous curve

Ch. 11 Number of upper incisors 5 4 3 2 anterior 1 anterior none or 1 2 small posterior

Ch. 12 Number of lower incisors 4 3 2 1 none or small posterior

Ch. 13 Position of upper anteriormost incisors or alveoli contacting or closely approximated on the midline separated by broad gap

Ch. 14 Anteriormost upper incisor procumbent absent present

Ch. 15 Second anteriormost upper incisor projecting anteriorly absent present

Ch. 16 Upper incisor size subequal anteriormost is the largest close to twice the size of the following incisors second anteriormost incisor is the largest close to twice the size of the adjacent incisors third incisor is the largest close to twice the size of the adjacent incisors

Ch. 17 Anteriormost upper incisor shape conical mediolaterally compressed anteroposteriorly compressed cusped one major and one minor spatulate

- Ch. 18** Upper anteriormost incisor root closed and rooted hypsodont in premaxilla only hypsodont extending into maxilla hypsodont in maxilla
- Ch. 19** Enamel distribution on upper anterior dentition incisors surrounds tooth discontinuous posteriorly
- Ch. 20** Ultimate upper incisor in premaxilla between premaxilla and maxilla in maxilla
- Ch. 21** Lower anteriormost incisor size small subequal to subsequent incisor greatly enlarged reduced smaller than subsequent
- Ch. 22** Anteriormost lower incisor shape conical mediolaterally compressed anteroposteriorly compressed cusped one major and one minor spatulate
- Ch. 23** Lower anteriormost incisor procumbency absent present
- Ch. 24** Lower anteriormost incisor growth closed and determinate open and indeterminate ever growing
- Ch. 25** Lower anteriormost incisor root length not extended posteriorly below p1 extending posteriorly below p1 extending posteriorly below penultimate or ultimate premolar extending posteriorly below molars
- Ch. 26** Lower anteriormost incisor enamel covers whole incisor discontinuous posteriorly
- Ch. 27** Shape of incisor arcade transverse U shaped sharply angled at first incisor or parallel sided
- Ch. 28** Lower posterior incisor procumbent absent present
- Ch. 29** Staggered lower third incisor i3 absent present
- Ch. 30** Upper canine presence present absent
- Ch. 31** Upper canine size enlarged small
- Ch. 32** Upper canine roots two one
- Ch. 33** Lower canine presence present absent
- Ch. 34** Lower canine size enlarged small
- Ch. 35** Lower canine roots two one
- Ch. 36** Canines diverging externally uppers and or lowers absent present
- Ch. 37** Lower canine procumbency absent present
- Ch. 38** Deciduous canine present absent
- Ch. 39** Number of premolars five including retained dP3 four three two or less
- Ch. 40** dP1 dp1 dP2 dp2 replacement present absent
- Ch. 41** Tall trenchant premolar presence absent present

- Ch. 42** Tall trenchant premolar position in ultimate premolar position in penultimate premolar position
- Ch. 43** First upper premolar P1 procumbency absent present
- Ch. 44** First upper molar P1 number of roots one two three
- Ch. 45** First upper premolar P1 posterior diastema absent present
- Ch. 46** First upper premolar P1 protocone presence absent present
- Ch. 47** First upper premolar P1 protocone small swelling or ridge discrete cusp
- Ch. 48** Second upper premolar P2 protocone presence absent present
- Ch. 49** Second upper premolar P2 protocone size small swelling or ridge lacks basin discrete cusp with basin
- Ch. 50** Third upper premolar roots only for taxa with five premolars and retaining p3 P3 one two
- Ch. 51** Penultimate upper premolar P4 protocone presence absent present
- Ch. 52** Penultimate upper premolar P4 protocone development small lingual bulge large and basined
- Ch. 53** Vertically developed cylindrical parastyle separated from paracone by a deep vertical sulcus on labial edge of upper cheek teeth absent present
- Ch. 54** Penultimate upper premolar P4 metacone presence absent or vestigial present
- Ch. 55** Penultimate upper premolar P4 metacone development large swelling
- Ch. 56** Penultimate upper premolar P4 parastylar lobe presence present absent
- Ch. 57** Penultimate upper premolar P4 parastylar lobe development well developed and prominent lobe expanded lobe but not prominent
- Ch. 58** Penultimate upper premolar P4 metastylar lobe presence absent present
- Ch. 59** Penultimate upper premolar P4 metastylar lobe expanded lobe but not prominent well developed prominent lobe
- Ch. 60** Penultimate upper premolar P4 roots one two three four
- Ch. 61** Penultimate upper premolar P4 paraconule absent present
- Ch. 62** Penultimate upper premolar P4 metaconule absent present
- Ch. 63** Ultimate upper premolar P5 protocone presence present absent
- Ch. 64** Ultimate upper premolar P5 protocone size smaller than paracone approaches paracone in height
- Ch. 65** Ultimate upper premolar P5 metacone presence present absent

- Ch. 66** Ultimate upper premolar P5 metacone size swelling metacone connate to paracone large metacone and paracone distinctly separate
- Ch. 67** Ultimate upper premolar P5 parastylar lobe presence present absent
- Ch. 68** Ultimate upper premolar P5 metastylar lobe presence present absent
- Ch. 69** Ultimate upper premolar P5 parastylar and metastylar lobes relative size absent or vestigial subequal parastylar larger metastylar larger
- Ch. 70** Ultimate upper premolar P5 precingulum absent present
- Ch. 71** Ultimate upper premolar P5 postcingulum presence absent present
- Ch. 72** Ultimate upper premolar P5 postcingulum height lower than protocone level with protocone
- Ch. 73** Double V shaped penultimate and ultimate upper premolars paracone and protocone V shaped absent present
- Ch. 74** Ultimate upper premolar P5 paraconule presence absent present
- Ch. 75** Ultimate upper premolar P5 metaconule absent present
- Ch. 76** Ultimate upper premolar P5 endocingulum absent present connect pre and post cingulae
- Ch. 77** Penultimate upper premolar P4 length compared to ultimate upper premolar P5 P4 is much shorter P4 P5 length 0.7 P4 is somewhat shorter 0.7 to 0.84 P4 is subequal to P5 0.85 to 0.99 P4 is longer than P5 1.0
- Ch. 78** Ultimate upper premolar P5 size occlusal surface area to M1 smaller or subequal larger
- Ch. 79** First lower premolar p1 roots two one
- Ch. 80** First lower premolar p1 orientation in line with jaw axis oblique
- Ch. 81** Diastema separating first and second lower premolar absent gap less than one tooth root present subequal to one tooth root diameter
- Ch. 82** Second lower premolar p2 talonid heel absent present
- Ch. 83** Second lower premolar p2 metaconid presence absent present
- Ch. 84** Second lower premolar p2 metaconid size present as small swelling or ridge appressed against flank of protoconid present as a distinct cusp
- Ch. 85** Third premolar p3 size only for taxa with 5 premolars longer than p2 shorter than p2
- Ch. 86** Third lower premolar dp3 number of roots two one
- Ch. 87** Penultimate lower premolar p4 paraconid absent present

Ch. 88 Penultimate lower premolar p4 paraconid development small subtle swelling or cuspid on prominent anterior shelf small cusp enlarged cusp

Ch. 89 Penultimate lower premolar p4 metaconid presence present absent

Ch. 90 Penultimate lower premolar p4 metaconid development swelling or metaconid connate appressed to paraconid metaconid and paraconid distinctly separate

Ch. 91 Penultimate lower premolar p4 talonid cusps one cusp two cusps three or more cusps talonid consists of single central mesiodistally aligned blade

Ch. 92 Ultimate lower premolar paraconid presence present absent

Ch. 93 Ultimate lower premolar p5 paraconid height low less than half the height of the protoconid high half the height of the protoconid or more

Ch. 94 Ultimate lower premolar paraconid size small cuspid or swelling evident. Score applicable to taxa with a prominent anterior shelf where small prominence is evident but hard to discern strong cusp discrete but small cusp in relation to other cusps enlarged cusp

Ch. 95 Ultimate lower premolar p5 metaconid presence present absent

Ch. 96 Ultimate lower premolar p5 metaconid development swelling metaconid present as a small bulge on posteromedial side of protoconid present as a distinct and separate cusp present but reduced to lingual ridge

Ch. 97 Ultimate lower premolar p5 postmetaconid cristid presence absent present

Ch. 98 Ultimate lower premolar p5 postmetaconid cristid development small cristid present but does not descend to talonid cristid present and descends to talonid

Ch. 99 Ultimate lower premolar p5 talonid presence present absent

Ch. 100 Ultimate lower premolar p5 talonid width narrower than anterior crown as wide as anterior crown

Ch. 101 Ultimate lower premolar p5 talonid cusps talonid basined or at least non trenchant with one cusp basined with two cusps evident basined with three or more cusps evident talonid trenchant and consists of single central mesiodistally aligned blade

Ch. 102 Ultimate lower premolar p5 anterolingual cingulid absent present

Ch. 103 Length of ultimate lower premolar p5 longer than penultimate more than 1.25 times longer subequal no more than 1.25 times longer or less than penultimate

Ch. 104 Ultimate lower premolar p5 width wide length width or 1.4 narrow length width or 1.4

Ch. 105 Size area of upper molars M1 vs. M2 M1 is much larger more than 120 larger both teeth are subequal 80 120 M1 is much smaller less than 80

Ch. 106 Size area of upper M2 vs M3 M2 is much larger more than 120 both teeth are subequal 80 to 120 M2 is much smaller less than 80 M2 is much larger more than 120

Ch. 107 Size area of upper molars M1 vs. M3 M1 is much larger more than 120 larger Both teeth are subequal 80 120 M1 is much smaller less than 80

Ch. 108 Size area of lower molars m1 vs. m2 m1 is much larger more than 120 larger teeth are subequal 80 120 m1 is much smaller less than 80

Ch. 109 Size area of lower m2 vs m3 m2 is much larger more than 120 both teeth are subequal 80 to 120 m2 is smaller less than 80 m2 is much larger more than 120

Ch. 110 Size area of lower molars m1 vs. m3 m1 is much larger more than 120 larger teeth are subequal 80 120 m1 is much smaller less than 80

Ch. 111 Number of upper molars four three two

Ch. 112 Number of lower molars four three two

Ch. 113 Molar cusp form secodont bunodont selenodont zalambdodont

Ch. 114 Molar cusp convergence erect cusp form may be conical or more blade like converge apically tend to be more conical in form

Ch. 115 Upper molar M2 shape as long as wide or longer square mesiodistal length mesial labiolingual width 1.0 wider than long length more than 75 and less than 99 width much wider than long transverse length less than 75 width

Ch. 116 Upper molars styler shelf presence absent present

Ch. 117 Upper molars styler shelf width present and 50 or more of tooth width present but less than 50 but more than 25 present but less than 25 absent

Ch. 118 Upper molars styler shelf development continuous around buccal surface of tooth discontinuous

Ch. 119 Upper molars parastylar lobe presence present absent

Ch. 120 Upper molars metastylar lobe presence present absent

Ch. 121 Upper molars metastylar and parastylar lobes relative buccal extent parastylar more buccal lobes subequal metastylar more buccal

Ch. 122 Upper first molar M1 parastylar lobe position to paracone anterolabial to paracone anterior to paracone

Ch. 123 Upper second molar M2 parastylar lobe width measured to stylocone or stylocone position more than 30 total width less than 30 but more than 20 20 or less

Ch. 124 Upper molar preparastyle presence absent present

Ch. 125 Upper molar styler cusp A parastyle presence present absent or vestigial

- Ch. 126** Upper molar stylar cusp A parastyle size subequal to larger than B distinct but smaller than B
- Ch. 127** Upper molar stylar cusp B stylocone presence present absent or vestigial
- Ch. 128** Upper molar stylar cusp B stylocone size to paracone smaller but distinctive subequal
- Ch. 129** Upper molar stylar cusp C mesostyle presence absent present
- Ch. 130** Upper molars stylar cusp D presence present absent
- Ch. 131** Upper molar stylar cusp D size smaller or subequal to B larger than B
- Ch. 132** Upper molar stylar cusp E metastyle presence present absent or vestigial
- Ch. 133** Upper molar stylar cusp E metastyle size directly lingual to D or D position distal to D or D position
- Ch. 134** Upper molars preparacingulum presence present absent
- Ch. 135** Upper molar preparacingulum development interrupted between stylar margin and paraconule continuous between stylar margin and more lingual cingulum exact one characterised later
- Ch. 136** Upper molar ectoflexus presence present absent
- Ch. 137** Upper molar ectoflexus development present only on penultimate molar M2 on penultimate and preceding molars M1 M2 present on all molars present on M2 M3
- Ch. 138** Relative size of metacone and paracone on M2 metacone noticeably smaller than paracone metacone and paracone subequal metacone larger than paracone
- Ch. 139** Metacone position to paracone on M1 or M2 metacone labial approximately at same level metacone lingual
- Ch. 140** Orientation of the preparacrista on penultimate and ante penultimate molars and premolars in the case of molariform premolars deflected labially and tend to be aligned with or sub parallel to paracone protocone axis shifted anteriorly forming a distinct angle with paracone PROTOCONE not metacone axis
- Ch. 141** Upper molar paracone and metacone bases meet at base or closely adjoined distinctly separate but may be connected by a centrocrista
- Ch. 142** Upper molar preparacrista strong from labial edge of paracone to stylocone or stylar shelf weak from base of paracone or absent
- Ch. 143** Upper molar cuspsate preparacrista presence present absent
- Ch. 144** Upper molar centrocrista presence present absent
- Ch. 145** Upper molar centrocrista shape in occlusal view straight V shaped

- Ch. 146** Upper molar postmetacrista presence absent present
- Ch. 147** Upper molar postmetacrista development prominent and extends from side of metacone to metastyle salient expanded posterolabially weak from base of metacone or absent
- Ch. 148** Upper molars postmetacrista cusplate cusplate not cusplate
- Ch. 149** Upper molars preprotocrista presence present absent
- Ch. 150** Upper molars preprotocrista extent does not extend buccally beyond paracone does extend buccally beyond paracone
- Ch. 151** Upper molars buccal edges of paracone and metacone distinctly swollen slightly convex flat to concave
- Ch. 152** Upper molars postprotocrista presence present absent
- Ch. 153** Upper molars postprotocrista extent extends to mid lingual surface of metacone extends to distal surface of metacone
- Ch. 154** Upper molars postvallum wear presence absent present
- Ch. 155** Development of postvallum wear extent Present but only by the first rank postmetacrista Present with second rank wear postprotocrista below postmetacrista but the second rank does not reach labially below the base of the metacone present with second rank wear extending to metastylar lobe metacingulum
- Ch. 156** Upper molar paraconule presence absent present
- Ch. 157** Upper molar paraconule position prominent closer to protocone prominent midway or closer to paracone
- Ch. 158** Upper molar metaconule presence absent present
- Ch. 159** Metaconule position closer to protocone midway or closer to metacone
- Ch. 160** Upper molar metaconule mesiodistal position approximately in line with protocone and metacone positioned distal to line between protocone and metacone
- Ch. 161** Upper molar relative conule development conules subequal in size metaconule larger and more developed paraconule larger and more developed
- Ch. 162** Upper molar conular cristae presence absent present
- Ch. 163** Upper molar internal conular cristae present but indistinctive distinctive and wing like
- Ch. 164** Upper molar conular cristae development weak not as prominent as conules strong and high so more prominent than actual conules
- Ch. 165** Upper molar paraconule preparaconular cristae presence absent present
- Ch. 166** Upper molar paraconule preparaconular cristae development low high
- Ch. 167** Upper molar paraconule postparaconular cristae presence absent present

- Ch. 168** Upper molar paraconule postparaconular cristae development low high
- Ch. 169** Upper molar paraconule premetaconular cristae presence absent present
- Ch. 170** Upper molar paraconule premetaconular cristae development low high
- Ch. 171** Upper molar paraconule postmetaconular cristae presence absent present
- Ch. 172** Upper molar paraconule postmetaconular cristae development low high
- Ch. 173** Upper molar conular region width narrow less than 30 total tooth width moderate 30 50 total tooth width wide more than 50 total tooth width
- Ch. 174** Upper molar protocone presence present absent
- Ch. 175** Upper molar protocone development small without trigon basin small with distinct trigon basin larger basin somewhat expanded mesiodistally distal portion expanded
- Ch. 176** Upper molar protocone mesiodistal expansion absent subequal or smaller than paracone present protocone larger than paracone
- Ch. 177** Upper molar protocone procumbent absent present
- Ch. 178** Upper molar protocone apex buccolingual position no shift sits within lingual 10 20 of tooth width moderate shift sits within 21 30 of tooth width from lingual edge substantial shift positioned more than 31 of tooth width from lingual edge creating shallow lingual protocone slope
- Ch. 179** Upper molar protocone height low lower than paracone and or metacone tall approaching or subequal to paracone and metacone taller equal or higher than paracone and or metacone
- Ch. 180** Upper molar protocone apex mesiodistal position protocone apex positioned on mesiodistal midline of the tooth protocone apex shifted somewhat mesially closer to paracone but not to buccolingual axis of paracone axis protocone apex shifted mesially to buccolingual axis of paracone apex or further mesial
- Ch. 181** Upper molar protocone paracone crista absent present crista extends from protocone to base of paracone may extend onto flank of paracone
- Ch. 182** Upper molar precingulum presence present absent
- Ch. 183** Upper molar precingulum extent labial edge of the precingulum lingual to paraconule labial edge of precingulum and reaching buccally passed paraconule
- Ch. 184** Upper molar secondary precingulum presence absent present second precingulum positioned dorsal to first
- Ch. 185** Upper molar postcingulum presence present absent
- Ch. 186** Upper molar postcingulum extent remains lingual to metaconule extending buccally passed metaconule but not to buccal margin extending to buccal margin

Ch. 187 Upper molar postcingulum morphology thin shelf may be narrower than hypocone if present thickened shelf along entire length may be as deep or near as deep as hypocone region

Ch. 188 Upper molar postcingulum position lower than protocone subequal in height to protocone

Ch. 189 Upper molar secondary postcingulum presence absent present

Ch. 190 Upper molar metacingulum and postmetaconule wing development metacingulum and postmetaconule wing form continuous shelf exclusive to postcingulum metacingulum and postcingulum form a continuous shelf which may or may not be interrupted by postmetaconule wing

Ch. 191 Upper molar hypocone presence absent present

Ch. 192 Upper molar hypocone lobe development swelling or small cusp on postcingulum enlarged to form distinct basal lobe that is smaller and does not extend lingually beyond base of protocone base of hypocone extending lingually beyond base of protocone but protocone maintains lingual exposure base of hypocone enveloping base of protocone lingually

Ch. 193 Upper molar hypocone cusp number single hypocone cusp swelling ridge present on any molar present with two or more cusps hypocone with hypostyle on any molar

Ch. 194 Upper molar hypocone lobe postcingulum development along tooth row equally or near equally developed on all molars increases in size and development posteriorly along tooth row decreases in size and development posteriorly along tooth row

Ch. 195 Upper molar hypocone mesiodistal position mesial to metacone directly lingual to metacone distal to metacone

Ch. 196 Upper molar hypocone lobe shape hypocone lobe cylindrically expanded base is roughly subequal to apex in size hypocone lobe base expanded with swollen bulbous base inverted cone shape hypocone base massive i.e covers protocone slope

Ch. 197 Upper molar crest extending between hypocone and protocone absent present

Ch. 198 Molar protostyle pericone presence absent present

Ch. 199 Molar protostyle pericone development small swelling or cusp smaller than hypocone large cusp subequal in size to hypocone

Ch. 200 Upper molar precingulum protostyle development precingulum forms a narrow shelf along its entire length precingulum forms a deeper shelf and maybe slightly swollen in the position of the protostyle but cusp is lacking similar in to postcingulum precingulum present as prominent shelf with protostyle subequal to postcingulum

- Ch. 201** Upper molar protostyle mesiodistal position distal to paracone directly lingual to paracone mesial to paracone
- Ch. 202** Upper molar pre and postcingulum separate continuous so as to form an endocingulum
- Ch. 203** Upper molars number of roots excluding ultimate molar three four more than four
- Ch. 204** Ultimate upper molar number of roots one two three four or more
- Ch. 205** Upper molar lingual root position supporting paracone supporting trigon
- Ch. 206** Ultimate upper molar width to penultimate subequal smaller
- Ch. 207** Ultimate upper molar metastylar lobe absent present
- Ch. 208** Presence of a crochet oblique loph joining the ectoloph or centrocrista to the metaloph or posterior edge of molar between metacone and protocone absent present
- Ch. 209** Lower molar shape very wide m1 length distal width 1.20 wide or to 1.20 and 1.35 narrow or to 1.35 and 1.50 very narrow or 1.50
- Ch. 210** Lower molar paraconid presence present absent or vestigial
- Ch. 211** Lower molar paraconid development along tooth row present and subequal on all molars decreases in development posteriorly along molar series increases in development posteriorly along molar series
- Ch. 212** Lower molar paraconid position relative other trigonid cusps paraconid forms distinct cusp separate from metaconid and or protoconid paraconid may be evident as a relatively large cusp or swelling but tightly appressed against mesial flank of metaconid or protoconid
- Ch. 213** Lower molar paraconid height paraconid shorter than metaconid subequal to metaconid paraconid taller than metaconid
- Ch. 214** Lower molar paraconid position Paraconid positioned on lingual margin Paraconid offset from lingual margin but still closer to lingual side than centre Paraconid closer but not directly on mesiodistal midline of tooth Paraconid on mesiodistal midline of tooth
- Ch. 215** Lower molar paraconid projection erect projects anteriorly
- Ch. 216** Lower molar mesiolingual vertical crest of paraconid rounded forming a keel
- Ch. 217** Lower molar paracristid notch notched continuous mesiolingual curve without a notch forms distinct mesially directed crest that rises mesiodorsal to protoconid without a notch
- Ch. 218** Lower molar premetacristid presence absent present
- Ch. 219** Lower molar postmetacristid presence absent present

Ch. 220 Lower molar postmetacristid development does not off talonid basin strong so as to close off or nearly close off talonid basin

Ch. 221 Lower molar trigonid configuration open paracristid protocristid angle more than 50 degrees more acute angle between 36 and 49 degrees anteroposteriorly compressed angle less than 35 paraconid absent or highly reduced resulting in wide open trigonid

Ch. 222 Lower molar talonid configuration elongate talonid cusp configuration with small angle less than 90 degrees formed by postcristid between the hypoconid entoconid and hypoconulid open talonid cusp configuration with a large angle 90 degrees or more

Ch. 223 Lower molar protoconid height tallest cusp on trigonid subequal to metaconid and or paraconid smaller than metaconid and or paraconid

Ch. 224 Lower molar protocristid orientation oblique transverse

Ch. 225 Lower molar mesiobuccal cingular cusp f presence absent present

Ch. 226 Lower molar mesiobuccal cingular cusp f development of shelf positioned on a distinct posteroventrally directed cingular shelf positioned on a shelf which continues along buccal border of tooth

Ch. 227 First and second molar lingual cingulid presence absent or weak present

Ch. 228 Lingual cingulid on lower molars development discontinuous may be restricted to only lingual flank of paraconid well developed along entire lingual margin of tooth

Ch. 229 Lower molar mesiolingual cingular cusp e presence absent present

Ch. 230 Ultimate lower molar lingual cingulid presence absent present

Ch. 231 Ultimate lower molar lingual cingulid development discontinuous well developed continuous cingulid

Ch. 232 Lower molar cristid obliqua presence present absent

Ch. 233 Lower molar cristid obliqua completeness incomplete does not reach trigonid wall metacristid may be present complete reaches trigonid wall

Ch. 234 Lower molar cristid obliqua termination at trigonid wall attaching lingual to notch in protocristid attaching at or labial to notch in protocristid attaching below middle posterior of protoconid buccally placed

Ch. 235 Lower molar trigonid height twice or more the height of talonid less than twice the height of talonid subequal to trigonid

Ch. 236 Lower molar trigonid to talonid length long more than 75 of total tooth length some shortening 51 75 of total total length anteroposterior compression of trigonid 50 or less of total length

Ch. 237 Lower molar Talonid width to trigonid width very narrow subequal to base of metaconid talonid narrower than trigonid talonid subequal to wider than trigonid

Ch. 238 Lower molar hypoconulid presence present absent

Ch. 239 Lower molar hypoconulid position in posteromedial position lingually placed with slight approximation to entoconid close approximation connate to entoconid

Ch. 240 Ultimate lower molar hypoconulid form short and erect tall and sharply recurved posteriorly procumbent

Ch. 241 Lower molar entoconid presence absent present

Ch. 242 Lower molar entoconid size smaller than hypoconid and or hypoconulid subequal to larger than hypoconid and or hypoconulid

Ch. 243 Lower molar m1 m2 entoconid position distolingual to hypoconid directly lingual to hypoconid mesiolingual to hypoconid

Ch. 244 Ultimate lower molar entoconid position distolingual to hypoconid directly lingual to hypoconid mesiolingual to hypoconid

Ch. 245 Lower molar entocristid presence present absent

Ch. 246 Lower molar entocristid development extends to the base of the distal wall of the metaconid to meet postmetacristid talonid basin enclosed lingually extends more mesioventrolingually on distolingual base of metaconid to lingual cingulid if present entoconid present but entocristid weak to absent talonid basin widely open lingually

Ch. 247 Lower molar entocristid denovo crest presence absent present

Ch. 248 Lower molar postentocristid height lower than hypoconulid higher than hypoconulid

Ch. 249 Lower molar postentocristid orientation oblique buccolingually transverse

Ch. 250 Lower molar hypoconid cristid obliqua denovo crest presence absent denovo crest present extending mesioventrally from hypoconid separate from crista obliqua

Ch. 251 Lower molar mesoconid presence absent present

Ch. 252 Lower molar hypolophid presence absent present

Ch. 253 Lower molar entoconid transversely expanded into entolophid and not connected to hypoconulid absent present

Ch. 254 Lower molar buccal postcingulid presence absent present

Ch. 255 Last lower molar length to penultimate lower molar subequal or larger smaller

Ch. 256 Lower molar hypsodonty presence absent present

Ch. 257 Lower molar hypsodonty degree of development high height of lingual distention below level marked by enamel root juncture at midline equals about 1 3 tooth width higher height of lingual distention below level marked by enamel root juncture at midline equal approx. 1 2 of tooth width

Ch. 258 Mandible number of mental foramina two or more one

Ch. 259 Mandible anteriormost mental foramen below incisors or anteriormost mandible below p1 or p1 position below p2 or p2 position more posterior

Ch. 260 Mandible posteriormost mental foramen in canine and anterior premolar region below penultimate premolar below ultimate premolar at ultimate premolar and first molar junction or more posterior

Ch. 261 Mandible depth of mandibular body shallow and long deep and short

Ch. 262 Mandible retromolar space between ultimate molar and coronoid process absent present

Ch. 263 Mandible coronoid process height higher than condyle even with condyle

Ch. 264 Mandible coronoid process width broad approximating two molar lengths narrow less than two molar lengths

Ch. 265 Mandible angle between anterior border of coronoid process and horizontal alveolar border of cheek teeth distinctly obtuse 135 145 degrees obtuse 110 134 degrees vertical 90 109 degrees acute tilted anteriorly less than 90 degrees

Ch. 266 Mandible coronoid crest presence absent or weak present

Ch. 267 Mandible coronoid crest thickness present and transversely thick hypertrophied and laterally flaring creating a deep masseteric fossa posterior to it

Ch. 268 Mandible ridge ventral to the masseteric fossa presence present absent

Ch. 269 Mandible portion of the mandibular ramus ventral to the masseteric fossa position dorsoventrally narrow crest or ridge with a dorsoventral height less than half that of the mandibular body dorsoventrally broad ridge or elevated area with a dorsoventral height more than half that of the mandibular body

Ch. 270 Mandible anteroventral extension of masseteric fossa onto mandibular body presence absent present

Ch. 271 Mandible anteroventral extension of masseteric fossa onto mandibular body extent extending anteriorly onto body below molars extending below ultimate premolar or anterior to this point

Ch. 272 Mandible labial mandibular foramen absent present

Ch. 273 Mandible. condyloid crest absent present

Ch. 274 Mandible posterior shelf of masseteric fossa absent present

Ch. 275 Mandible angular process projection posteriorly directed medially inflected posteroventrally directed posterodorsally directed

Ch. 276 Mandible angular process length length less than ramus length equal or greater than ramus length

Ch. 277 Mandible angular process shape in lateral view hook like with width in lateral view of base lesser than length hook like with width of base subequal to or wider than length plate like no hook distinct more or less rounded or sub rectangular triangular

Ch. 278 Mandible angular process apex vertical position low below the level of the alveolar plane elevated near or above alveolar plane

Ch. 279 Mandible anteroposterior position of the dorsal root of the angular process level with or posterior to the vertical level of the condyloid process anterior to the vertical level of the condyloid process

Ch. 280 Mandible condylar process peduncle presence present absent

Ch. 281 Mandible condyle shape ovoid wider than long with tapered ends cylindrical wider than than along with flat ends anteroposteriorly elongate as long as wide or longer

Ch. 282 Mandible condyle position to tooth row at approximately the same level or slightly above above by approximately one molar length above by two molar lengths or more

Ch. 283 Mandible mandibular symphysis shape tapered anterodorsal to posteroventral angle less than or equal to 60 degrees deep tapered anterodorsal to posteroventral angle more than 60 degrees

Ch. 284 Mandible mandibular symphysis posterior extent first premolar or p1 position or more anterior second premolar p2 or more anterior penultimate premolar p4 or more posterior

Ch. 285 Mandible mandibular symphysis unfused fused

Ch. 286 Mandible Meckels sulcus presence present absent

Ch. 287 Mandible Meckels sulcus position parallel to ventral border of mandibular body convergent with ventral border of mandibular body

Ch. 288 Mandible coronoid facet presence present absent

Ch. 289 Mandible mandibular foramen vertical position near ventral margin of dentary recessed dorsally from ventral margin but below level of alveolar plane at the level of the alveolar plane above alveolar plane

Ch. 290 Mandible mandibular foramen position dorsal to prominent oblique subpterygoid ridge present absent

Ch. 291 Septomaxilla presence present absent

- Ch. 292** Facial process of premaxilla posterodorsal process dorsal extent does not nasal posterodorsally does reach nasal
- Ch. 293** Premaxilla posterodorsal process posterior extent remains anterior does not extend beyond canine extends beyond canine and but not to frontal extends to contact frontal posteriorly
- Ch. 294** Posterodorsal facial process of premaxilla posterodorsal finger like process wedged between the maxilla and nasal not wedged lacks a finger like process
- Ch. 295** Paracanine fossa between posterior incisor and upper canine presence absent present
- Ch. 296** Paracanine fossa between posterior incisor and upper canine development distinctly excavated in the tooth row with a crest like lateral margin opened laterally but remaining on the tooth row opened laterally and dorsally expanded on the lateral edge of the rostrum
- Ch. 297** Lateral margin of paracanine fossa formed by maxilla formed by maxilla and premaxilla formed by premaxilla
- Ch. 298** Infraorbital foramen presence present absent
- Ch. 299** Infraorbital foramen number of openings multiple single
- Ch. 300** Infraorbital foramen position dorsal to penultimate premolar or more anterior dorsal to ultimate premolar or more anterior dorsal to first molar or more posterior
- Ch. 301** Infraorbital canal length long longer than greatest diameter of the anterior opening short shorter than or roughly equal to greatest diameter of the anterior opening
- Ch. 302** Width of nasals widest posteriorly sides sub parallel widest anteriorly
- Ch. 303** Shape ratio of the nasals length mean width nasals length less than or equal to five times their mean width nasals length more than five times their mean width
- Ch. 304** Nasal overhangs external nasal aperture present absent
- Ch. 305** Nasal of adults fused together but not to surrounding bones absent present
- Ch. 306** Naso frontal suture with medial process of frontals wedged between nasals present absent
- Ch. 307** Nasofrontal suture position posterior to or even with anterior edge of orbital rim well anterior to orbital rim
- Ch. 308** Nasal foramina present absent
- Ch. 309** Fronto maxillary contact on rostrum absent present
- Ch. 310** Anterior maxillary process of frontal wedged between the nasal and maxilla absent or vestigial present elongate and thin

Ch. 311 Preorbital length relative to postorbital length less than one third of the total length more than one third of the total length

Ch. 312 Lacrimal present absent

Ch. 313 Facial process of lacrimal presence absent present

Ch. 314 Facial process of lacrimal shape large external wing on the rostrum at the anterior edge of the orbit small rectangular or crescentic

Ch. 315 Lacrimal tubercle present absent

Ch. 316 Lacrimal foramen exposed on face because lateral edge of the foramen is reduced or absent present absent

Ch. 317 Lacrimal foramen exits two one

Ch. 318 Lacrimal foramen composition lacrimal maxilla jugal

Ch. 319 Translacrimal canal absent present

Ch. 320 Nasal processes of the premaxillae tuberosity at the anterior apices of the premaxillae on the anterior floor of the nasal opening absent present

Ch. 321 Palatal process of premaxilla does not reach to canine alveolus does reach or nearly reach to canine alveolus

Ch. 322 Premaxillary maxillary suture on palate shape transverse wedge shaped pointing anteriorly wedge shaped pointing posteriorly

Ch. 323 Incisive foramen presence present absent

Ch. 324 Incisive foramen size short half or less than half the maximal palatal length of the premaxilla along the sagittal plane elongate more than half the length of the premaxilla

Ch. 325 Incisive foramen composition between maxilla and premaxilla within premaxilla

Ch. 326 Palatal vacuities absent present

Ch. 327 Major palatine foramen well individualised opening within maxilla and or palatine multiple small foramina in maxilla and or palatine

Ch. 328 Anterior extent of palatine on palate posterior to first upper molar level with first upper molar anterior to first upper molar

Ch. 329 Palatal expansion with regard to the last molar posterior even anterior

Ch. 330 Postpalatine torus absent present

Ch. 331 Posterior nasal palatine spine weak or absent prominent

Ch. 332 Minor palate foramen groove presence present absent

Ch. 333 Passageway of the minor palatine foramen or groove totally enclosed in the minor palatine foramen in a groove on the posteromedial edge of the palate as a result of the posterior opening of the minor palatine foramen no posterior bony bridge

Ch. 334 Minor palatine foramen composition maxilla palatine pterygoid

Ch. 335 Maxilla expansion posterior to ultimate molar absent present

Ch. 336 Posterior edge of anterior zygomatic root aligned with last molar or more posterior aligned between M1 and M2 aligned with ultimate upper premolar or more anterior

Ch. 337 Zygomatic process of maxilla present absent or vestigial

Ch. 338 Jugal present absent

Ch. 339 Jugal contribution to anteroventral edge of the orbit present contributes to anteroventral orbit and zygoma absent only contributes to zygoma

Ch. 340 Maxillary jugal contact bifurcated absent present

Ch. 341 Zygomatic arch complete arch incomplete arch

Ch. 342 Zygomatic arch morphology stout large overlap between jugal and squamosal to form robust arch delicate

Ch. 343 Orientation of the anterior root of zygoma in anterior view oblique extends dorsally transverse roughly horizontal extends ventrally

Ch. 344 Vertical position of posterior root of zygoma relative to foramen magnum at the same level posterior root positioned more dorsal

Ch. 345 Shape of zygomatic arches in dorsal view not protruding much laterally smoothly curved or parallel to sagittal plane protruding laterally largely exceeding other parts of skull laterally with a large posterior corner

Ch. 346 Molar roots exposed in orbit floor absent present

Ch. 347 Palatine extends into posterior opening of the infraorbital canal present absent

Ch. 348 Lacrimal contributes to maxillary foramen present absent

Ch. 349 Groove connects maxillary and sphenopalatine foramina absent present

Ch. 350 Sphenopalatine foramen contribution palatine maxilla frontal

Ch. 351 Sphenopalatine foramen proximal approximated to maxillary foramen absent present

Ch. 352 Maxilla contribution to orbital wall no contribution in orbital wall large dorsal process contributing to orbital wall

Ch. 353 Frontal and maxilla contact in orbital wall absent present

- Ch. 354** Orbital process of palatine present absent palatine excluded from medial wall or only a thin sliver in ventromedial wall
- Ch. 355** Ethmoid exposure in orbit absent present
- Ch. 356** Ethmoid foramen between frontal and orbitosphenoid within frontal
- Ch. 357** Foramen for frontal diploic vein absent present
- Ch. 358** Position of frontal diploic foramina relative to postorbital process or tuberosity posterior even or anterior
- Ch. 359** Supraorbital frontal postorbital foramen presence present absent
- Ch. 360** Supraorbital frontal postorbital foramen position on skull roof often extending anteriorly as a groove on the maxilla and or nasal more laterally on the dorsal edge of the orbit and or postorbital process groove variably present
- Ch. 361** Postorbital process presence present absent
- Ch. 362** Postorbital process development prominent weak
- Ch. 363** Postorbital process composition frontal parietal
- Ch. 364** Postorbital bar absent present
- Ch. 365** Dorsal process of jugal absent present
- Ch. 366** Optic foramen confluent with sphenorbital fissure well separated from sphenorbital fissure
- Ch. 367** Optic foramen position narrowly separated from sphenorbital fissure broadly separated from sphenorbital fissure
- Ch. 368** Orbitosphenoid expansion presence absent present
- Ch. 369** Orbitosphenoid expansion direction expanded anteriorly from optic foramen or with anterior process for forms without optic foramen expanded dorsally from optic foramen not expanded confined to optic foramen and vicinity
- Ch. 370** Suboptic foramen absent present
- Ch. 371** Orbitotemporal canal present absent
- Ch. 372** Frontal alisphenoid contact presence absent present
- Ch. 373** Frontal alisphenoid contact extent small alisphenoid contacting frontal at anterior corner with more extensive contact approx. 50 percent of dorsal margin
- Ch. 374** Sphenorbital fissure confluent with foramen rotundum i.e. there is no foramen rotundum per se and the V2 exits with the V1 through the sphenorbital fissure absent present
- Ch. 375** Frontal length on midline of skull roof less than half length of parietal subequal to slightly smaller than parietal more than 50 longer than parietal

- Ch. 376** Frontoparietal suture transverse with anterior process of parietal off the midline with anterior process of parietal on the midline
- Ch. 377** Temporal lines meet to form sagittal crest present absent
- Ch. 378** Interparietal absent present
- Ch. 379** Nuchal crest level with or anterior to level of foramen magnum extends posterior to level of foramen magnum
- Ch. 380** Nuchal crest in dorsal view deeply notched on medial line bilobate morphology and V shaped opening posteriorly transverse near straight median point posterior to lateral parts of the crest V shaped morphology opening anteriorly
- Ch. 381** Anterior lamina of petrosal presence present absent
- Ch. 382** Anterior lamina of petrosal exposure present and exposed on lateral braincase wall internal to braincase and small to vestigial
- Ch. 383** Squama of squamosal absent present
- Ch. 384** Foramina for temporal rami presence present absent
- Ch. 385** Foramina for temporal rami position in petrosal in parietal and or squama of the squamosal in squamosal including squamosal parietal suture
- Ch. 386** Choanae as wide as posterior palate distinctly narrower
- Ch. 387** Vomer contacts pterygoid present absent
- Ch. 388** Pterygoids contact on midline in roof of basipharyngeal canal present absent
- Ch. 389** Pterygopalatine crests present absent
- Ch. 390** Midline crest in basipharyngeal canal absent present
- Ch. 391** Entopterygoid presence present absent
- Ch. 392** Entopterygoid process posterior extension ends at anterior basisphenoid approaches ear region
- Ch. 393** Midline cordiform rod like eminence on basisphenoid absent present
- Ch. 394** Ectopterygoid process of alisphenoid presence absent or fused with entopterygoid present
- Ch. 395** Ectopterygoid process of alisphenoid extent present terminates at anterior basisphenoid present approaches ear region posteriorly
- Ch. 396** Ectopterygoid process shape Long crest or triangular blade small process spine or tubercle long crest triangular blade small spine small tubercle
- Ch. 397** Ectopterygoid process shape 2

Ch. 398 Ectopterygoid crests blades or tubercles orientation sub parallel and facing ventromedially diverging and facing mostly posteriorly

Ch. 399 Transverse canal foramen presence absent present

Ch. 400 Exit for maxillary nerve V2 via foramen rotundum relative to alisphenoid between the posterior edge of the alisphenoid anteriorly and the anterior lamina of the petrosal posteriorly within the alisphenoid at anterior end of alisphenoid

Ch. 401 Number of exits for mandibular branch of trigeminal nerve V3 two or more one

Ch. 402 Foramen ovale composition in anterior lamina of the petrosal between petrosal and alisphenoid in alisphenoid between alisphenoid and squamosal

Ch. 403 Foramen ovale position on lateral wall of braincase on ventral surface of the skull facing ventrally on the ventral side of the skull and facing anteroventrally

Ch. 404 Alisphenoid canal absent present

Ch. 405 Posterior opening of alisphenoid canal separated from foramen ovale in common depression with foramen ovale

Ch. 406 Posterior border of hypophyseal fossa located just anterior to basisphenoid basioccipital suture position relative to posterior edge of foramen ovale anterior to or roughly even with posterior edge of foramen ovale well posterior to posterior edge of foramen ovale

Ch. 407 Position of dentary articulation relative to fenestra vestibuli at same level anterior

Ch. 408 Glenoid fossa position on zygoma partially on braincase majority on braincase

Ch. 409 Glenoid fossa shape concave or concave posteriorly and flat anteriorly open anteriorly trough like anteroposteriorly elongate and concave with the major axis of fossa directed anteroposteriorly anteroposteriorly short with the major axis of fossa directed anteroposteriorly or flat concavoconvex circular ovoid mediolateral width up to twice anteroposterior length elongate ovoid mediolateral width greater than twice anteroposterior length

Ch. 410 Glenoid fossa shape 2

Ch. 411 Glenoid fossa surface topology flat slightly concave concave

Ch. 412 Glenoid fossa dorsoventral position relative to roof of basipharyngeal canal approximately level dorsal to it

Ch. 413 Glenoid process of jugal presence absent present

Ch. 414 Glenoid process of jugal facet presence with articular facet without facet

Ch. 415 Glenoid process of alisphenoid absent present

- Ch. 416** Postglenoid process presence present absent or highly reduced
- Ch. 417** Postglenoid process width subequal or slightly narrower in width to glenoid cavity approximately half the width of the glenoid cavity
- Ch. 418** Postglenoid foramen absent present
- Ch. 419** Postglenoid foramen position positioned posterior to postglenoid process glenoid fossa positioned medial or anteromedial to postglenoid process within glenoid fossa on lateral aspect of braincase
- Ch. 420** Postglenoid eminence of the squamosal absent present
- Ch. 421** Postglenoid foramen composition within squamosal posterior edge of squamosal
- Ch. 422** Suprameatal foramen absent present
- Ch. 423** Entoglenoid process of squamosal position present absent separate from postglenoid process continuous with postglenoid process
- Ch. 424** Entoglenoid process of squamosal position 2 State zero State one
- Ch. 425** Posttympanic crest of squamosal absent present
- Ch. 426** Carotid opening presence on basicranium present absent
- Ch. 427** Carotid opening form incisure notch enclosed foramen
- Ch. 428** Carotid opening position within basisphenoid between basisphenoid and petrosal
- Ch. 429** Floor of cavum epiptericum floor presence absent open as a pyriform fenestra present
- Ch. 430** Floor of cavum epiptericum floor composition floored by petrosal petrosal and alisphenoid primarily or exclusively squamosal
- Ch. 431** Posterodorsal extension of tympanic process of the alisphenoid which forms the roof of the anterior region of the tympanic cavity absent present
- Ch. 432** Basisphenoid tympanic process vestigial or absent present contributing to anteromedial bulla
- Ch. 433** Basicochlear fissure closed patent
- Ch. 434** Epitympanic wing medial to promontorium presence absent present
- Ch. 435** Epitympanic wing medial to promontorium form flat thickened
- Ch. 436** Rostral tympanic process of the petrosal presence present absent
- Ch. 437** Rostral tympanic process of the petrosal development small to moderate ridge contributing to posterodorsomedial bulla tall ridge contributing to ventral bulla

- Ch. 438** Course of internal carotid artery lateral transpromontorial medial perbullar or extrabullar
- Ch. 439** Boney canals for intratympanic carotid system transpromontorial internal carotid plus stapedial artery absent present
- Ch. 440** Deep groove for internal carotid artery excavated on the apex of the promontorium absent present
- Ch. 441** Perbullar carotid canal for medial internal carotid absent present
- Ch. 442** Sulcus or canal for stapedial artery on promontorium present absent
- Ch. 443** Stapedial ratio length width of fenestra vestibuli rounded less than 1.8 ellipital more than 1.8
- Ch. 444** Coiling of cochlea less than 360 360 or greater
- Ch. 445** Promontorium shape flat globose
- Ch. 446** Promontorium depth most ventral point relative to basioccipital even or ventral to basioccipital dorsal to basioccipital
- Ch. 447** Facial nerve intratympanic course open in sulcus open anteriorly in canal posteriorly in canal
- Ch. 448** Tympanic aperture of hiatus Fallopii on cerebral face of petrosal at anterior edge of petrosal on tympanic face of petrosal via fenestra semilunar
- Ch. 449** Prootic canal present absent
- Ch. 450** Prootic canal length and orientation long and vertical short and vertical short and horizontal
- Ch. 451** Lateral flange parallels length of promontorium greatly reduced or absent
- Ch. 452** Anterior extension of bony shelf lateral to promontorium lateral trough or tegmen tympani does not reach the apex of the promontorium anteriorly and confined posterolaterally extends as far anteriorly as the apex of the promontorium extends further anteriorly than the apex of the promontorium
- Ch. 453** Width of bony shelf lateral to promontorium tegmen tympani uniform expanded anteriorly
- Ch. 454** Inflation of bony shelf lateral to promontorium lateral trough or tegmen tympani absent present
- Ch. 455** Stapedial canal on tegmen tympani absent present
- Ch. 456** Tensor tympani fossa on the petrosal shallow or vestigial deep fossa
- Ch. 457** Area occupied by tensor tympani fossa small and or poorly excavated large
- Ch. 458** Location of tensor tympani fossa mostly medial or ventromedial to the cavum supracochleare strictly ventral or lateral to it not medial

- Ch. 459** Medial process of squamosal in tympanic cavity absent present
- Ch. 460** Hypotympanic sinus presence absent present
- Ch. 461** Hypotympanic sinus contributing elements alisphenoid petrosal squamosal
- Ch. 462** Epitympanic recess presence present absent not a visible recess
- Ch. 463** Epitympanic recess vs fossa incudis size subequal epitympanic recess larger
- Ch. 464** Epitympanic recess lateral wall squamosal contribution with small contribution from squamosal to posterolateral wall with extensive contribution from squamosal to lateral wall with no squamosal contribution
- Ch. 465** Fossa incudis relationship with epitympanic recess continuous with epitympanic recess separated from epitympanic recess
- Ch. 466** Squamosal epitympanic sinus absent present
- Ch. 467** Floor ventral to fossa incudis presence present absent
- Ch. 468** Floor ventral to fossa incudis floor composition floor formed by squamosal floor formed by ectotympanic floor formed by petrosal
- Ch. 469** Fossa incudis position relative to fenestra vestibuli lateral anterolateral
- Ch. 470** Foramen for superior ramus of the stapedia artery presence present absent
- Ch. 471** Foramen for superior ramus of the stapedia artery position on petrosal on petrosal squamosal suture
- Ch. 472** Position of foramen for superior ramus of the stapedia artery relative to the fenestra vestibuli posterior or lateral anterior
- Ch. 473** Ascending canal passage for the superior ramus of the stapedia artery presence present absent
- Ch. 474** Ascending canal passage for the superior ramus of the stapedia artery intramural in the petrosal intracranial
- Ch. 475** Diameter of the stapedius fossa approximately twice size of fenestra vestibuli distinctly less than twice the size of the diameter of the fenestra vestibuli small and shallow
- Ch. 476** Cochlear canaliculus visible middle ear space absent present
- Ch. 477** Stapedial fossa and postpromontorial tympanic sinus distinct separated by a break in slope or a crest merged almost indistinct
- Ch. 478** Cochlear fossula vestigial or absent distinct pit behind fenestra cochleae
- Ch. 479** External aperture of cochlear fossula fenestra cochleae in Wible posteromedial to fenestra vestibuli posterior to fenestra vestibuli
- Ch. 480** Posterior septum shields fenestra cochleae absent present

- Ch. 481** Mastoid process protuberance presence present absent
- Ch. 482** Mastoid process orientation present and vertical angled anteroventrally
- Ch. 483** Posterior border of the middle ear cavity medial to the stylomastoid notch and lateral to the lateral edge of the jugular foramen straight or convex anteriorly concave or deeply notched
- Ch. 484** Crista interfenestralis and lateral caudal tympanic process connected by curved ridge absent present
- Ch. 485** Medial caudal tympanic process of the petrosal presence present absent
- Ch. 486** Medial caudal tympanic process of the petrosal height low high i.e. inflated into bullar wall
- Ch. 487** Medial tympanic process composition petrosal petrosal and exoccipital
- Ch. 488** Inferior petrosal sinus intrapetrosal horizontal between petrosal basisphenoid and basioccipital intracranial entering cranial cavity on the anterior edge of the jugular foramen intracranial entering cranial cavity via a foramen at mid length of the medial border of the promontorium
- Ch. 489** Size of jugular foramen relative to external aperture of fenestra cochleae smaller or subequal larger
- Ch. 490** Jugular foramen and inferior petrosal sinus confluent separated
- Ch. 491** Hypoglossal foramen presence present absent
- Ch. 492** Hypoglossal foramen number of openings two or more one
- Ch. 493** Size of the opening which houses the hypoglossal foramen smaller than jugular foramen subequal to larger than jugular foramen
- Ch. 494** Hypoglossal foramen ventral opening on exoccipital in a fossa on a flat to convex bony surface
- Ch. 495** Paraoccipital process presence absent present
- Ch. 496** Paraoccipital process of the exoccipital projection direction vertically directed posteriorly directed anteriorly directed
- Ch. 497** Ectotympanic phaneric or visible in ventral view aphaneric hidden by auditory bulla
- Ch. 498** Ectotympanic shape ring like fusiform expanded contributing to bullar floor
- Ch. 499** Anterior crus of ectotympanic exhibits broad contact with squamosal absent present
- Ch. 500** Anterior crus of ectotympanic articulation with petrosal absent present
- Ch. 501** Elongate ossified external acoustic meatus absent present
- Ch. 502** Roof of external acoustic meatus formed by petrosal formed by squamosal

- Ch. 503** Entotympanic distinct in adults absent present
- Ch. 504** Position of sulcus for anterior distributary of transverse sinus to subarcuate fossa anterolateral posterolateral
- Ch. 505** Hyoid pit for ectotympanic or between ectotympanic and exoccipital absent present
- Ch. 506** Hyoid arch contributes to bullar floor absent present
- Ch. 507** Dorsum sellae tall low
- Ch. 508** Posterior clinoid process contacts apex of the promontorium absent present
- Ch. 509** Wall separating cavum supracochleare and epiptericum presence absent present
- Ch. 510** Wall separating cavum supracochleare and epiptericum completeness incomplete with fenestra semilunaris complete
- Ch. 511** Crista petrosa vestigial or absent present
- Ch. 512** Subarcuate fossa morphology sub spherical with constricted aperture diameter of aperture is smaller than maximum diameter of the fossa cylindrical diameter more or less constant conical or shallow depression aperture is the widest diameter
- Ch. 513** Anterior semicircular canal does form lateral wall of subarcuate fossa does not form lateral wall of subarcuate fossa
- Ch. 514** Internal acoustic meatus depth deep with thick prefacial commissure shallow with thin prefacial commissure
- Ch. 515** Prefacial commissure thick thin
- Ch. 516** Posttemporal canal present absent
- Ch. 517** Posttemporal canal composition posterior opening posterior opening between petrosal and squamosal within petrosal
- Ch. 518** Posttemporal canal position on occiput dorsal to external acoustic meatus
- Ch. 519** Mastoid foramen foramina absent present
- Ch. 520** Amastoidy or lack of occipital exposure of the mastoid absent present
- Ch. 521** Dorsal margin of foramen magnum formed by exoccipitals by exoccipitals and supraoccipital
- Ch. 522** Dorsal relief of lambdoid crest continuous with dorsal margin of zygomatic arch absent present
- Ch. 523** Atlantal foramen present absent
- Ch. 524** Atlas neural arch fused absent present

- Ch. 525** Atlas neural arch and intercentrum fused absent present
- Ch. 526** Suture between atlantal and axial parts of the axis present absent
- Ch. 527** Axis with extra pair of transverse processes on ventral surface present absent
- Ch. 528** Axis anterior facets prezygapophyses and dens connection not linked linked and facets extend ventral to dens
- Ch. 529** Inferior lamellae on posterior cervical vertebrae present absent
- Ch. 530** C7 or last transverse foramen present absent
- Ch. 531** Number of thoracic vertebrae 13 or fewer 15 or more
- Ch. 532** Number of lumbar vertebrae six or more five or fewer
- Ch. 533** Xenarthrous articulation in addition to the pre and post zygapophyses of lumbar vertebrae absent present
- Ch. 534** Number of sacral vertebrae two three four or more
- Ch. 535** Sacral vertebra fused to pelvis absent present
- Ch. 536** Scapula infraspinous fossa size area to supraspinous fossa infraspinous fossa larger subequal supraspinous larger
- Ch. 537** Suprascapular incisure absent present
- Ch. 538** Scapula acromion presence absent present
- Ch. 539** Scapula apex of scapula acromion extent reaches distal to glenoid articulation with humerus remains proximal
- Ch. 540** Scapula metacromion presence absent present
- Ch. 541** Scapula metacromion extent small large larger
- Ch. 542** Scapula tuber spinae absent present
- Ch. 543** Humerus elevation of the greater tubercle of humerus relative to the humeral head ventral to humeral head even or dorsal to humeral head
- Ch. 544** Humerus extension of deltopectoral region on humerus does not extend beyond 50 length of humerus shaft extends to distal shaft over 50 length of shaft
- Ch. 545** Humerus deltopectoral tuberosity presence present absent
- Ch. 546** Humerus lateral epicondylar crest presence present absent
- Ch. 547** Humerus epicondylar crest development weak limited lateral projection in line with lateral edge of capitulum shelf like projects further laterally than the lateral edge of the capitulum
- Ch. 548** Humerus medial epicondyle development large projection slightly expanded weak

Ch. 549 Humerus medial epicondyle projection direction medial posteromedial posterior

Ch. 550 Humerus entepicondylar foramen present absent

Ch. 551 Humerus supratrochlear foramen absent present

Ch. 552 Humerus surface for articulation with ulna cylindrical trochlea in posterior view with a vestigial ulnar condyle in anterior view cylindrical trochlea without an ulnar condyle cylindrical trochlea extending to the anterior ventral side

Ch. 553 Radial articulation on humerus rounded radial condyle capitulum anteriorly but cylindrical posteriorly capitulum forming a continuous synovial surface with the ulnar trochlea cylindrical in anterior and posterior views

Ch. 554 Radius articulation with distal humerus single fossa two fossae

Ch. 555 Radius capitular eminence absent present

Ch. 556 Radius articulation with carpals single fossa two fossae

Ch. 557 Radius and ulna distal fusion absent present

Ch. 558 Manus scaphoid and lunate separate fused

Ch. 559 Manus os centrale present absent

Ch. 560 Pelvis pubic symphysis extensive narrow

Ch. 561 Pelvis epipubic bone present absent

Ch. 562 Femur articular surface of femoral head extended posterolaterally limited to sphere of femoral head

Ch. 563 Femur fovea for ligamentum teres on femur head presence present absent

Ch. 564 Femur fovea for ligamentum teres on femur head does not interrupt margin of articular surface does interrupt margin of articular surface

Ch. 565 Femur height of greater trochanter to femoral head greater trochanter lower subequal greater trochanter higher

Ch. 566 Femur size of lesser trochanter large forms a well defined prominent projecting flange small forms a small boney ridge

Ch. 567 Femur less trochanter direction of projection medial posteromedial posterior

Ch. 568 Femur third trochanter absent present

Ch. 569 Femur third trochanter size large moderate small

Ch. 570 Femur pectineal tubercle absent or vestigial distinct

Ch. 571 Proportions of distal femoral epiphysis in distal view subequal anteroposterior and mediolateral dimensions longer anteroposteriorly than mediolaterally mediolaterally wider than anteroposteriorly long

- Ch. 572** Ossified patella absent present
- Ch. 573** Articulation between femur and fibula absent present
- Ch. 574** Tibia and fibula proximal fusion absent present
- Ch. 575** Tibia and fibula distal fusion absent present
- Ch. 576** Astragalus depth of trochlear groove lateral tibial facet shallow slightly concave articular surface moderately deep U shaped deep V shaped
- Ch. 577** Astragalus squatting facet presence absent present
- Ch. 578** Astragalus angle between medial and lateral tibia facet approximately 90 degrees greater than 110 degrees
- Ch. 579** Astragalus angle between fibula facet and lateral tibia facet 180 intermediate 90
- Ch. 580** Astragalus fibular facet size small protuberance larger protuberance
- Ch. 581** Astragalus radius of lateral trochlear keel greater than medial keel subequal less than medial keel
- Ch. 582** Astragalus cotylar fossa absent present
- Ch. 583** Astragalus pit on dorsal surface to lock tibia when pes dorsiflexed absent present
- Ch. 584** Astragalus contact between sustentacular and navicular facets on astragalus absent present
- Ch. 585** Astragalus medial plantar tubercle vestigial or absent present
- Ch. 586** Astragalus sustentacular facet lateral extent does reach medial edge of neck does not medial edge of neck
- Ch. 587** Astragalus head shape convex concave flat concavoconvex trochleated
- Ch. 588** Astragalus head dimensions mediolaterally broad width and depth subequal really mediolaterally broad define for horse etc
- Ch. 589** Astragalus head orientation relative to body mediolateral long axis of head orientated in line near in line with mediolateral long axis of the body when view anteriorly head on mediolateral long axis of head orientated at an angle 5 degrees or greater relative to mediolateral long axis of body
- Ch. 590** Astragalus head features facet for cuboid absent present
- Ch. 591** Astragalus astragalar canal presence present absent
- Ch. 592** Astragalus relative proportions mediolateral width of head relative to neck neck is more than or equal to 80 width of head neck is less than 80 width of head

- Ch. 593** Astragalus relative proportions mediolateral width of neck relative to trochlea neck is equal to or more than 60 width of trochlea neck is less than 60 width of trochlea
- Ch. 594** Astragalus relative proportions width of head relative to trochlea head is equal to or more than 70 width of trochlea head is less than 70 width of trochlea
- Ch. 595** Os tibiale sesamoid presence present absent
- Ch. 596** Calcaneum ectal calcaneoastagalal facet longest dimension anteromedial to posterolateral anteroposterior posteromedial to anterolateral
- Ch. 597** Calcaneum ectal facet surface orientation lateral or very near lateral laterodorsal dorsal or very near dorsal
- Ch. 598** Calcaneum ectal facet position medial edge of facet does not come close to reaching medial edge of calcaneal tuber medial edge of facet positioned close to medial edge of tuber so facet orientation is strongly oblique i.e. Arctocyon
- Ch. 599** Calcaneum contact overlap between ectal and sustentacular facets absent present
- Ch. 600** Calcaneum degree of overlap between ectal and sustentacular facets partial overlap complete overlap
- Ch. 601** Calcaneum sustentacular facet mediolateral orientation medial dorsal
- Ch. 602** Calcaneum sustentacular facet expanded onto body absent present
- Ch. 603** Calcaneum sustentacular facet features small accessory facet connecting it to cuboid facet absent present
- Ch. 604** Calcaneum sustentacular facet position on body on or very close to anterior border of calcaneum set back from anterior border to that cuboid facet forms a distinct protrusion
- Ch. 605** Calcaneum peroneal tubercle present absent
- Ch. 606** Calcaneum peroneal tubercle development small protuberance or ridge large laterally prominent process
- Ch. 607** Calcaneum anterior peroneal tubercle position protruding anteriorly beyond calcaneocuboid facet anterior but non protruding distal to anterior end of calcaneum
- Ch. 608** Calcaneum peroneal tubercle crest absent present
- Ch. 609** Calcaneum plantar tubercle presence present absent
- Ch. 610** Calcaneum plantar tubercle position at distal margin more proximal posterior than distal margin
- Ch. 611** Calcaneum tuber calcis ventral margin curvature present absent
- Ch. 612** Calcaneum facet for fibula present absent

Ch. 613 Calcaneum orientation of mediolateral axis of cuboid facet relative to long axis of calcaneum less than 70 degrees 70 to 85 degrees more than 85 degrees

Ch. 614 Calcaneum proportions of cuboid facet facet deeper dorsoplantar than wide mediolateral facet depth and width subequal facet wider mediolateral than deep dorsoplantar

Ch. 615 Calcaneum groove for tendon of flexor hallucis longis and flexor fibularis on the posterior edge of the sustentaculum calcaneum absent present

Ch. 616 P5 parastyle absent present

Ch. 617 P5 stylocone absent present

Ch. 618 P5 metastyle absent present

Ch. 619 Distolingual cusp on upper molars absent present

Ch. 620 Twinned metaconule on upper molars absent present

Ch. 621 Lower molars pre entoconulid absent present

Ch. 622 Lower molars post entoconulid absent present

Ch. 623 Lower molars multicuspid in the hypoconulid position absent one cuspid as hypoconulid present more than one cuspid

Ch. 624 Upper premolars hypselodonty present absent

Ch. 625 Upper molars hypselodonty present absent

Ch. 626 Lower premolars hypselodonty present absent

Ch. 627 Lower molars hypselodonty present absent

Ch. 628 Lower anterior premolars size smaller than posterior premolars longer than posterior premolars

Ch. 629 Upper anterior premolars size smaller than posterior premolars longer than posterior premolars

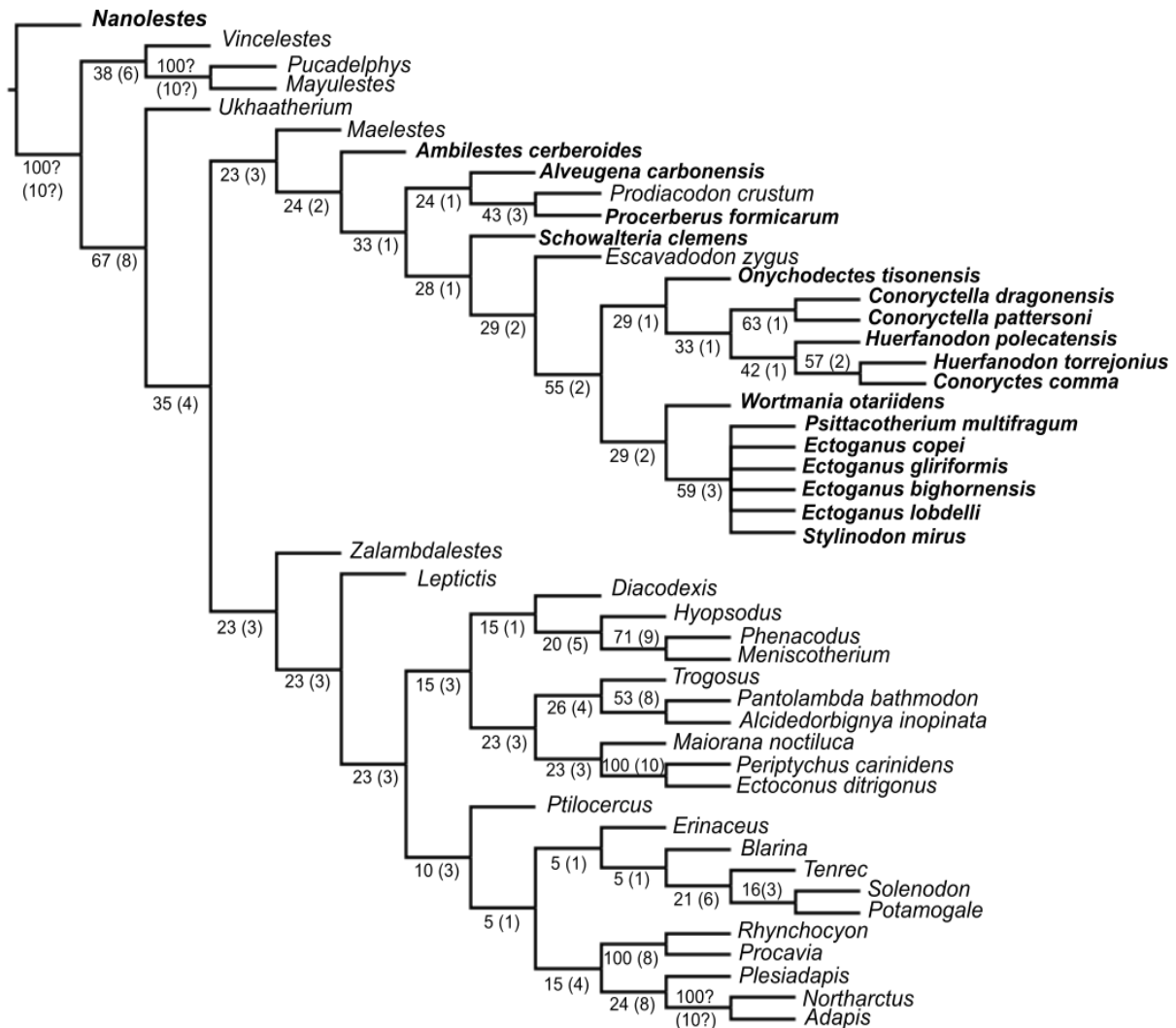
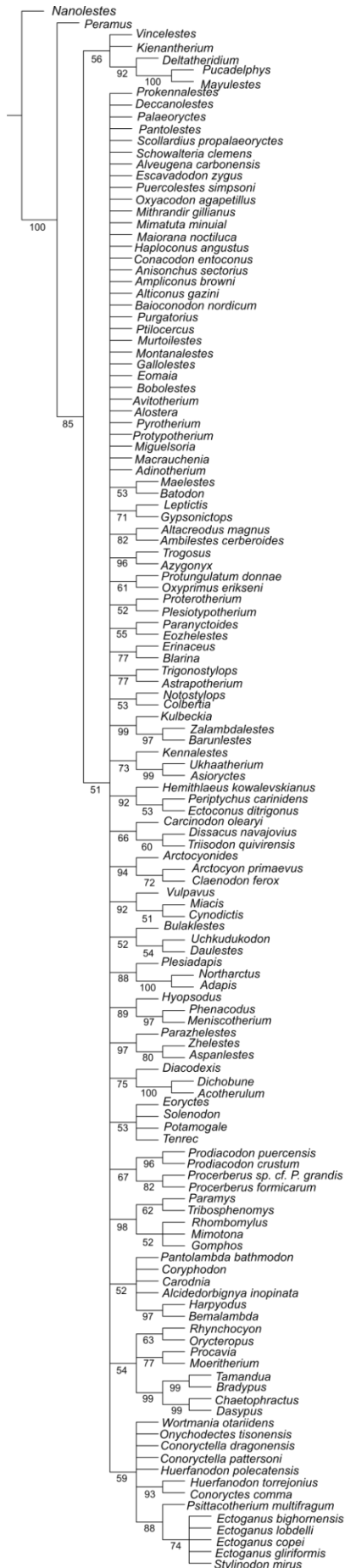


Figure A31: Bremmer support of relative (absolute) values, after pruning the least scored taxa of the analysis. Taeniodonta and potential related taxa are highlighted in bold.

Figure A32 (next page): Tree produced after New Technology search and TBR, followed by resampling Jackknife method. Taeniodonta and potential related taxa are highlighted in bold and Jackknife support values are under each node.



Time calibrate tree

Table A5. The "int_times.csv", used in the R code. This is to create the interval times used in the study. To make them equal, the time periods were divided further.

| Interval times | Start time | End time |
|----------------|------------|----------|
| Late_Lancia | 68 | 66 |
| Pu1 | 66 | 65.7 |
| Pu2 | 65.7 | 65.3 |
| Pu3 | 65.3 | 64.8 |
| To1_a | 64.8 | 64.15 |
| To1_b | 64.15 | 63.5 |
| Tj2-Tj3 | 63.5 | 62.8 |
| Tj4-Tj5 | 62.5 | 62.5 |
| To3 | 62.5 | 61.8 |
| To3_b | 61.8 | 61 |
| Tiff_a | 61 | 60.3 |
| Tiff_b | 60.3 | 59.6 |
| Tiff_c | 59.6 | 58.9 |
| Tiff_d | 58.9 | 58.2 |
| Tiff_e | 58.2 | 57.5 |
| Tiff_f | 57.5 | 56.8 |
| Clarkf_a | 56.8 | 56.1 |
| Clarkf_b | 56.1 | 55.4 |
| Wa0 | 55.4 | 55 |
| Wa1 | 55 | 54.7 |

| | | |
|------------|-------|-------|
| Wa2 | 54.7 | 54.1 |
| Wa3 | 54.1 | 53.35 |
| Wa4 | 53.35 | 52.9 |
| L. Wasat_a | 52.9 | 52.25 |
| L. Wasat_b | 52.25 | 51.6 |
| L. Wasat_c | 51.6 | 50.95 |
| L. Wasat_d | 50.95 | 50.3 |
| Bridg_a | 50.3 | 49.6 |
| Bridg_b | 49.6 | 48.9 |
| Bridg_c | 48.9 | 48.2 |
| Bridg_d | 48.2 | 47.5 |
| Bridg_e | 47.5 | 46.8 |
| Bridg_f | 46.8 | 46.2 |
| Uintan_a | 46.2 | 45.5 |
| Uintan_b | 45.5 | 44.8 |
| Uintan_c | 44.8 | 44.1 |
| Uintan_d | 44.1 | 43.4 |
| Uintan_e | 43.4 | 42.7 |
| Uintan_f | 42.7 | 42 |
| Uintan_g | 42 | 41.2 |
| Uintan_h | 41.2 | 40.4 |

Table A6a. The "taxon_times.csv", used in the R code. The numbers in the FAD_Ma and LAD_Ma are referring to the rows of the time intervals table (table A5).

| Taxa | FAD_Ma | LAD_Ma |
|---------------------------------------|--------|--------|
| <i>Procerberus_formicarum</i> | 2 | 6 |
| <i>Procerberus_sp._cf._P._grandis</i> | 2 | 6 |
| <i>Prodiacodon_crustum</i> | 2 | 6 |
| <i>Puercolestes_simpsoni</i> | 3 | 4 |
| <i>Prodiacodon_puercensis</i> | 5 | 10 |
| <i>Escavadodon_zygus</i> | 7 | 10 |
| <i>Alveugena_carbonensis</i> | 3 | 3 |
| <i>Schowalteria_clemens</i> | 1 | 2 |
| <i>Onychodectes_tisonensis</i> | 3 | 4 |
| <i>Conoryctes_comma</i> | 8 | 10 |
| <i>Huerfanodon_torrejonius</i> | 8 | 8 |
| <i>Huerfanodon_polecatensis</i> | 9 | 10 |
| <i>Conoryctella_pattersoni</i> | 7 | 7 |
| <i>Conoryctella_dragonensis</i> | 5 | 7 |
| <i>Wortmania_otariidens</i> | 3 | 4 |
| <i>Psittacotherium_multifragum</i> | 7 | 16 |
| <i>Ectoganus_copei</i> | 17 | 18 |
| <i>Ectoganus_gliriformis</i> | 20 | 27 |
| <i>Stylinodon_mirus</i> | 28 | 41 |

Table A6b. The "taxon_times2.csv", used in the R code.

| Taxa | FAD_Ma | LAD_Ma |
|---------------------------------------|--------|--------|
| <i>Procerberus_formicarum</i> | 66 | 63.5 |
| <i>Procerberus_sp._cf._P._grandis</i> | 66 | 63.5 |
| <i>Prodiacodon_crustum</i> | 66 | 63.5 |
| <i>Puercolestes_simpsoni</i> | 65.7 | 64.8 |
| <i>Prodiacodon_puercensis</i> | 64.8 | 61 |
| <i>Escavadodon_zygus</i> | 63.5 | 61 |
| <i>Alveugena_carbonensis</i> | 65.7 | 65.3 |
| <i>Schowalteria_clemensi</i> | 68 | 66 |
| <i>Onychodectes_tisonensis</i> | 65.7 | 64.8 |
| <i>Conoryctes_comma</i> | 62.8 | 61 |
| <i>Huerfanodon_torrejonius</i> | 62.8 | 62.5 |
| <i>Huerfanodon_polecatensis</i> | 62.5 | 61 |
| <i>Conoryctella_pattersoni</i> | 63.5 | 62.8 |
| <i>Conoryctella_dragonensis</i> | 64.8 | 62.8 |
| <i>Wortmania_otariidens</i> | 65.7 | 64.8 |
| <i>Psittacotherium_multifragum</i> | 62.5 | 56.8 |
| <i>Ectoganus_copei</i> | 56.8 | 55.4 |
| <i>Ectoganus_gliriformis</i> | 55 | 50.3 |
| <i>Stylinodon_mirus</i> | 50.3 | 40.4 |

R code

Code used in R to produce the time-calibrated tree. The geological ranges of the taxa were taken from the literature.

```

library("ape")
library("maps")
library("paleotree")
library("phytools")
library("geoscale")
library("strap") #geological scale
library("ggplot2")
library("phangorn")
etwd("C:/Users/kynig/Downloads/Final_phylogeny/Final2")
tree_ts<-read.nexus("Final_consensus_2.nex")
plot(root_ts,cex=.3)
#taxa range for age
taxon.times<-read.csv("taxon_times.csv",row.names=1)
int.times<-read.csv("int_times.csv",row.names=1)
ts.range<-list(int.times,taxon.times)
#bin_cal3TimePaleoPhy method
likFun<-make_durationFreqDisc(ts.range)
spRes<-optim(parInit(likFun),likFun,lower=parLower(likFun),upper=parUpper(likFun),
             method="L-BFGS-B",control=list(maxit=1000000))
#sampling PROBABILITY per bin
sProb <- spRes[[1]][1]
#calculate meanInt, use an average int.length
intLength<--apply(ts.range[[1]],1,diff)

```

```

hist(intLength)
meanInt <-mean(apply(ts.range[[1]], 1, diff))
sRate <- sProb2sRate(sProb,int.length = meanInt)

#extinction rate and branching rate (see above) divide by int.length...
divRate <- spRes[[1]][1]/meanInt

#calibrated tree
tree_ts1 <- bin_cal3TimePaleoPhy(tree_ts, ts.range,brRate = divRate, extRate =
divRate, sampRate = sRate, ntrees = 100, plot = FALSE)

multiDiv(tree_ts1)

show(meanInt)

show(sRate)

#Average tree - takes about ~7 mins
tree_ts2<-averageTree(tree_ts1, method="quadratic.path.difference")

#plot with ages FAD and LAD
tree_ts2$root.time <- 68
FL.times<-read.csv("taxon_times2.csv", header=T,row.names=1)
ages1<-as.data.frame(FL.times[,c(1,2)])
ages1$FAD<-as.numeric(ages1$FAD)
ages1$LAD<-as.numeric(ages1$LAD)
colnames(ages1)<-c("FAD", "LAD")

time.tree2<-geoscalePhylo(tree=ladderize((root(tree_ts2,outgroup
=c("Puercolestes_simpsoni"), resolved.root=TRUE)),right=FALSE), ages=ages1,
units=c("Period", "Epoch", "Age"), boxes="Epoch", cex.tip=0.4, cex.age=0.3,
cex.ts=0.5, label.offset=0, x.lim=c(37,70), lwd=2, width=0.5)

```

Appendix to Chapter 3

Table A7. A list of the new specimens studied from the San Juan Basin of *Conoryctes comma*, the localities they were found and their biozones.

| Specimen number | Associated elements | Locality | Biozone |
|-----------------|---|---|---------|
| NMMNH P-19494 | M1, M2, p4, distal tibia, partial femur | Upper horizon of West Flank of Torreon Wash | Tj6 |
| NMMNH P-48198 | Vertebrae, os coxae, tibia, astragalus, calcaneum | Upper horizon of West Flank of Torreon Wash | Tj6 |
| NMMNH P-48052 | Atlas, vertebrae, ribs, proximal ulna, metacarpals, phalanges and ungual, proximal and distal tibia, parts of proximal and distal femur, patella, astragalus, calcaneum | Upper horizon of West Flank of Torreon Wash | Tj6 |
| NMMNH P-61789 | Partial humerus, partial os coxae | Upper horizon of West Flank of Torreon Wash | Tj6 |
| NMMNH P-77896 | Distal humerus, partial os coxae | Upper horizon of West Flank of Torreon Wash | Tj6 |
| NMMNH P-21509 | Vertebrae, proximal tibia, astragalus | Upper horizon of East Flank of Torreon Wash | Tj6 |

| | | | |
|-------------------|---|-------------------------|-----|
| NMMNH P-
79457 | vertebrae, sacrum, radius,
metacarpals, phalanges
and ungual, proximal
femur | Red Mesa | Tj5 |
| NMMNH P-
47700 | Vertebrae, partial os
coxae, metatarsals,
phalanges and unguals | Angel Peak, Kutz Canyon | Tj4 |
| NMMNH P-
47866 | calcaneum | Angel Peak, Kutz Canyon | Tj4 |

Table A8. Teeth measurements of specimen NMMNH P-19494, *Conoryctes comma*, from San Juan Basin.

| Teeth | Buccolingual width (mm) | Anteroposterior length (mm) |
|-------|-------------------------|-----------------------------|
| M1 | 13.82 | 8.31 |
| M2 | 13.34 | 7.61 |
| p4 | 8.21 | 5.91 |

Table A9. Measurements of vertebrae of *Conoryctes comma*.

| Specimen | | mm |
|---------------|--|-------|
| NMMNH P-21509 | Caudal vertebra body
anteroposterior length | 21.31 |
| | Caudal vertebra body mediolateral
width | 15.61 |
| NMMNH P-48052 | Axis body anteroposterior length | 12.57 |

| | | |
|---------------|---|-------|
| | Axis body mediolateral width | 16.33 |
| | Caudal body anteroposterior length | 26.24 |
| | Caudal body mediolateral width | 16.94 |
| NMMNH P-79457 | Cervical body mediolateral width | 12.57 |
| | Cervical body anteroposterior length | 7.71 |
| | Thoracic body mediolateral width | 13.59 |
| | Thoracic body anteroposterior length | 10.61 |
| | Lumbar body mediolateral width | 17.48 |
| | Lumbar body anteroposterior length | 19.06 |
| | Sacral vertebra body mediolateral width | 54.41 |
| | Sacral vertebra body anteroposterior length | 41.35 |
| NMMNH P-48198 | Lumbar body mediolateral width | 21.75 |
| | Lumbar body anteroposterior length | 20.76 |
| | Caudal body mediolateral width | 15.12 |
| | Caudal body anteroposterior length | 18.42 |
| NMMNH P-47700 | Cervical body mediolateral width | 14.6 |
| | Cervical body anteroposterior length | 8.04 |

| | | |
|--|------------------------------------|-------|
| | Lumbar body mediolateral width | 15.14 |
| | Lumbar body anteroposterior length | 16.64 |
| | Caudal body mediolateral width | 14.3 |
| | Caudal body anteroposterior length | 25.38 |

Table A10. Measurements of the humerus from the new specimens of *Conoryctes comma*.

| Specimen | | mm |
|---------------|---------------------------------------|-------|
| NMMNH P-48052 | Humeral head mediolateral width | 13.22 |
| | Humeral head proximodistal length | 14.39 |
| NMMNH P-77896 | Maximum distal mediolateral width | 53.31 |
| | Maximum distal humeral trochlea width | 9.8 |

Table A11. Measurements of the ulna, *Conoryctes comma*.

| Specimen | | mm |
|---------------|------------------|-------|
| NMMNH P-48052 | Olecranon height | 19.43 |

Table A12. Measurements of the radius, *Conoryctes comma*. Numbers are referring to the measurements as seen in Figure A31.

| Specimen | | mm |
|---------------|--------------------------------|--------|
| NMMNH P-79457 | Total proximodistal length (1) | 56.12* |

| | | |
|--|---|-------|
| | Mediolateral width of the proximal epiphysis (2) | 10.27 |
| | Mediolateral width of the distal epiphysis (3) | 11.18 |
| | Mediolateral width at the middle of the shaft (4) | 7.97* |
| | Anteroposterior width of the proximal epiphysis (5) | 7.56 |
| | Anteroposterior width at the middle of the shaft (6) | 4.83* |
| | Anteroposterior width of the distal epiphysis (7) | 10.89 |
| | Anteroposterior width of the distal articular fovea (8) | 6.93 |

Table A13. Measurements of the metacarpals, *Conoryctes comma*.

| Specimen | | mm |
|----------------|--|-------|
| NMMNH P-79457 | | |
| II metacarpals | Total length | 14.04 |
| | Perimeter at midshaft | 18 |
| | Mediolateral width of the proximal epiphysis | 5.24 |
| | Mediolateral width of the distal epiphysis | 7.34 |

| | | |
|----------------|---|-------|
| | Anteroposterior width of the proximal epiphysis | 6.19 |
| | Anteroposterior width of the proximal epiphysis | 5.21 |
| V metacarpals | Total length | 13.84 |
| | Perimeter at midshaft | 17 |
| | Mediolateral width of the proximal epiphysis | 5.92 |
| | Mediolateral width of the distal epiphysis | 6.09 |
| | Anteroposterior width of the proximal epiphysis | 4.69 |
| | Anteroposterior width of the proximal epiphysis | 4.80 |
| <hr/> | | |
| NMMNH P-48052 | | |
| II metacarpals | Total length | 14.2 |
| | Perimeter at midshaft | 19 |
| | Mediolateral width of the proximal epiphysis | 5.21 |
| | Mediolateral width of the distal epiphysis | 7.73 |
| | Anteroposterior width of the proximal epiphysis | 6.25 |

| | | |
|--|---|------|
| | Anteroposterior width of proximal epiphysis | 5.67 |
|--|---|------|

Table A14. Measurements of the pelvis, *Conoryctes comma*. Numbers are referring to the measurements as seen in Figure A35.

| Specimen | | mm |
|---------------|--|-------|
| NMMNH P-48198 | Length of the lunate surface (1) | 22.10 |
| | Width of the lunate surface (2) | 20.57 |
| | Length from the tip of the ischiatic tuberosity to the iliopectineal eminence (3) | 44.41 |
| | Total length of the fossae attaching the sacrum on the ventral view of the ilium (4) | 38.55 |
| | Length of the fossa closer to the greater ischiatic notch (5) | 16.49 |
| | Length of the fossa on the wing of the ilium (6) | 21.88 |
| NMMNH P-47700 | Length of the lunate surface (1) | 20.29 |
| | Length from the tip of the ischiatic tuberosity to the iliopectineal eminence (3) | 41.46 |

Table A15. Measurements of the femur, *Conoryctes comma*. Numbers are referring to the measurements as seen in Figure A36.

| Specimen | | mm |
|---------------|--|-------|
| NMMNH P-48052 | Femoral head mediolateral width
(3) | 14.31 |
| | Femoral head proximodistal length
(4) | 16.31 |
| NMMNH P-79457 | Total mediolateral width of the
proximal epiphysis(1) | 31.34 |
| | Femoral head anteroposterior
length (2) | 15.89 |
| | Femoral head mediolateral width
(3) | 15.40 |
| | Femoral head proximodistal length
(4) | 11.96 |

Table A16. Measurements of the patella, *Conoryctes comma*.

| Specimen | | mm |
|---------------|------------------------|-------|
| NMMNH P-48052 | Anteroposterior length | 7.45 |
| | Mediolateral width | 12.57 |
| | Proximodistal length | 14.93 |

Table A17. Measurements of the tibia, *Conoryctes comma*. Numbers are referring to the measurements as seen in Figure A37.

| Specimen | | mm |
|---------------|---|--------|
| NMMNH P-19494 | Distal tibia mediolateral width (3) | 19.62 |
| | Distal tibia anteroposterior total length (6) | 16.33 |
| NMMNH P-21509 | Proximal tibia mediolateral width (2) | 21.45 |
| | Proximal fibular facet mediolateral width (4) | 5.62 |
| | Proximal fibular facet anteroposterior length (5) | 7.57 |
| | Proximal tibia anteroposterior total length (7) | 23.03* |
| NMMNH P-48052 | Distal tibia mediolateral width (3) | 20.39 |
| | Proximal fibular facet mediolateral width (4) | 5.61 |
| | Proximal fibular facet anteroposterior length (5) | 7.07 |
| | Distal tibia anteroposterior total length (6) | 14.79 |
| | Proximal tibia anteroposterior total length (7) | 22.23* |
| NMMNH P-48198 | Total proximodistal length (1) | 50.80 |

| | | |
|---------------|--|--------|
| | Proximal tibia mediolateral width
(2) | 27.68 |
| | Distal tibia mediolateral width (3) | 21.52 |
| | Proximal fibular facet mediolateral
width (4) | 6.32 |
| | Proximal fibular facet
anteroposterior length (5) | 7.62 |
| | Distal tibia anteroposterior total
length (6) | 14.41 |
| | Proximal tibia anteroposterior total
length (7) | 17.87 |
| NMMNH P-47700 | Proximal tibia mediolateral width
(2) | 29.06* |
| | Proximal fibular facet mediolateral
width (4) | 3.97* |
| | Proximal fibular facet
anteroposterior length (5) | 6.30* |
| | Proximal tibia anteroposterior total
length (7) | 20.27* |

Table A18. Measurements of the astragalus, *Conoryctes comma*. Numbers are referring to the measurements as seen in Figure A38.

| Specimen | | mm |
|---------------|---|--------|
| NMMNH P-21509 | Mediolateral total width of the astragalar body (1) | 16.62 |
| | Mediolateral total width of the astragalar head (2) | 12.33 |
| | Anteroposterior length of the astragalar neck and head (3) | 11.71 |
| | Mediolateral total width of the astragalar neck (4) | 9.13 |
| | Mediolateral total width of the anteriormost edge of the astragalar body (5) | 13.62 |
| | Mediolateral total width of the posteriormost edge of the astragalar body (6) | 13.44* |
| | The anteroposterior total length of the astragalus (7) | 24.5 |
| | Anteroposterior length of the ectal facet (8) | 11.53* |
| | Mediolateral width of the ectal facet (9) | 7.5* |
| | Anteroposterior length of the sustentacular facet (10) | 5.5* |

| | | |
|---------------|--|--------|
| | Mediolateral width of the sustentacular facet (11) | 5.89* |
| | Anteroposterior length of the medial tibial facet (12) | 12.06* |
| | Dorsoplantar width of the medial tibial facet (13) | 8.08 |
| | Dorsoplantar width of the astragalar head (14) | 6.72 |
| | Anteroposterior length of the lateral tibial facet (15) | 11.28 |
| | Dorsoplantar width of the lateral tibial facet (16) | 10.32 |
| NMMNH P-48052 | Mediolateral total width of the astragalar body (1) | 18.68 |
| | Mediolateral total width of the astragalar head (2) | 10.37 |
| | Anteroposterior length of the astragalar neck and head (3) | 9.89 |
| | Mediolateral total width of the astragalar neck (4) | 7.67* |
| | Mediolateral total width of the anteriormost edge of the astragalar body (5) | 12.20 |

| | | |
|---------------|---|--------|
| | Mediolateral total width of the posteriormost edge of the astragalar body (6) | 13.01 |
| | Anteroposterior total length of the astragalus (7) | 22.63* |
| | Anteroposterior length of the ectal facet (8) | 6.33* |
| | Anteroposterior length of the sustentacular facet (10) | 7.94* |
| | Mediolateral width of the sustentacular facet (11) | 6.44* |
| | Anteroposterior length of the medial tibial facet (12) | 10.42* |
| | Dorsoplantar width of the medial tibial facet (13) | 8.52* |
| | Dorsoplantar width of the astragalar head (14) | 6.36 |
| | Anteroposterior length of the lateral tibial facet (15) | 9.95* |
| | Dorsoplantar width of the lateral tibial facet (16) | 8.11* |
| NMMNH P-48198 | Mediolateral total width of the astragalar body (1) | 19.45 |

| | | |
|--|--|-------|
| | Mediolateral total width of the astragalar head (2) | 12.53 |
| | Anteroposterior length of the astragalar neck and head (3) | 11.89 |
| | Mediolateral total width of the astragalar neck (4) | 8.73* |
| | Mediolateral total width of the anteriormost edge of the astragalar body (5) | 15.15 |
| | Mediolateral total width of the posterior most edge of the astragalar body (6) | 13.78 |
| | Anteroposterior total length of the astragalus (7) | 23.97 |
| | Anteroposterior length of the ectal facet (8) | 11.6 |
| | Mediolateral width of the ectal facet (9) | 7.96 |
| | Anteroposterior length of the sustentacular facet (10) | 8.12 |
| | Mediolateral width of the sustentacular facet (11) | 6.44 |
| | Anteroposterior length of the medial tibial facet (12) | 11.12 |

| | | |
|--|---|-------|
| | Dorsoplantar width of the medial tibial facet (13) | 10.35 |
| | Dorsoplantar width of the astragalar head (14) | 7.72 |
| | Anteroposterior length of the lateral tibial facet (15) | 12.13 |
| | Dorsoplantar width of the lateral tibial facet (16) | 11.73 |

Table A19. Measurements of the calcaneum, *Conoryctes comma*. Numbers are referring to the measurements as seen in Figure A39.

| Specimen | | mm |
|---------------|---|-------|
| NMMNH P-47866 | Total anteroposterior length (1) | 27.78 |
| | Total mediolateral width between the sustentacular facet and the peroneal process (2) | 18.73 |
| | Anteroposterior length of the ectal facet (3) | 9.85 |
| | Mediolateral width of the ectal facet (4) | 6.96 |
| | Anteroposterior length of the sustentacular facet (5) | 6.77 |

| | | |
|--|--|-------|
| | Mediolateral width of the sustentacular facet (6) | 6.56 |
| | Mediolateral width of the cuboid facet (7) | 7.72 |
| | Dorsoplantar length of the cuboid facet (8) | 6.77 |
| | Anteroposterior length of the peroneal process (9) | 5.69 |
| | Distance between the tuber calcanei and the most posterior edge of the ectal facet (10) | 12.10 |
| | Distance between the most anterior edge of the ectal facet and the most anterior part of the calcaneum (11) | 7.21 |
| | Distance between the most posterior edge of the ectal facet and the most anterior part of the calcaneum (12) | 15.65 |
| | Mediolateral width of the tuber calcaneum at the middle point (13) | 6.86 |
| | Dorsoplantar length of the anterior edge of the calcaneum (14) | 11.68 |

| | | |
|---------------|---|-------|
| | Dorsoplantar length at the middle point of the calcaneum (15) | 11.55 |
| | Dorsoplantar length of the tubercle calcanei (16) | 10.13 |
| | Mediolateral width of the anterior plantar tubercle (17) | 4.51 |
| NMMNH P-48052 | Total anteroposterior length (1) | 33.98 |
| | Anteroposterior length of the ectal facet (3) | 11.09 |
| | Mediolateral width of the ectal facet (4) | 9.68 |
| | Mediolateral width of the cuboid facet (7) | 8.66 |
| | Dorsoplantar length of the cuboid facet (8) | 7.76 |
| | Anteroposterior length of the peroneal process (9) | 7.04 |
| | Distance between the tubercle calcanei and the most posterior edge of the ectal facet (10) | 17.22 |
| | Distance between the most anterior edge of the ectal facet and the most anterior part of the calcaneum (11) | 8.10 |

| | | |
|--------------------------|--|-------|
| | Distance between the most posterior edge of the ectal facet and the most anterior part of the calcaneum (12) | 17.14 |
| | Mediolateral width of the tuber calcaneum at the middle point (13) | 6.81 |
| | Dorsoplantar length of the anterior edge of the calcaneum (14) | 11.67 |
| | Dorsoplantar length at the middle point of the calcaneum (15) | 14.28 |
| | Dorsoplantar length of the tubercle calcanei (16) | 10.57 |
| | Mediolateral width of the anterior plantar tubercle (17) | 4.77 |
| NMMNH P-48198
(right) | Total anteroposterior length (1) | 34.12 |
| | Anteroposterior length of the ectal facet (3) | 10.89 |
| | Mediolateral width of the ectal facet (4) | 6.16 |
| | Anteroposterior length of the sustentacular facet (5) | 6.90 |
| | Mediolateral width of the sustentacular facet (6) | 7.31 |

| | |
|--|-------|
| Mediolateral width of the cuboid facet (7) | 8.46 |
| Dorsoplantar length of the cuboid facet (8) | 6.46 |
| Distance between the tuber calcanei and the most posterior edge of the ectal facet (10) | 18.11 |
| Distance between the most anterior edge of the ectal facet and the most anterior part of the calcaneum (11) | 8.63 |
| Distance between the most posterior edge of the ectal facet and the most anterior part of the calcaneum (12) | 16.48 |
| Mediolateral width of the tuber calcaneum at the middle point (13) | 7.72 |
| Dorsoplantar length of the anterior edge of the calcaneum (14) | 13.08 |
| Dorsoplantar length at the middle point of the calcaneum (15) | 14.63 |
| Dorsoplantar length of the tubercle calcanei (16) | 10.65 |

| | | |
|-------------------------|---|-------|
| NMMNH P-48198
(left) | Total anteroposterior length (1) | 33.78 |
| | Anteroposterior length of the ectal
facet (3) | 9.95 |
| | Mediolateral width of the ectal
facet (4) | 5.54 |
| | Mediolateral width of the cuboid
facet (7) | 7.48* |
| | Dorsoplantar length of the cuboid
facet (8) | 6.48 |
| | Distance between the tuber
calcanei and the most posterior
edge of the ectal facet (10) | 18.08 |
| | Distance between the most
anterior edge of the ectal facet and
the most anterior part of the
calcaneum (11) | 8.26 |
| | Distance between the most
posterior edge of the ectal facet
and the most anterior part of the
calcaneum (12) | 16.02 |
| | Mediolateral width of the tuber
calcaneum at the middle point (13) | 8.12 |

| | | |
|--|--|-------|
| | Dorsoplantar length of the anterior edge of the calcaneum (14) | 13.18 |
| | Dorsoplantar length at the middle point of the calcaneum (15) | 14.10 |
| | Dorsoplantar length of the tubercle calcanei (16) | 11.52 |

Table A20. Measurements of the metatarsals, *Conoryctes comma*.

| Specimen | | mm |
|----------------|---|-------|
| NMMNH P-47700 | | |
| IV metatarsals | total length | 28.35 |
| | perimeter at midshaft | 21 |
| | mediolateral width of the proximal epiphysis | 5.68 |
| | mediolateral width of the distal epiphysis | 8.39 |
| | anteroposterior width of the proximal epiphysis | 8.23 |
| | anteroposterior width of the proximal epiphysis | 5.83 |
| V metatarsals | total length | 14.27 |
| | perimeter at midshaft | 1.5 |
| | mediolateral width of the proximal epiphysis | 5.98 |

| | | |
|--|---|------|
| | mediolateral width of the distal epiphysis | 5.72 |
| | anteroposterior width of the proximal epiphysis | 5.45 |
| | anteroposterior width of the proximal epiphysis | 3.95 |



Figure A33: Right and left ulna and left ulna of the specimen (top photos) and of the cervical vertebrae (bottom photo). These postcranial are associated with USNM 22484 after Schoch (1986), but were first associated with specimen USNM 22483 of *Triisodon*. I agree with associating them to *Triisodon*. Scale bar is 1cm.

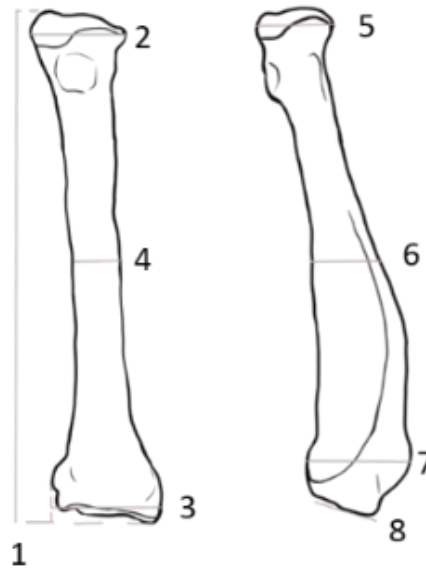


Figure A34: Drawing of the measurements taken of the radius. Total proximodistal length (1), mediolateral width of the proximal epiphysis (2), mediolateral width of the distal epiphysis (3), mediolateral width at the middle of the shaft (4), anteroposterior width of the proximal epiphysis (5), anteroposterior width at the middle of the shaft (6), anteroposterior width of the distal epiphysis (7), anteroposterior width of the distal articular fovea (8).

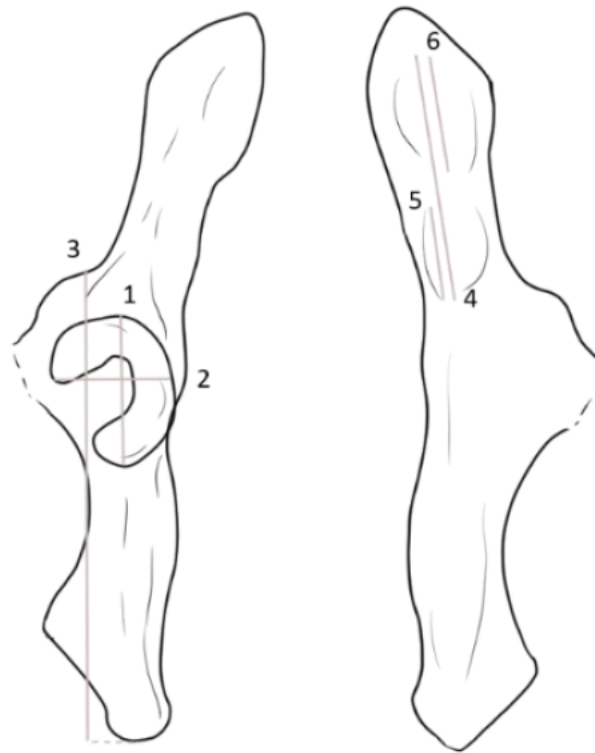


Figure A35: Drawing of the measurements taken of the pelvis. Length of the lunate surface (1), width of the lunate surface (2), length from the tip of the ischiatic tuberosity to the iliopectineal eminence (3), total length of the fossae attaching the sacrum on the ventral view of the ilium (4), length of the fossa closer to the greater ischiatic notch (5), length of the fossa on the wing of the ilium (6).

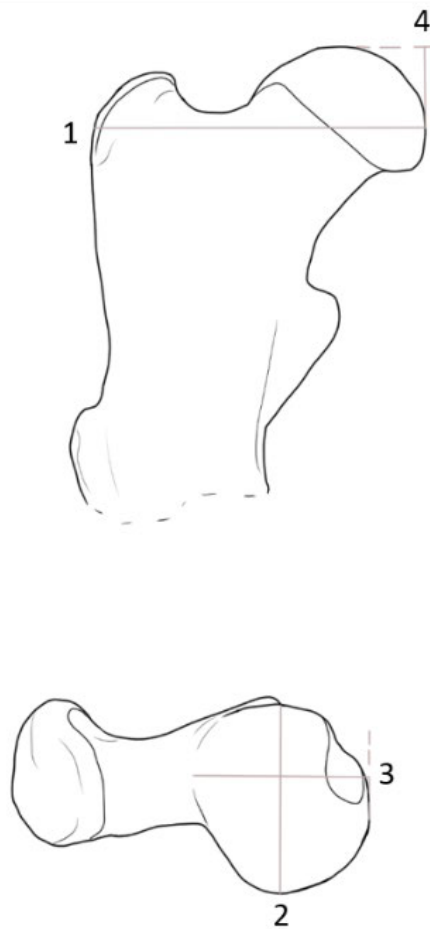


Figure A36: Drawing of the measurements taken of the femur. Total mediolateral width of the proximal epiphysis (1), femoral head anteroposterior length (2), femoral head mediolateral width (3), femoral head proximodistal length (4).

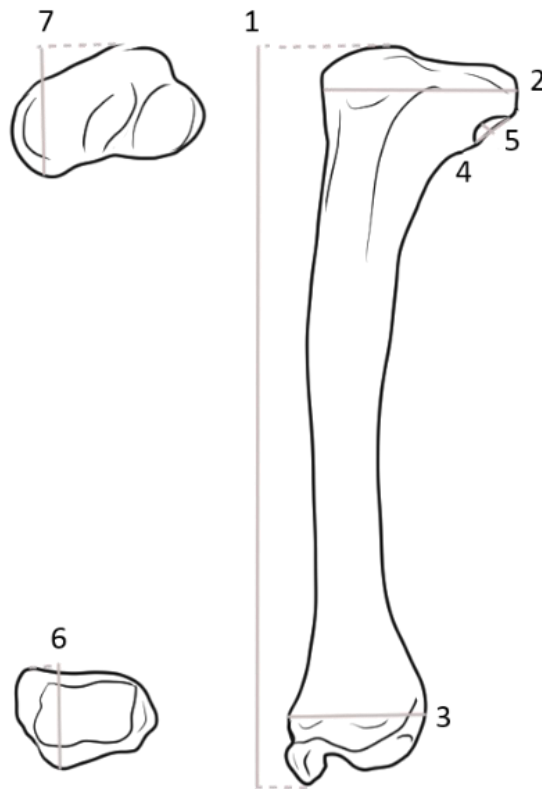


Figure A37: Drawing of the measurements taken of the tibia. Total proximodistal length (1), proximal tibia mediolateral width (2), distal tibia mediolateral width (3), proximal fibular facet mediolateral width (4), proximal fibular facet anteroposterior length (5), distal tibia anteroposterior total length (6), proximal tibia anteroposterior total length (7).

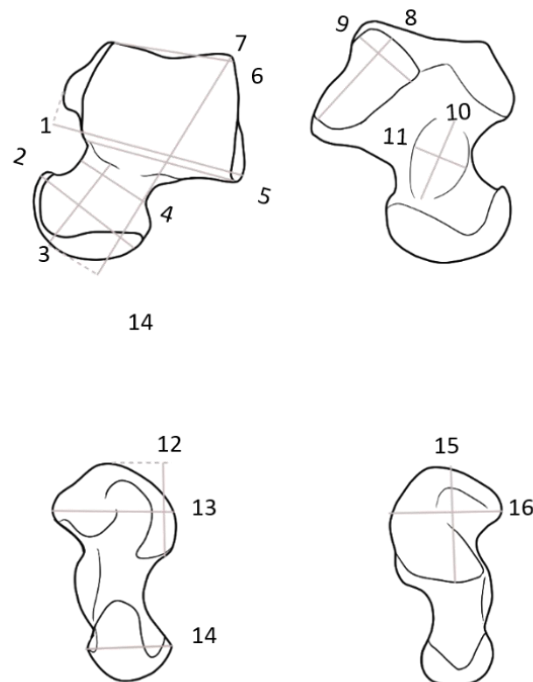


Figure A38: Drawing of measurements of the astragalus. Mediolateral total width of the astragalar body (1), mediolateral total width of the astragalar head (2), anteroposterior length of the astragalar neck and head (3), mediolateral total width of the astragalar neck (4), mediolateral total width of the anterior most edge of the astragalar body (5), mediolateral total width of the posterior most edge of the astragalar body (6), anteroposterior total length of the astragalus (7), anteroposterior length of the ectal facet (8), mediolateral width of the ectal facet (9), anteroposterior length of the sustentacular facet (10), mediolateral width of the sustentacular facet (11), anteroposterior length of the medial tibial facet (12), dorsoplantar width of the medial tibial facet (13), dorsoplantar width of the astragalar head (14), anteroposterior length of the lateral tibial facet (15), dorsoplantar width of the lateral tibial facet (16).

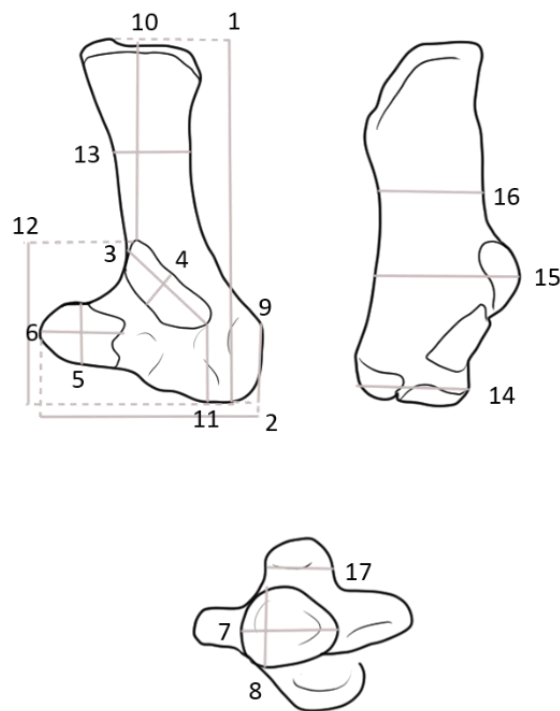


Figure A39: Drawing of the measurements taken on the calcaneum. Total anteroposterior length (1), total mediolateral width between the sustentacular facet and the peroneal process (2), anteroposterior length of the ectal facet (3), mediolateral width of the ectal facet (4), anteroposterior length of the sustentacular facet (5), mediolateral width of the sustentacular facet (6), mediolateral width of the cuboid facet (7), dorsoplantar length of the cuboid facet (8), anteroposterior length of the peroneal process (9), distance the tuber calcanei to the most posterior edge of the ectal facet (10), distance between the most anterior edge of the ectal facet and the most anterior part of the calcaneum (11), distance between the most posterior edge of the ectal facet and the most anterior part of the calcaneum (12), mediolateral width of the tuber calcaneum at the middle point (13), dorsoplantar length of the anterior edge of the calcaneum (14), dorsoplantar length at the middle point of the calcaneum (15), dorsoplantar length of the tubercle calcanei (16), mediolateral width of the anterior plantar tubercle (17).

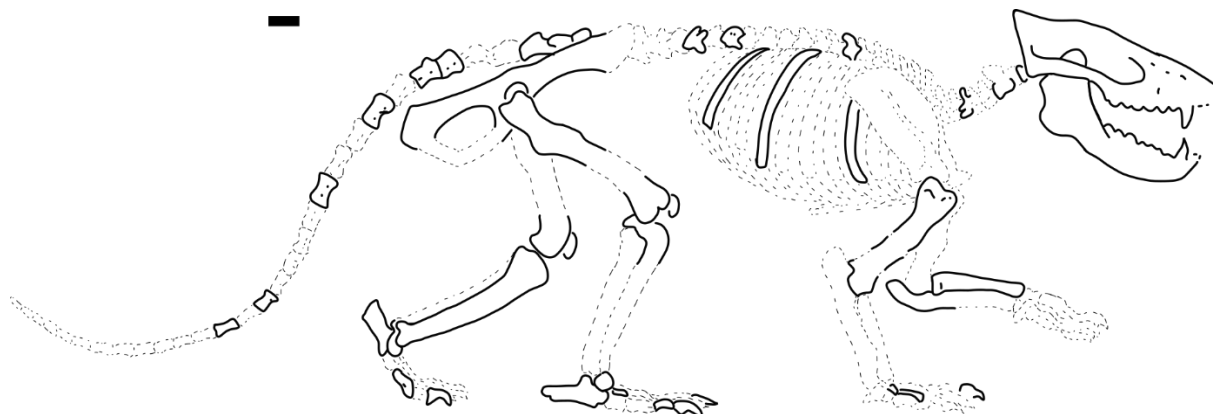


Figure A40: Drawing of the skeleton of *Conoryctes comma* based on the known specimens of the genus. In bold the postcranial elements described in this study. Scale bar is 1cm.

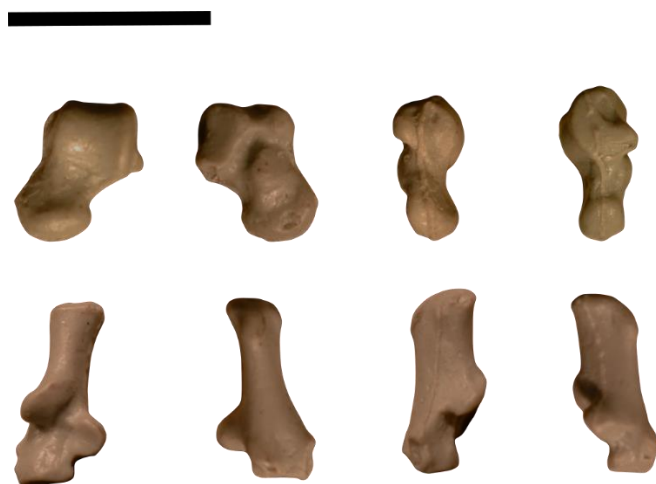


Figure A41: Tarsals of *Procerberus* (astragalus AMNH 117454, calcaneum AMNH 117455) in dorsal, plantar, lateral, and medial views. Scale bar is 1cm.



Figure A42: Humerus of *Onychodectes tisonensis* (AMNH 16410) in posterior, and anterior views. Scale bar is 1cm.



Figure A43: Ulna of *Onychodectes tisonensis* (AMNH 16410) in medial, anterior, and lateral views. Scale bar is 1cm.



Figure A44: Astragalus of *Onychodectes tisonensis* (AMNH 3405) in dorsal, plantar, lateral, and medial views. Scale bar is 1cm.



Figure A45: Ulna of *Conoryctella pattersoni* (NMMNH P-25056, old label UNM B-1528) in lateral, anterior and medial views. Scale bar is 1cm.



Figure A46: Ulna of *Psittacotherium multifragum* (AMNH 16560) in medial, lateral, and anterior views, and lateral view of the radius (AMNH 16560). Note the distal parts of the fossils are made of plaster. Scale bar is 1cm.



Figure A47: Manus of *Psittacotherium multifragum* (AMNH 2453) in anterior view in plaster. Note some of the phalanges are made of plaster. Scale bar is 1cm.



Figure A48: Femur of *Psittacotherium multifragum* (TMM 41364-1) in posterior, medial, lateral, and anterior views. Photos provided by my supervisor, Tom Williamson. Note the presence of a gap in the middle of the shaft. Scale bar is 1cm.



Figure A49: Tibia of *Psittacotherium multifragum* (TMM 41364-1) anterior, lateral, and posterior views and the proximal epiphysis of the tibia. Photos provided by my supervisor, Tom Williamson. Scale bar is 1cm.

